

DEVELOPMENT & CHARACTERIZATION OF MICROWAVE ABSORBERS

A THESIS

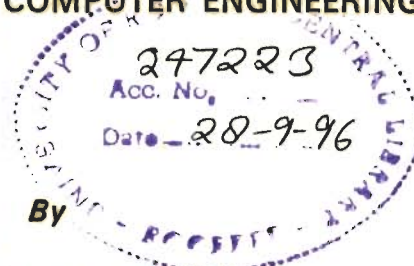
*Submitted in fulfilment of the
requirements for the award of the degree*

of

DOCTOR OF PHILOSOPHY

in

ELECTRONICS AND COMPUTER ENGINEERING



CHAITANYA KUMAR M.V.



**DEPARTMENT OF ELECTRONICS AND COMPUTER ENGINEERING
UNIVERSITY OF ROORKEE
ROORKEE - 247 667, INDIA**


SEPTEMBER, 1994

matris


CANDIDATE'S DECLARATION

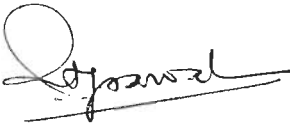
I hereby certify that the work which is being presented in the thesis entitled Development & Characterization Of Microwave Absorbers' in fulfilment of the requirement for the award of the Degree of Doctor of Philosophy and submitted in the Department of Electronics and Computer Engineering of the University is an authentic record of my own work carried out during a period from 3rd July 1991 to 28 September 1994, under the supervision of Dr. S.C.Gupta, Dr. N.K.Agrawal and Dr. P.S.Mishra.


The matter presented in this thesis has not been submitted by me for the award of any other degree of this or any other University.


(Chaitanya Kumar M. V.)

This is to certify that the above statement made by the candidate is correct to the best of our knowledge.


(Dr. S.C.Gupta)
Professor
Department of Electronics
and Computer Engg.


(Dr. N.K.Agrawal)
Professor
Department of Electronics
and Computer Engg.
University of Roorkee, Roorkee, India.

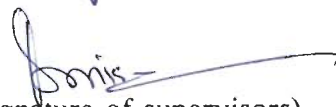

(Dr. P.S.Mishra)
Professor
Department of
Metallurgical Engg.

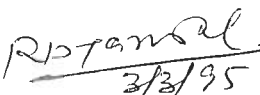
Date : 20.9.94.

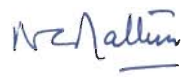
The Ph.D. Viva-Voce examination of Shri Chaitanya Kumar M. V., Research Scholar, has been held on March 3, 1995

1) 

2) 

3) 
(Signature of supervisors)


(Signature of H.O.D.)


(Signature of
External Examiner)

ABSTRACT

Microwaves span over a wide frequency spectrum, but in this particular subject of study, material-composites in the form of planar thin sheets, have been analyzed and designed to absorb microwave energy in the frequency range of 2-18 GHz. Various design approaches have been formulated for the design and analysis of thin planar absorbers. An impedance matching technique has been formulated to match thin planar absorbers to free space, without increasing the overall thickness of the absorber.

A generalized design approach is formulated with Cobalt-substituted Barium Hexa Ferrite (Co-BHF) as the lossy material for the design of broad band absorbers. Broad banding is achieved by combining the material and thickness absorption effects in the absorber. The design formulation has been practically verified by fabricating of an absorber for broad band operation over Ku-band, with a constraint of 2mm on the thickness of the absorber. The close agreement between the theoretically predicted and experimentally obtained absorption characteristics has validated the formulation.

A mathematical model for the theoretical analysis and design of microwave absorbers has been formulated, based on the evaluation of the overall reflection coefficient of the absorber. The design criteria for two types namely, matched and resonant absorbers are established. The design criteria for the matched absorber indicates that it is best suited for broad band operation and a predominantly magnetic type of material will have to be employed to realize matched absorber in practice. The design criteria for the resonant absorber implies that, resonant absorbers are narrow band absorbers.

Absorbers one each for matched (broad band operation over Ku-Band) and resonant (narrow band operation in X-Band) criteria with an added constraint on thickness of 2mm were designed and fabricated. Co-BHF and carbon have been used as the lossy materials along with silicone/neoprene rubber as the binder in the design. A very close agreement between the theoretically predicted and experimentally determined performance for both types of absorbers justifies the proposed mathematical model.

Waterman's T-matrix approach has been utilized in a multiple scattering formulation, to determine the bulk or effective propagation constant for the composite absorbing medium, as a function of particle (scatterer) size and shape, volume concentration of the lossy material, orientation and position of the scatterer in the binder or host matrix. In the multiple scattering model, T-matrix is used to represent the effect of size and shape of individual lossy particles and the random nature of orientation of the particles in the host matrix. An average over all possible position is performed using the two-point joint probability function, which in turn is defined by the radial distribution function obtained under the self consistent approximation. A closed form solution of the dispersion equation for a ferrite polymer composite is obtained under the long wavelength approximation.

The designed and fabricated matched absorber performance is verified using this approach. This model describes more closely the practical behavior of the absorber than the earlier method, thus proving that bulk properties have to be considered, when high loss materials are employed in the design.

Employing the proposed model, the optimum configuration for a ferrite-rubber composite, such as size of the spherical particles (scatterer), volume

concentration of the ferrite and thickness of the absorber were determined for broad band operation over X-Band within 3mm thickness limitation. The experimentally determined absorption characteristics for the designed and fabricated absorber of thickness 2.3mm, displays good agreement with the theoretically predicted curve as a broad band absorber, except for the shift in the absorption peak.

An impedance matching technique was formulated to overcome the mismatching (at the free space-absorber interface) problem associated with thin planar absorbers. A thin conducting screen perforated with an array of structures has been employed as the Impedance Matching Layer (IMS). Jerusalem cross and double square loop array structures were found to be promising candidates for IMS application from a number of structures that were experimentally examined. A simple equivalent circuit approach was formulated for the design analysis of the composite structure formed by incorporating the IMS at the front end of the absorber. Equivalent circuit models available in literature, to analyze the array of Jerusalem cross and double square loops have been utilized in the design of the IML's. The effect of the various parameters of the array on the overall performance of the absorber have been analyzed and critical parameters identified.

Using the proposed equivalent circuit model, with Jerusalem cross as the IMS structure, the Co-BHF rubber absorber designed using the first technique discussed above, which practically provided around 8dB absorption over 12-18 GHz., was impedance matched into (i) operating as a narrow band absorber with a peak absorption of over 30dB; and (ii) operating as broad band absorber with bandwidth over 8 to 18 GHz., with a marked increase in the level of absorption through out the band. The close agreement between the theoretically predicted absorption

characteristics and the experimentally determined values for both the cases consolidates the proposed impedance technique. With double square loop array as the IMS structure, the absorber was impedance matched to operate as broad band absorber to provide 10 GHz (8-18 GHz) bandwidth.

An established approach to overcome the mismatching (at the free space-absorber interface) problem associated with planar absorbers is to construct an impedance taper employing a multilayered structure. This approach has been extended to the case of thin planar absorbers. Generalized design equations have been arrived at, for a plane wave at arbitrary angle of incidence, as a function of number of layers, concentration of the lossy material in each layer, individual layer thickness, and the overall thickness of the absorber. As a special case of multilayered structure when the number of layers is one, a single layer absorber was designed using the multilayered approach, to operate as a broad band absorber (X-Band) over $\pm 45^\circ$ incidence angle. A limitation on the overall thickness of the absorber of 3mm was also met. Iron powder has been used in the design as the lossy material along with silicone rubber as the binder. The designed and fabricated absorber of 2.3mm thick, displays a practical absorption characteristics which matches very closely with the theoretically predicted curves.

One of the major problems faced in translating the theoretical design into practical absorbers is dispersing the lossy particles uniformly in the host medium. In this context, Secondary Electron and Optical microscopic analysis were done on samples fabricated with different dispersing aids. The type and critical concentration of the dispersing aid, and the method for dispersion, for particular applications have been identified.

ACKNOWLEDGEMENTS

The author expresses his deep sense of gratitude to his supervisors, Dr. S. C. Gupta, Dr. N. K. Agrawal, Professors, Department of Electronics and Computer Engineering and Dr. P. S. Mishra, Professor, Department of Metallurgical Engineering, for their valuable guidance, sincere advice and above all the friendliness shared with him.

The co-operation and help extended by the Professor and Head, Department of Electronics and Computer Engineering; Professor and Head, Department of Metallurgical Engineering, is gratefully acknowledged.

Thanks are also due to the staff of Computer centre, workshop, PCB lab., Advance Microwave lab., Department of Electronics and Computer Engineering; Metal Forming and Heat treatment lab., Department of Metallurgical Engineering. The co-operation extended by S.K. Bhattacharjee of stores is gratefully acknowledged.

I thank all fellow research scholars for their encouragement, co-operation, valuable suggestions and help rendered during the course of my work.

The author is indebted to DRDO, Ministry of Defence, for sponsoring research in the Department on 'Development of Thin Radar Absorbers', under whose grant the work presented in this thesis was carried out. The author also thanks, CSIR, Govt. of India, for providing the necessary fellowship support for his research work.

This acknowledgement would be incomplete, without a mention of gratitude to the members of the author's family, who had to put up with all sorts of inconveniences due to his persual of research under loss of pay!.

Finally the author is grateful to the authorities of Sri Jayamarajendra College of Engineering, Mysore, for granting him with necessary leave.

Chaitanya Kumar M V.

(Chaitanya Kumar M V)

CONTENTS

ABSTRACT	(i)
ACKNOWLEDGEMENTS	(v)
CONTENTS	(vi)
CHAPTER I : INTRODUCTION	1
1.1 Prelude.	1
1.2 Microwave absorbers : Application.	4
1.3.0 Microwave absorbers : A Classification.	6
1.3.1 Absorbers Based On The Material Properties.	7
1.3.2 Absorbers Based On The Geometrical Properties.	8
1.4.0 Microwave absorbers : A General Design Guideline.	9
1.4.1 General Guidelines Of Electrical Performance	10
1.4.2 General Guidelines On Physical Performance	11
1.5 Organization Of This Dissertation.	11
CHAPTER II : PREVIEW	13
2.1 Introduction.	13
2.2 Microwave Absorbers : A Review.	13
2.3 Multiple Scattering Theory : A Review.	21
2.4 Impedance Matching Technique : A Review.	24
2.5 Statement Of The Problem.	26
CHAPTER III : A GENERALIZED APPROACH FOR THE DESIGN OF BROAD BAND MICROWAVE ABSORBER.	29
3.1 Introduction.	29
3.2 Theory.	30
3.3 Design Examples For Single Layer Broad Band Absorbers.	34
3.4 Experimental Results.	35
3.5 Conclusions.	38
Appendix 3.1	40
CHAPTER IV : DESIGN CRITERIA FOR MICROWAVE ABSORBERS	43
4.1 Introduction.	43
4.2 Theory.	43
4.2.1 Design Criteria For Matched Absorber.	47
4.2.2 Design Criteria For Resonant Absorber.	48
4.3.0 Design Examples.	39
4.3.1 Design Of A Matched Absorber.	50
4.3.2 Design Of A Resonant Absorber.	51
4.4 Fabrication Of Absorbers.	52
4.5 Experimental Results.	52
4.6 Conclusions.	53

CHAPTER V : CHARATERIZATION OF THE ABSORBING MEDIA BY ITS BULK PROPERTIES	57
5.1 Introduction.	57
5.2 Wave Propagation Through Randomly Distributed And Oriented Scatterers : Multiple Scattering Theory	59
5.3 Configurational Averaging : The Average Or Effective Wave Number In The Media.	68
5.4 Analytical Expression For The Wave Number Under The Long Wavelength Approximation.	72
5.5 Radial Distribution Function.	73
5.6 Organization Of The computer Programme.	77
5.7 Analysis Of Absorbers Using Effective Or Average Wave Number.	79
5.8 Design Analysis Of A Broad Band Absorber.	83
5.9 Experimentale Results.	90
5.10 Conclusions	90
Appendix 5.1	92
Appendix 5.2	96
Appendix 5.3	98
Appendix 5.4	106
Appendix 5.5	110
 CHAPTER VI : AN IMPEDANCE MATCHING TECHNIQUE TO IMPROVE THE PERFORMANCE OF THIN PLANAR ABSORBERS.	 111
6.1 Introduction.	111
6.2 An Experimental Investigation To Asses The Impedance Matching Property Of A Conducting Screen Perforated With An Array Of Apertures.	113
6.3 Theory Of Impedance Matched Absorber.	116
6.4.0 Analysis Of An IMA With Periodic Array Of Jerusalem Cross Apertures As The IMS.	117
6.4.1 Design Examples.	125
6.4.2 Fabrication Of IMS And IMA.	126
6.4.3 Discussion And Experimental Results.	126
6.5.0 Analysis Of An IMA With Periodic Array Of Double Square Loops As The IMS.	136
6.5.1 Design Example.	137
6.6 Conclusions.	137
Appendix 6.1	146
 CHAPTER VII : DESIGN ANALYSIS OF A MULTILAYER ABSORBER	 151
7.1 Introduction.	151
7.2 Analysis Of Multilayered Absorber.	151
7.2.1 Electric field Parallel To The Plane Of Incidence.	152
7.2.2 Electric field Perpendicular To The Plane Of Incidence.	155
7.3 Design And Experimental results.	157
7.4 Conclusions.	160

CHAPTER VIII : MICROWAVE ABSORBERS : FABRICATIONAL ASPECTS	167
8.1 Introduction	167
8.2 An Experimental Investigation : Analysis of Particulate Dispersion In Rubber.	167
8.3.0 Fabrication Of The Rubber-Absorber Sheet.	174
8.3.1 Preparation Of The Lossy material.	174
8.3.2 Preparation Of Co-BHF.	175
8.3.3 Preparation Procedure.	176
8.3.4 Estimation Of Cobalt Content in the Barium ferrite.	177
8.3.5 Preparation Of The Standard Solution.	178
8.3.6 Determination Of The Concentration Curve.	178
8.3.7 Preparation Of The Solution Of The Unknown Cobalt Compound.	178
8.3.8 Estimation Of Cobalt Content In The Sample.	179
8.3.9 Estimation Of Complex Permeability Of Co-BHF : Determination Of F_r for Co-BHF.	180
8.3.10 Experimentation.	180
8.3.11 Preparation Of Waveguide Sample.	180
8.3.12 Experimental Procedure.	181
8.3.13 Analysis Of The Data.	182
8.3.14 Preparation Of Ferrite.	185
8.4 Fabrication Of The Sheet.	185
8.5.0 Fabrication Of Impedance Matching Surfaces.	186
8.5.1 Preparation Of The Art Work.	187
8.5.2 Preparation Of The Negatives.	187
8.5.3 Preparation Of A Mask ON The Copper Sheet.	187
8.5.4 Preparation Of The IMS In Its Final Form.	188
8.6.0 Materials Used To Absorb Electromagnetic Energy At Microwave Frequencies.	188
8.6.1 Carbon.	189
8.6.2 Iron Powder.	189
8.6.3 Ferrites.	189
8.6.4 Loss Mechanism In Ferrites (Magnetic Losses).	191
8.7 Conclusion.	192
Appendix 8.1	194
CHAPTER IX : DISCUSSIONS AND CONCLUSIONS	197
9.1 Discussions and Conclusion.	197
9.2 Scope Of Future Work.	204
References	207
Appendix I	225

CHAPTER I

INTRODUCTION

1.1 PRELUDE :

Advanced technologies present unusual challenges and opportunities for researchers in India. The unusual challenges arise from the common perception, particularly in western nations, that their availability to countries, such as India should be restricted, since these advanced technologies are needed in sophisticated weapon systems. Challenges also arise in translating science into technology. Emerging electronic technologies are most certainly useful in sophisticated weapon systems. There can be no dispute about this. However, the same technologies also find a host of applications in modern day communications and industry, state of the art and cost effective communication and informatic systems and, computer and control instrumentation cannot be built without such technologies. Interestingly, denial of technology, itself offers many unique opportunities for research and development.

Techniques for Radar Cross Section Reduction (RCSR) of weapon platforms have been practiced for many years, but it has been the development of the so-called 'stealth' aircraft, the F-117A fighter and B-2 bomber, that has brought this technology into prominence. While such aircrafts, epitomize low observability targets. The underlying technique of RCSR are applicable to other weapon platforms as well.

In addition, existing assets are being examined to asses what palliative

measures can be adopted to reduce their RCS. The work presented in this thesis describes an investigation into one of the major techniques that can be employed to reduce the RCS of existing structures.

A reduction of RCS at one viewing angle is usually accompanied by an enhancement at another when target surfaces are reshaped or reoriented to achieve the reduction [1-3]. On the other hand if radar absorbing coatings [simply called 'absorbers' henceforth] are used, the reduction is achieved by dissipation of energy within the material. Thus reduction in one direction does not effect the RCS in other direction. But addition of absorber is a compromise as it increases weight, volume and surface maintenance problems.

Such absorbers should be thin, light in weight and provide specified absorption over the desired frequency spectrum. Microwaves span over a wide frequency spectrum, but in this particular subject of study, it is proposed to formulate a material-composite in the form of planar thin sheets, which can absorb microwave energy in the frequency range of 2-18 GHz., so that they can be employed to coat existing assets to reduce RCS or achieve suppression of electromagnetic interference.

We are led to believe, similar work presented in this thesis, may be going on or has been done, especially in the various industrial and government research laboratories of the advanced countries. But due to the sensitive nature of the work, or may be of a proprietary nature, is not easily available at large, especially the practical aspect of the problem in translating science into production technology.

The basic feature of the absorbers is that substances either exist or can be

fabricated whose indices of refraction are complex numbers. In the index of refraction which includes both the electric and magnetic effects, it is the imaginary part which accounts for the loss. At microwave frequencies the loss occurs because of finite conductivity of the material as well as due to a kind of molecular friction which occurs when molecules attempt to follow the alternating fields of an impressed wave. It is customary to include the effects of all types of loss at molecular level, in the permittivity and permeability of the material at the macroscopic level.

The presence of the electric field component in microwaves introduces the possibility of dielectric and magnetic losses. Hence, while it is obvious that for microwaves to penetrate a material to any appreciable depth its resistivity must be very high; this defines, the first requirement of materials for microwave applications.

A Thin coating of material can be theoretically designed to give any desired reflectivity over a specified bandwidth. But the realization of the material in practice, imposes a severe constraint at microwave frequencies. Ideally, we should be able to have control over the material permittivity, permeability and the loss tangents, but this is rarely achieved as most materials have a high permittivity and low values of permeabilities in the microwave region. Thus characteristics impedance of the material ' Z ', then becomes less than unity leading to a mismatch at the air-material interface (the Z of free space being unity), which in turn prevents the wave from entering into the material. This defines the second and most important requirement for microwave absorption - If an absorber is to be efficient, the material must not only attenuate the waves penetrating its volume, but also present a good match to the incident waves at the air-material interface.

In the absence of any constraints on volume and or weight of the absorber, then sufficient absorption of energy over a wide bandwidth can be obtained by increasing the thickness of the material and shaping its geometry. The electromagnetic reflectivity over a frequency range in combination with the material weight, depth, cost and durability will however determine the effectiveness of an absorber.

1.2 MICROWAVE ABSORBERS : APPLICATIONS

The increased need for absorbers has resulted from the following two on going developments

1) The greater number of electronic systems being incorporated into weapon platforms has resulted in corresponding growth in electromagnetic interference. These problems include false images, increased clutter on radars and reduced performance because of system to system coupling. Microwave absorbers can be effectively used to eliminate these types of problems.

The lack of space available on modern warships causes electronic systems to be placed in close proximity. Often a signal or its harmonics from one system will be received by or will interfere with an adjacent system. This problem has become especially acute with the powerful broad band jammers currently being deployed, but it can be eliminated or minimized by constructing absorber barriers.

Today's modern warship has a wide variety of electronic systems on board. Navigational and target acquisition radars, communications equipment, etc are all mounted on a large metal superstructure. This arrangement creates two major

problems:-

- (a) false images from self reflections, and
- (b) system to system interference.

False images or ghosts are indirect radar returns resulting from specular reflections of radar energy off the ships own superstructures. False echoes cause navigational hazards and if severe enough can make radar navigation impossible. False returns to target acquisition and fire control systems can cause the system to lock on to the false images. These problems can be eliminated through the use of tuned frequency, elastomeric absorber. Tuned to the frequency of the radar, the absorber is bonded to masts, stacks, yard arms and other reflecting structures. By properly situating the material, false echoes can be reduced.

2) There are even greater requirements for reduced radar cross section (RCS) of weapon systems, not only is there a need to reduce a vehicles signature but equally important is to reduce the signature of various Electronic Warfare (EW) systems and payloads attached to these vehicles. Absorbers play a key role in the stealth technology and their use is a major factor in radar cross section reduction.

The past few years have seen a tremendous increased interest in the area of radar-cross-section reductions (RCSR) paralleled by an increasing requirement for absorbers. Absorbers have become an integral part of a weapon system's electronic counter measures package. When used in an integrative Electronic Warfare approach, the use of absorber can improve survivability by: Increasing the amount of power necessary for an enemy radar to gain detection, there by tending to increase radar's detectability. Deceiving an enemy into misjudging vehicle size and shape.

Reducing the amount of chaff that needs to be dispersed and carried on board for decoy and seduction.

Antenna pattern improvement is an area of universal application of microwave absorbers. Conductive objects in the near field of an antenna can greatly alter its free-space propagation characteristics. The net effect of this is wider main beam with increased side lobes. This condition can reduce system discrimination and increase the possibility of side lobe jamming. The application of absorber to the conductive areas will effectively match out radiation in these directions and return the system to its designed free-space characteristics. A variety of antenna systems have to use absorbers for this problem, to coat feeds, struts and mounts which act as reflectors.

Considering the on going developments discussed above, depending on the system involved, single frequency, dual frequency or broad band absorbers will have to be used.

1.3.0 MICROWAVE ABSORBERS : A CLASSIFICATION

Microwave absorbers or Radar absorbers may be loosely classified as "narrow band" and "broad band" absorbers. Narrow band absorbers provide absorption at discrete frequencies. As such these find applications as an interference layer, there by preventing interference between any two systems. Broad band absorber on the other hand, in principle, provides absorption at all the frequencies within a band. Outside a frequency band the absorbers become ineffective because of changes in material properties with corresponding change in frequency. Broad band absorbers can be used to reduce the radar cross sections of targets, as well as for coating

the interior of an anechoic chamber.

Further absorbers can be broadly classified into the following,

- a.* Absorbers based on the material properties; and
- b.* Absorbers based on the structural properties.

1.3.1 ABSORBERS BASED ON THE MATERIAL PROPERTIES

These can further be classified into five types

- a.* Those utilizing dielectric loss;
- b.* Those utilizing magnetic loss;
- c.* Resonant absorbers;
- d.* Hybrid absorbers, and
- e.* Circuit analog absorbers.

In the first type the loss is mainly due to the imaginary part of permittivity, ϵ'' ; while in the second it is mainly due to the imaginary part of permeability, μ'' . These absorbers offer the advantage of compactness, because they are typically a fraction of the thickness of dielectric absorbers and at the same time they are heavy in comparison.

If the thickness of an absorber backed by a perfect conductor, is made equal to the quarter wavelength of the frequency to be absorbed, then it offers an open circuit to the incident wave giving rise to absorption. Such absorbers are known as resonant absorbers.

A combination of the above three results in an hybrid absorber, which are employed to obtain higher peak absorption and larger bandwidth.

The term Circuit Analog Absorbers is derived from the fact that geometrical patterns are often defined in terms of their effective resistance, capacitance and inductance. These are then used in the analysis and design of an absorber. The Salisbury screen and Jaumann absorbers (the earliest types of absorbers) use resistive sheets for their operation, which have only a real part to their admittance, as the matching elements. Significant flexibility can be achieved in the design process if the sheets can have a susceptance as well as a conductance. This imaginary part can be generated by replacing the continuous resistive sheet with one whose conducting material has been deposited in appropriate geometrical patterns. However, optimization of the variables controlling the admittance properties is complicated.

1.3.2 ABSORBERS BASED ON THE GEOMETRICAL PROPERTIES

Absorber can be structurally subdivided into pyramidal type, tapered impedance type and thin coating type.

Pyramidal type are a class of broad band absorbers which take the form of pyramids or wedges of synthetic rubber or plastic foam loaded with an electrically lossy material. The geometrical transition may also be combined in some cases with an electrical transition by increasing the loss towards the base of the pyramids. The length of these pyramids are usually several free-space wavelengths long (*i.e.* in excess of 10λ). Absorption of the order of 30-50 dBs over a wide band of frequencies and $\pm 60^\circ$ incident angle can be achieved by these absorbers.

Tapered impedance are a class of absorbers used to match the impedance between free space and a perfect conductor by changing the properties of each layers. The

layers are so arranged that they become progressively thicker and have higher permittivity and permeability values in the direction of the incident plane wave. The optimum method for the design of such absorbers would be to determine analytically the μ & ϵ values required as a function of distance into the material to limit the reflection coefficient over a given frequency range, subject to angle of incidence and thickness constraints. The number of layers will have some effect on the overall performance, but the thickness of absorber cannot fulfill the practical values. This can lead to either bulky layers of materials or laminar structures that are too complicated to manufacture.

Thin coating type are a class of absorbers used where space is a premium. Since these are coatings, they can assume any shape and hence can be used to coat on an existing target thereby reducing its RCS.

1.4.0 MICROWAVE ABSORBERS : A GENERAL DESIGN GUIDELINE

A wide variety of absorber materials are needed for use in RCS reduction. There are trade off involved in use of each candidate material. To optimize the use of absorber in a design, there are three sets of parameters that should be critically analysed; electrical, physical and application.

It has not been possible to achieve the goal of DC to daylight absorbers as yet but considerable attempts have been made to broaden frequency coverage in the microwave region. In optimizing the absorber use, the threat should be defined as clearly as possible. The following question need to be asked.

- (1) What is the frequency band of interest ?
- (2) Is the coverage needed over the entire region or just at specific

frequencies ?

(3) What is the order of importance in coverage ?

Perhaps at frequency f_0 , 25 dB absorption is needed. However at f_1 only 10 dB is required and at f_2 12 dB is acceptable. By setting these priorities a design can more readily be reached.

(4) Will the absorber be used to absorb specular energy or is the application such that at high angles of incidence radiation must be attenuated ?

By answering these questions the various trade offs in electrical performance can be examined and an optimum absorber derived.

1.4.1 GENERAL GUIDELINES OF ELECTRICAL PERFORMANCE :

(1) The broader the frequency coverage, the thicker, heavier, and more expensive the absorber.

(2) The lower the minimum frequency coverage the thicker and heavier the absorber. Of equal importance to the materials, electrical performance is its physical performance, which includes environmental characteristics and mechanical properties.

Again a series of questions can help to clarify the parameters of major importance.

(1) What is the application environment? will the absorber be enclosed or subjected to the out door environment ?

(2) What environment forces will be degrading the absorber? such as Salt Water, Ozone, Oxygen, Ultra violet light, fuels, oils, chemicals nuclear radiations, gases ?

(3) Over what temperature range will the material be used ?

(4) What mechanical stress will be placed on the absorber: vibration, thermal shock, elongation, wind ?

(5) What is the expected life time of the absorber? like in case of missile applications the requirement may not be of the same degree of physical integrity as in ship or aircraft applications.

1.4.2 GENERAL GUIDANCE ON PHYSICAL PERFORMANCE :

(1) The elastomeric-type (rubber) absorbers have better environment resistance than broad band foam types.

(2) Neoprene is widely used in Naval applications because of superior weather resistance.

(3) Absorbers can be encapsulated in fiber reinforced plastics to develop required mechanical properties.

1.5 ORGANIZATION OF THIS DISSERTATION

In the next chapter a brief review of the work done in related fields are discussed, and the statement of the problem presented. The third and fourth chapter's are devoted to the development of the theoretical approaches for design and development of microwave absorbers. Design equations are arrived at, and hence design criterions established, for narrow as well as broad band absorbers. Absorbers are then designed and practically implemented, and their results compared with theoretically predicted values.

Waterman's T-Matrix approach is utilized in the fifth chapter, along with statistical averaging in a multiple scattering formalism, to evaluate the effective

or average properties of a absorbing media. Absobers designed and developed in the preceding chapters are then analyzed by the multiple scattering formalism. It is shown that the properties of the absorbing media is characterized by its bulk or average properties. Broad band absorbers are designed employing the multiple scattering formalism, and fabricated. It was found that there is good agreement between the theortically predicted absorption and experimentally determined values.

In the sixth chapter, an impedance matching technique is proposed and developed, to match the absorber to free space. The matching is obtained by the addition of a impedance matching screen (layer) at the front end of the absorber. Narrow as well as broad band absorbers have been developed using the proposed design model. The model is validated by the good agreement obtained between the theoretically predicted absorption and practically determined curves. An established approach to over come the impedance matching problem is to employ a multilayer construction for the absorber. In seventh chapter, the design analysis of a multilayer absorber based on layer structure model is discussed.

Eigth chapter is devoted to the fabrication aspect, wherein a brief procedure is given for the fabrication of the absorber as well as the impedance matching layer. The procedures adopted to prepare the lossy materials are also described.

Brief conclusions are drawn in the final chapter. The scope for future work in this area are also discussed.

CHAPTER II

PREVIEW

2.1 INTRODUCTION

Before getting into the business of reviewing the work in the field, it is important to note that thin sheet absorbers are usually formulated by dispersing lossy material in fine powder form (called 'filler'), in a suitable media (called 'host or binder'). In some cases loss aiding structures/molecules may also be added along with the filler into the binder.

2.2 MICROWAVE ABSORBERS : A REVIEW

One of the earliest type of absorbers developed was the Salisbury screen absorber [4]. In which a resistive sheet of 377 ohms per square inch, is placed one quarter wavelength from the metal surface to be shielded, with the aid of a spacer. Since the criteria of quarter wavelength can be satisfied at one frequency only, this type of absorbers tend to be narrow band absorbers.

An extension of the Salisbury type absorber is the Jaumann absorber [2], in which a number of screens are layered to increase the bandwidth of operation. The conductivity of the resistive sheets exponentially increases from a high resistive sheet at the front end to a low resistive back sheet. But the Jaumann absorbers due to their principle of operation tend to be bulky.

Dallenback layer was yet another earlier type of absorbers developed. It consists of a lossy layer backed by a perfect conductor. This construction is still

in use today, employing different types of lossy layers. Knott [5], has theoretically demonstrated with this type of construction to obtain maximum absorption, the layer thickness should be one quarter wavelength for a predominantly dielectric type material, while it is one half wavelength for a predominantly magnetic material. Absorbers which satisfy the above thickness criteria are commonly known as resonant absorbers, and due to the 'resonance' this type of absorbers display narrow band operation.

Many researchers [6-12], have adopted the resonant technique to design and develop single layer absorbers using different materials. Numerous ways and means were also investigated to improve the performance of resonant absorbers. Shimizu and Nishikata [6], have reported the development of a resonant absorber, in which the lossy layer comprises of a resistive cloth, made of conductive yarn wound in a grid pattern. It is further reported that the resistive cloth displays, susceptance as well as frequency characteristics. They have also done extensive experimentation [7], and have arrived at the optimum configuration for a carbon-rubber absorbers to operate as a narrow band absorber in X-Band. They have also investigated the effect of rolling speed and direction of rolling employed during manufacture of the rubber sheet. Which introduces anisotropy in the permittivity of the composite, and hence arrived at an optimum speed for rolling.

Mirtaheri et al [8,9], have experimentally demonstrated that addition of magnetic loss in the form of ferrites, will increase the operating bandwidth 4.6 times over the dielectric or carbon-rubber absorber. They have also noted that addition of magnetic loss will decrease the thickness of the absorber. The effect of magnetic loss on the bandwidth has also been observed by Natio et al [10], who have noted experimentally, that addition of ferrite in small relative weight ratio

(0.2%) of rubber, doubles the effective bandwidth of a carbon-rubber (weight ratio of 1:1) resonant absorber.

Dong et al [11], have obtained around 8% relative bandwidth, with a peak absorption of 20 dB, in a 1.4-1.6mm thick ferrite-rubber absorber operating in the X-Band. Natio and Mizumoto [12], have experimentally studied the effect of doping carbon in the order of 1-10% by volume of rubber, on the operating performance of a ferrite-rubber resonant type absorber. Their results indicate that addition of carbon in small quantities, will result in reduction in the thickness by 30%, for a given absorption-frequency bandwidth operation.

Natio [13] and Natio and Suetake [14], have experimentally observed that for a given ferrite-rubber composite, the matching frequency or the frequency at which absorption is maximum and matching thickness or the thickness at which maximum absorption is achieved are different and independent of each other.

Chino et al [15], have utilized, Zinc Titanate powder as the lossy material in a ferroelectric-rubber resonant absorber. Their results for 1.65mm thick absorber indicate a very narrow band (480 MHz) operation around 8.6 GHz.

Fernandez and Valenzuela [16], have described a graphical method for designing single layer absorbers, based on the loss angles in the material. Ahmad and Abdul Sada [17], have theoretically analyzed a single layer absorber, using the Maxwell's equations. Criteria's for Zero or near Zero reflection coefficient have been arrived for the single layer absorber.

Plas et al [18], have proposed a modification to the Salisbury type absorber to improve its performance. Where in the continuous resistive sheet is replaced

with one whose conducting material is deposited in appropriate geometrical patterns. They have utilized the spectral iteration technique proposed by Tsao and Mitra [19], to solve for the current distribution on the screen and hence the impedance of the periodic array of sheet conductors. Equivalent techniques are then applied in the subsequent design and analysis of the resulting absorber.

Vardhan et al [20], have exhaustively analyzed using a multiple scattering formulation, the effect of particles size and shape of the filler, the particulate distribution in the host media and the volume concentration of the filler in the host matrix, on the microwave attenuation properties of a ferrite-resin composite. Their theoretical results are in excellent agreement with the experimental work of Ueno and Ogaswara [21].

Kukimi et al [22] and Aoto et al [23,24], have analyzed the absorber, by representing it by an equivalent circuit, comprising of electric and magnetic nodes. Each element in the equivalent circuit includes the medium constants (permittivity and permeability) of the absorber. A transient analysis on the equivalent circuit employing numerical technique is then proposed to be made to determine the field components and hence analyze the absorber. In this approach the loss in the media is totally characterized by the magnetic loss tangent and the dielectric loss parameter is neglected.

Chiral inclusion (in the form of miniature conductive helices), which possess the property of circular dichorism at microwave frequency have been theoretically investigated by Jaggard and Enghata [25], Jaggard et al [26,27] and Basseri et al [28] for microwave absorptive applications. These chiral inclusion promise to aid the microwave absorption mechanism by changing the polarization of the wave inside

the media. The effect of chiral inclusion is thus to increase path length of the wave inside the absorber, or in other words an increase in the interaction time between the media and the wave. Thus increasing the absorption that can be derived from the absorber.

The effect of chiral inclusion in a dielectric media have also been analyzed theoretically as well as experimentally by Guire et al [29] and Lakhtakia et al [30] on microwave absorption of the composite material. They have reported the synthesis of a chiral-dielectric slab as an absorber which displays broad band characteristics both at normal as well as at oblique incident angles. The reported absorber displays broad band absorber characteristics over Ku-Band. Vardhan et al [31], have studied the effect of chiral inclusion in a magnetic media comprising of ferrite and resin composite. Researchers working on chirality have used modification to the Maxwells equations to account for the chirality parameter and then analyzed by transmission line theory [25-27]. While the extended boundary condition or T-matrix approach has been utilized in [28-31].

Pitman et al [32], have proposed another approach where in the electrical characteristics (permittivity and permeability) of the filler and binder are experimentally determined. Design and analysis of the resonant type absorber, is done using the data so collected. They have also described two techniques for the determination of the electrical parameters.

An extension of the dielectric based resonant absorber, is the graded dielectric absorber [2]. Where in an electric grading is obtained from a low concentration (lossy inclusion) at the front end to a very high concentration at the rear. The low loss front layer enables the abosrber to present an impedance

equal to that of free space and thus, improving the operating performance of resonant absorbers. The grading can be achieved in a single layer with increasing concentration of the dielectric in the layer, or by staggering a number of layers together. In order to obtain the required grading for matching with free space, the graded dielectric absorbers end up being bulky.

In order to achieve broader operating bandwidth, many workers [33-46], have employed a multilayered construction backed by a conductor. Fante and Michael [33], have proposed layering Salisbury type absorbers to obtain maximally flat response or absorption over a broad band. They have also arrived at a recurring relationship for the response as a function of the number of screens, appropriate values of permittivity and spacer thickness used to separate the screens. A similar approach is also suggested by Morris [34], who has employed an optimization technique to obtain specified input impedances at a number of frequencies, thereby increasing the bandwidth of operation. Optimization is performed for the dielectric constants of the spacers, number of interleaving screens, resistance and lumped capacitance of the screens. The capacitances are generated by using an array of discs.

Perni and Cohen [35], have employed a layered media approach to design and develop a multilayered absorber to operate over a wide angle of incidence. A highly lossy base layer is matched to free space by covering it with a number of dielectric layers. The dielectric constants of the layers are so designed to bend the incoming wave, such that it penetrates the lossy layer at near normal incidence.

Natio and Sueteki [36], have proposed a convergent impedance technique for the design of multilayered absorber at normal incidence. The multilayer is constructed

by layering the narrow band absorbers such that their characteristics impedances converges to a fixed value. In essence the technique aims to achieve a normalized impedance matching from 1 to 0.

Another approach put forth by Ono and Suzuki [37,38], for the design and analysis of multilayered absorber is to consider the construction, as a cascade of elements having different characteristics impedances. Then, starting with an impedance transformer, each element is replaced by its lossy dielectric counterpart for analysis purposes. The design analysis is extended to the case of oblique incidence by the same authors [39]. The work of Ono and Ikuta [40], is similar in nature, but they have extended the approach to the generalized case of oblique incidence.

Amin and James [41], have proposed layered structure models and have utilized an optimization technique for the design analysis of a multilayered absorber for broad band operation at normal incidence. For a minimum 10 dB absorption over 2-18 GHz operational bandwidth specification, they have optimized a four layered absorber with overall thickness of 7.5mm. The optimized parameters include type and amount of binder to be used in each layer, individual layer thickness, and the ferromagnetic resonance frequency for Cobalt substituted Barium Hexa ferrite, used as the lossy material. Results reported by the authors [41] indicate that they have achieved around 10 dB absorption from 8-18 GHz experimentally from the four layered structure.

The investigation of Kyung et al [42], shows that the centre frequency of absorption for a laminated ferrites/or ferrite-dielectric layers shifts between the frequency ranges in which the monolithic ferrites are useful. They have also shown

that the effective bandwidth of the laminate can arbitrarily be changed by employing different composition and thickness.

Miyazaki and Tanova [43], have employed the characteristic matrix method described in [44], to construct and analyze a multilayered absorber to provide 17 dB absorption around 11 GHz. The total thickness of the dielectric based absorber was 10.8mm. Their analysis shows that increase in the value of permittivity and conductivity with the direction of stratification improves the absorption performance.

Hatakeyama and Inui [45], have used a two layered construction for the design of a broad band absorber to operate over X-band and over ± 45 degree incidence angle. The two layers are formed with a ferrite-rubber sheet (1st layer) as the impedance transformer to match a low impedance (2nd layer) resonator to free space, obtained by dispersing short metallic fibres in a ferrite-rubber matrix. The absorber of total thickness 4.6mm experimentally behaves as a broad band absorber over X-Band, at rated oblique angle of incidence.

Varaprasad and Paramasweran [46], have employed a two layered construction to develop an absorbing coating that, provides 10-20 dB absorption in the X-Band. The lossy layer consists of 123 oxide conductor incorporated with short brass fibres in a resin matrix, a ferrite-resin second layer, matches the lossy layer to free space.

Sivigelj et al [47], have theoretically analyzed a two layered periodic arrangement of helices, for thier application as microwave absorbers. They have shown that as the pitch to length ratio decreases more number of layers of helix are required to maintain a minimum reflectivity level.

Ueno and Ogaswara [21], have investigated the Radio wave suppression by ferrites and have tabulated the values of permittivity and permeability as a function of frequency (1 - 10 GHz) for ferrites. Their investigation and the experimental work of Jha and Banthia [48], demonstrates that ferrites are strong candidate materials for microwave absorption. Yet another composite used in the design of resonant type absorber is Acetylene black carbon-rubber [49,50]. The experimental work by Hashimoto and Shimizu [51], indicate that the rolling process employed during manufacture of rubber sheet, results in anisotropy and that for a carbon-rubber absorber, the carbon particles tend to align themselves along the direction of rolling, leading to the principle direction of the imaginary part of permittivity being aligned along the direction.

Veinger et al [52], have experimentally demonstrated that absorption in magnetic-rubber type absorbers, not only depends on the type of magnetic filler employed but is also strongly influenced by the polymer properties as well, contrary to the belief that the polymer matrix acts only as a host dielectric binder.

2.3 MULTIPLE SCATTERING THEORY : A REVIEW

The effect of multiple scattering on the coherent wave are of great practical importance, in particular the dependance on concentration at wavelengths comparable to scatter-size. At very low concentration ($\leq 1\%$ by volume), multiple scattering can be neglected and each scatter can be treated as independent [53]. However, in our practical situations of metal filled polymers, where the concentration can be as high as 50%, the multiple scattering cannot be neglected.

Analytical closed form solutions for the scattering problem exists for only a limited class of objects for which the wave equation is separable. Further more if the object composition is complex, i.e., it is composed of dielectric and metallic material, the problem becomes more complicated. Over the last two decades, several numerical techniques have been developed to handle these problems. These techniques include for example, the Fredholm integral equation approach [54], various Moment methods [55-58], Finite difference time domain [59], Finite element [60-62], and Extended boundary condition method [63-65]. Some of these techniques are more suitable for implementation to certain size or shape and their computational requirements vary accordingly. An excellent discussion on some of these methods, their computational aspects and the limitation on their applicability can be found in [66-68].

If one limits himself to the three dimensional scatterer with axis of symmetry and attempts to consider the problem of multiple scattering of identical scatterers, then, the Extended Boundary Condition (EBC) method has the advantage of great flexibility. Since in the EBC method, the scattered field is computed without explicitly evaluating either the field inside the body or the field on the body's surface [69]. Which in fact implies restrictions on the shape of the body's surface. This restrictions are over come by the Waterman's T-matrix approach [70,71], to evaluate fields on the bodies, whose surface can have any arbitrary shape, under the null field principle.

Foldy [72], introduced the multiple scattering formulism either closing or truncating the resulting system of integral equations through the use of a

heuristic approximation, and obtained a closed form expression for the wave number of the coherent wave for the simple case of scant scatterers. Lax [73,74], developed an improved closure approximation through Quasi Crystalline Approximation (QCA), which involves the two-particle correlation function. Through careful analysis in a series of papers, Twersky [75-80], provided a much needed insight into the various orders of multiple scattering using different forms of pair-correlation functions. The analysis in reference [79,80] and the work of Tsang and Kong [81], is particularly interesting, in that they have used the scaled particle equations of a state of gas of hard spheres, to obtain improvements to the 'hole correction integral' through Virial expression and Percus-Yevick Approximation (P-YA) to the pair correlation function. The hole correction is characterized by the conditional probability equal to zero, within a hole of radius equal to the diameter of the scatterer and uniform distribution outside the 'hole'.

Recently, Vardhan et al and others [20, 82-88], have presented a multiple scattering formalism which lends itself to numerical computation for high frequencies of the incident plane wave as well as more realistic geometry for the inhomogeneties. The dynamic properties of composite media have been studied in [82] using an ensemble averaging. The ensemble averaging resulted in a hierarchy of equations for the average field with higher and higher order correlation functions. This hierarchy has been truncated using QCA of Lax [20,21] and in [82-85], only the hole correction is employed, which gave nonphysical results for higher concentrations [81]. For a dense distribution of scatterers, higher order statistics for the pair correlation derived under QCA, P-YA and the Self-Consistent Approximations (SCA) have been utilized in [20] along with Waterman's T-Matrix to arrive at the effective properties of the composite media.

The T-Matrix approach is employed in this work, as a tool to analyze and determine the effective properties of the absorbing media, via the multiple scattering formalism.

2.4 IMPEDANCE MATCHING TECHNIQUE : A REVIEW

Many research workers [34,35,36,45,46], have adopted the impedance matching technique to improve the performance of absorbers. Wherein the impedance matching is achieved by layering a number of layers, whose electrical parameters are so designed, so that they present an impedance equal to that of free space at the free space-absorber interface. In particular the work of Hatakeyama and Inui [45] is interesting, due to the fact that, they have utilized only two layers to realize an composite absorber that provides above 20 dB absorption over complete X-Band at $\pm 45^\circ$ angle incidence. The first layer, a highly lossy layer is impedance matched to free space by a second layer-an impedance transformer. Both the layers are based on using ferrite/rubber composites. The only draw back of such a design, is the large thickness of the absorber, which consequently makes the absorber to be very heavy.

The work of Plas et al [18], is an indicator to the fact that conducting material when deposited in appropriate geometrical patterns will improve the performance of absorbers. Apart from this work, conducting screen perforated with apertures or its complementary screen, a free standing array of structures have not been found reported in literature, to the best of the author's knowledge, in the context of impedance matching of microwave absorbers till now.

However, such screens have been extensively used for various applications. For examples as an artificial dielectric [89], antenna radome [90-93], and as microwave

frequency selective surfaces [94-96]. Various techniques [97-112], have been adopted to analyze free standing as well as dielectric backed screens. The moment method and the spectral analysis method are the most favored techniques to analyze such screens [103]. The effect of truncating the array is analyzed in [103, 114]. But the work of Langley and Drinkwater, and others [110-113], is of particular interest. Their equivalent circuit approach, being simple lends itself rather well to our concept of impedance matching.

Various geometrical structures analyzed in this context are; Circular patch or aperture [91,93]; Square patch or aperture [91,93]; Dipoles [99]; Crossed dipoles [101]; Jerusalem cross [102,110]; Annular rings or Circular loops [109]; Single square loop [111]; and Double square loops [112]. In the context of impedance matching, a geometry that produces a response which is relatively insensitive to the angle of incidence of illuminating field, is highly desired. The Jerusalem cross geometry has been found [102,103] to be one of the promising candidates satisfying this criterion.

Research work in the area of design and development of absorbers is thus largely experimental, and hence empirical. An unsatisfactory aspect of the empirical approach is the large number of experimental parameters, which must be tested in search of an optimal design. There is often no assurance that the final design so obtained is the best. Further attempts at the design and development of broad band absorbers has resulted in either the absorber being bulky or complicated structure, difficult to realize practically. It is advantageous to approach the absorber design problem systematically through, modeling and application of mathematical optimization. The outcome of such an approach will indicate what properties to look for to achieve an optimized design for a given application.

The theoretical design and development of absorbers, single layer, multilayer or composite absorbers in this work are modeled on the simple concept of impedance matching in a microwave transmission line.

2.5 STATEMENT OF THE PROBLEM

In the design and analysis of absorbers the following specifications were set, along with a specified constraint on the thickness of the absorber: (i) Narrow Band absorbers, minimum 15dB absorption over a 1 GHz., bandwidth; and (ii) Broad band absorbers, minimum 10dB absorption over a operational bandwidth ≥ 2 GHz.

- ▶ A generalized design approach is formulated with Cobalt-substituted Barium Hexa Ferrite (Co-BHF) as the lossy material for the design and development of broad band absorbers. Broad banding is achieved by combining the material and thickness absorption effects in the absorber. Broad band absorbers to operate over each of S-; C-; X- and Ku-Bands are theoretically designed. The design formulation has been practically verified by fabricating of an absorber for broad band operation over Ku-band, with a constraint of 2mm on the thickness of the absorber.
- ▶ A mathematical model for the theoretical analysis and design of microwave absorbers has been formulated, based on the evaluation of the overall reflection coefficient of the absorber. The design criteria for two types namely, matched and resonant absorbers are established. Absorbers one each for matched (broad band operation over Ku-Band) and resonant (narrow band operation in X-Band) criteria with an added constraint on thickness of 2mm were designed and fabricated.
- ▶ For a multilayered absorber, generalized design equations have been arrived

at, for a plane wave at arbitrary angle of incidence, as a function of number of layers, concentration and properties of the lossy material in each layer, individual layer thickness, and the overall thickness absorber.

▶ Waterman's T-matrix approach has been utilized in a multiple scattering formulation, to determine the bulk or effective propagation constant for the composite absorbing medium, as a function of particle (scatterer) size and shape, volume concentration of the lossy material, orientation and position of the scatterer in the binder or host matrix. Employing the proposed model, the optimum configuration for a ferrite-rubber composite, such as size of the spherical particles, volume concentration of the ferrite and thickness of the absorber were determined for broad band operation over X-Band within 3mm thickness limitation.

▶ An impedance matching technique is formulated to overcome the mismatching (at the free space-absorber interface) problem associated with thin planar absorbers. A thin conducting screen perforated with an array of structures has been employed as the Impedance Matching Layer. A simple equivalent circuit approach is formulated for the design analysis of the composite structure formed by incorporating the impedance matching layer at the front end of the absorber. Both narrow as well as broad band absorbers are developed using this technique, within a thickness constraint of 2mm.

▶ A detailed experimental study has been done, to identify the type and amount of aids that have to be employed to obtain uniform distribution of the filler particles in the host media.

CHAPTER III

A GENERALIZED APPROACH FOR THE DESIGN OF BROAD BAND MICROWAVE ABSORBERS

3.1 INTRODUCTION

In this chapter the theoretical as well as the practical design of a single layer microwave absorber which gives more than 10 dB absorption in a desired frequency band, is discussed.

Single layer thin sheet absorbers are generally made by dispersing a lossy material in a suitable binder. The peak absorption obtained depends on the thickness 'd' (called resonant absorption), as well as on the properties of the lossy material (called material absorption) used. The resonant and material absorption effects are independent of each other. It was formulated that by combining these two independent absorption effects, with the aid of a suitable lossy material, the overall absorption bandwidth will be considerably increased, at normal incidences of the electromagnetic wave.

In the search of a lossy material through which the proposed broad banding technique could be practically implemented, the work by Amin and James [41], on Cobalt substituted Barium Hexa Ferrite (Co-BHF) was found interesting. Co-BHF, had earlier been reported [115] to give significant values of μ_r , the relative complex permeability at microwave frequencies. They provide the additional advantage of controlling the Ferromagnetic resonance frequency (f_r) at any desired frequency between 2 to 46 GHz. It is found [41,116], that Co-BHF with $\mu_r \approx 5$ gives excellent

absorption at ferromagnetic resonance, and has been used as the lossy material in the analysis.

The computer simulated results for a single layer absorber of thickness 7.5mm, (curve 'a' of Fig 5, in [41]) is reproduced as curve 'a' in Fig 3.1. The absorber was designed by dispersing Co-BHF with a ferromagnetic resonance frequency (f_r) of 7.5 GHz., in rubber. The first peak is due to the quarter wavelength effect (resonant absorption) while the second is due to the f_r of Co-BHF (material absorption). The order of the two peaks are determined by the choice of the material constants (f_r and thickness). Employing the proposed combination of the two effects, i.e., for the same f_r of 7.5 GHz., and a quarter wavelength thickness (at 7.5GHz) of 1.51mm the simulated results are plotted as curve 'b' in Fig 3.1. If a minimum 10dB absorption is taken as a criterion for bandwidth considerations then the large increment in the bandwidth can be observed from Fig 3.1, thus justifying our formulation.

3.2 THEORY

Consider an infinitely conducting plane coated with a uniform layer of material (Absorber) of thickness d , whose complex relative permittivity and permeability are given by ϵ_r and μ_r respectively. Let a uniform plane wave travelling in the positive Z direction, be incident on the surface of the absorber at an angle of θ_0 as shown in the Fig 3.2. If the interface point 'o' is chosen as the origin of a co-ordinate axis system, then the incident and reflected field (E_i and E_r) in different regions can be written as

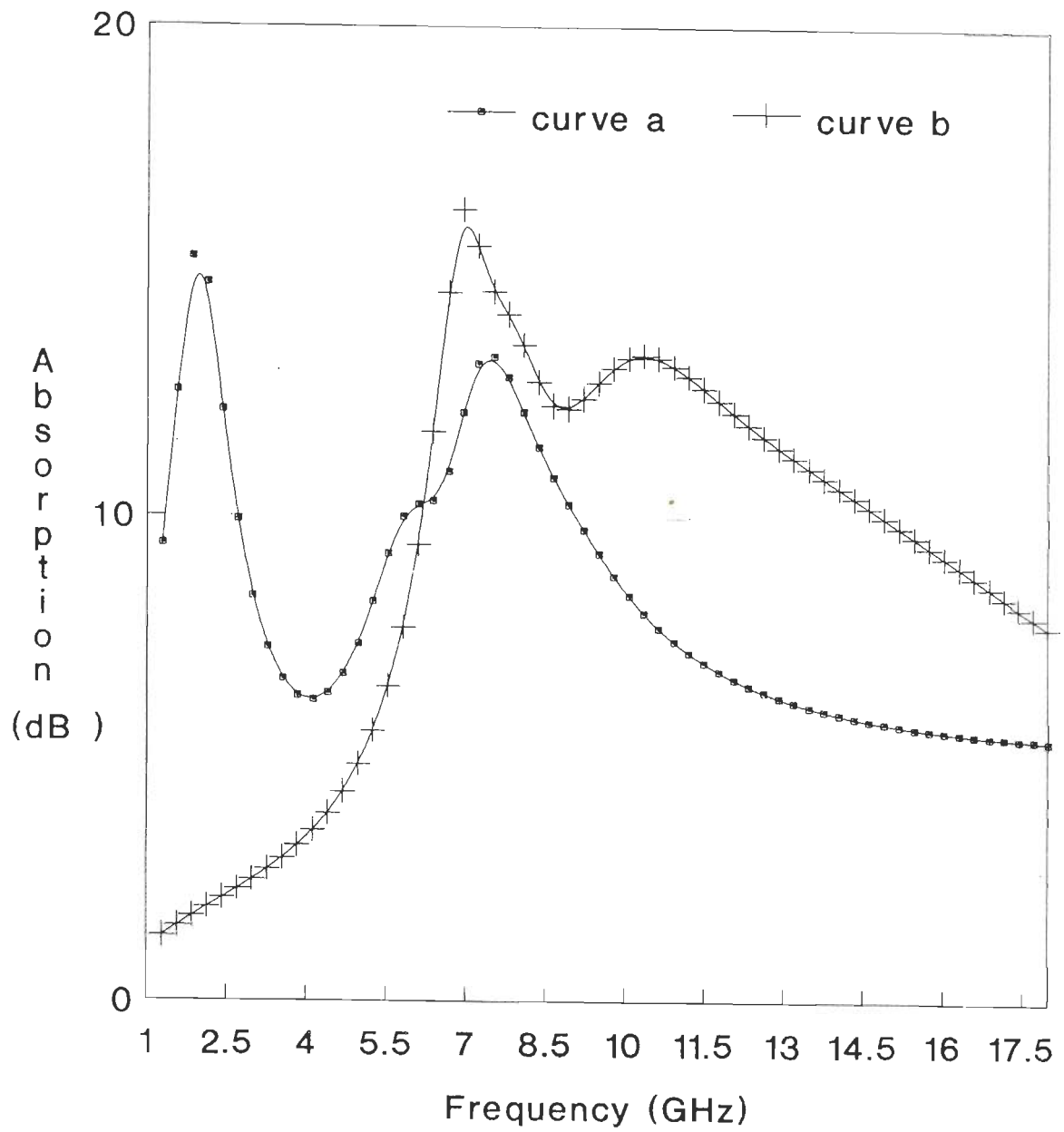


Fig 3.1 Computer simulated results to show the increment in the bandwidth of a single layer absorber.

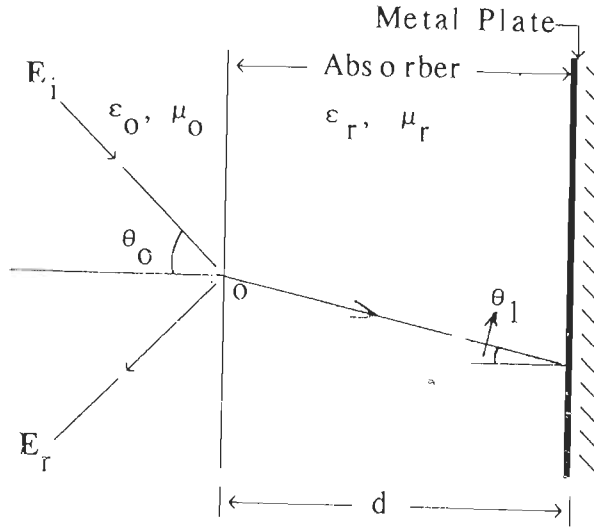


Fig 3.2 Geometry of a Single Layer absorber.

$$E_{ii} = a_{ii} e^{j\{\omega t - k_j(x \sin\theta_i + z \sin\theta_i)\}} \quad 3.1$$

$$E_{ir} = b_{ir} e^{j\{\omega t - k_j(x \sin\theta_i - z \sin\theta_i)\}} \quad 3.2$$

where a_i 's and b_i 's are the amplitudes of the incident and reflected fields, ω the angular frequency, k_i the complex wave number and θ the angle of incidence. Then the reflection coefficient R_{jo} , at the front surface of the absorber is given by [117]

$$R_{jo} = (Z_{jm} - 1)/(Z_{jm} + 1) \quad 3.3$$

where j stands for the type of polarization of the incident wave. Thus, if the incident field is polarized perpendicular to the plane of incidence, the impedance parameter Z_{jm} , is given by

$$Z_{nm} = \frac{\mu_r \cos\theta_1}{N \cos\theta_0} \tanh(kd \cos\theta_1) \quad 3.3a$$

where, $\sin\theta_0 = N \sin\theta_1$ and $N = \sqrt{\epsilon_r \mu_r}$.

Further, if the incident field is polarized parallel to the plane of incidence, the impedance parameter Z_{pm} is given by

$$Z_{pm} = \frac{\mu_r \cos\theta_0}{N \cos\theta_1} \tanh(kd \cos\theta_1) \quad 3.4b$$

For normal incidence we have, $Z_{nm} = Z_{pm} = Z_m$ and is given by

$$Z_m = \sqrt{\mu_r/\epsilon_r} \tanh(kd) \quad 3.5$$

The frequency dispersion characteristics of μ_r for Co-BHF, can be represented as [41]

$$\mu_r' = \frac{4.0}{\sqrt{1 + (f-f_r)^2}} 2^{\cosh \frac{2(f-f_r)}{f+f_r/2}} \quad 3.6a$$

$$\text{and } \mu_r'' = \mu_r'(f-1.0) \quad 3.6b$$

where f and f_r are in GHz.

The maximum available value of $\epsilon_r = 10-j1$ for the Co-BHF and $\epsilon_r = 5-j0.2$ for the rubber were assumed. The values of permittivity and permeability is diluted by the addition of rubber as the binder and can be computed, using the Lichtenecker [118] equations as,

$$\left. \begin{aligned} \log |x_e| &= \sum_1^N V_i \log |x_i| \\ \tan\delta_{x_e} &= \sum_1^N V_i \tan\delta_{x_i} \\ \sum_1^N V_i &= 1 \end{aligned} \right\} \quad 3.6c$$

where x can either be ϵ_r or μ_r , V_i the volume fraction of the i^{th} inclusion, $\tan\delta = x''/x'$ and x_e is the equivalent x of the composite. Thus if individual values of ϵ_r (or μ_r) of the binder and filler are known, then using the above equation the equivalent values of ϵ_r (or μ_r) can be determined for the composite medium as a function of the volume concentration of filler inclusion.

The thickness of the Absorber will then be given as

$$d = \lambda_r / [4\text{real}(\sqrt{\epsilon\mu})] \quad 3.7$$

where λ_r is the wavelength at f_r , ϵ and μ are the equivalent permittivity and permeability of the ferrite - rubber composite material.

The absorption can then be computed from the relation,

$$A = -20\log_{10}|R_{j0}| \quad 3.8$$

A computer code in FORTRAN was written to compute the absorption using Eq.'s (3.5) to (3.8). The program (abs.for) listing is given in Appendix 3.1

3.3 DESIGN EXAMPLES FOR SINGLE LAYER BROADBAND ABSORBERS

The specifications that was chosen was a minimum 10dB absorption over S-; C-; X-; or Ku-Band. In addition a constraint on the thickness of the absorber was also set as 5mm (in S- and C-Bands) and 3mm (in X- and Ku-Bands). Since the specifications was itself non-unique, in the sense that beyond a given level the absorption could fluctuate in an unspecified manner, it is advantageous to approach the absorber design through the application of a mathematical optimization. Since our optimization problem is a multi variable one with constraints on the variables, an existing multi variable-constraint optimization subroutine based on the flexible tolerance [119] method was utilized. The listing of the routine is given in Appendix I.

The above multivariable optimization method does not lead to unique solution in practice, due to the non-uniqueness of the specifications. In practice the routine would have to be run several times with different numerical weights, so that a variety of possible solutions could be inspected. Since some degree of

inspection is involved, it is important to investigate whether, the design data can be chosen entirely by inspection. Hence given a specification, it becomes imperative to select the design parameters by trial and error inspection of the simulated results given by Eq.'s (3.5)-(3.8), along with an iterative application of the optimization process.

For the design problem on hand, the optimization subroutine was run several times with different numerical weights along with Eq.'s (3.5)-(3.8) and the optimized values for f_r and ferrite:rubber ratio (volume) were selected as listed in Table 3.1. The computer simulated absorption characteristics for the designed absorbers whose design parameters are listed in Table 3.1 are plotted in Fig 3.3.

Table 3.1

Band	Frequency range (GHz)	f_r (GHz)	Ferrite : binder	Thickness (mm)
S	2 - 4	2.1	55:45%	6.72
C	4 - 8	4.44	55:45%	3.9
X	8 - 12.4	8.4	48:52	2.5
Ku	12.4 - 18	12.75	45:55	1.8

The designed thickness for the absorber in S-Band has violated the set constraint, this is due to the practical limitation on the amount of filler that can be loaded into the silicone rubber (binder) used. The thickness can be brought within the limitations by adding small amount of carbon [12] along with the filler.

3.4 EXPERIMENTAL RESULTS

Due to the practical limitation of fabricating higher thickness sheets at this juncture, only the fabrication of the absorber sheet for operation over Ku-band was

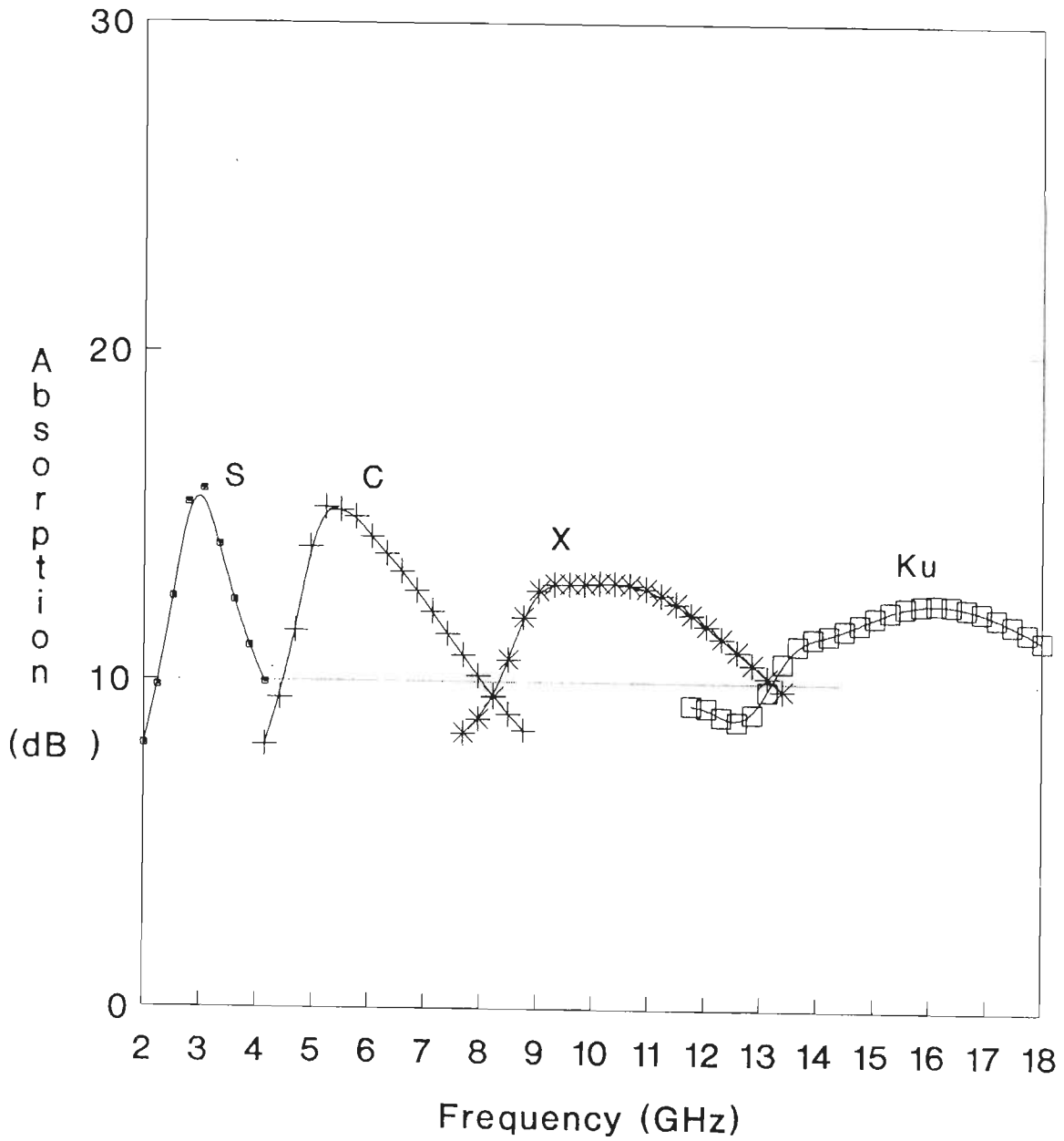


Fig 3.3 Theoretically simulated absorption curves for broad band absorbers.
(Design details in Table 3.1)

taken up [120, 121]. The Co-BHF was prepared employing conventional ceramic procedure for preparing metal-oxide powders. The particle size was controlled to less than 15 microns, by repeatedly grinding in ball mill and then sieving the powder through an appropriate mesh screen. The ferrite-rubber in the required ratio of 45%:55% was mixed in a two roll mill and fabricated into a sheet of dimension 300 X 300 X 1.8mm by hot pressing.

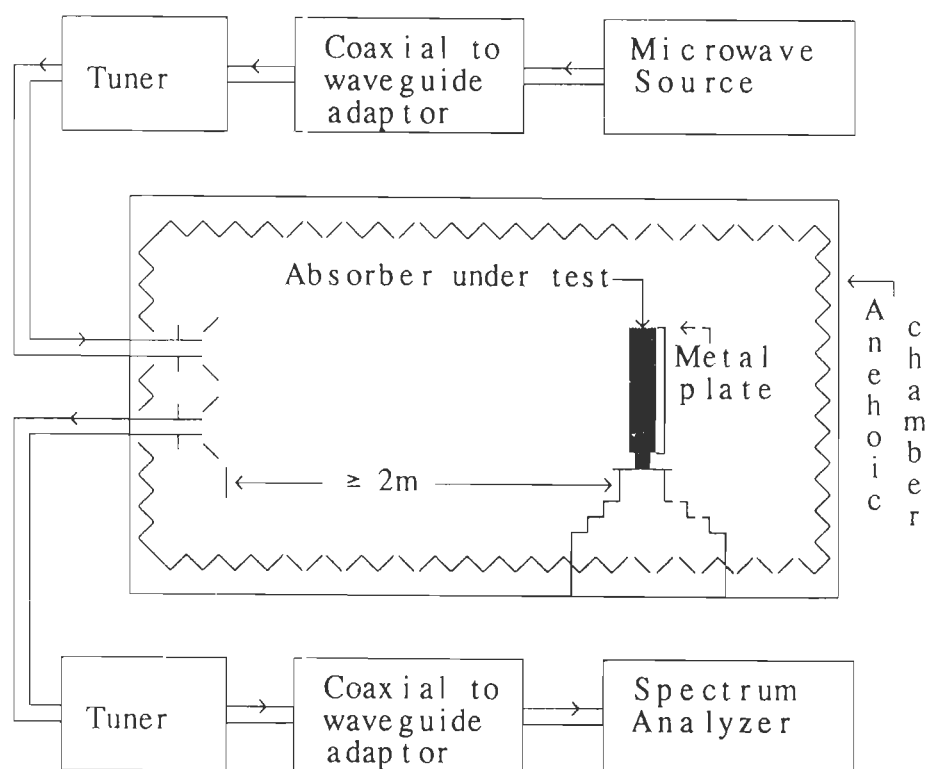


Fig 3.4 Experimental set up employed to determine the absorption characteristics of the absorbers.

A free space bistatic measurement setup operating in the frequency range of 8 - 18 GHz. as shown in Fig 3.4 was employed to measure $|R_{no}|$ and $|R_{po}|$. The rectangular to waveguide and waveguide to rectangular adaptors are used as mode transitions for the bistatic measurement setup. Two incident waves namely E_p and E_n can be realized by appropriately rotating the transmitting and receiving antennas

along with the mode transitions with respect to the plane of the absorber sample. For measurement at normal incidence the two horn's were placed side by side to realize a quasi monostatic measurement setup. Further it was ensured that there was no direct coupling between the antennas.

The reflectivity of the planar absorber and the reflectivity of a metal plate of the same dimensions as that of the absorber were measured. The absorption provided by the absorber is the difference of the two measurements. The absorption characteristics obtained for normal incidence are plotted in Fig 3.5.

3.5 CONCLUSION

A generalized approach for the theoretical design and analysis of a single layer absorber with broad band characteristics is discussed in this chapter. Generalized because one need not search for different approaches /materials while designing broad band absorbers for various frequency band. One needs to vary only the concentration of the filler in the binder to achieve broad band operation.

Absorbers to give a minimum 10dB absorption over S,C,X or Ku-bands respectively have been theoretically designed. The absorber for operation over Ku-band has been fabricated and tested. The experimentally obtained absorptions follow the same pattern and agree closely with the theoretical results, thus validating the proposed design approach. As can be observed from the Fig 3.5 a minimum of 8 dB absorption has been achieved over the desired frequency band, which is 2 dB less than the desired value. The experimentally obtained absorptions are 2-3dB less than the theoretically predicted values, which could be due to the practical limitation of the fabrication process.

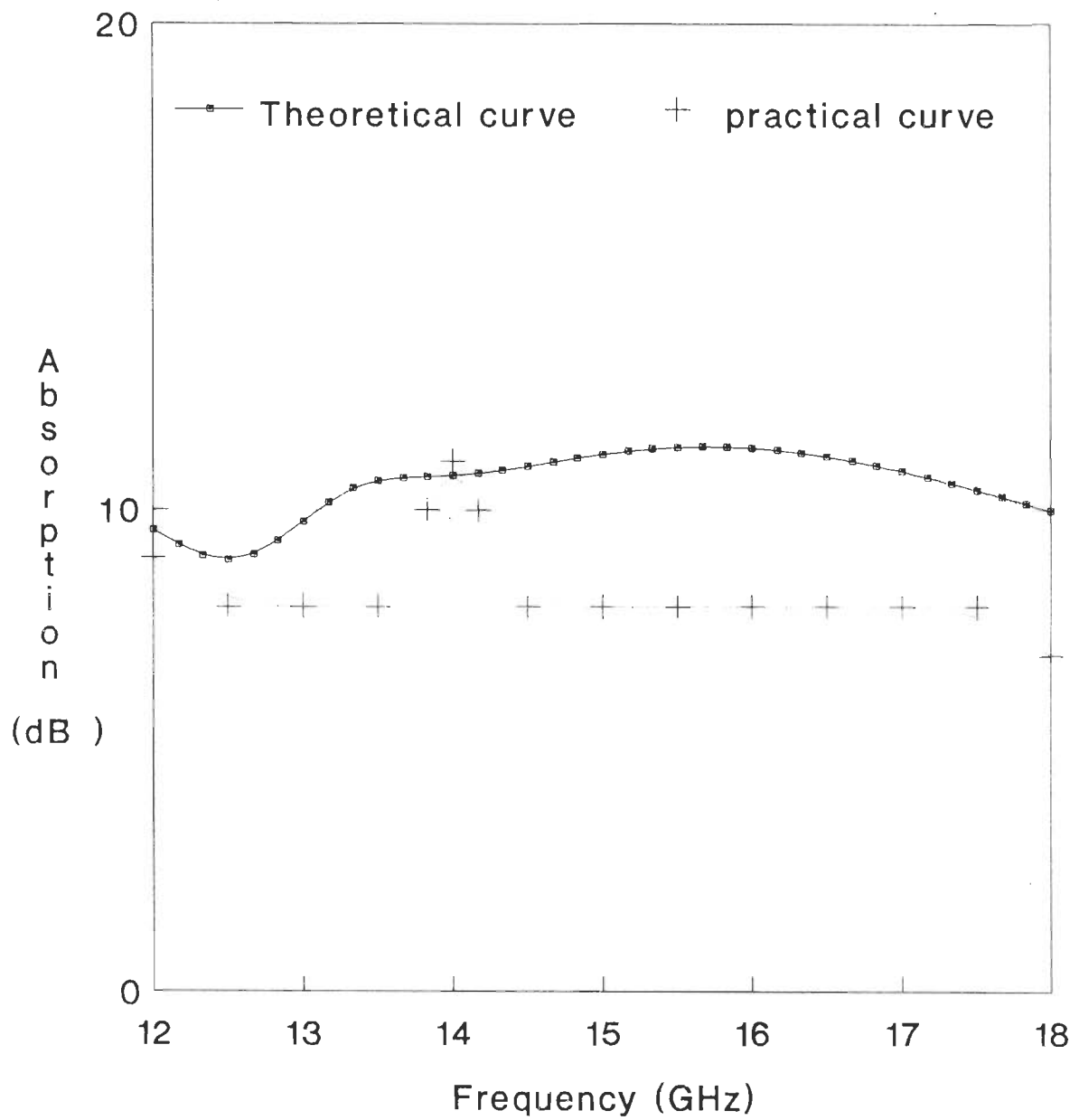


Fig 3.5 Absorption characteristics for the designed and fabricated (Co-BHF)-rubber absorber.

APPENDIX 3.1

```

c  abs.for
c  Program to compute the absorption using Eq.3.5-3.8

c  pf(1), volume fraction of filler
c  pf(2), volume fraction of binder
c  pf(1) + pf(2) = 1
c  fr, ferromagnetic resonance of Co-BHF (ferrite) in GHz
c  al, thickness of absorber in mm.
c  epr(1,2) and epi(1,2), real and imaginary part of
c  permittivity (filler, binder)
complex ep(10),e,u,q,b,a8,a9,qd,qs,c1,ak,b1,xy, up(10)
dimension af(250),epr(10),epi(10),pf(10)
open(unit=6,file='abs.in.in',status='old')
open(unit=5,file='abs.out',status='new')
fh = 20.
fl = 7.
dinc = abs(fh-fl)/60.0
pi=3.1415927
u0 = 12.56637E-07
e0 = 8.854E-12
z0 = 377.0
read(6,*)(pf(i),i=1,2)
read(6,*)fr
read(6,*)al
read(6,*)(epr(i),epi(i),i=1,2)
af(0) = fl-dinc
c1=(0.0,1.0)
do 10 i = 1,2
ep(i) = cmplx(epr(i),-epi(i))
10 continue
call eque(ep,pf,xy)
s1=real(xy)
s2=aimag(xy)
e = xy * e0
d = al/1000.
do 50 k = 1,60
af(k) = af(k-1) + dinc
fl = af(k)
call perm(fl,fr,xy)
up(1) = xy
up(2) = cmplx(1.0,0.0)
call eque(up,pf,xy)
u = xy * u0
ak = 2. * pi * af(k) * 1.e+09 * csqrt(e * u)
a8 =-c1*2.0*ak * d
q = cexp(a8)
qd = 1.0 - q
qs = 1.0 + q
b1 = (qd/qs)*csqrt(u/e)

```

```

xy = (b1-z0)/(b1+z0)
r = cabs(xy)
da = -20.0 * alog10(r)
write(5,1)af(k),da
write(*,1)af(k),da
1   format(2f10.2)
50  continue
    stop
    end
    subroutine eque(u1,pf,xa)
c   subroutine eque to compute the equivalent
c   e/u based on Lichenecker's equation (Eq. 3.6c)
    complex xa,u1(10)
    dimension pf(10)
    xa = 0.0
    pi = 0.0
    ai = 0.0
    tx = 0.0
    do 100 i = 1,2
    as = cabs(u1(i))
    as1 = abs(as)
    ai = ai + pf(i) * log(as1)
    b1 = aimag(u1(i))
    b2 = real(u1(i))
    tnd = b1/b2
    tx = tx + pf(i) * tnd
    pi = pi + pf(i)
100 continue
    del = atan(tx)
    as = exp(ai)
    b2 = as * cos(del)
    b1 = as * sin(del)
    xa = cmplx(b2,b1)
    return
    end

c   subroutine to compute the permeability (Eq.3.6a & b)
    subroutine perm(f1,fsr,us)
    complex us
    us = 0.0
    s1 = 1.0
    afc = f1 + 1.0
    do 525 j1=1,2
    afc=afc-1.0
    a1 = afc - fsr
    a2 = fsr + afc/2.0
    a3 = 2.0 * a1/a2
    ch = cosh(a3)
    a4 = a1*a1
    a5 = sqrt(s1 + a4)
    xy = 4.0 * ch/a5
    if (j1.eq.1) then

```

```
    ur = xy
    else
    ui = xy
    endif
525 continue
    us = cmplx(ur,-ui)
    return
end
```

Listing of a typical input file (abs.in)

```
.45,.55
12.63
1.8
10.0,1.0,5.0,0.2
```

CHAPTER IV

DESIGN CRITERIA FOR MICROWAVE ABSORBERS

4.1 INTRODUCTION

The main principle behind the approach discussed in this chapter, is based on using the parameters of the overall reflection coefficient, in arriving at the design criterions for absorbers. Two types of absorbers are considered theoretically and their performance verified experimentally. The first one (usable as a RCS reducer) is designed such that the reflection coefficient between free space and the coating is zero. The second (usable as a interference suppressor) is designed such that the overall reflection coefficient vanishes.

4.2 THEORY

The coating of a planar target surface with a thin absorber of thickness 'd', would constitute a three layered system with interfaces at air-absorber (1st interface) and absorber-target surface (2nd interface).

Let a transverse electromagnetic wave propagating in the Z-direction be incident at an arbitrary angle θ_i on the surface of the absorber. Part of this wave would be reflected back, giving rise to the primary reflected wave and part of it would be refracted into the absorber triggering a series of secondary reflected waves [122,123] from the absorber surface as shown in the Fig. 4.1.

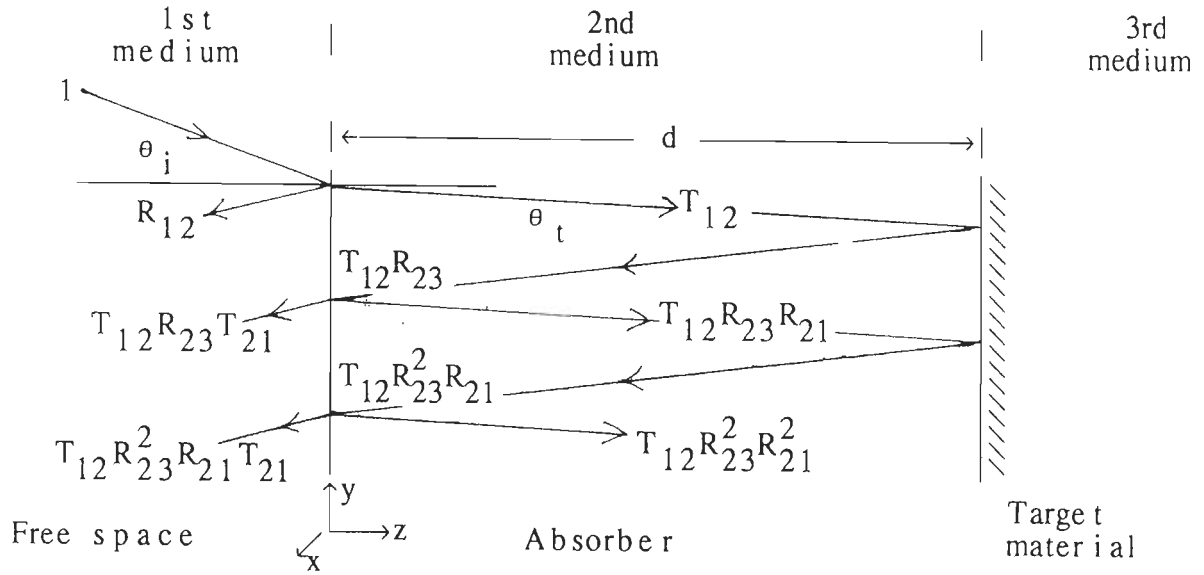


Fig 4.1 Geometry Of The Problem

Our objective is to minimize or eliminate the overall reflection coefficient, which is the ratio of the algebraic sum of all reflected field intensities to the incident field intensity. To this end we proceed as follows :

The electric field intensity at a distance 'z' from the 1st interface in the absorber media can be written as [124]

$$\mathbf{E} = E_m e^{j(\omega t - kz)} \quad 4.1$$

where E_m the amplitude of the field in the medium and

$$k = (2\pi/\lambda)\sqrt{\epsilon_r \mu_r} \quad 4.2$$

is the wave number in the medium, λ the free space wavelength. $\epsilon_r = \epsilon_r' - j\epsilon_r''$ and $\mu_r = \mu_r' - j\mu_r''$ are the complex relative permittivity and permeability of the absorber,

$$\begin{aligned} \sqrt{\epsilon_r \mu_r} &= \sqrt{\epsilon_r' \mu_r' - \epsilon_r'' \mu_r'' - j(\epsilon_r' \mu_r'' + \epsilon_r'' \mu_r')} \\ &= n - jp \end{aligned} \quad 4.3a$$

where n and p are the refractive index and absorption index.

The distance parameter z , can be expressed as

$$z = \frac{d}{\cos \theta_t} \quad 4.3b$$

where,

$$\cos \theta_t = \sqrt{\frac{1}{\{1 - [\sin(\theta_i)/n]^2\}}} \quad 4.3c$$

and

$$n = \frac{\sin(\theta_i)}{\sin(\theta_t)} \quad 4.3d$$

Substituting Eq.'s (4.2) and (4.3) into (4.1), we obtain the expression for the wave propagation in the absorber media as

$$E = E_m [e^{(2\pi/\lambda)(-\alpha_1 + j\beta_1)d}] e^{j\omega t} \quad 4.4a$$

where,

$$\alpha_1 = pn/\xi, \quad 4.4b$$

$$\beta_1 = n^2/\xi, \quad 4.4c$$

and

$$\xi = \sqrt{n^2 - \sin^2(\theta_i)} \quad 4.4d$$

The field intensity E_{1a} at the 2nd interface can now be expressed (with time dependence suppressed) as

$$E_{1a} = T_{12} E_o [e^{(2\pi/\lambda)(-\alpha_1 + j\beta_1)d}] \quad 4.5$$

where T_{12} is the transmission coefficient at the 1st interface.

In order to remove the dependence on polarization within the absorbing media we impose the condition given by Crispin [117] as

$$n \gg 1 \quad 4.6$$

physically this assumption means that the wave inside the absorber is travelling in a direction, which is normal/near normal to the surface. With this restriction, $n^2 \gg \sin^2(\theta_i)$ and thus from Eq. (4.4d) $\xi = n$ and hence $\alpha_1 = p$; $\beta_1 = n$. Using these we define two new variables α and β as

$$\alpha = 4\pi dp/\lambda = 2(2\pi d/\lambda)\alpha_1 \quad 4.7a$$

and

$$\beta = 4\pi dn/\lambda = 2(2\pi d/\lambda)\beta_1 \quad 4.7b$$

The field intensity E_{1b} at the 1st interface using Eq. (4.5) and (4.7) can be written as

$$E_{1b} = R_{23}T_{12}E_0e^{-\alpha+j\beta} \quad 4.8$$

where R_{23} is the reflection coefficient at the 2nd interface.

E_{r2} , the first of the several secondary reflected waves from the absorber surface is given by $E_{r2} = E_{1b} \cdot T_{21}$, T_{21} the transmission coefficient due to the interface from medium 2 to medium 1; or

$$E_{r2} = R_{23}T_{21}T_{12}E_0e^{-\alpha+j\beta} \quad 4.9$$

But

$$1 + R_{12} = T_{12} \quad \text{and} \quad R_{12} = -R_{21}$$

hence $T_{21} \cdot T_{12} = 1 - R_{12}^2$ using this in Eq. (4.9) we have

$$E_{r2} = R_{23}(1 - R_{12}^2)E_0e^{-\alpha+j\beta} \quad 4.10$$

Similarly we obtain E_{r3} , the second of secondary reflected wave as

$$E_{r3} = -R_{12} \cdot R_{23}^2(1 - R_{12}^2)E_0 \cdot e^{2(-\alpha+j\beta)}$$

or in general the higher numbered secondary reflected waves can be represented by

$$E_{rN} = (-1)^N R_{12}^{N-2} R_{23}^{N-1} (1 - R_{12}^2) E_0 e^{(N-1)(-\alpha+j\beta)} \quad N \geq 3, \dots, N \quad 4.11$$

The total reflected field can then be written as

$$E_r = E_0 \left[R_{12} + (1 - R_{12}^2) \sum_{N=2}^N (-1)^N \cdot R_{12}^{N-2} \cdot R_{23}^{N-1} \cdot e^{(N-1)(-\alpha+j\beta)} \right] \quad 4.12$$

The overall reflection coefficient is $R = E_r/E_0$, i.e.,

$$R = R_{12} + (1 - R_{12}^2) \cdot \sum_{N=2}^N (-1)^N \cdot R_{12}^{N-2} \cdot R_{23}^{N-1} \cdot e^{(N-1)(-\alpha+j\beta)}$$

Invoking the binomial theorem over the summation, we obtain

$$R \cong R_{12} + (1 - R_{12}^2) [R_{23} e^{(-\alpha+j\beta)}] / [1 + R_{12} R_{23} e^{(-\alpha+j\beta)}]$$

$$= [R_{12} + e^{(-\alpha+j\beta)}]/[1 + R_{12}R_{23} e^{(-\alpha+j\beta)}] \quad 4.13$$

If medium 3 is considered to be a good conductor, then the above expression simplifies to

$$R = \frac{R_{12} + e^{(-\alpha+j\beta)}}{1 + R_{12} e^{(-\alpha+j\beta)}} \quad 4.14$$

then the reflection loss or absorption provided by the absorber is given by

$$A = -20\log_{10}|R| \quad 4.15$$

It can be observed from expression (4.14), that the major contribution to the overall reflection coefficient R , is the primary reflected wave. Hence (i) the overall reflection coefficient can be reduced by eliminating the primary reflected wave, leading to a matched absorber and (ii) the overall reflection itself can be eliminated leading to a resonant absorber.

4.2.1 DESIGN CRITERIA FOR A MATCHED ABSORBER

It is desired that, for matched absorber $R_{12} = 0$;

and R_{12} is given by

$$R_{12} = E_{r1}/E_o = (\eta_2 - \eta_1)/(\eta_2 + \eta_1) \quad 4.16$$

where $\eta_1 = (\mu_o/\epsilon_o)^{1/2}$ and $\eta_2 = (\mu_o\mu_r/\epsilon_o\epsilon_r)^{1/2}$ are the intrinsic impedance of medium 1 and medium 2 respectively. Substituting these values in Eq. (4.16), we obtain the matching conditions as

$$\mu_r = \epsilon_r \quad 4.17$$

The overall reflection coefficient can also be written in terms of p and n as

$$R_{12} = \frac{[\mu_r - (n - jp)]}{[\mu_r + (n + jp)]} \quad 4.18a$$

for $R_{12} = 0$; we have

$$\mu_r = \mu_r' - j\mu_r'' = n - jp \quad 4.18b$$

thus we obtain another set of condition for the matching layer as

$$n = \mu_r' \quad 4.19a$$

$$\text{and } p = \mu_r'' \quad 4.19b$$

The absence of ϵ_r terms in the above condition for a matched absorber explicitly implies that, for a matched absorber, the absorption index and refractive index are functions of permeability only. Hence a predominantly magnetic type of material will have to be employed to realize a matched absorber in practice.

The overall reflection coefficient is then given by

$$R = e^{(-\alpha + j\beta)}$$

$$\text{and } |R| = e^{-\alpha} \quad 4.20a$$

For the condition obtained in Eq. (4.17) and layer thickness thin, we have [117]

$$2\pi d/\lambda = -j/\mu_r$$

using Eq. (4.18b) in the above Eq., we obtain an expression for the thickness of the matched absorber as

$$d = \lambda/(2\pi p) \quad 4.20b$$

Thus the overall reflection coefficient can be further reduced by making α larger or from Eq. (4.7a) increasing p , the absorption index.

4.2.2 DESIGN CRITERIA FOR A RESONANT ABSORBER

The resonant absorber is desired to provide zero reflected signal or $R = 0$; Hence from Eq. (4.14), we have

$$R_{12} = -e^{(-\alpha + j\beta)} = e^{-\alpha + j(\beta - \pi)} \quad 4.21$$

$$\text{Also, } |R_{12}| = e^{-\alpha} \quad 4.22a$$

$$\text{and phase, } \angle R_{12} = \beta - \pi = \delta \quad 4.22b$$

For most materials in the microwave frequency region, $\epsilon_r' \gg \epsilon_r''$ and $\mu_r' \gg \mu_r''$, hence $\epsilon_r \cong \epsilon_r'$ and $\mu_r \cong \mu_r'$, then R_{12} is a real constant, this implies that $\delta = 0$ or $\beta = \pi$.

From Eq.s (4.18a) and (4.22a), we obtain

$$\alpha = \frac{1}{2} \ln \left[\frac{(\mu_r + n)^2 + p^2}{(\mu_r - n)^2 + p^2} \right] \quad 4.23$$

substituting the value of α from Eq. (4.7a) in (4.23), we obtain the amplitude condition for the resonant absorber as given by

$$d = (\lambda/8\pi p) \ln \left[\frac{(\mu_r + n)^2 + p^2}{(\mu_r - n)^2 + p^2} \right] \quad 4.24$$

and for $\delta = 0$; Using Eq. (4.7b) we obtain the phase condition for the resonant absorber to be given by

$$d = \lambda/4n \quad 4.25$$

The thickness of the resonant absorber has to satisfy both the amplitude and phase conditions represented by Eq. (4.24) and (4.25). Simultaneous satisfaction of both the condition is seldom achieved in practice. The phase condition is generally satisfied, leading to the well known quarter wavelength absorber.

4.3.0 DESIGN EXAMPLES

Thin absorbers are generally made by dispersing a lossy material in preferably powder form (Ex. graphite, ferrite etc) in a binder (Ex. rubber, resin etc). Thus the effective properties of such a mixtures would depend upon the size and shape

[125] of the lossy particulate inclusions in general, and in particular on the volume concentration c , of the lossy material in the binder. Many models [118,126,127] are available to predict the effective properties of such mixtures. If one considers spherical particles, then the model proposed by Lichtenecker [118] has been found to be valid over a wide range of volume concentration and has been used in our computation.

4.3.1 DESIGN OF A MATCHED ABSORBER

A design specification of minimum 10 dB absorption over Ku-band (12-18 GHz) and thickness less than 2 mm was set for an absorber that can be employed for RCS reduction.

The matching condition represented by Eq. (4.17) is an ideal condition, which can not be realized practically with known lossy material [128, 129]. The only material that approaches towards this electrical property in the microwave region is Cobalt-Substituted Barium Hexagonal Ferrite (Co-BHF) with μ_r reaching to 5 at resonance. They also provide the additional advantage of controlling [41, 116] the ferromagnetic resonance (f_r), at any desired frequency (f) between 2 and 46 GHz. Hence Co-BHF was selected as lossy material along with silicone/neoprene rubber as the binder.

The ferromagnetic resonance frequency f_r , can be varied by varying δ_s , the amount of Cobalt substituted. The variation of f_r with δ_s can be represented [116,118,132], by the empirical relation,

$$\delta_s = 1.097163 - 0.0223806f_r \quad 4.26$$

Thus δ_s , the amount of Cobalt required to be doped, can be determined for any

247223



f_r between 3.9 to 46 GHz. The frequency dispersion characteristics of μ_r for Co-BHF [41], can be represented as

$$\mu_r'(f) = \frac{4}{\sqrt{1+(f-f_r)^2}} \text{Cosh} \frac{2(f-f_r)}{f + f_r/2} \quad 4.27a$$

$$\text{and } \mu_r''(f) = \mu_r'(f - 1.0) \quad 4.27b$$

where f and f_r are in GHz.

The maximum available value [41] of $\epsilon_r = 10-1j$ for Co-BHF and $\epsilon_r = 5 - j0.2$ for rubber [133] was assumed.

The design was made using the flexible tolerance method [119], a multivariable constraint optimization subroutine (Appendix I). The optimization subroutine was used since the bandwidth requirement was itself non-unique, in the sense that beyond a given level the absorption could fluctuate in an unspecified manner. The optimization subroutine was run along with Eq.'s (4.20a) and (4.20b) several times with different numerical weights and the optimized values of 12.75 GHz, 45% and 1.8 mm as the values of ferromagnetic resonance frequency of Co-BHF, volume concentration of the lossy material in the binder and thickness of the absorber respectively were selected to meet the design specification.

4.3.2 DESIGN OF A RESONANT ABSORBER

For an absorber that could be employed as an electromagnetic wave interference suppressor, a design specifications of ≥ 25 dB at 8.5 GHz within a thickness constraint of 2 mm were set. Co-BHF was again employed as the lossy material along with silicone rubber as the Binder. Carbon was used (in addition to Co-BHF) to reduce the thickness [12], and also to increase the peak absorption.

The flexible-Tolerance optimization subroutine was once again employed along with Eq.'s (4.7a), (4.22a) and (4.25) to determine the volume ratios of Co-BHF and Carbon in the binder. The optimization subroutine was run several times with different numerical weights and the optimized values of 8.5 GHz, 52%, 18%, and 1.76mm as the f_r of Co-BHF, volume concentration of Co-BHF, and carbon; and the thickness of the absorber respectively were selected to meet the design specification.

4.4 FABRICATION OF ABSORBERS

Co-BHF for the two absorbers with $f_r = 8.5$ and 12.75 GHz were prepared using the conventional Ceramic procedure and the particle size were controlled to ≤ 35 microns sieving with an appropriate mesh.

The ferrite-rubber and ferrite-Carbon-rubber in the required volume ratios were mixed in a two roll mill and cured in a hot press into sheets of dimensions $300 \times 300 \times 1.8$ mm.

4.5 EXPERIMENTAL RESULTS

A free space quasi mono static measurement set up operating in X- or Ku-bands as shown in Fig 3.4 was employed to determine the absorption characteristics of the fabricated absorbers. Measurement were carried out in an anechoic chamber. The two horns were suitable isolated such that there were no direct coupling between the transmitting and receiving antennas. The reflectivity of the planar absorber and that due to a metal plate of the same dimensions as that of the absorber were measured. The absorption provided by the absorber is the difference of the two

measurements.

The theoretically predicted and experimentally obtained absorption characteristics for the designed and fabricated matched and resonant absorbers are shown in the Fig 4.2 and 4.3 respectively. The practical performance of the matched absorber over the entire Ku-Band follows very closely with the theoretically predicted values. Further the experimentally determined resonant frequency and absorption for the resonant absorber behaves well with its theoretical counterpart. The shift in the resonant frequency is attributed to the fact that theoretically computed thickness for the absorber was 1.76mm, while the fabricated thickness is 1.8mm.

4.6 CONCLUSION

A mathematical model for the theoretical analysis and design of two types of absorbers have been developed. Their correctness has been validated by the design, fabrication, and experimental testing of an absorber for each type; to reduce RCS and electromagnetic interference in the region of 8-18 GHz with an added thickness constraint of 2 mm.

Further, Matched layer is designed to eliminate the front surface reflection while the resonant absorber is designed to theoretically reduce the overall reflection coefficient R to zero. It is apparent from Eq. (4.24) and (4.25) that, the resonant conditions are λ dependent. Hence, this type can generally be employed as single frequency absorber or for narrow band operation. While the absence of an explicit λ term in the condition for the matched layer, Eq. (4.17) and (4.19), makes these absorbers best suited for broad band operation.

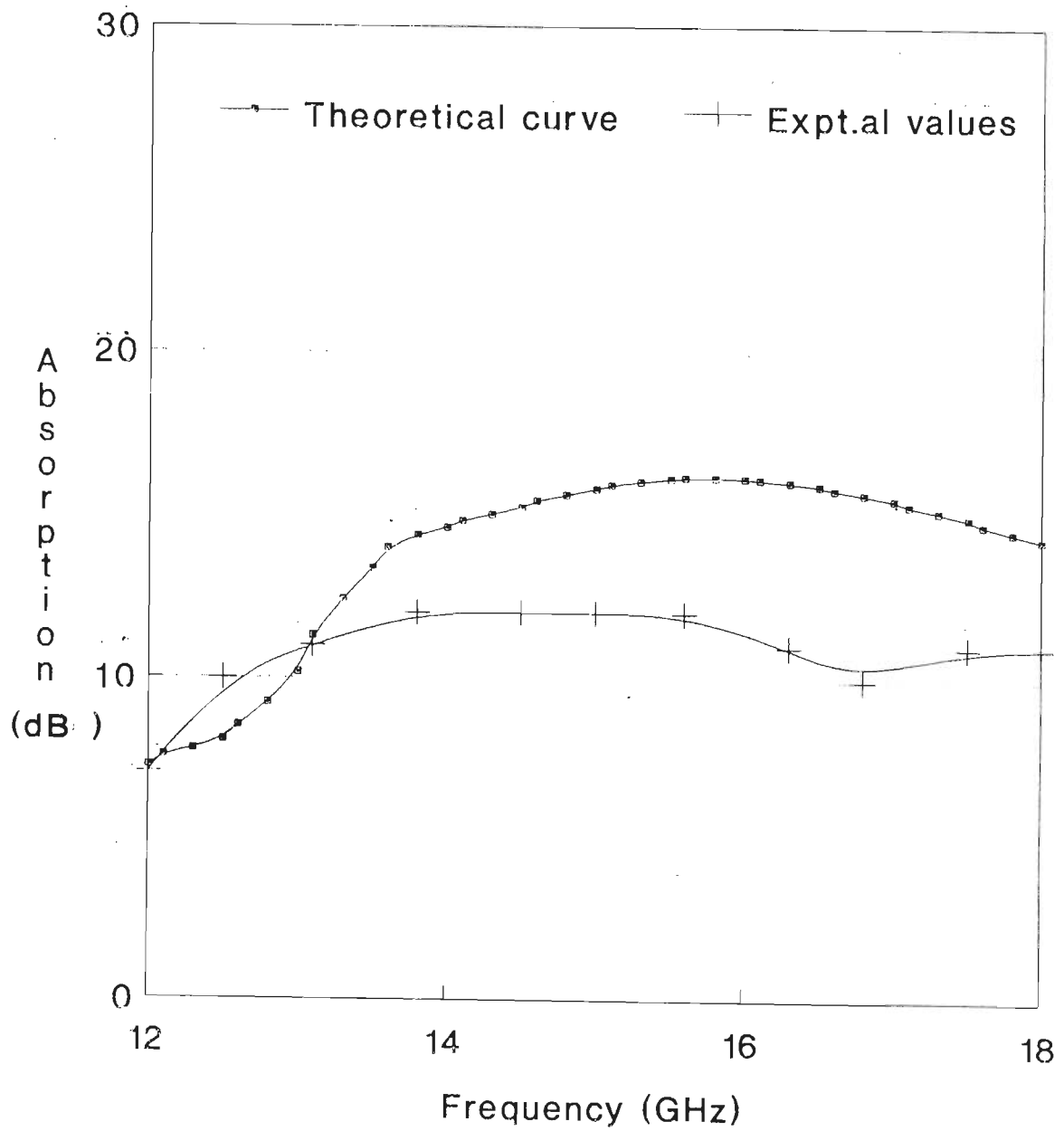


Fig 4.2 Theoretical and experimental absorption characteristics for the matched absorber

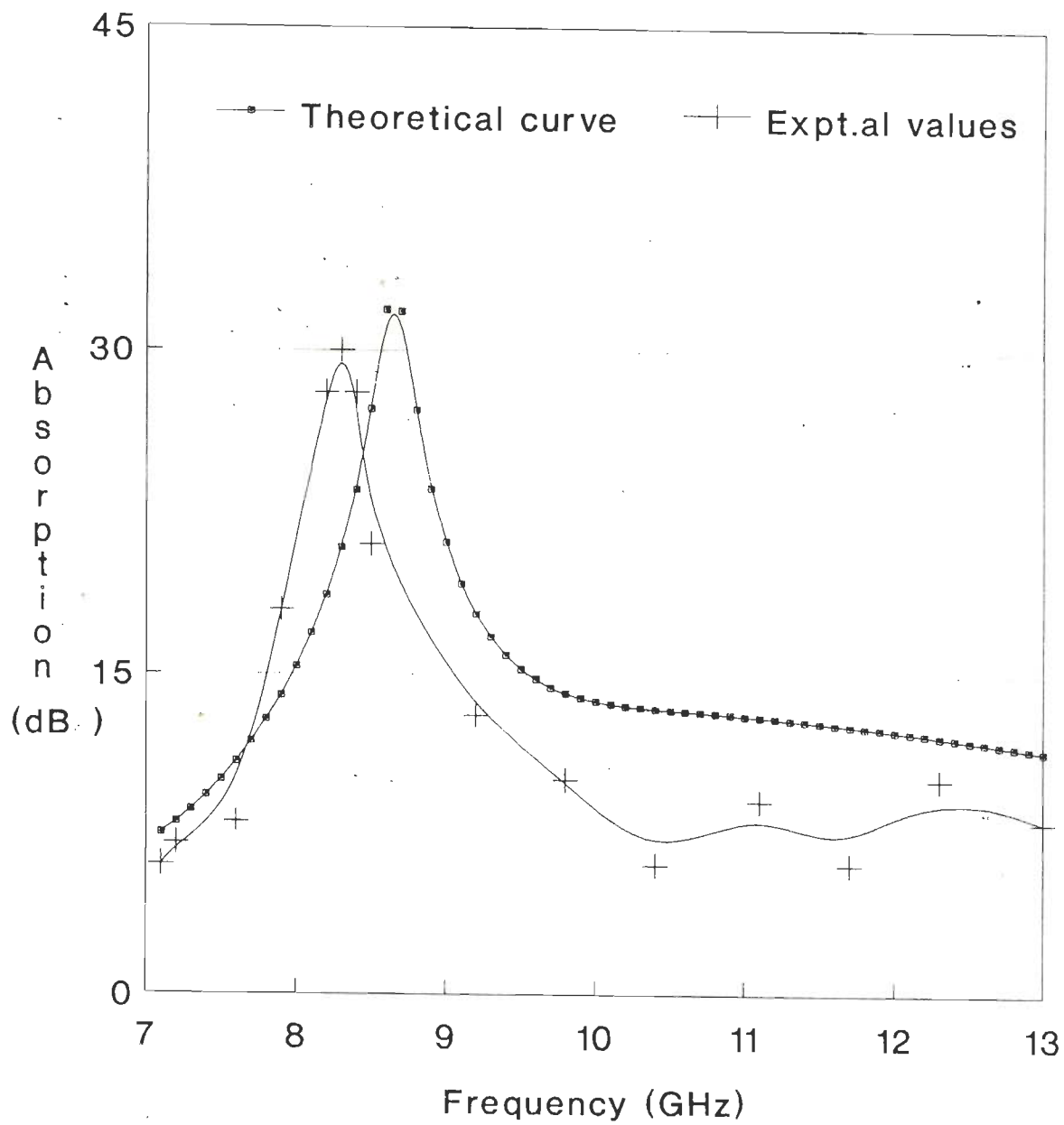


Fig 4.3 Theoretical and experimental absorption characteristics for the resonant absorber

CHAPTER V

CHARACTERIZATION OF THE ABSORBING MEDIA BY ITS BULK PROPERTIES

5.1 INTRODUCTION

Materials for which the microwave behavior of a point in its media depends on the characteristics of the field at all neighboring points, are known as bulk reacting. Most microwave absorbing materials behave in this manner, because microwaves can propagate within the medium to provide communication between points in the media. If the region of influence due to propagation within the medium is relatively small compared to the wavelength of the field, then the behavior of the media is approximately point reacting. The microwave behavior of an ideal point reacting media depends only on the local conditions. The behavior of such a media can be characterized solely by its input impedance, a quantity which is easily measured. In practice, bulk reacting materials are often assumed to be point reacting. This approach has the advantage of simplicity since the impedance is easily represented. It is also widely believed that point reaction is a good approximation even though its accuracy is strongly dependent on the composition of the material in question.

But, in our situation, the medium cannot be assumed to be point reacting due to the following reasons :

- (i) the penetration distance of the wave into the media is small, compared to

the wavelength of the external field;

(ii) the material (absorber) is backed by a perfectly conducting layer or reflecting surface; and

(iii) the layer thickness is small compared to both the penetration distance and the wavelength in the media,

Further, the multiple scattering effects in the media cannot be ignored [53,134,135], in particular the dependence on concentration at wavelengths comparable to scatter's size. At very low concentration, multiple scattering can be neglected and each scatterer be treated as independent. However, in our practical situation of metal filled polymers, wherein the concentration can be as high as 50%, multiple scattering cannot be neglected. The scattering of a single scatterer or particle can be simply represented by the T-matrix [70-71], and the effect of multiple scattering can be taken into account, by performing a configurational averaging on the system.

In most theoretical investigation, scatterers are assumed to be spherical in shape and bear a uniform distribution, although this may not be the case in practice [82,86,136-137]. When the volume concentration occupied by the scatterers becomes large enough to consider their relative positions, detailed knowledge of the positional distribution of the scatterers is needed. This entails a consideration of inter-body forces as in the many body problem of statistical mechanics. At a minimum, the pair correlation function is required in analyzing the problem. If the concentration of the particles happens to be small, random lattice gas statistics can be applied, otherwise the spatial distribution of these scatterers cannot be described by spherical statistics alone. The reason, which is

quite obvious, is that the pair correlation function, instead of being a function of only the separation distance between a pair of scatterers, becomes also a function of the orientation of the vector joining the two scatterers. The non-spherical statistics involved in the analysis is the pair correlation function for aligned scatterers. Of all the approximations using spherical statistics for non-spherical scatterers, that using an equal volume or circumscribing sphere appears to be the best [138] if the actual statistics are not known. Herein a circumscribing sphere approximation is utilized.

5.2 WAVE PROPAGATION THROUGH RANDOMLY DISTRIBUTED AND ORIENTED SCATTERERS : MULTIPLE SCATTERING THEORY

Let in a medium referred to as the host or matrix (characterized by the complex permittivity and permeability by $\epsilon_{r2} = \epsilon'_{r2} - j\epsilon''_{r2}$ and $\mu_{r2} = \mu'_{r2} - j\mu''_{r2}$ respectively) be a random distribution of randomly oriented scatterers (characterized by the complex permittivity and permeability by ϵ_{r1} and μ_{r1} respectively), as shown in Fig 5.1. The number of scatterers N and the embedding volume V are both large, but when $N/V = \eta_0$, the number density is finite.

Consider the propagation of plane harmonic electromagnetic wave of unit amplitude, $e^{j\omega t}$ time dependence (suppressed), and a wave vector K given by

$$E^{inc}(r) = \hat{n} e^{-Kr} \quad 5.1$$

where \hat{n} is the unit normal vector. Let such a wave be incident on system depicted in Fig 5.1. The incident wave is assumed to be propagating in the positive Z direction, thus $Kr = kz$, where k is the free space wave number. O_i and O_j refer to the centres of the i^{th} and j^{th} scatterers. Let E^S be the field scattered by a given scatterer and E^t the field inside the scatterer, Both E^S and E^t satisfies the

vector Helmholtz equation

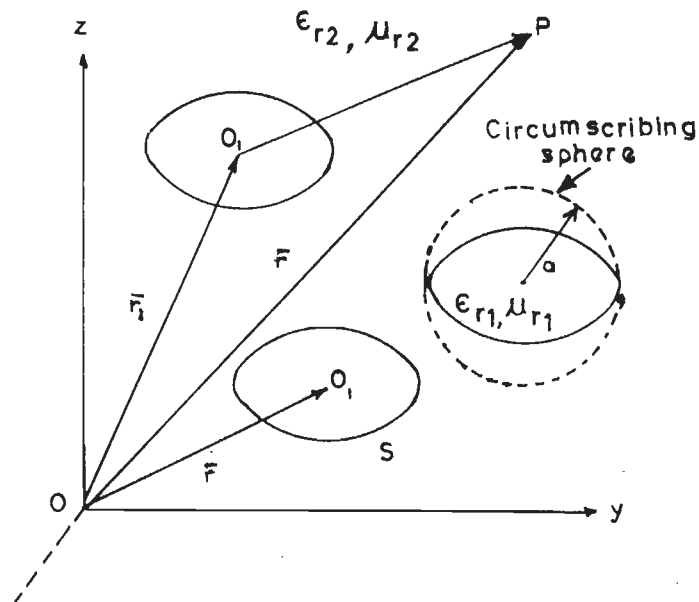


Fig 5.1

$$\nabla \times (\nabla \times E^S) - k_2^2 E^S = 0 \quad 5.2a$$

$$\nabla \times [\nabla \times E^t(r)] - k_1^2 E^t(r) = 0 \quad 5.2b$$

where k_1 and k_2 are the wave numbers in the scatterer and the host medium respectively.

The total electric field at any point in the host medium is the sum of the incident field and the fields scattered by all scatterers. Thus

$$E(r) = E^{\text{inc}}(r) + \sum_i^N E_i^S(r-r_i) \quad 5.3$$

where $E_i^S(r-r_i)$ is the field scattered by the i^{th} scatterer to the point of

observation r .

The field that excites a given scatterer E_i^e , can be written as

$$E_i^e(r) = E^{\text{inc}}(r) + \sum_{j \neq i}^N E_j^s(r-r_j); \quad a \leq |r-r_j| \leq 2a \quad 5.4$$

where 'a' is the radius of the imaginary circumscribing sphere. The second term of Eq. (5.4) refers to summation of the scattered fields due to all scatterers except the i^{th} . (E^e is used to differentiate between the externally incident field E^{inc} , produced by a source at infinity and the field actually incident on a scatterer)

From Eq. (5.3) and (5.4) we have

$$E(r) = E_i^e(r) + E_i^s(r) \quad 5.4a$$

so that the exciting field and scatterer are defined in a self-consistent manner.

The fields E_i^e , E^{inc} and E_j^s can be expanded [Appendix 5.1] using in vector spherical functions, \mathfrak{M} 's and \mathfrak{N} 's as follows.

$$E_j^s(r) = \sum_{n=0}^{\infty} \sum_{m=-n}^n [B_n^{m(j)} \mathfrak{M}_{nm}^j(r-r_j) + C_n^{m(j)} \mathfrak{N}_{nm}^j(r-r_j)] \quad 5.5$$

$$E_i^e(r) = \sum_{n=0}^{\infty} \sum_{m=-n}^n [b_n^{m(i)} \mathfrak{M}_{nm}^i(r-r_i) + c_n^{m(i)} \mathfrak{N}_{nm}^i(r-r_i)] \quad 5.6$$

$$\text{and } E^{\text{inc}} = \frac{e^{-jKr_i}}{2j} \sum_{n=1}^{\infty} \sum_{m=-n}^n [\alpha_n^m \mathfrak{M}_{mn}'(r-r_i) + \beta_n^m \mathfrak{N}_{mn}'(r-r_i)] \quad 5.7$$

where,

$$\alpha_n^m = \frac{(2n+1)j^n}{n(n+1)} [\delta_{m,1} + n(n+1)\delta_{m,-1}]; \quad 5.7a$$

$$\beta_n^m = \frac{(2n+1)j^n}{n(n+1)} [\delta_{m,1} - n(n+1)\delta_{m,-1}]; \quad 5.7b$$

and δ_{mn} is the Kronecker delta;

In the above two expressions B & C are the unknown expansion coefficients,

while b & c are the known exciting field expansion coefficients. The basis set of Eq. (5.6) is chosen to satisfy the radiation condition at infinity for the scattered field E_j^S , and the basis set of Eq. (5.7) is chosen such that, regularity of the exciting field E_i^E , in the region $0 \leq |\bar{r}-\bar{r}_i| \leq 2a$ is maintained.

The wave functions \mathfrak{M} 's and \mathfrak{N} 's, which are the solutions to the vector Helmholtz equation (Eq.5.2's) in spherical coordinates, can be written as [124, page 415]

$$\mathfrak{M}_{mn}(\bar{r}) = \nabla \times [\bar{r} h_n(kr) Y_{mn}(\theta, \phi)] \quad 5.8a$$

$$\mathfrak{N}_{mn}(\bar{r}) = (1/k) \nabla \times \mathfrak{M}_{mn} \quad 5.8b$$

where, $Y_{mn}(\theta, \phi) = P_n^m(\cos\theta) e^{jm\phi}$; \mathfrak{M}' and \mathfrak{N}' are obtained by replacing h_n by J_n , the spherical Bessel function in Eq. (5.8), with P_n^m the Legendre polynomial.

Substituting Eq.'s (5.5)-(5.8) into (5.4), we have

$$\begin{aligned} \sum_{n=0}^{\infty} \sum_{m=-n}^n [b_n^{m(i)} \mathfrak{M}_n^{i(r-r_i)} + c_n^{m(i)} \mathfrak{N}_n^{i(r-r_i)}] = \\ e^{-jKr_i} \sum_{n=1}^{\infty} \sum_{m=-n}^n [\alpha_n^m \mathfrak{M}'_{mn}(r-r_i) + \beta_n^m \mathfrak{N}'_{mn}(r-r_i)] \\ + \sum_{j \neq i}^N \sum_{n=0}^{\infty} \sum_{m=-n}^n [B_n^{m(j)} \mathfrak{M}_{nm}^j(r-r_j) + C_n^{m(j)} \mathfrak{N}_{nm}^j(r-r_j)] \quad 5.9 \end{aligned}$$

In the above expression E_i^E and E^{inc} are referred to a co-ordinate system at O_i , while E_j^S refers to an origin at O_j . To eliminate this ambiguity, we utilize the translation theorem for vector spherical function. Which states that for the system shown in the Fig. 5.2 (with the co-ordinate axis at O_i and O_j parallel to XYZ axes), and $\sigma_{\tau n \nu w}$ representing the translation of the basis function from the j^{th} scatterer to the i^{th} scatterer, the translation is

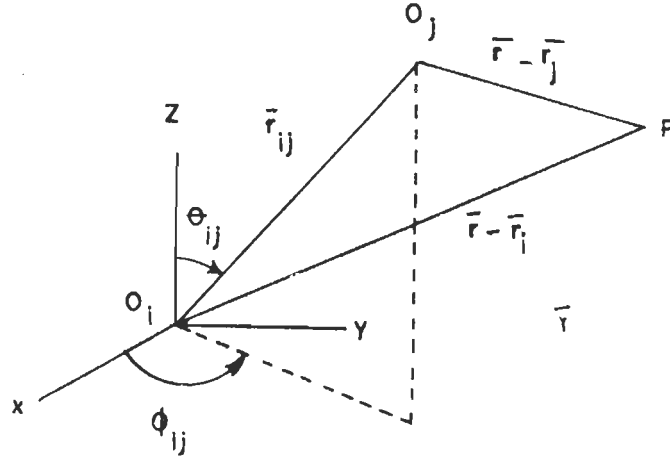


Fig 5.2

$$\chi_{\tau n}^j = \sum_{\nu w} \sigma_{\tau n \nu w} (r-r_j) \chi_{\nu w}^{(i)} \quad 5.10$$

Using (5.10) we can rewrite the basis functions as

$$\mathfrak{M}_{mn}^j = \sum_{\nu=0}^{\infty} \sum_{w=-\nu}^{\nu} [B_{\nu w}^{mn} \mathfrak{M}_{\nu w}^{(i)} + C_{\nu w}^{mn} \mathfrak{M}_{\nu w}^{(i)}] \quad 5.11a$$

$$\mathfrak{M}_{mn}^j = \sum_{\nu=0}^{\infty} \sum_{w=-\nu}^{\nu} [C_{\nu w}^{mn} \mathfrak{M}_{\nu w}^{(i)} + B_{\nu w}^{mn} \mathfrak{M}_{\nu w}^{(i)}] \quad 5.11b$$

where again prime indicates the replacement of h_n by J_n , and $B_{\nu w}^{mn}$, $C_{\nu w}^{mn}$, the functions resulting from the application of the translation theorem are obtained [139] as,

$$B_{\nu w}^{mn} = \sum_{q=|n-\nu|+1}^{n+\nu} (-1)^w (j)^{\nu+q-n} a(m, n | -w, \nu | q) b(n, \nu, q) h_q(kr_{ij}) \cdot P_q^{m-\nu} \cos(\theta_{ij}) e^{-j(m-w)\phi_{ij}} \quad 5.12a$$

$$C_{\nu w}^{mn} = \sum_{q=|n-\nu|+1}^{n+\nu} (-1)^{w+1} (j)^{\nu+q-n} b(n,\nu,q) a(m,n|-w,\nu|q,q-1) \cdot h_q(kr_{ij}) P_q^{m-\nu} \cos(\theta_{ij}) e^{-j(m-w)\phi_{ij}} \quad 5.12b$$

Where, the coefficients a's, b's in the above equations can be obtained in the work by Cruzan [139].

Utilizing the above translated expansion coefficients (Eq. 5.11 and 5.12) in Eq. (5.9) one obtains the expansion of Eq. (5.4) in vector spherical harmonics with respect to an origin O_i centered at the i^{th} scatterer. Invoking the orthogonality of the basis function and with some algebraic manipulation, we can write the exciting field expansion coefficients as

$$b_n^{m(i)} = \frac{2n+1}{n(n+1)} j^n \frac{e^{-jKr_i}}{2j} [\delta_{m,1} + n(n+1)\delta_{m,-1}] + \sum_{j \neq i}^N \sum_{n_1=0}^{\infty} \sum_{m_1=-n_1}^{n_1} [B_{n_1}^{m_1(j)} B_{mn}^{m_1 n_1}(r_i-r_j) + C_{n_1}^{m_1(j)} C_{mn}^{m_1 n_1}(r_i-r_j)] \quad 5.13a$$

$$\text{and } c_n^{m(i)} = \frac{2n+1}{n(n+1)} j^n \frac{e^{-jKr_i}}{2j} [\delta_{m,1} + n(n+1)\delta_{m,-1}] + \sum_{j \neq i}^N \sum_{n_1=0}^{\infty} \sum_{m_1=-n_1}^{n_1} [B_{n_1}^{m_1(j)} C_{mn}^{m_1 n_1}(r_i-r_j) + B_{n_1}^{m_1(j)} B_{mn}^{m_1 n_1}(r_i-r_j)] \quad 5.13b$$

where $\sum_{j \neq i}^N$ denotes the summation over all scatterers except the i^{th} scatterer, and $B_{mn}^{m_1 n_1}$ and $C_{mn}^{m_1 n_1}$ are the functions resulting from the translation theorem of the

vector spherical function. Expression (5.13) is thus a relation between the known expansion coefficient (b_n^m, c_n^m) of the exciting field and the unknown expansion coefficients (B_n^m, C_n^m) of the scattered fields.

If the total field outside a given scatterer is the algebraic sum of the incident and scattered fields, the unknown scattered-field expansion coefficient can be related to the incident-field expansion coefficient using Watermans [70,71] or Transition matrix (T-Matrix) approach. Since $[E_j^e(r) + E_j^s(r)]$ is the total field at any point in the medium, the expansion coefficient of the scattered field by the j^{th} scatterer can be related to the coefficient of the field exciting the j^{th} scatterer through the T-Matrix by [140],

$$\begin{bmatrix} B_n^{l(i)} \\ C_n^{l(i)} \end{bmatrix} = \begin{bmatrix} (T^{11})_{nm}^{lp} & (T^{12})_{nm}^{lp} \\ (T^{21})_{nm}^{lp} & (T^{22})_{nm}^{lp} \end{bmatrix} \begin{bmatrix} b_n^p \\ c_n^p \end{bmatrix} \quad 5.14$$

where summation over m and p indices is implied by repeated index conventions.

The T-matrix of a scatterer, depends only on the frequency, geometry and nature of the scatterer. The elements of the T-Matrix involve surface integrals which can be evaluated in closed form for spherical geometry, while for arbitrary shaped surface geometry, a numerical method will have to be employed. The T-Matrix for a single scatterer is of the form [140a, 140b]

$$[T_n] = [Q_n^{11}] [Q_n^{31}] \quad 5.15$$

where

$$Q_n^{ij} = \begin{bmatrix} K_n^{ij} + (\mu_{rn} \epsilon_{rn})^{1/2} J_n^{ij} & L_n^{ij} + (\mu_{rn} \epsilon_{rn})^{1/2} I_n^{ij} \\ I_n^{ij} + (\mu_{rn} \epsilon_{rn})^{1/2} L_n^{ij} & J_n^{ij} + (\mu_{rn} \epsilon_{rn})^{1/2} K_n^{ij} \end{bmatrix} \quad 5.16$$

and I, J, K and L are surface integrals given by,

$$[I_n^{ij}]_{lm} = \frac{k_{n+1}^2}{\pi} \int_{S_i} \hat{n}_n \mathfrak{M}_l^i(k_{n+1}r) \times \mathfrak{M}_m^j(k_n r) ds \quad 5.16a$$

J, K and L are obtained by replacing the cross product in the above equation by $\mathfrak{M} \times \mathfrak{N}$, $\mathfrak{N} \times \mathfrak{M}$ and $\mathfrak{N} \times \mathfrak{N}$ respectively.

If we consider the case of identical scatterers, then the T-Matrix for all individual scatterers would be identical or same and Eq. (5.14) can be written in a simple form as

$$\begin{bmatrix} B \\ C \end{bmatrix} = \begin{bmatrix} T^{11} & T^{12} \\ T^{21} & T^{22} \end{bmatrix} \begin{bmatrix} b \\ c \end{bmatrix} = [T] \begin{bmatrix} b \\ c \end{bmatrix} \quad 5.17$$

For aligned identical scatterers, if the T-Matrix is computed with respect to the xyz axes, then the T-Matrix of all N scatterers is the same. However if the orientation of each scatterer with respect to xyz axes is defined by the Euler angles $\alpha_i, \beta_i, \gamma_i$ as shown in Fig 5.3, then the T-Matrix of the i^{th} scatterer is a function of the Euler angles and is defined [141] as

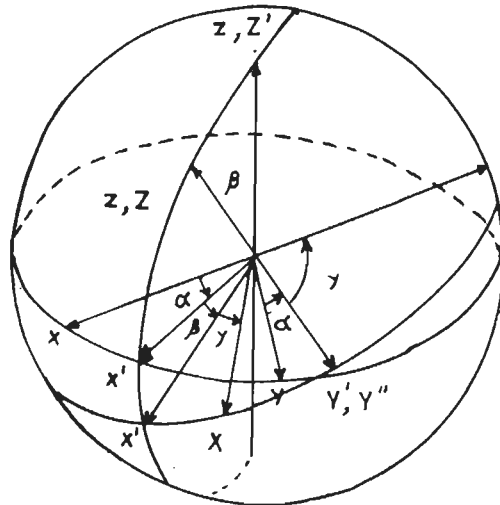


Fig 5.3 Euler angles

$$T = D \hat{T} D^{-1} \quad 5.18a$$

where \hat{T} is the T-matrix of a scatterer evaluated with respect to the set of coordinates axes natural to the scatterer (XYZ), and is independent of position and orientation and is, hence, the same for identical scatterers. D is the rotation matrix given by Edmonds [141] as

$$D_{mm'}^n(\alpha, \beta, \gamma) = e^{-jm\alpha} d_{mm'}^n(\beta) e^{-jm'\gamma} \quad 5.18b$$

where

$$d_{mm'}^n(\beta) = \left[\frac{(n+m)!(n-m)!}{(n+m')!(n-m')!} \right]^{1/2} \left[\cos(\beta/2) \right]^{m+m'} \left[\sin(\beta/2) \right]^{m-m'} \cdot P_{n-m}^{(n-m', m+m')}(\cos(\beta)) \quad 5.18c$$

and P is the Jacobi polynomial, which can be expressed in terms of the associated Legendre polynomials [141].

The T-Matrix averaged over all possible orientations of the scatterer may then be written as

$$\begin{aligned} \langle T_{nm, n'm'} \rangle &= \frac{1}{8\pi^2} \int_0^{2\pi} d\alpha \int_0^{2\pi} d\gamma \int_0^{2\pi} d\beta \sin(\beta) \sum_{m_1, m_2} [D_{mm_1}^n(\alpha, \beta, \gamma) \\ &\quad \cdot \hat{T}_{nm_1, n'm_2} (D^{-1})_{m_2, m'}^{n'}(\alpha, \beta, \gamma)] \\ &= \frac{1}{2n+1} \sum_{m_1, m_2} \hat{T}_{nm_1, n'm_2} \delta_{mm_2} \delta_{mm'} \delta_{nn'} \\ &= \hat{T}_{nm, nm'} \end{aligned} \quad 5.19$$

Thus,

$$\begin{bmatrix} B_n^{l(i)} \\ C_n^{l(i)} \end{bmatrix} = \begin{bmatrix} \langle T^{11} \rangle_{nm}^{lp} & \langle T^{12} \rangle_{nm}^{lp} \\ \langle T^{21} \rangle_{nm}^{lp} & \langle T^{22} \rangle_{nm}^{lp} \end{bmatrix} \begin{bmatrix} b_n^p \\ c_n^p \end{bmatrix} \quad 5.20$$

now provides the relationship between the scattered field expansion coefficient and the exciting field expansion coefficient, with the T-matrix described by Eq. (5.19).

5.3 CONFIGURATIONAL AVERAGING : THE AVERAGE OR EFFECTIVE WAVENUMBER IN THE MEDIUM

It now remains to perform an average over all possible positions. To this end, we define a probability density function of finding the first scatterer at r_1 , the second at r_2 and so on by $p(r_1, r_2, \dots, r_N)$. Which in turn may be expressed [142], in terms of conditional probability $p(r_j/r_i)$, of finding a scatterer at r_j if a scatterer is known to be at r_i . If the scatterers are randomly distributed, the positions of all scatterers are equally probable within the volume V accessible to the scatterers, and hence

$$P(r_i) = \begin{cases} \eta_0/N, & r_i \in V \\ 0, & r_i \notin V \end{cases}$$

in addition, for non overlap of the imaginary spherical shells circumscribing each scatterer, we approximate the conditional density as

$$P(r_j/r_i) = \begin{cases} \eta_0/N, & |r_j - r_i| \geq 2a \\ 0, & |r_j - r_i| \leq 2a \end{cases} \quad 5.21$$

The two point joint probability function described in Eq. (5.21) above can in turn be defined [86], in terms of the radial distribution function $g(|r_j - r_i|)$, with an exclusion surface or 'hole' corresponding to a sphere of radius 'a' as follows

$$P(r_j/r_i) = \begin{cases} \frac{1}{V}g(|r_j - r_i|) & |r_j - r_i| \geq 2a \\ 0, & |r_j - r_i| \leq 2a \end{cases} \quad 5.22$$

where V is the large but finite volume occupied by the scatterers and 'a' is the

largest radius of the sphere circumscribing the scatterer.

Multiplying both sides of Eq. (5.20) by (5.22), we obtain the configurational average of B and C:

$$\begin{bmatrix} \langle B_{nm}^l(i) \rangle_i \\ \langle C_{nm}^l(i) \rangle_i \end{bmatrix} = \begin{bmatrix} \langle T^{11} \rangle & \langle T^{12} \rangle \\ \langle T^{21} \rangle & \langle T^{22} \rangle \end{bmatrix} \begin{bmatrix} \langle \psi_{n_1 m_1}^i \rangle \\ \langle \chi_{n_1 m_1}^i \rangle \end{bmatrix} \quad 5.23$$

The above equation indicates that the conditional average with one scatterer fixed viz., $[\langle B_n^l \rangle_i, \langle C_n^l \rangle_i]$ is given in terms of the conditional average with two scatterers fixed, viz., $[\langle B_{n_1}^{l_1} \rangle_{ij}, \langle C_{n_1}^{l_1} \rangle_{ij}]$, and so on. To close the system we use the quasi crystalline approximation suggested by Lax [73,74],

$$\left. \begin{aligned} \langle B_n^{m(j)} \rangle_{ij} &\cong \langle B_n^{m(j)} \rangle_j \\ \langle C_n^{m(j)} \rangle_{ij} &\cong \langle C_n^{m(j)} \rangle_j \end{aligned} \right\} i \neq j \quad 5.24$$

which implies that there is no correlation between the i^{th} and j^{th} scatterer other than there should be no interpenetration of any two scatterers. ψ and χ in Eq. (5.23) can now be expressed as

$$\begin{aligned} \langle \psi_{n_1 m_1}^i \rangle &= \frac{2n_1+1}{n_1(n_1+1)} j^{n_1} \frac{e^{-jKr_i}}{2j} [\delta_{m_1,1} + n_1(n_1+1)\delta_{m_1,-1}] \\ &+ \frac{1}{V} \sum_{j \neq i} \sum_{n_2=0}^{\infty} \sum_{m_2=-n_2}^{n_2} \int_V [\langle B_{n_2 m_2}^j \rangle B_{n_1 m_1}^{n_2 m_2}(r_i-r_j) \\ &+ \langle C_{n_2 m_2}^j \rangle C_{n_1 m_1}^{n_2 m_2}(r_i-r_j)] g(|r_j-r_i|) dr_j \end{aligned} \quad 5.25a$$

$$\langle \chi_{n_1 m_1}^i \rangle = \frac{2n_1+1}{n_1(n_1+1)} j^{n_1} \frac{e^{-jKr_i}}{2j} [\delta_{m_1,1} + n_1(n_1+1)\delta_{m_1,-1}]$$

$$\begin{aligned}
& + \frac{1}{V} \sum_{j \neq i}^N \sum_{n_2=0}^{\infty} \sum_{m_2=-n_2}^{n_2} \int_{V'} [\langle B_{n_2 m_2}^j \rangle C_{n_1 m_1}^{n_2 m_2}(r_i - r_j) \\
& + \langle C_{n_2 m_2}^j \rangle B_{n_1 m_1}^{n_2 m_2}(r_i - r_j)] g(|r_j - r_i|) dr_j
\end{aligned} \tag{5.25b}$$

where V' denotes the volume of the medium excluding the volume of the sphere 'a'.

For identical scatterers $\sum_{j \neq i}^N$ can be replaced by $(N-1)$ and

$$4\pi(N-1)a^3/3V = c \tag{5.26}$$

the volume concentration of 'scatterers' provided N is large.

With the above coherent averaging of the fields, the medium with microstructural inhomogeneities, is replaced with a macroscopically homogeneous medium. In such a medium, let plane waves propagate with an average or effective wave number K , with unknown amplitudes Y and Z :

$$\langle B_{nm}^i \rangle_i = Y_{nm} e^{-jKr_i} \tag{5.27a}$$

and $\langle C_{nm}^i \rangle_i = Z_{nm} e^{-jKr_i} \tag{5.27b}$

Utilizing the above Eq. in (5.25) and invoking the extinction theorem to cancel the incident term on the right side of Eq. (5.25a) and (5.25b), we obtain an infinite system of equations for the unknowns as [20]

$$\begin{aligned}
Y_{nm} = & \sum_{q=|n_1-n_2|}^{|n_1+n_2|} \sum_{n_1=0}^{\infty} \sum_{n_2=0}^{\infty} \sum_{m_1=-n_1}^{n_1} \sum_{m_2=n_2}^{n_2} (-1)^{m_2} j^{n_2-n_1} \delta_{m_1, m_2} \\
& \cdot (JH)_q \left\{ Y_{n_2 m_2} \left[\langle T^{11} \rangle_{nm, n_1 m_1} a(n_2, n_1, q) a(m_2, n_2 | -m_1, n_1 | q) \right. \right. \\
& \left. \left. - \langle T^{12} \rangle_{nm, n_1 m_1} b(n_2, n_1, q) a(m_2, n_2 | -m_1, n_1 | q, q-1) \right] \right\}
\end{aligned}$$

$$\begin{aligned}
& + Z_{n_2 m_2} \left[\langle T^{12} \rangle_{nm, n_1 m_1} a(n_2, n_1, q) a(m_2, n_2 | -m_1, n_1 | q) \right. \\
& \left. - \langle T^{11} \rangle_{nm, n_1 m_1} b(n_2, n_1, q) a(m_2, n_2 | -m_1, n_1 | q, q-1) \right] \} \quad 5.27c
\end{aligned}$$

$$\begin{aligned}
\text{and } Z_{nm} &= \sum_{q=|n_1-n_2|}^{|n_1+n_2|} \sum_{n_1=0}^{\infty} \sum_{n_2=0}^{\infty} \sum_{m_1=-n_1}^{n_1} \sum_{m_2=n_2}^{n_2} (-1)^{m_2} j^{n_2-n_1} \delta_{m_1, m_2} \\
& \cdot (JH)_q \left\{ Y_{n_2 m_2} \left[\langle T^{21} \rangle_{nm, n_1 m_1} a(n_2, n_1, q) a(m_2, n_2 | -m_1, n_1 | q) \right. \right. \\
& \left. \left. - \langle T^{22} \rangle_{nm, n_1 m_1} b(n_2, n_1, q) a(m_2, n_2 | -m_1, n_1 | q, q-1) \right] \right. \\
& \left. + Z_{n_2 m_2} \left[\langle T^{22} \rangle_{nm, n_1 m_1} a(n_2, n_1, q) a(m_2, n_2 | -m_1, n_1 | q) \right. \right. \\
& \left. \left. - \langle T^{21} \rangle_{nm, n_1 m_1} b(n_2, n_1, q) a(m_2, n_2 | -m_1, n_1 | q, q-1) \right] \right\} \quad 5.27d
\end{aligned}$$

The term $(JH)_q$ is defined as [20]

$$\begin{aligned}
(JH)_q &= \{6c / [(ka)^2 - (Ka)^2]\} [2Kaj_q(2Ka)h'_q(2ka) \\
& - 2Kah_q(2ka)j'_q(2Ka)] + 24c \int_1^{\infty} x^2 [g(x) - 1] h_q(2kax) j_q(2Kax) dx \quad 5.28
\end{aligned}$$

where $x = |r_i - r_j| / 2a$, j_q and h_q are the spherical bessel functions and prime indicates differentiations with respect to the arguments. The solution to Eq. (5.27) can be realized by setting the determinant of the coefficient matrix generated by Eq. (5.27) to zero, thus obtaining the value for the effective or average wave number in the media.

5.4 ANALYTICAL EXPRESSION FOR EFFECTIVE WAVENUMBER UNDER LONG WAVELENGTH APPROXIMATION

For the case of thin absorbers we have

$$a \ll d \leq \lambda, \quad (5.29)$$

where a is the scatterer or particle radius, d the thickness of the absorber and λ the free space wavelength. Hence invoking the long wavelength approximation, and retaining only the dipole terms in Eq. (5.27), we obtain the determinant of the coefficient matrix generated by Eq. (5.27) as

$$\begin{vmatrix} (T^{11})_{11} (JH_0 + \frac{1}{2} JH_2)^{-1} & \frac{3}{2} (T^{22})_{11} JH_1 \\ \frac{3}{2} (T^{11})_{11} JH_1 & (T^{22})_{11} (JH_0 + \frac{1}{2} JH_2)^{-1} \end{vmatrix} = 0 \quad (5.30)$$

and for spherical particles the dipole term of the T-Matrix takes the form

$$(T^{11})_{11} = \frac{-\{\mu_{r1} j_{11}^{-[2j_{12}-(k_2 a)j_{22}]} - \mu_{r2} j_{12} [2j_{11}-(k_1 a)j_{21}]\}}{\{\mu_{r1} j_{11}^{-[2h_{12}-(k_2 a)h_{22}]} - \mu_{r2} h_{12} [2j_{11}-(k_1 a)j_{21}]\}} \quad (5.31a)$$

$$(T^{22})_{11} = \frac{-\{\mu_{r1} j_{12} [2j_{11}-(k_1 a)j_{21}] - \mu_{r2} (\epsilon_{r1} \mu_{r1} / \epsilon_{r2} \mu_{r2}) j_{11} [2j_{12}-(k_2 a)j_{22}]\}}{\mu_{r1} h_{12} [2j_{11}-(k_1 a)j_{21}] - \mu_{r2} (\epsilon_{r1} \mu_{r1} / \epsilon_{r2} \mu_{r2}) j_{11} [2h_{12}-(k_2 a)h_{22}]} \quad (5.31b)$$

According to symmetry of the T-Matrix for a spherical scatterer:

$$(T^{12})_{11} = (T^{22})_{11} = 0.$$

The hole correction term $(JH)_n$ in Eq. (5.30) is given by

$$\begin{aligned} (JH)_n &= \{6c / [(ka)^2 - (Ka)^2]\} [2Kaj_n(2Ka)h'_n(2ka) - 2Kah_n(2ka) \cdot j'_n(2Ka)] \\ &+ 24c \int_1^\infty x^2 [g(x) - 1] h_n(2kax) j_n(2Kax) dx \end{aligned} \quad (5.32)$$

with the following notation for

$j_{nm} = j_n(k_m a)$ spherical Bessel function

$h_{nm} = h_n(k_m a)$ spherical Hankel function ($n, m = 1, 2$).

Eq. (5.30) is in the form of a transcendental equation and can be solved by searching for the value of K in the complex plane, using Muller's method [143], described in Appendix 5.2.

5.5 RADIAL DISTRIBUTION FUNCTION

The discrete random medium is considered as a statistical ensemble of non-impenetrable spheres. In the statistical mechanics literature this is synonymous with an ensemble of 'hard' spheres. The radial distribution $g(r)$ is defined in terms of the two-particle joint probability density $p(r_j/r_i)$; Eq. (5.22). Equation (5.22) implies that the particles are hard (no interpenetration) and the excluded volume is a sphere of radius 'a' although the particles themselves may not be spherical. The function $g(r)$, ($r = r_{ij}$), is called the pair correlation function and depends only on $|r_{ij}| = |r_j - r_i|$; because of translational invariance of the system under consideration. Several theories and calculations are available for determining $g(r)$, namely the Hypernetted-Chain equation (HNC), the Percus-Yevick approximation (P-YA), the Self-Consistent Approximation (SCA), Monte Carlo calculations, etc. Fuller details regarding these and other forms of the distribution are nicely discussed by Twersky in [144].

The pair correlation function for an ensemble of particles depends on the nature and range of the interparticle forces. The average of several measurements of a statistical variable that characterizes an ensemble will depend on the pair correlation function. To obtain expressions for the pair correlation function, one

needs a description of the interparticle forces. In our case, we assume that the scatterers behave like effective hard spheres. Percus and Yevick [145] have obtained an approximate integral equation for the pair correlation function of a classical fluid in equilibrium. The statistics of the fluid are the same as those of the ensemble of discrete hard particles that we are considering.

Although integral expressions for the correlation functions also result in a hierarchy, Percus and Yevick [145] have truncated the hierarchy by making certain approximations that results in a self-consistent relation between the pair correlation function $g(r)$ and the direct correlation function $C(r)$. The direct correlation function can be defined to be the direct effect of scatterer S_1 on S_2 , which roughly has the range of interparticle potential and also an indirect effect due to the effect of S_1 on S_3 , which in turn has an effect on S_2 . Since scatterer S_3 can be any scatterer of the system, it will include a sum on all scatterers and an integration over the volume of the system. But P-YA is a strong statement of the extremely short range nature of the direct correlation function [146]. The integral equation put forward by Percus and Yevick is of the form

$$\tau(r) = 1 + \eta_0 \int_{r' < 2a} \tau(r') dr' - \eta_0 \int_{\substack{r' < 2a \\ |r-r'| > 2a}} \tau(r') \tau(r-r') dr' \quad 5.33$$

where,

$$\left. \begin{aligned} \tau(r) &= g(r) & r > 2a \\ g(r) &= 0 & r < 2a \\ \tau(r) &= -C(r) & r < 2a \\ C(r) &= 0 & r > 2a \end{aligned} \right\} \quad 5.33a$$

The P-YA fails as the concentration approaches the close packing factor for hard spheres and is expected to be good for $c < 0.4$ (c is defined in Eq.5.26).

Another approximation to $g(r)$ is the HNC, which differs from the P-YA in that the direct correlation function $C(r)$ has a longer range. In general, P-YA is expected to be better than HNC. Both P-YA and HNC are good approximations to $g(r)$ at low concentrations but are appreciably in error at high concentrations.

The reason for this error is that when an approximate theory as P-YA for $g(r)$ is used to calculate the pressure, two different values are obtained, via the pressure and compressibility equations [147]. An exact theory for $g(r)$ should give the same values for pressure from both equations. Rowlinson [148] has suggested a method known as the self-consistent approximation for optimizing the P-YA and removing the ambiguity in the pressure, by assuming that the direct correlation function may be written as

$$C_{SCA}(r) = C_{P-YA}(r) + \phi C_{HNC}(r) \quad 5.34$$

where ϕ is an adjustable parameter which depends on concentration but not separation r and C_{SCA} is the self-consistent approximation of the direct correlation function. Using Eq. (5.33) and (5.34) the ambiguity in pressure value is resolved self-consistently by adjusting the function ϕ . This leads to an integral equation for $g(r)$, which is then solved numerically. The SCA is thus an improvement over P-YA and HNC at higher concentrations. A general computer program to compute the g_{SCA} is given by McQuarrie [147]. Tabulated values found in literature [149] for g_{SCA} were not found suitable, since they are given for short ranges only. Hence the general computer program given in the work by Mcquarrie is most suitable for our present applications. A representative plot of g_{SCA} is shown [147] in Fig 5.4. The general computer program to obtain g_{SCA} in term of r is listed as subroutine GR in Appendix 5.3.

For even higher concentration than that is considered here one's choice for

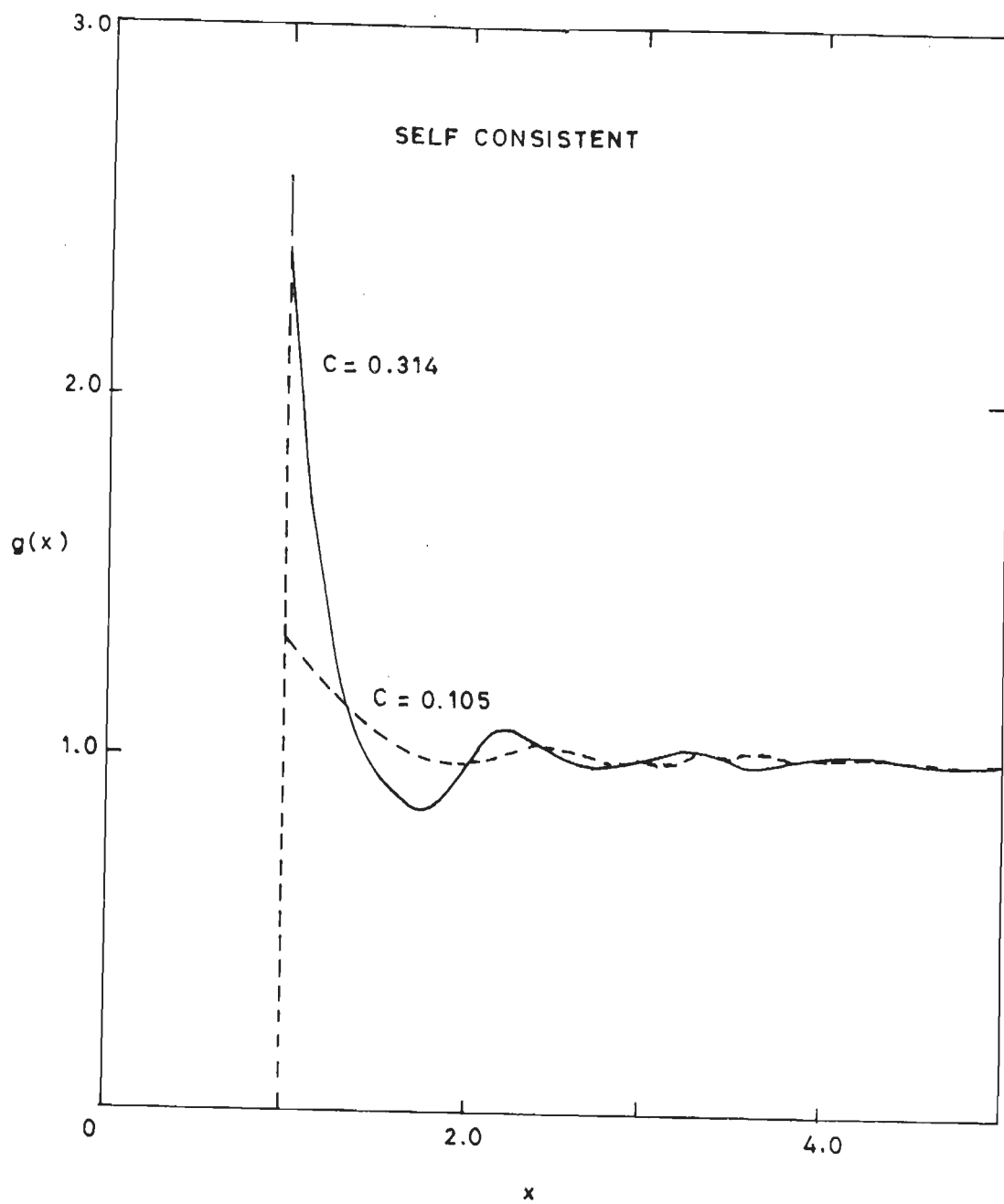


Fig 5.4 The Self-consistent correlation function for 'hard' spheres [147].

$g(r)$ would perhaps rest on the Monte Carlo calculations [138].

5.6 ORGANIZATION OF THE COMPUTER PROGRAM

A computer program in FORTRAN was developed to solve Eq. (5.30) for effective or average wave number. The Muller technique (Appendix 5.2) was employed to search the effective wave number in the complex plane. The listing of the computer program is given in Appendix 5.3. The organization of the program is explained in Fig 5.5a and 5.5b.

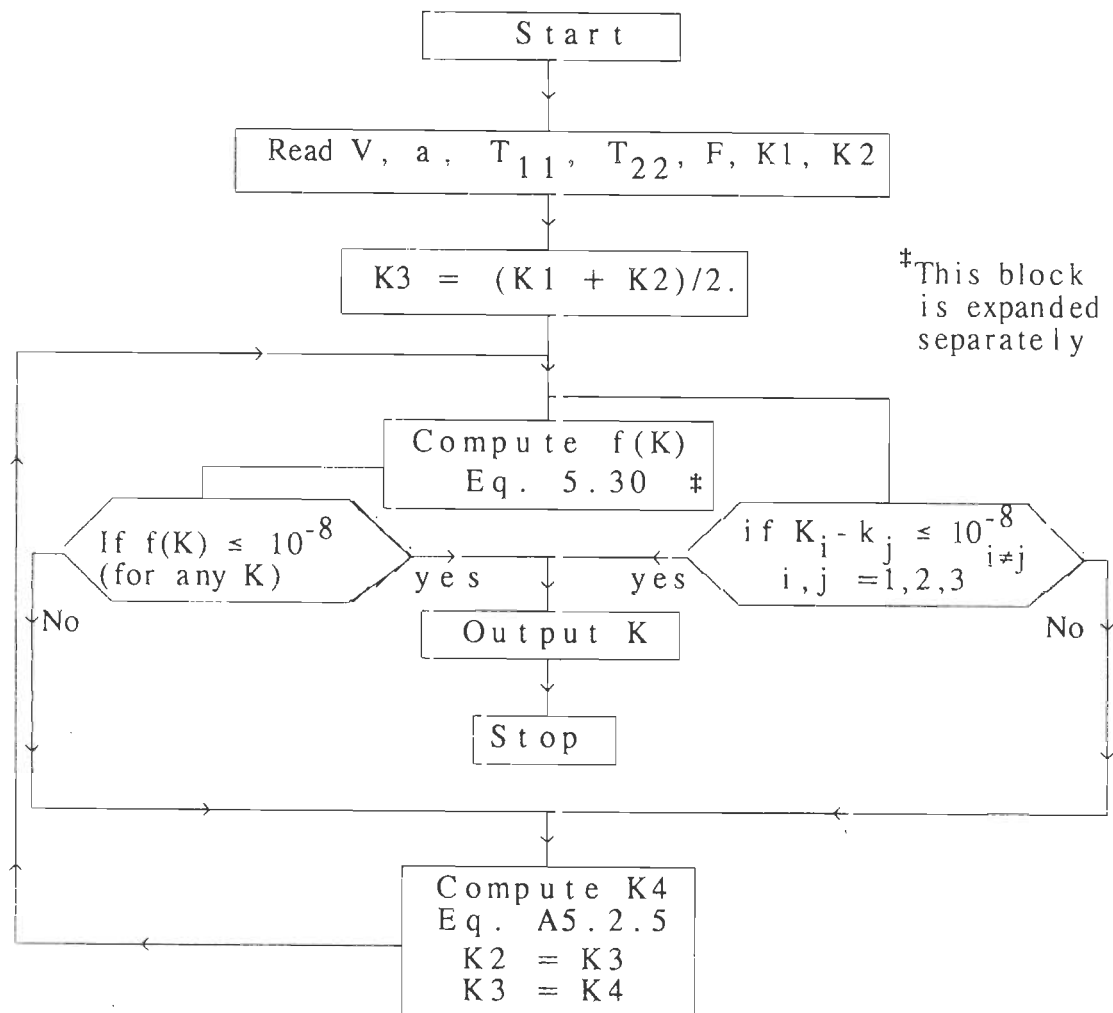


Fig 5.5a

The inputs for this program are

V , the volume concentration of the lossy material,

a , the average particle radius,

T_{11} and T_{22} are the elements of the T-Matrix, and $K1$, $K2$ are initial assumed values for wave number, computed in Appendix 5.4

The output of this program is the effective or average wave number K .

Expansion of the block # in Fig 5.5a

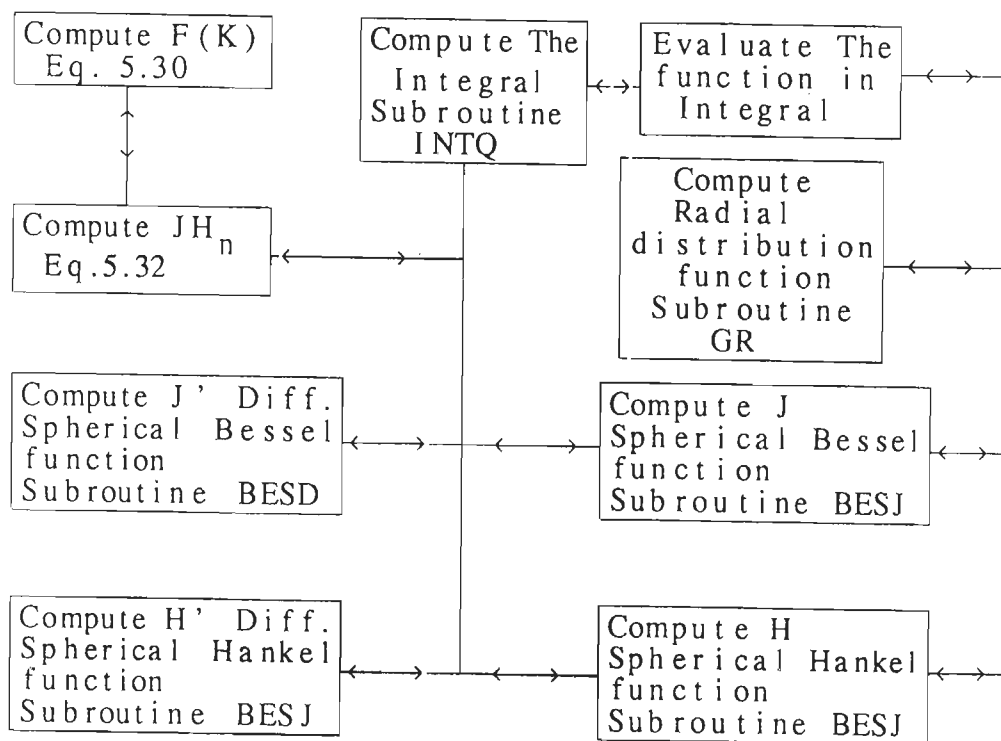


Fig 5.5b

The elements of the T-Matrix (Eq. 5.31) are computed using the computer program listed in Appendix 5.4, and the organization of the program is explained in Fig 5.6

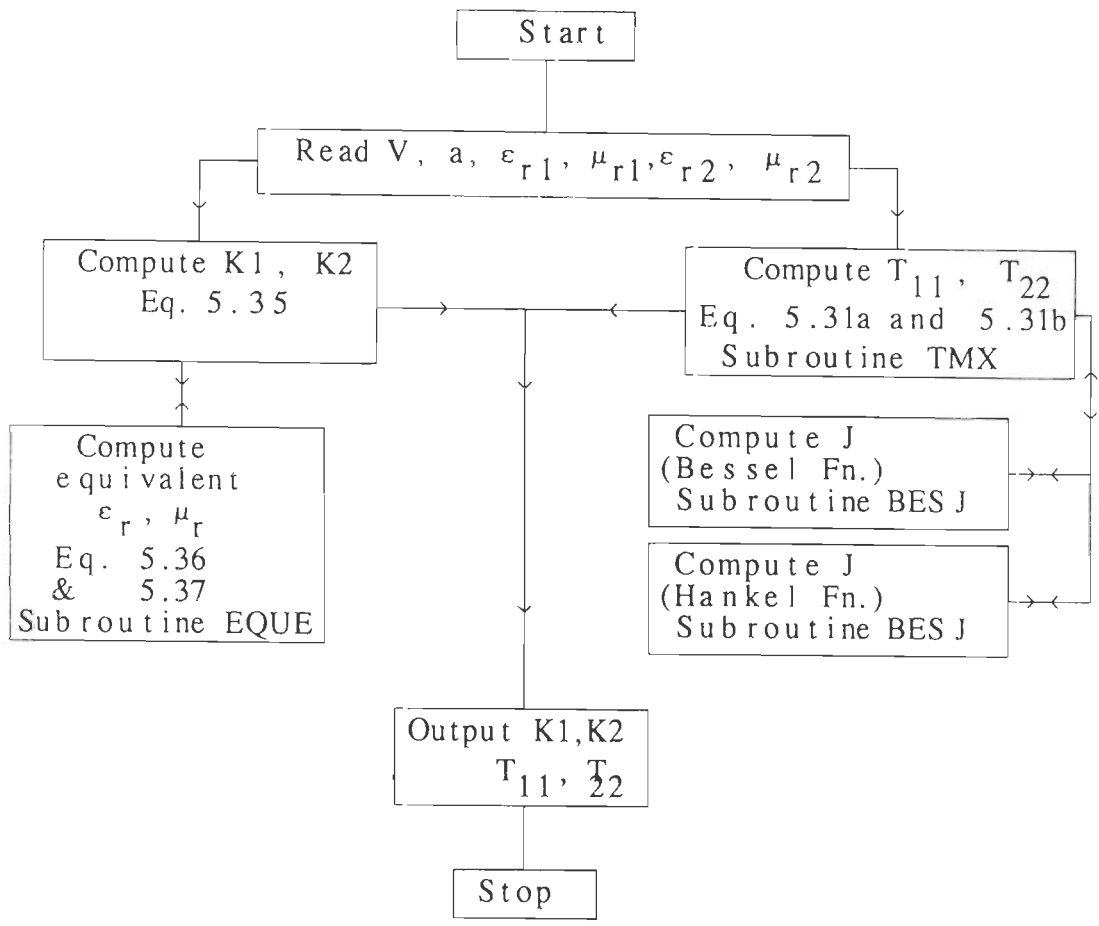


Fig 5.6

Since initial guess for the wave number are required in Muller technique, initial values for normalized wave number K, were computed using the following equations.

$$K = \sqrt{\mu_{re} \epsilon_{re}} \tag{5.35}$$

where μ_{re} and ϵ_{re} the effective permeability and permittivity respectively for the medium is computed using the Lichtenecker's formula, Eq (3.6c).

The subroutine listed in Appendix 5.4 computes two roots of Eq. (5.35) as the initial values for K, which were then utilized by the Muller technique to search for effective wave number in the complex plane.

The inputs to the program listed in Appendix 5.4 are

V , the volume concentration of the lossy material,

a , the average particle radius,

ϵ_{r1} , and ϵ_{r2} the complex relative permittivity of the lossy material and binder respectively,

μ_{r1} , and μ_{r2} the complex relative permeability of the lossy material and binder respectively.

The outputs of this program are T_{11} , T_{22} (the elements of the T-Matrix) and $K1$, $K2$ the initial values for Muller technique, to determine the effective wave number of the media.

The loss is then computed using Eq. (4.15) and (4.7a). Appendix 5.5 gives the program listing to compute Eq. (4.15),

5.7 ANALYSIS OF ABSORBERS USING EFFECTIVE WAVE NUMBER

The broad band absorbers designed, fabricated and tested in chapter III and IV (named as BBA and MBA for convenience) are analyzed, by estimating their theoretical performance with the wave number determined now, by solving Eq. (5.30). The design parameters for the two broad band absorbers obtained in chapter III and IV are tabulated in Table 5.1.

The simulated absorption pattern with effective wave number now computed using Eq. (5.30), along with results in chapter III for BBA are plotted in Fig 5.7. It can be observed from the curves that simulation of the performance of BBA, via., the T-matrix approach for the wave number, reproduces the experimentally determined absorption pattern of the absorber. Also it reproduces the small resonance peak,

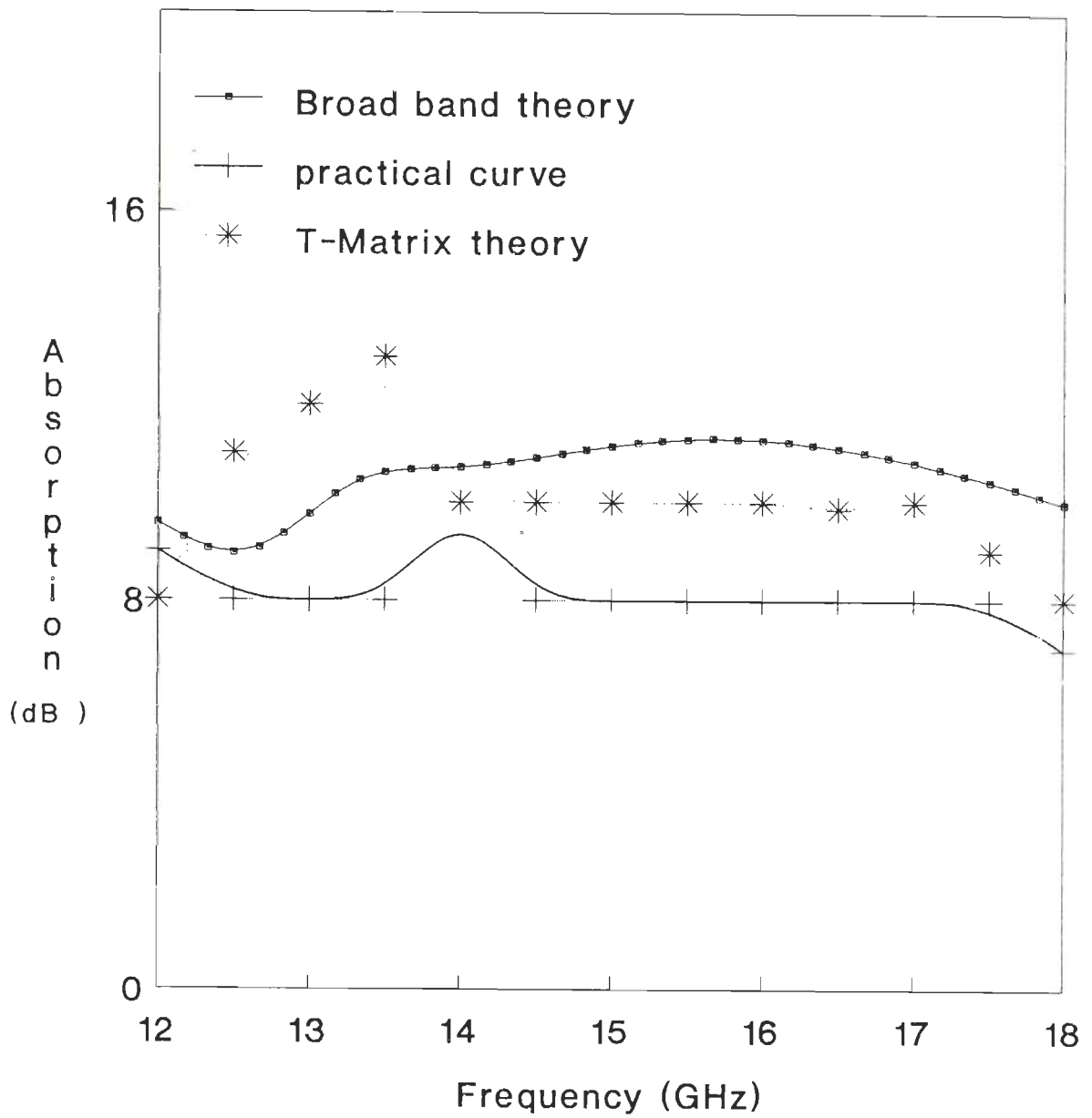


Fig 5.7 Absorption characteristics for the designed and fabricated BBA.

that was experimentally observed in the absorber, which was absent in the simulation by the earlier approach.

Table 5.1

Particulars	BBA	MBA
Lossy (LM) Material	Co-BHF	Co-BHF
Binder (B)	Silicone rubber	Silicone rubber
LM : B	45:55%	45:55%
f_r of Co-BHF	12.63 GHz	12.63 GHz
Absorber thickness	1.8mm	1.8mm
Average particle size	10microns	30microns

The resonance or peak absorption frequency has deviated by approximately 0.5 GHz higher than theoretically predicted value. Further the absorption at resonance is only around 3-4 dB higher than the flatter response region. Which is well followed by the experimentally obtained characteristics with a swell of 2-3 dB over the flatter region at the peaking frequency (14GHz).

The performance of MBA and the theoretical results obtained through the T-matrix approach for the effective number are plotted in Fig 5.8. It is easily observed that simulation of absorber performance with effective wave number, displays the flatter response of the absorber obtained experimentally through out the entire frequency band.

Further though the design of BBA and MBA absorbers were done for broad band operation over Ku-Band, using different design approaches. Both types of absorbers

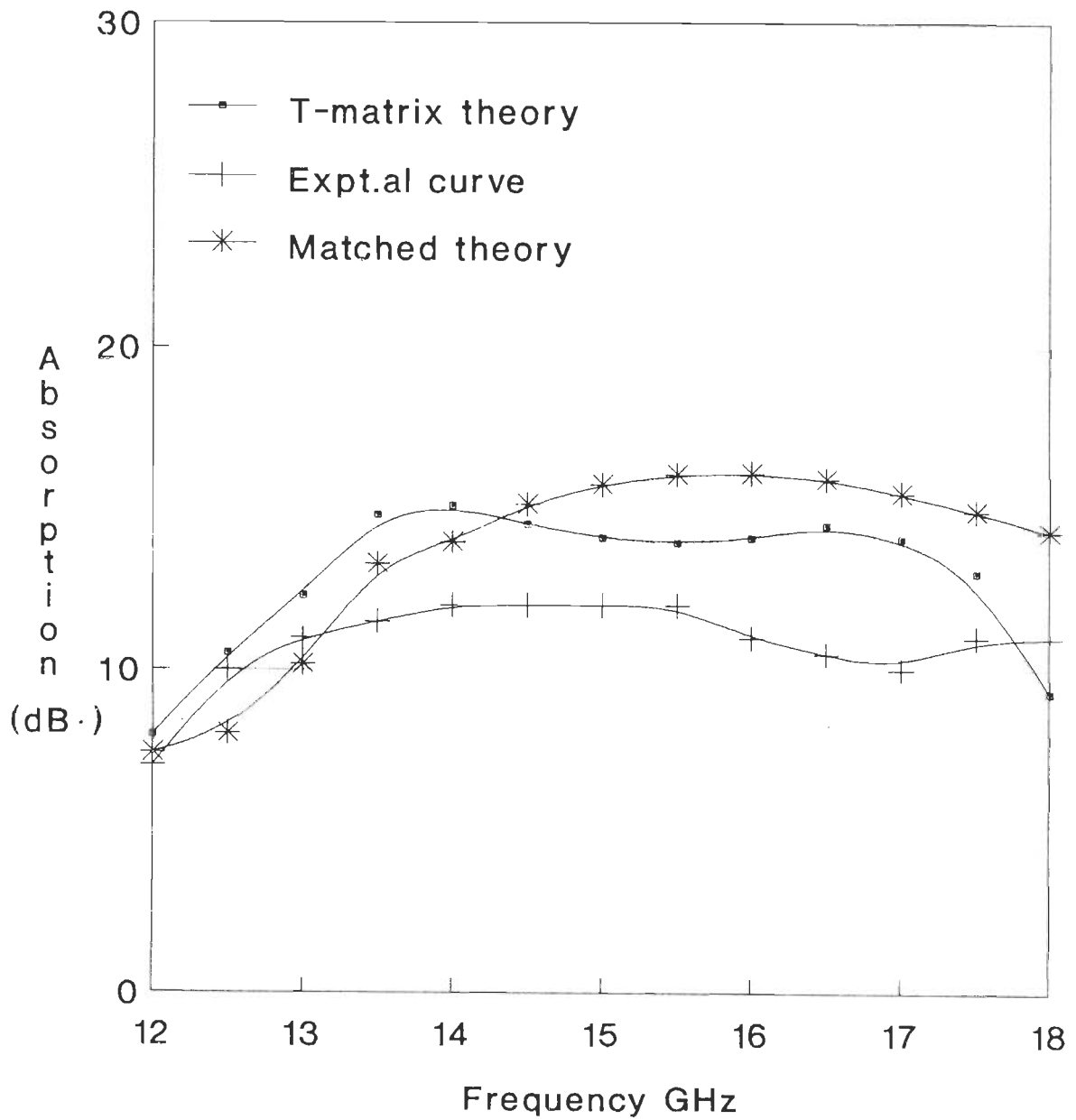


Fig 5.8 Absorption characteristics for the designed and fabricated matched absorber.

have the same lossy material, binder, identical thickness and volume concentration of the lossy material. But differ only in the average particle size of the Co-BHF used. Yet, it can be observed from Fig 5.7 and 5.8., that MBA displays higher absorption characteristics through out the frequency band, in both theoretical as well as experimental results. Thus bringing to light the importance of the effect of average particle size on overall absorption.

The general decrease of 2-3 dB absorption in experimentally obtained results compared to the theoretically predicted values, is due to the practical limitations of the fabrication process.

5.8 DESIGN ANALYSIS OF A BROAD BAND MICROWAVE ABSORBER

Ferrites (Fe_3O_4) have been used by many workers [8-14], to design and develop resonant type absorbers or to improve performance of resonant type absorbers. Ferrites have been comprehensively analyzed by many authors [10-14, 20,21,48], for their microwave absorptive properties. They have concluded that ferrite is a very strong candidate, especially due to its high magnetic loss tangent.

Hence, ferrite was selected as the lossy material to design and develop an absorber to operate as a broad band absorber over X-Band, within a thickness constraint of 3mm. The design was made using the flexible tolerance optimization subroutine [119], in a iterative manner to obtain the required microwave absorptive properties, within practicably achievable parameters. The values of ϵ_r and μ_r at 10 GHz for ferrite was deduced from the data tabulated by Von Hippal [133], and the from the results of [45] as

$$\epsilon_r = 15 - j1.2 \quad 5.36a$$

$$\mu_r = 0.9 - j1.0$$

5.36b

which were assumed to be constant over X-Band.

The optimization subroutine was run several times with different numerical weights along with Eq. (4.15), (4.7a), (4.22a) and further Eq (5.30) was used to solve for the effective wave number in the media. The real part of which enables to determine the refractive index of the absorber- composite. The thickness of the absorber was then computed through Eq. (4.25). The optimized parameters for the absorbers which were chosen from a number of iterative trails are tabulated in Table 5.2.

Table 5. 2

Particulars	Absorber
Lossy (LM) Material	Ferrite
Binder (B)	Silicone rubber
LM : B	45 : 55 %
Absorber thickness	2.3mm
Average particle size	20microns

The complex effective wave number obtained by Eq. 5.30 for the designed volume concentration of ferrite in rubber, as a function of average particle size 'a' is plotted in Fig 5.9a and 5.9b at 8 GHz, while in Fig 5.10a and 5.10b it is plotted at 10 GHz. The significance of 'a' can be easily felt from these two graphs. The absorption index p, which is inferred from the imaginary part of the effective wave number, increases significantly as the average particle size is lowered. It reaches

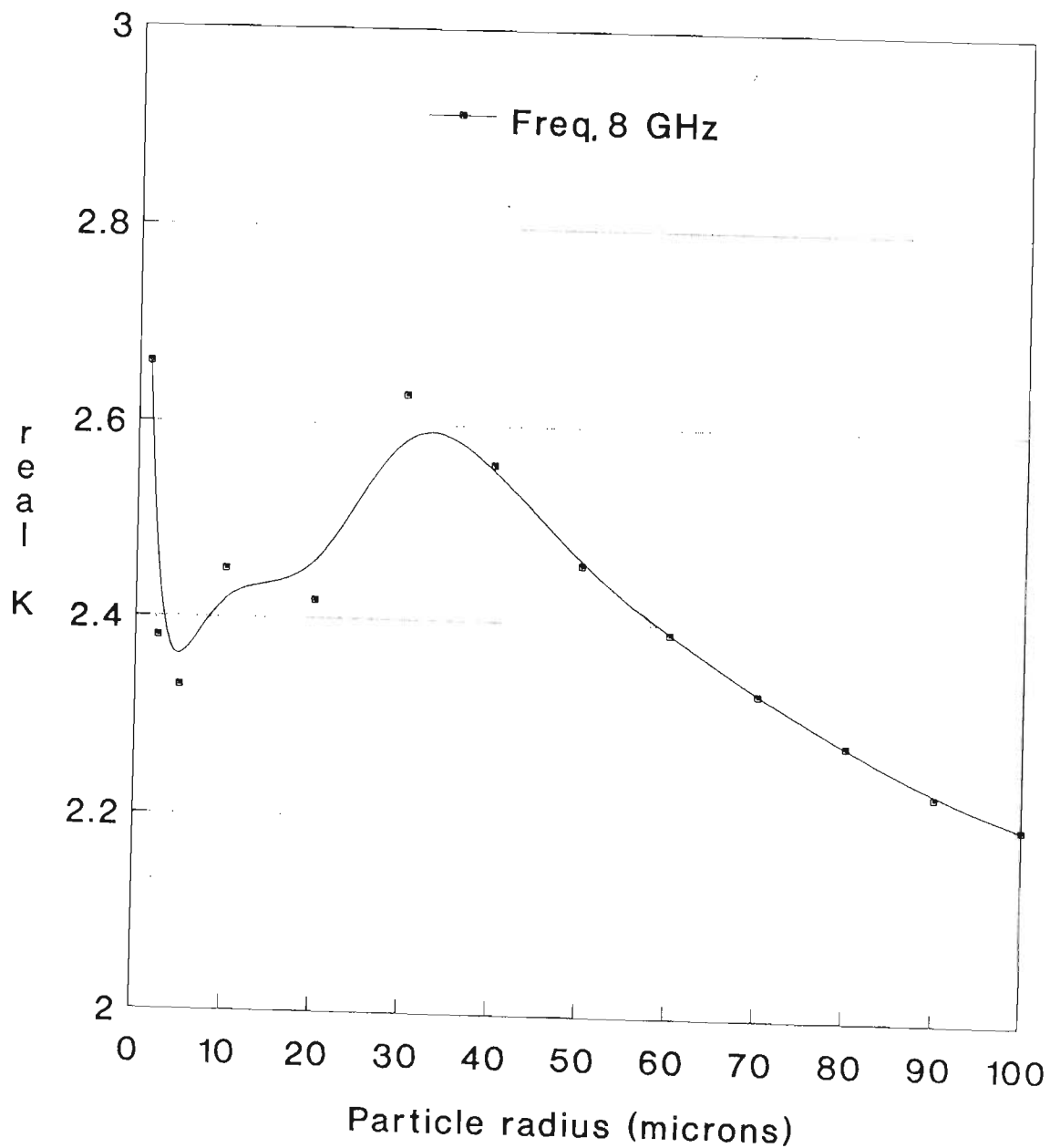


Fig 5.9a Variations of Normalized value of the real part of the effective wavenumber with particle size for spherical Fe O particles in rubber.

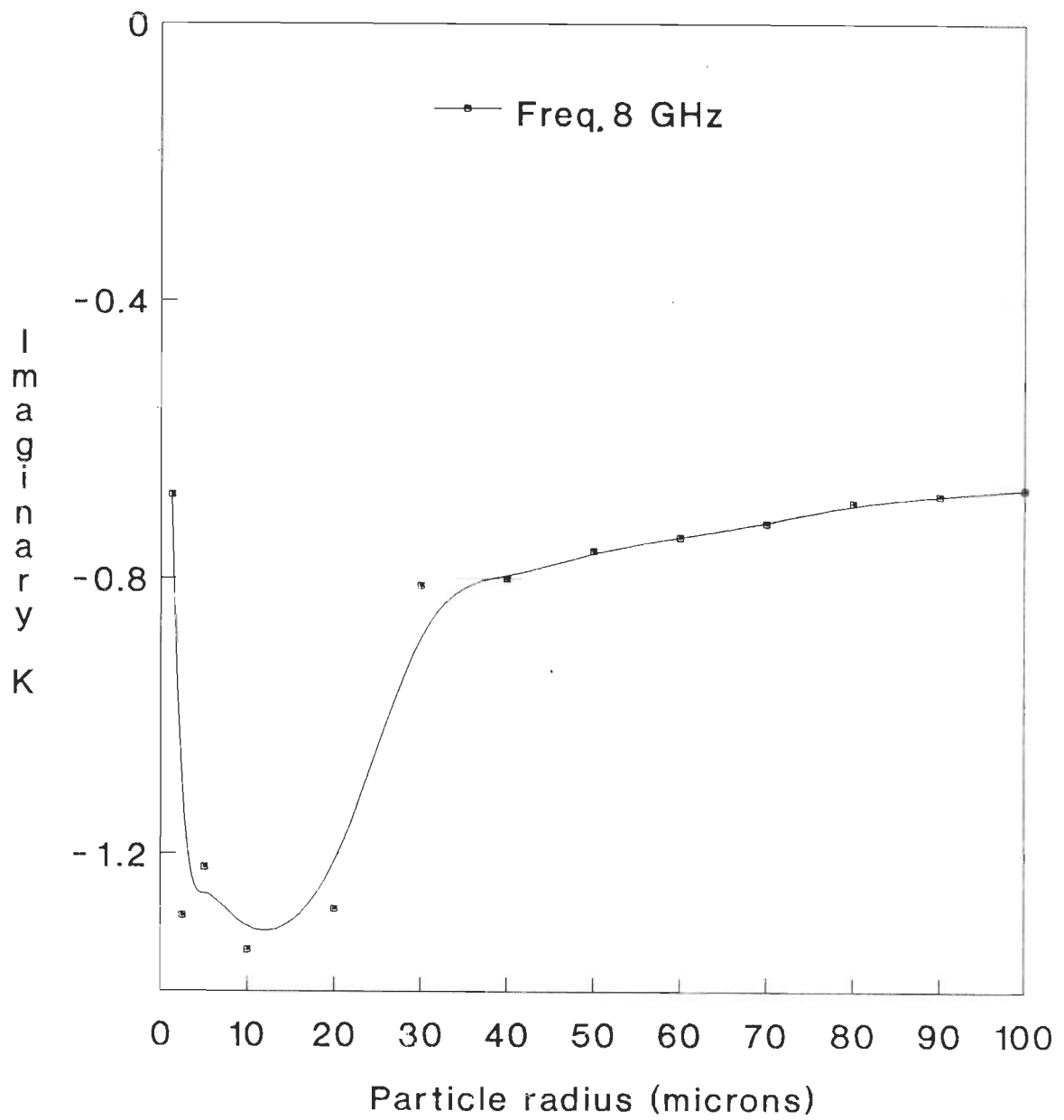


Fig 5.9b Variation of the imaginary part of the effective wavenumber with particle size for spherical Fe O particles in rubber.

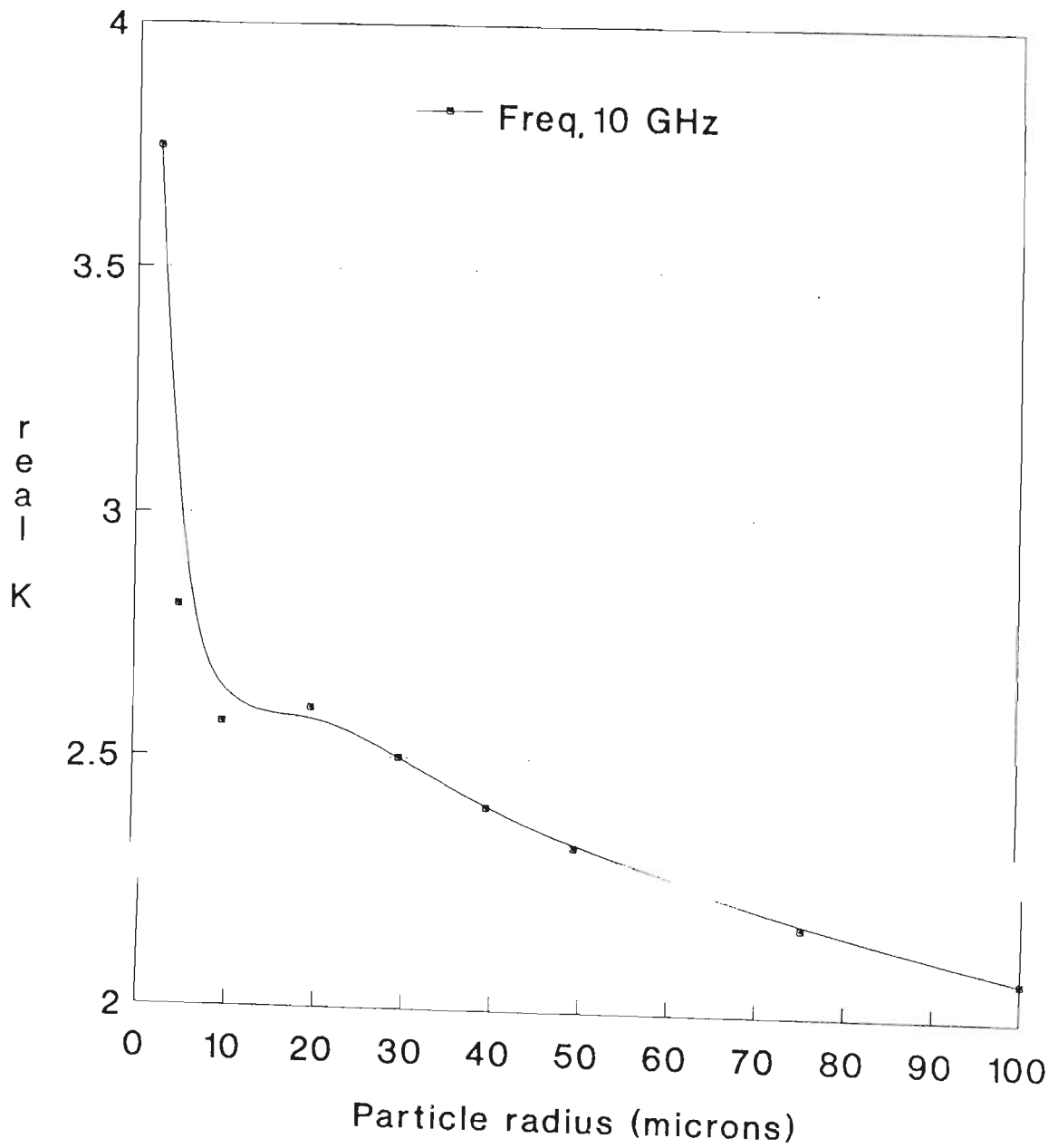


Fig 5.10a Variation of the real part of the effective wave-number with particle size for spherical Fe O particles in rubber

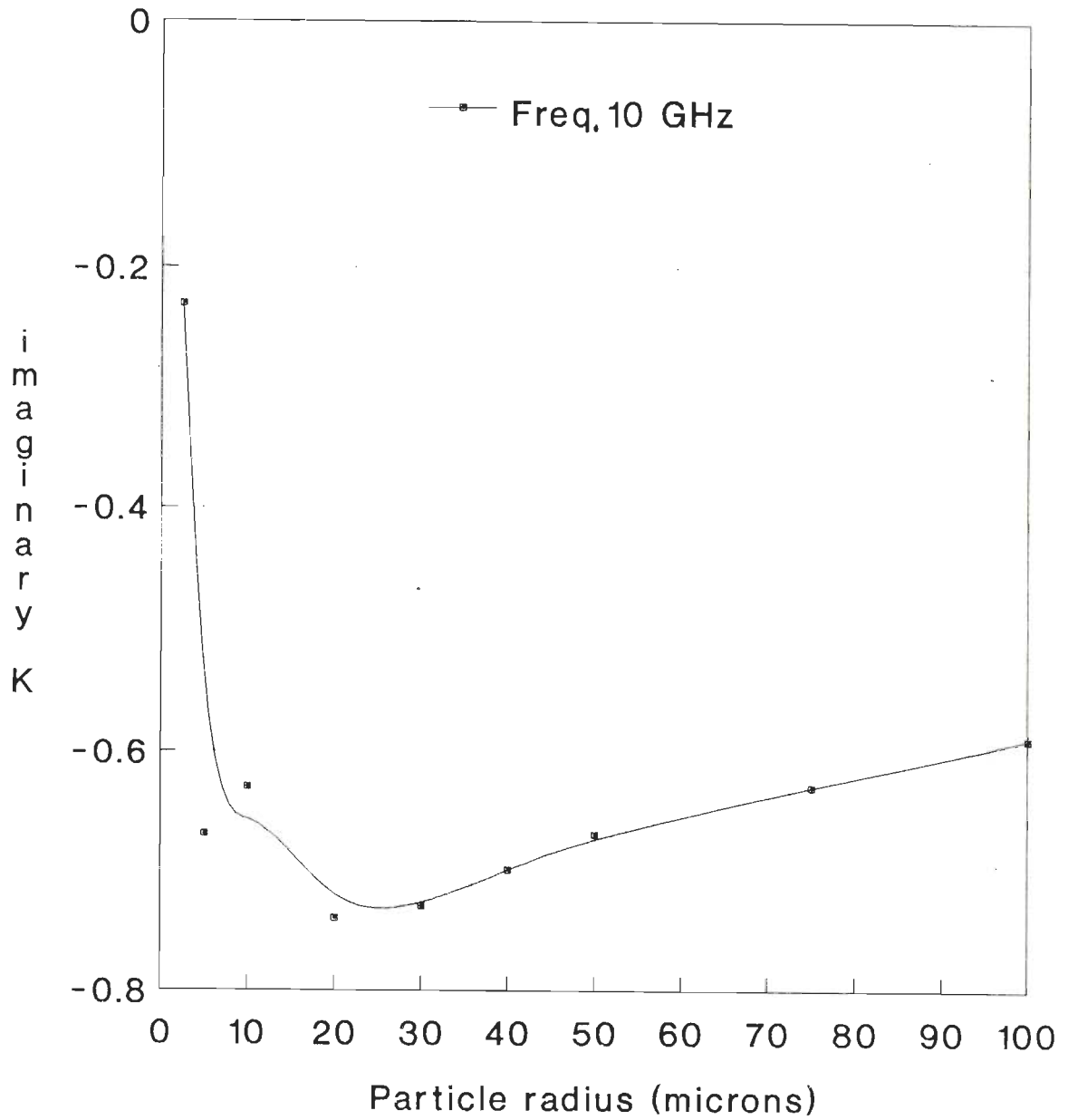


Fig 5.10b Variation of the imaginary part of the effective wavenumber with particle size for spherical Fe O particles in rubber.

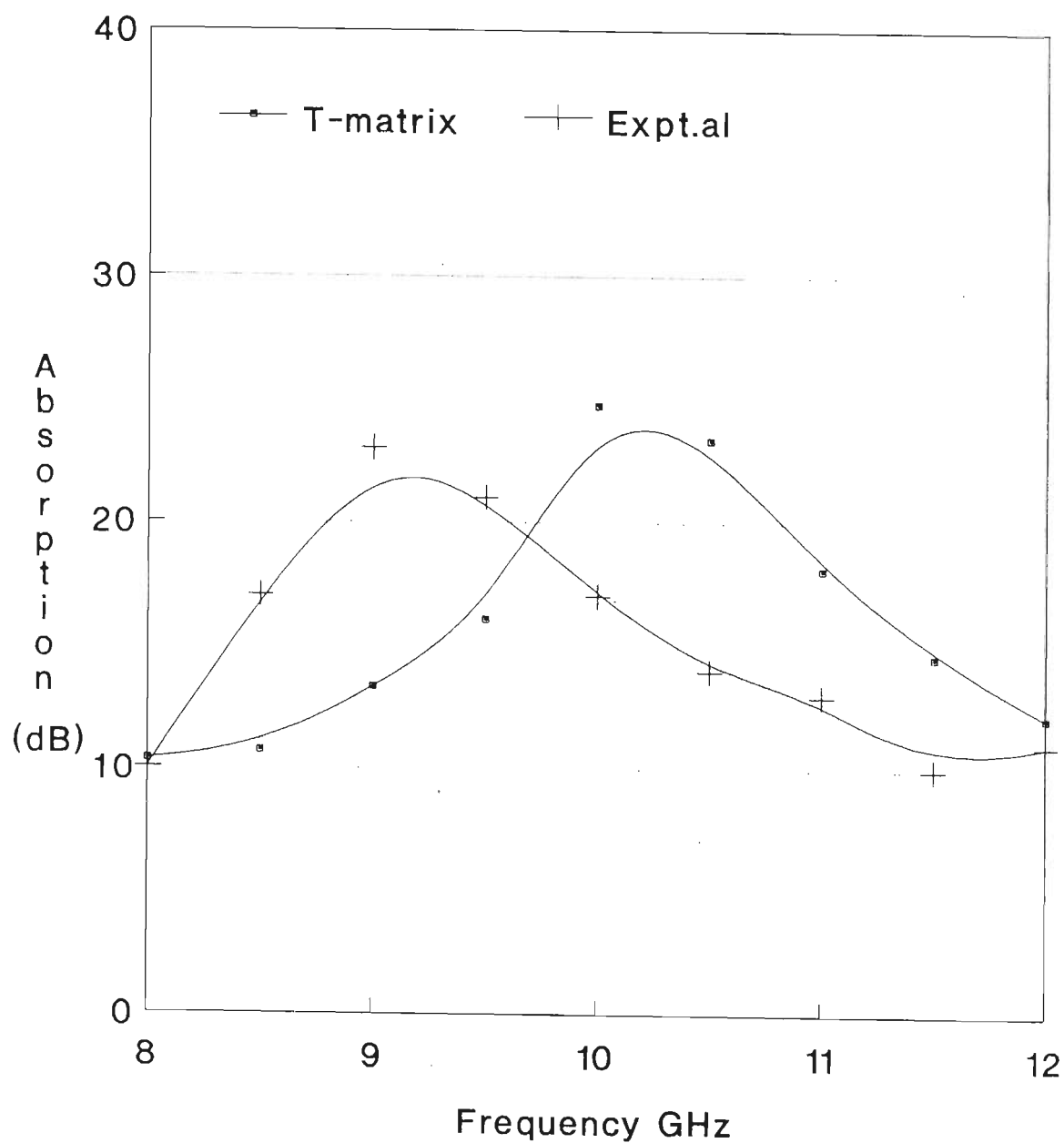


Fig 5.11 Absorption characteristics for the designed and fabricated ferrite-rubber absorber.

a maximum around 20-30 microns, implying that higher absorption can be achieved over this range of particle size.

5.9 EXPERIMENTAL RESULTS

Ferrite, the lossy material required was prepared in the laboratory, since our first venture with commercially available ferrite powder proved unsuccessful. A highly pure ferrite powder, with near spherical shape was prepared using the wet method described in chapter 8. The ferrite and rubber in the required ratio were mixed in a two roll mill and then hot pressed into a sheet of 2.6mm.

The measurement set up shown in Fig 3.4 was once again employed to determine experimentally the absorption characteristics of the fabricated absorber. Theoretically simulated and experimentally obtained absorption curves for the absorber are shown in Fig 5.11. The absorber behaves well as an broad band absorber, as seen from the experimentally obtained curve. It provides a minimum 10 dB absorption over entire X-Band. However the experimentally obtained peak absorption frequency is observed (Fig 5.11) to have shifted by 1 GHz from the corresponding theoretical value.

5.10 CONCLUSION :

Waterman's T-matrix approach has been utilized in a multiple scattering formulation, to determine the bulk or effective propagation constant for the composite absorbing medium, as a function of particle (scatterer) size and shape, volume concentration of the lossy material, orientation and position of the scatterer in the binder or host matrix. In the multiple scattering model, T-matrix

is used to represent the effect of size and shape of individual lossy particles and the random nature of orientation of the particles in the host matrix. An average over all possible position is performed using the two-point joint probability function, which in turn is defined by the radial distribution function obtained under the self consistent approximation. A closed form solution of the equation for the wave number in composite media is obtained under the long wavelength approximation.

The designed and fabricated BBA and MBA broad band absorber's performance, were verified using this approach. This model describes more closely the practical behavior of the absorbers than the earlier methods, thus proving that bulk properties have to be considered, when high loss materials are employed in the design.

Employing the proposed model, the optimum configuration for a ferrite-rubber composite, such as size of the spherical particles (scatterer), volume concentration of the ferrite and thickness of the absorber were determined for broad band operation over X-Band within 3 mm thickness limitation. Experimentally a minimum 10dB absorption over entire X-Band (8-12 GHz), has been achieved by the designed and fabricated absorber of thickness 2.3 mm. Which is in good agreement (Fig 5.11) with the theoretically predicted curve as a broad band absorber, except for the shift in the peak absorption frequency. The effect of particle size on the performance of the absorber has been analyzed and experimental results confirm the theoretical analysis.

Expansion Of Vector Plane Waves [124]

Within any closed domain of a homogeneous, isotropic medium from which sources have been excluded, all vectors E , B , D and H , the vector potential and the Hertzian vectors- satisfy one and the same differential equation. If C is any such vector, then

$$\nabla^2 C - \mu\epsilon \frac{\partial^2 C}{\partial t^2} - \mu\sigma \frac{\partial C}{\partial t} = 0 \quad \text{A5.1}$$

The above equation can be rewritten as

$$\nabla \nabla \cdot C - \nabla \nabla \times \nabla \times C + K^2 C = 0 \quad \text{A5.2}$$

The vector C can be resolved into its rectangular components as

$$\nabla^2 C_i + K^2 C_i = 0; \quad i = x, y, z. \quad \text{A5.3}$$

where K is the complex wave number in the media.

Let a solution to Eq. (A5.2) given by vector functions \mathfrak{M} and \mathfrak{N} , as

$$\mathfrak{M} = \nabla \times (I_1 u(r)\psi) = \frac{1}{K} \nabla \times \mathfrak{N} \quad \text{A5.4}$$

where $u(r)$ is an unknown scalar function of r . Then if \mathfrak{M}_1 , \mathfrak{M}_2 and \mathfrak{M}_3 are the R , θ and ϕ components of \mathfrak{M} in a spherical coordinate system, we have

$$\mathfrak{M}_1 = 0; \quad \mathfrak{M}_2 = \frac{1}{R \sin\theta} \frac{\partial}{\partial \phi}(u\psi); \quad \text{and} \quad \mathfrak{M}_3 = -\frac{1}{R} \frac{\partial}{\partial \theta}(u\psi) \quad \text{A5.5}$$

The divergence of \mathfrak{M} is zero and expanding $\nabla \times \nabla \times \mathfrak{M} - K^2 \mathfrak{M} = 0$, into R , θ and ϕ components, we find that the R component is zero. In spherical coordinates both the tangential components (θ and ϕ) components are identical and will be zero provided $u(r)$ is such that

$$\frac{\partial^2}{\partial R^2}(u\psi) + \frac{1}{R \sin\theta} \frac{\partial}{\partial \theta} \left[\sin\theta \frac{\partial}{\partial \theta}(u\psi) \right] + \frac{1}{R^2 \sin^2\theta} \frac{\partial^2}{\partial \phi^2}(u\psi) + K^2 u\psi = 0 \quad \text{A5.6}$$

If, we choose $u(r) = R$, then the above equation will reduce to

$$\nabla^2 \psi + K^2 \psi = 0 \quad \text{A5.7}$$

Thus in spherical coordinates Eq. (A5.2) is satisfied by

$$\mathfrak{M} = \nabla \times R\psi = \frac{1}{K} \nabla \times \mathfrak{N} \quad \text{A5.8}$$

whose components are

$$\mathfrak{M}_1 = 0; \quad \mathfrak{M}_2 = \frac{1}{\sin\theta} \frac{\partial \psi}{\partial \phi}; \quad \text{and} \quad \mathfrak{M}_3 = -\frac{\partial \psi}{\partial \theta} \quad \text{A5.9}$$

From the relation $K\mathfrak{N} = \nabla \times \mathfrak{M}$ the components of a third solution can be easily found,

$$K\mathfrak{N}_1 = \frac{\partial^2 (r\psi)}{\partial R^2} + K^2 R\psi; \quad \text{A5.10a}$$

$$\mathfrak{N}_2 = \frac{1}{KR} \frac{\partial (r\psi)}{\partial R \partial \theta}; \quad \text{A5.10b}$$

$$\text{and} \quad \mathfrak{N}_3 = \frac{1}{KR} \frac{1}{\sin\theta} \frac{\partial (r\psi)}{\partial R \partial \theta} \quad \text{A5.10c}$$

It now remains to obtain the expansion for the incident vector wave represented by,

$$f(z) = ae^{-jkz} = a e^{-jKr \cos\theta} \quad \text{A5.11}$$

to this end we proceed as follows-

$$\text{Let} \quad \psi_{nm} = f_{onm}^e e^{j\omega t} \quad \text{A5.12}$$

where f , is the characteristic solution, and can be expressed as

$$f_{onm}^e = \frac{\cos m\phi}{\sin m\theta} P_n^m(\cos\theta) z_n(kR) \quad \text{A5.13a}$$

and $z_n(kR)$ is defined as =

$$\begin{aligned} z_n(kR) &= \sum_{n=0}^{\infty} (2n+1) P_n(\cos\gamma) j_n(kR) h_n^{(1)}(kR_1) \quad (R_o < r_1) \\ &= \sum_{n=0}^{\infty} (2n+1) P_n(\cos\gamma) j_n(kR) h_n^{(1)}(kR_o) \quad (R_1 < r_o) \end{aligned} \quad \text{A5.13b}$$

where 'o' and '1' correspond to observation and source points.

To obtain explicit expression for the vector wave functions \mathfrak{M} and \mathfrak{N} , we need to carry out the differentiation of Eq. (A5.13) as required by Eq. (A5.9) and Eq. (A5.10). The time factor is split off by writing $\mathfrak{M} = me^{j\omega t}$ and $\mathfrak{N} = ne^{j\omega t}$ and we find, the expression for the vector wave functions \mathfrak{M} and \mathfrak{N} as

$$m_{onm}^e = \mp \frac{m}{\sin\theta} z_n(kR) P_n^m(\cos\theta) \frac{\sin m\phi}{\cos m\phi} I_2 - z_n(kR) \frac{\partial P_n^m(\cos\theta)}{\partial\theta} \frac{\cos m\phi}{\sin m\phi} I_3 \quad \text{A5.14}$$

$$n_{onm}^e = \frac{n(n+1)}{kR} z_n(kR) P_n^m(\cos\theta) \frac{\cos m\phi}{\sin m\phi} I_1 + \frac{1}{kR} \frac{\partial}{\partial R} [R z_n(kR)] \frac{\partial P_n^m(\cos\theta)}{\partial\theta} \frac{\cos m\phi}{\sin m\phi} I_2 \mp \frac{1}{kR} \frac{m}{\sin\theta} \frac{\partial}{\partial R} [R z_n(kR)] P_n^m(\cos\theta) \frac{\sin m\phi}{\cos m\phi} I_3 \quad \text{A5.15}$$

where I_j are the unit vectors for the spherical coordinate system.

The vector a in Eq. (A5.11) can be resolved into three vectors directed along the x-, y-, and z-axis respectively as

$$a_x = \sin\theta \cos\phi I_1 + \cos\theta \cos\phi I_2 - \sin\phi I_3, \quad \text{A5.16a}$$

$$a_y = \sin\theta \sin\phi I_1 + \cos\theta \sin\phi I_2 - \cos\phi I_3, \quad \text{A5.16b}$$

$$a_z = \cos\theta I_1 - \sin\theta I_2 \quad \text{A5.16b}$$

Now the divergence of the vector functions a_x and a_y is zero and consequently they may be expanded in terms of the characteristic functions m and n alone. At $R = 0$, the field is finite and we shall, therefore, require functions of the first kind. Whence upon consideration of the odd and even properties of Eq. (A5.14) and (A5.15), we set up the expansion

$$a_x = e^{-jKR} \cos\theta \sum_{n=0}^{\infty} \sum_{m=-n}^n (a_n m_{nm}^{(1)} + b_n n_{nm}^{(1)}) \quad \text{A5.17}$$

Utilizing the orthogonality relations for the functions, we obtain the coefficients as

$$a_n = \frac{2n + 1}{n(n + 1)} (j)^n \quad \text{A5.18a}$$

$$b_n = -\frac{2n + 1}{n(n + 1)} (j)^{n+1} \quad \text{A5.18b}$$

hence,

$$a_x = e^{-jkz} \sum_{n=0}^{\infty} \sum_{m=-n}^n j^n \frac{2n + 1}{n(n + 1)} [m_{omn}^{(1)} - jn_{emn}^{(1)}] \quad \text{A5.19a}$$

Similarly, we can obtain a_y as

$$a_y = e^{-jkz} \sum_{n=0}^{\infty} \sum_{m=-n}^n j^{n+1} \frac{2n + 1}{n(n + 1)} [m_{omn}^{(1)} + jn_{emn}^{(1)}] \quad \text{A5.19a}$$

The expansion for E^s , E^e and E^{inc} in Eq. (5.6) - (5.7), are obtained by applying the above procedure for each field vector.

Muller Technique To Determine Complex Roots.

Muller method [143] is useful for obtaining the complex roots of a function, and it is reasonably straight forward to implement as a computer program.

Given three points, the technique involves the construction of a quadratic polynomial that passes through the given three points $(x_i, f(x_i))$. One of the roots of this polynomial is used as an improved estimate for a root of the function $f(x)$.

The quadratic polynomial is given by

$$p(x) = f(x_3) + w(x - x_3) + f[x_3, x_2, x_1](x - x_3)^2 \quad \text{B5.1}$$

where $w = f[x_3, x_2] + f[x_3, x_1] - f[x_1, x_2]$

The divided differences $f[x_i, x_j]$ and $f[x_i, x_j, x_k]$ are defined [143, page 9] as

$$f[x_i, x_j] = \frac{f(x_j) - f(x_i)}{x_j - x_i} \quad \text{B5.2}$$

$$\text{and } f[x_i, x_j, x_k] = \frac{f[x_j, x_j] - f[x_i, x_j]}{x_k - x_i} \quad \text{B5.3}$$

we need to find the smallest value of $x - x_3$ that satisfies Eq. (B5.1), thus finding the root closest to x_3 . The solution is

$$x - x_3 = \frac{-w \pm \sqrt{w^2 - 4f(x_2)f[x_2, x_1, x_0]}}{2f[x_2, x_1, x_0]} \quad \text{B5.4}$$

with the sign chosen to minimize the numerator. Because of the loss-of-significance errors implicit in this formula, we rationalize the numerator, to obtain the new

iteration formula as

$$x_4 = x_3 - \frac{2f(x_3)}{w \pm \sqrt{w^2 - 4f(x_3)f[x_3, x_2, x_1]}} \quad \text{B5.5}$$

with the sign of the root chosen to maximize the denominator.

With two initial assumptions for the root, a third root is constructed in between the assumed initial roots. Repeat Eq. (B5.5) recursively to define a sequence of iterates $\{x_n: n \geq 0\}$. If they converge to a point α , then α is a root of the polynomial. Else if $|f(\alpha)| \leq \epsilon$, a very small positive quantity then α , can be considered as an approximate root of the polynomial. Herein both these approaches have been employed to arrive at the roots of Eq. (5.30).

\$DEBUG

```

C   TMSB.FOR
COMPLEX T11,T22,AK(6),JH(5),AKA(5),FX(6),FX12,FX23,FX31
COMPLEX FX13,A,B,C,D,AK2,AKF
OPEN(UNIT=1,FILE='FKINI.DAT',STATUS='OLD')
OPEN(UNIT=4,FILE='FTME.DAT',STATUS='OLD')
OPEN(UNIT=2,FILE='FTMB.OUT',STATUS='NEW')
OPEN(UNIT=3,FILE='FTMSB.DAT',STATUS='NEW')
PI = 3.1415927
U0 = 12.56637E-07
E0 = 8.854E-12
FX(0)=(0,0)
AK(0)=(0,0)
READ(1,*)V,AR
DO 1000 KLI=1,21
READ(1,*)AF,(AK(I),I=1,2)
READ(4,*)T11,T22
AK(3)=(AK(1)+AK(2))/2.
AK0=2.*PI*AF*1.E+09*SQRT(E0*U0)
AK0=AK0*(AR*1.E-06)
AK(3)=(AK(1)+AK(2))/2.
1  DO 100 I = 1,4
   IF(I.EQ.4)THEN
C   MULLER's QUADRATIC INTERPOLATION TO DETERMINE K FOR FX=0
C   REF : K E ATKINSON, AN INTRODUCTION TO NUMERICAL ANALYSIS,
C   PP 72-74.
FX12=(FX(2)-FX(1))/(AK(2)-AK(1))
FX23=(FX(3)-FX(2))/(AK(3)-AK(2))
FX31=(FX(1)-FX(3))/(AK(1)-AK(3))
FX13=(FX23-FX12)/(AK(3)-AK(1))
B=FX23+FX31-FX12
D=CSQRT(B*B-(4.*FX(3)*FX13))
A=B+D
C=B-D
IF(CABS(A).GT.CABS(C))THEN
D=A
ELSE
D=C
ENDIF
AK(4)=AK(3)-(2.*FX(3)/D)
ENDIF
AKA(I)=AK(I)*(AR*1.E-06)*AK0
DO 10 J=1,5
JH(J)=(0.,0.)
10 CONTINUE
IF(CABS(AK(I)-AK(I-1)).LE.(1.E-08))THEN
WRITE(2,*)' ROOT CONVERGES TO '
WRITE(3,*)AK(I),AK(1)
WRITE(2,*)AK(I),FX(4)
WRITE(*,*)AK(I),AK(1)

```

```

WRITE(*,*)AK(3),FX(4)
WRITE(2,*)AF,AR,V
GO TO 1000
ENDIF
CALL JHN(V,AKO,AKA(I),JH)
T1=T11*(JH(0)+0.5*JH(2))-1.
T2=(3./2.)*T22*JH(1)
T3=(3./2.)*T11*JH(1)
T4=T22*(JH(0)+0.5*JH(2))-1.
FX(I)=T1*T4-T2*T3
WRITE(*,*)FX(I)
IF(I.NE.1)THEN
IF(CABS(FX(I)-FX(I-1)).LT.(1.E-08))THEN
WRITE(3,*)AK(I),AK(1)
WRITE(2,*)AK(I),FX(I)
WRITE(2,*)AF,AR,V
GO TO 1000
ENDIF
ENDIF
WRITE(*,*)AK(I),FX(I),AF
IF(CABS(FX(I)).LT.(1.E-08))THEN
WRITE(2,*) ' REQUIRED ROOT IS '
WRITE(3,*)AK(I),AK(1)
WRITE(2,*)AK(I),FX(I)
WRITE(2,*)AF,AR,V
GO TO 1000
ENDIF
100 CONTINUE
AK(2)=AK(3)
AK(3)=AK(4)
GO TO 1
C MULLER END's
1000 CONTINUE
STOP
END
SUBROUTINE JHN(C,KO,KA,JH)
COMPLEX KA,KA2,JH(5),BJ,BDJ,HK,HDK,QINT
REAL KO,KO2
AL=1.
UL=4.
KO2=2.*KO
KA2=2.*KA
DO 20 J = 1,3
J1=J-1
AJ1=J1
BJ=CMPLX(0,0)
BDJ=CMPLX(0,0)
HK=CMPLX(0,0)
HDK=CMPLX(0,0)
QINT=(0,0)
CALL BESJ(AJ1,KA2,BJ)
CALL BESJD(AJ1,KA2,BDJ)

```

```

CALL HANK(AJ1,KO2,HK)
CALL HANKD(AJ1,KO2,HDK)
CALL INTQ(AJ1,AL,UL,C,KO2,KA2,QINT)
JH(J)=((6.*C)/(KO*KO-KA*KA))*(KO2*BJ*HDK-KA2*HK*BDJ)
JH(J)=JH(J)+24.*C*QINT
20 CONTINUE
RETURN
END
SUBROUTINE INTQ(AJ1,A,B,C,KO2,KA2,QINT)
C INTEGRAL OF A FUNCTION BETWEEN a & b, BY TEN POINT
C GAUSS-LEGENDRE INTEGRATION.
COMPLEX KA2,QINT,X1,X2
DIMENSION X(5),W(5)
W(1)=0.2955242247
W(2)=0.2692667193
W(3)=0.2190863625
W(4)=0.1494513491
W(5)=0.0666713443
X(1)=0.1488743389
X(2)=0.4333953941
X(3)=0.6794095682
X(4)=0.8650633666
X(5)=0.9739065285
XM=0.5*(B+A)
XR=0.5*(B-A)
QINT=(0,0)
DO 11 J=1,5
DX=XR*X(J)
XS=XM+DX
XD=XM-DX
CALL FN(AJ1,C,KO2,KA2,XS,X1)
CALL FN(AJ1,C,KO2,KA2,XD,X2)
QINT=QINT+W(J)*(X1+X2)
11 CONTINUE
QINT=XR*QINT
RETURN
END
SUBROUTINE FN(AJ1,C,KO2,KA2,X,XY)
COMPLEX KA2,KA2X,XY,BJ,HK
REAL KO2,KO2X
KA2X=KA2*X
KO2X=KO2*X
BJ=CMPLX(0,0)
HK=CMPLX(0,0)
CALL BESJ(AJ1,KA2X,BJ)
CALL HANK(AJ1,KO2X,HK)
CALL GR(C,X,GX)
XY=X*X*(GX-1.)*HK*BJ
RETURN
END
SUBROUTINE GR(RH0,R1,GX)
C CALCULATION OF RADIAL DISTRIBUTION GO(R)

```

```

C USING HENDERSONS PROGRAM
C CORRECTION IS MADE TO P-Y GO(R) USING VERLET AND WIES METHOD
C RHO=DENSITY*(SIGMA=2a)**3
C R1=R/SIGMA (=R/2a)
C REF : STATISTICAL MECHANICS by McQUIRRI
COMPLEX EX12,IG102,IG202,IG212,IG222,IG302,IG312,IG322,IG332
COMPLEX IG402,IG412,IG422,IG432,IG442,IT2,EX2,IXL1C,IXL2C
COMPLEX IXL3C,IXL4C,IXL5C,ILTC,JX,ISPC,ISDPC
REAL LT,LT1,LT2,LP
PIE=3.14159265
K=0
RH0S=0.0
IF(K.NE.0)THEN
GO TO 1
ELSE
ENDIF
X=2.*PIE/3.
JX=CEXP(CMPLX(0,X))
K=1
ETAC=PIE/6.*RH0
ETA=ETAC*(1.-ETAC/16.)
ETAM=1.-ETA
BOT1=ETAM**4
TOP=1.+2.*ETA
TOP1=TOP*TOP
C1=TOP1/BOT1
BOT2=4.*BOT1
TOPP=2.+ETA
TOP2=TOPP*TOPP
C2=-TOP2/BOT2
C2=6.*ETA*C2
C3=ETA*C1/2.
C MADE A CHANGE IN THE ORDER OF THE FOLLOWING STATMENT !
C SHIFTING FROM LINE ORIGINAL PLACE TO HERE
1 IF(ABS(RH0-RH0S).LT.1.E-04)GO TO 10
RH0S=RH0
A1=0.75*ETA*ETA*(1.-ETA*(0.7117+0.114*ETA))/BOT1
A2=24.*(A1/ETA)*ETAM*ETAM/(1.+0.5*ETA)
A3=CUBER(ETAC/ETA)
ETA12=12.*ETA
LT1=1.+ETA/2.
LT2=1.+2.*ETA
LP=LT1
XETA=1./(1.-ETA)
ETA3=(1.-ETA)**2
SP1=1.
SP2=4.*ETA*XETA
SP3=6.*(ETA*XETA)**2
SDP1=2.
SDP2=SP2
STP=2.
FF=(3.-ETA)*ETA+3.

```

```

PAR=SQRT(1.+2.*(ETA**2/FF)**2)
YP=CUBER(1.+PAR)
YM=CUBER(1.-PAR)
PAR=CUBER(2.*ETA*FF)
T1=XETA*(-2*ETA+PAR*(YP+YM))
IT2=XETA*(-2*ETA+PAR*(YP*JX+YM/JX))
XF1=3.*ETA3
PAR=ETA3**2/ETA
XF2=PAR*3./4.
PAR=PAR*ETA3/ETA
XF3=PAR*3./8.
PAR=PAR*ETA3/ETA
XF4=PAR*9./32.
LT=LT1*T1+LT2
SDP=SDP1*T1+SDP2
SP=(SP1*T1+SP2)*T1+SP3
EX11=EXP(-T1)
XL1=(LT/SP)**2
XL2=15.*SDP**2-4.*SP*STP
XL3=LT+4.*T1*LP
XL4=LT*SDP/SP
XL5=2.*LT+3.*LP*T1
G101=T1*LT/XF1/SP
G201=-LT/XF2/SP**2
G211=LT*(1.-T1*(2.+SDP/SP))+2.*LP*T1
G221=LT*T1
G301=LT/XF3/SP**3
G311=LT**2*T1/SP**2*(3.*SDP**2-SP*STP)-3.*LT*SDP/SP*(LT+3.*T1*LP)+6.*LP
1 *(LT+LP*T1)
G321=LT*(6.*LP*T1+LT*(2.-3.*SDP*T1/SP))
G331=G221*LT
G401=-LT/XF4/SP**4
G411=5.*T1*XL1*LT/SP*SDP*(2.*SP*STP-3.*SDP**2)+XL1*XL2*XL3-
1 24.*LP*XL4*XL5+12.*LP**2*(3.*LT+2.*T1*LP)
G421=(T1*XL1*XL2-12.*(XL4*XL3-LP*XL5))*LT
G431=(-6.*T1*XL4+3.*XL3)*LT**2
G441=G331*LT
ILTC=LT1*IT2+LT2
ISDPC=SDP1*IT2+SDP2
ISPC=(SP1*IT2+SP2)*IT2+SP3
EX12=CEXP(-IT2)
IXL1C=(ILTC/ISPC)**2
IXL2C=15.*ISDPC**2.-4.*ISPC*STP
IXL3C=ILTC+4.*IT2*LP
IXL4C=ILTC*ISDPC/ISPC
IXL5C=2.*ILTC+3.*IT2*LP
IG102=IT2*ILTC/XF1/ISPC
IG202=-ILTC/XF2/ISPC**2
IG212=ILTC*(1.-IT2*(2.+ISDPC/ISPC))+2.*LP*IT2
IG222=ILTC*IT2
IG302=ILTC/XF3/ISPC**3
IG312=ILTC**2*IT2/ISPC**2*(3.*ISDPC**2-ISPC*STP)-3.*ILTC*

```



```

1 ISDPC/ISPC*(ILTC+3.*IT2*LP)+6.*LP*(ILTC+LP*IT2)
  IG322=ILTC*(6.*LP*IT2+ILTC*(2.-3.*ISDPC*IT2/ISPC))
  IG332=IG222*ILTC
  IG402=-ILTC/XF4/ISPC**4
  IG412=5.*IT2*IXL1C*ILTC/ISPC*ISDPC*(2.*ISPC*STP-3.*ISDPC**2)
1 +IXL1C*IXL2C*IXL3C-24.*LP*IXL4C*IXL5C+12.*LP**2*(3.*ILTC
2 +2.*IT2*LP)
  IG422=(IT2*IXL1C*IXL2C-12.*(IXL4C*IXL3C-LP*IXL5C))*ILTC
  IG432=(-6.*IT2*IXL4C+3.*IXL3C)*ILTC**2
  IG442=IG332*ILTC
10 R=R1*A3
  IF(R.GT.5.)THEN
  GX=1.
  GO TO 100
  ELSE
  GO TO 11
  ENDIF
11 IF(R.LE.0.99999)THEN
  R3=R**3
  GX=C1+C2*R+C3*R3
  GO TO 100
  ELSE
  GO TO 1010
  ENDIF
1010 RRG=0.
C FIRST SHELL CONTRIBUTION
  EX1=EX11*EXP(R*T1)
  EX2=EX12*CEXP(R*IT2)
  RRG=RRG+G101*EX1+2.*IG102*EX2
  IF(R.LE.2.)GO TO 99
C SECOND SHELL CONTRIBUTION
  EX1=EX1*EX11
  EX2=EX2*EX12
  RRG=RRG+G201*EX1*(G211+G221*R)+2.*IG202*EX2*(IG212+IG222*R)
  IF(R.LE.3.)GO TO 99
C THIRD SHELL CONTRIBUTION
  RX=R-3.
  EX1=EX1*EX11
  EX2=EX2*EX12
  RRG=RRG+G301*EX1*((G331*RX+G321)*RX+G311)+2.*IG302*
1 EX2*((IG332*RX+IG322)*RX+IG312)
  IF(R.LE.4.)GO TO 99
C FOURTH SHELL CONTRIBUTION
  RX=R-4.
  EX1=EX1*EX11
  EX2=EX2*EX12
  RRG=RRG+G401*EX1*(((G441*RX+G431)*RX+G421)*RX+G411)+
1 2.*IG402*EX2*(((IG442*RX+IG432)*RX+IG422)*RX+IG412)
99 Z=A2*(R1-1.)
  GX=RRG/R+A1/R1*EXP(-Z)*COS(Z)
100 CONTINUE
  RETURN

```

```

END
FUNCTION CUBER(X)
IF(X.LT.0)THEN
AX=-X
AA=AX**(1./3.)
CUBER=-AA
ELSE
CUBER=X**(1./3.)
ENDIF
RETURN
END
SUBROUTINE BESJD(ANU,Z,AJD)
C PROGRAM TO CALCULATE DIFFERENTIATION VALUES FOR SPHERICAL
C BESSEL FUNCTIONS OF ORDER 0 1 AND 2 (j's)
C REF : HANDBOOK OF MATHEMATICAL FUNCTIONS by ABRAMOWITZ
C PAGE 438 (10.1.21,22)
COMPLEX Z,AJD,AX,AXN,AX1
AN1=1.
IF(ANU-AN1)1,2,2
1 AN=ANU+1.
CALL BESJ(AN,Z,AX)
AJD=-AX
GO TO 4
2 CALL BESJ(ANU,Z,AXN)
AN=ANU-1.
CALL BESJ(AN,Z,AX1)
AJD=AX1-(((ANU+1.)/Z)*AXN)
4 CONTINUE
RETURN
END
SUBROUTINE BESJ(ANU,Z,AJ)
C PROGRAM TO CALCULATE SPHERICAL BESSEL FUNCTIONS OF ORDER
C 0 1 AND 2
C REF : HANDBOOK OF MATHEMATICAL FUNCTIONS by ABRAMOWITZ
C PAGE 438 (10.1.11)
COMPLEX Z,AJ
AN1=1.
IF(ANU-AN1)1,2,3
1 AJ=(CSIN(Z)/Z)
GO TO 4
2 AJ=((CSIN(Z)/(Z*Z))-(CCOS(Z)/Z))
GO TO 4
3 AJ=(3./(Z*Z*Z)-(1./Z))*CSIN(Z)-(3./(Z*Z))*CCOS(Z)
4 CONTINUE
RETURN
END
SUBROUTINE HANKD(ANU,Z,HD)
C PROGRAM TO CALCULATE DIFFERENTIATION VALUES FOR SPHERICAL
C BESSEL FUNCTIONS OF ORDER 0 1 AND 2 (j's)
C REF : HANDBOOK OF MATHEMATICAL FUNCTIONS by ABRAMOWITZ
C PAGE 438 (10.1.21,22)
COMPLEX Z,HD,AX,AXN,AX1

```

```

AN1=1.
IF(ANU-AN1)1,2,2
1 AN=ANU+1.
  CALL HANK(AN,Z,AX)
  HD=-AX
  GO TO 4
2 CALL HANK(ANU,Z,AXN)
  AN=ANU-1.
  CALL HANK(AN,Z,AX1)
  HD=AX1-(((ANU+1.)/Z)*AXN)
4 CONTINUE
  RETURN
  END
C PROGRAM TO CALCULATE SPHERICAL HANKEL FUNCTIONS OF ORDER
C 0 1 AND 2
C REF : HANDBOOK OF MATHEMATICAL FUNCTIONS by ABRAMOWITZ
C PAGE 437-438 (10.1.11,12) & 10.1.1
SUBROUTINE HANK(ANU,Z,H)
COMPLEX Z,AJ,AY,H,C
AN1=1.
C=CMPLX(0,1.)
IF(ANU-AN1)1,2,3
1 AJ=CSIN(Z)/Z
  AY=-CCOS(Z)/Z
  GO TO 4
2 AJ=(CSIN(Z)/(Z*Z))- (CCOS(Z)/Z)
  AY=- (CCOS(Z)/(Z*Z))- (CSIN(Z)/Z)
  GO TO 4
3 AJ=(3./(Z*Z*Z)-(1./Z))*CSIN(Z)-(3./(Z*Z))*CCOS(Z)
  AY=(-3./(Z*Z*Z)+(1./Z))*CCOS(Z)-(3./(Z*Z))*CSIN(Z)
4 CONTINUE
  H=AJ+C*AY
  RETURN
  END

```

```

$DEBUG
C   FKINI.FOR
C   PROGRAM TO COMPUTE THE INITIAL VALUES OF K's
COMPLEX E(2),U(2),AK(10),T11,T22,AK2
OPEN(UNIT=1,FILE='FER.DAT',STATUS='OLD')
OPEN(UNIT=2,FILE='FKINI.DAT',STATUS='NEW')
OPEN(UNIT=3,FILE='FTME.DAT',STATUS='NEW')
CALL BHF
PI = 3.1415927
U0 = 12.56637E-07
E0 = 8.854E-12
READ(1,*)V
READ(1,*)AR
READ(1,*)E(1)
READ(1,*)E(2)
READ(1,*)U(1)
READ(1,*)U(2)
E(1)=E(1)*E0
E(2)=E(2)*E0
U(2)=U(2)*U0
U(1)=U(1)*U0
AK(1)=(1,0)
WRITE(*,*)E(1),E(2),U(2)
AK2=CSQRT(E(2)*U(2))/SQRT(E0*U0)
WRITE(2,*)V,AR
WRITE(*,*)V,AR
DO 10 I=1,21
READ(1,*)AF
CALL TMX(E(1),E(2),U(1),U(2),AF,AR,T11,T22)
WRITE(*,*)T11,T22
CALL DKL(E,U,V,AK(2))
AK(2)=AK(2)/SQRT(E0*U0)
WRITE(2,*)AF,AK(2),AK(1)
WRITE(3,*)T11,T22
WRITE(*,*)AK(2),AK(1)
10  CONTINUE
STOP
END
SUBROUTINE DKL(E,U,V,AX)
C   SUBROUTINE TO COMPUTE K USING L'KER FORMULA
COMPLEX E,U,AX,E1,U1
CALL EQU(E,V,E1)
CALL EQU(U,V,U1)
AX=CSQRT(E1*U1)
RETURN
END
subroutine eque(u1,v,xa)
c   subroutine eque to compute the eqt. e/u based on dkl's eqn
complex xa,u1(2)
dimension pf(2)
xa = 0.0

```

```

pi = 0.0
ai = 0.0
tx = 0.0
pf(1)=v
pf(2)=1-v
do 100 i = 1,2
as = cabs(u1(i))
as1 = abs(as)
ai = ai + pf(i) * log(as1)
b1 = aimag(u1(i))
b2 = real(u1(i))
tnd = b1/b2
tx = tx + pf(i) * tnd
pi = pi + pf(i)
100 continue
del = atan(tx)
as = exp(ai)
b2 = as * cos(del)
b1 = as * sin(del)
xa = cmplx(b2,b1)
return
end

```

```

SUBROUTINE TMX(E1,E2,U1,U2,AF,AR,T11,T22)
C SUBROUTINE TO COMPUTE THE ELEMENTS OF THE T-MATRIX
C REF : EQN 18; VARDHAN, IEEE TRANS VOL MTT-34(2) 1986 P-254
COMPLEX E1,E2,U1,U2,EU1,EU2,AK1,AK2,AJ11,AJ12,AJ21,AJ22,
1 A(10),H12,H22,T11,T22

```

```

PI = 3.1415927
EU1=E1*U1
EU2=E2*U2
AK1=2.*PI*AF*1.E+09*(CSQRT(EU1))*(AR*1.E-06)
AK2=2.*PI*AF*1.E+09*(CSQRT(EU2))*(AR*1.E-06)
CALL BESJ(1.,AK1,AJ11)
CALL BESJ(1.,AK2,AJ12)
CALL BESJ(2.,AK1,AJ21)
CALL BESJ(2.,AK2,AJ22)
CALL HANK(1,AK2,H12)
CALL HANK(2,AK2,H22)
A(1)=2.*AJ12-AK2*AJ22
A(2)=2.*AJ11-AK1*AJ21
A(3)=2.*H12-AK2*H22
A(4)=2.*AJ11-AK1*AJ21
A(5)=U1*AJ11*A(1)-U2*AJ12*A(2)
A(6)=U1*AJ11*A(3)-U2*H12*A(4)
A(7)=U1*AJ12*A(2)-U2*(EU1/EU2)*AJ11*A(1)
A(8)=U1*H12*A(4)-U2*(EU1/EU2)*AJ11*A(3)
T11=-A(5)/A(6)
T22=-A(7)/A(8)
RETURN
END

```

```

SUBROUTINE BESJ(ANU,Z,AJ)
C PROGRAM TO CALCULATE SPHERICAL BESSEL FUNCTIONS OF ORDER

```

```

C   0 1 AND 2
C   REF : HANDBOOK OF MATHEMATICAL FUNCTIONS by ABRAMOWITZ
C   PAGE 438 (10.1.11)
      COMPLEX Z,AJ
      AN1=1.
      IF(ANU-AN1)1,2,3
1     AJ=(CSIN(Z)/Z)
      GO TO 4
2     AJ=((CSIN(Z)/(Z*Z))-(CCOS(Z)/Z))
      GO TO 4
3     AJ=(3./(Z*Z*Z)-(1./Z))*CSIN(Z)-(3./(Z*Z))*CCOS(Z)
4     CONTINUE
      RETURN
      END
C   PROGRAM TO CALCULATE SPHERICAL HANKEL FUNCTIONS OF ORDER
C   0 1 AND 2
C   REF : HANDBOOK OF MATHEMATICAL FUNCTIONS by ABRAMOWITZ
C   PAGE 437-438 (10.1.11,12) & 10.1.1
      SUBROUTINE HANK(ANU,Z,H)
      COMPLEX Z,AJ,AY,H,C
      H=(0,0)
      AN1=1.
      C=CMPLX(0,1.)
      IF(ANU-AN1)1,2,3
1     AJ=CSIN(Z)/Z
      AY=-CCOS(Z)/Z
      GO TO 4
2     AJ=(CSIN(Z)/(Z*Z))-(CCOS(Z)/Z)
      AY=-(CCOS(Z)/(Z*Z))-(CSIN(Z)/Z)
      GO TO 4
3     AJ=(3./(Z*Z*Z)-(1./Z))*CSIN(Z)-(3./(Z*Z))*CCOS(Z)
      AY=(-3./(Z*Z*Z)+(1./Z))*CCOS(Z)-(3./(Z*Z))*CSIN(Z)
4     CONTINUE
      H=AJ+C*AY
      RETURN
      END
C   SUBROUTINE BHF
C   PROGRAM TO COMPUTE THE VALUES OF PERMITTIVITY
C   PERMEABILITY OF Co-BHF.
      COMPLEX EP(2),UP,XY
      DIMENSION PF(2),EPR(2),EPI(2)
      OPEN(UNIT=7,FILE='BHF.IN',STATUS='OLD')
      OPEN(UNIT=8,FILE='BHF.DAT',STATUS='NEW')
      READ(7,*)(PF(I),I=1,2)
      READ(7,*)FR
      READ(7,*)AR
      READ(7,*)(EPR(I),EPI(I),I=1,2)
      WRITE(8,*)FR
      WRITE(8,*)PF(1)
      WRITE(8,*)AR
      DO 5 I=1,2
      EP(I)=CMPLX(EPR(I),-EPI(I))

```

```

WRITE(8,*)EP(I)
5  CONTINUE
   AF=7.5
   DO 10 I=1,21
   AF=AF+.5
   F1=AF
   CALL PERM(F1,FR,UP)
   WRITE(8,*)AF,UP
10  CONTINUE
   STOP
   END
c  subroutine to compute the permeability
   subroutine perm(f1,fsr,us)
   complex us
   us = 0.0
   s1 = 1.0
   afc = f1 + 1.0
   do 525 j1=1,2
   afc=afc-1.0
   a1 = afc - fsr
   a2 = fsr + afc/2.0
   a3 = 2.0 * a1/a2
   ch = cosh(a3)
   a4 = a1*a1
   a5 = sqrt(s1 + a4)
   xy = 4.0 * ch/a5
   if (j1.eq.1) then
   ur = xy
   else
   uj = xy
   endif
525 continue
   us = cmplx(ur,-ui)
   return
   end

```

APPENDIX 5.5

```

C   ABS.FOR
C   PROGRAM TO COMPUTE THE RETURN LOSS OR ABSORPTION (EQ. 4.15)
COMPLEX C1,AK,P,XY,ALPHA,R
DIMENSION PF(2)
OPEN(UNIT=1,FILE='FERQ.DAT',STATUS='OLD')
OPEN(UNIT=2,FILE='FTMSB.DAT',STATUS='OLD')
PI = 3.1415927
U0 = 12.56637E-07
E0 = 8.854E-12
C1=CMPLX(0.,1.)
WRITE(*,*) ' ENTER VALUE OF d '
READ(*,*)D
C   D=D/1000.
DO 100 I =1,21
READ(1,*)AF
READ(2,*)AK,XY
ALM=300./AF
P = -AIMAG(AK)
ALPHA=4.*PI*D*P/ALM
R=CEXP(-ALPHA)
DB=-20.*ALOG10(CABS(R))
D1=ALM/(2.*PI*P)
D2=ALM/(4.*REAL(AK))
WRITE(*,1)AF,DB,D1,D2
1  FORMAT(4F8.2)
100 CONTINUE
STOP
END

```


CHAPTER VI

AN IMPEDANCE MATCHING TECHNIQUE TO IMPROVE THE PERFORMANCE OF THIN PLANAR ABSORBERS

6.1 INTRODUCTION

In this chapter a simple Impedance Matching (IM) technique is formulated and discussed, to match a single layer microwave absorber with free space. A conducting screen perforated with an array of apertures have been considered as the impedance matching layer. The IM technique has been employed to design a broad band absorber (a minimum 10 dB absorption over a 6/10/12 GHz bandwidth), as well as a narrow band absorber (minimum 15 dB absorption over a 1 GHz bandwidth), within a thickness constraint of 2mm.

An efficient thin type microwave absorber must possess the following two properties; (i) attenuate or absorb the energy entering its media significantly and (ii) present a good match to the incident wave at the air-absorber interface. The first property will be met [2] by the material whose μ_r' , ϵ_r' , μ_r'' and ϵ_r'' are high and the second will be satisfied if $\mu_r' = \epsilon_r'$ and $\mu_r'' = \epsilon_r''$, where $\mu_r = \mu_r' - j\mu_r''$ and $\epsilon_r = \epsilon_r' - j\epsilon_r''$ are the relative complex permeability and permittivity of the absorber.

Since there are no known materials [128,129,133] which satisfies the above two conditions simultaneously and further for most of the known materials in the microwave region ϵ_r is greater than μ_r . Thus to obtain a high absorption, if one were to use a high ϵ_r material or resort to excessive loading of the lossy material

then this leads to mismatch at the air-absorber interface. Which in turn prevents the wave from entering the absorber medium. Further there is a physical limit to the level of loading a given binder. Such problems leading to mismatch can be minimized or avoided by incorporating an additional free space matching layer at the front end of the absorber.

Such an impedance matching layer should behave as a band pass filter and provide high impedance (complex) over the frequency range, in which the absorber is designed to operate. Further it is assumed that the thickness of the IMS is negligibly small so that it does not increase the overall thickness or weight of the absorber.

Measurements [150] have demonstrated that a thin conducting screen perforated with slots or apertures has band pass-band stop characteristics, when illuminated by the incident electromagnetic waves. This property makes these structures useful for many applications such as microwave filters [5], band pass radomes [90-93], artificial dielectrics [89], frequency selective surfaces [94-96], and antenna reflectors or ground planes.

Conducting screens perforated periodically with apertures are thus an excellent candidate material for impedance matching application. Such screens were named as Impedance Matching Screens (IMS).

On the lines of work done by Ott et al [150] an experimental investigation was done to assess the impedance matching property of a conducting screen perforated with apertures. The following section discusses the experimental investigations.

6.2 AN EXPERIMENTAL INVESTIGATION TO ASSES THE IMPEDANCE MATCHING PROPERTY OF A CONDUCTING SCREEN PERFORATED WITH AN ARRAY OF APERTURES

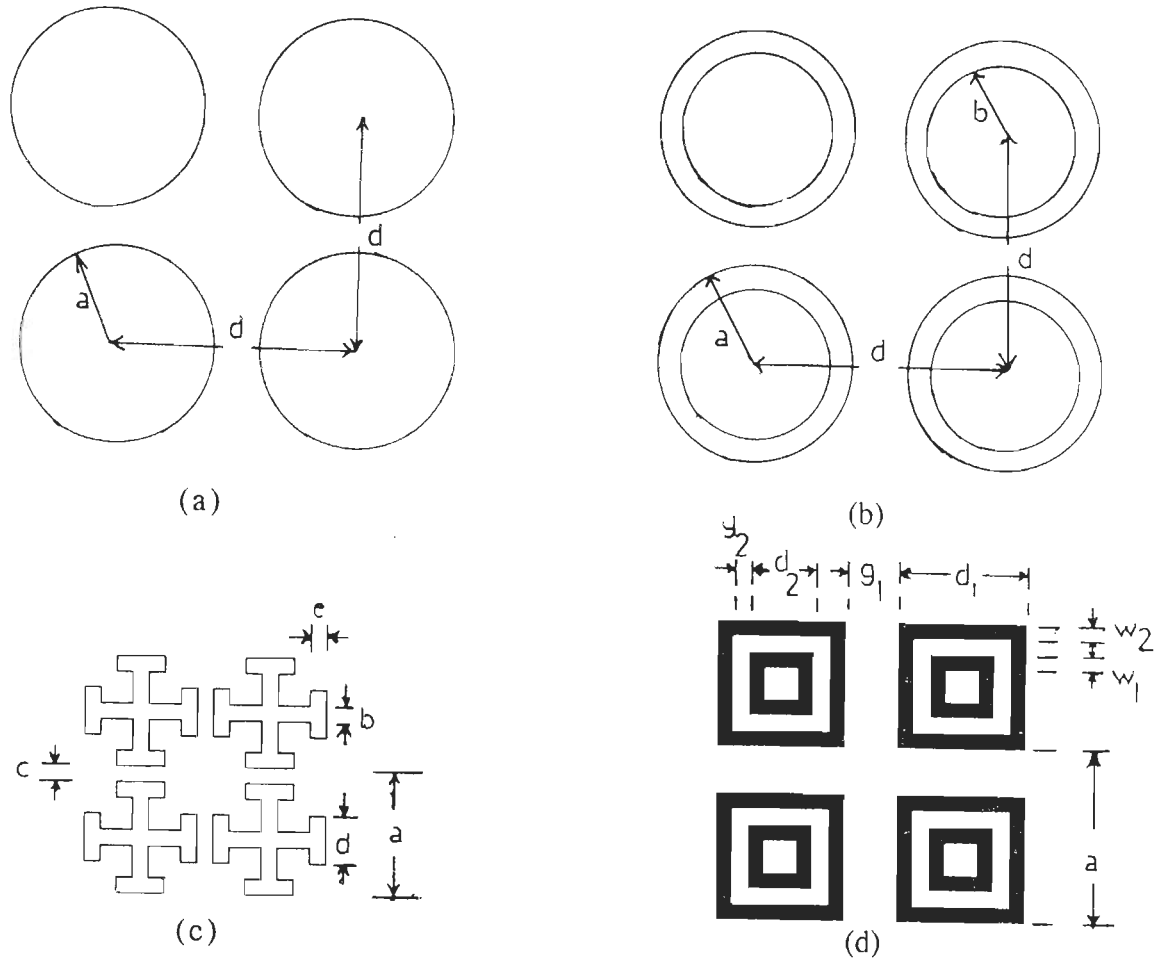


Fig 6.1 Geometry of the arrays of (a) Circular apertures; (b) Annular ring apertures; (c) Jerusalem cross apertures and (d) Double Square loops.

Screens perforated with an array of Circular Apertures (CA) [91], Annular Ring Apertures (ARA) [109], Jerusalem Cross Apertures (JCA) [151], and Double square loop (DSA) [152] shown in Fig 6.1 were considered for IMS application. The dimensional details for the array element for CA, ARA, JCA, and DSA are given Table 6.1.

A 12 X 12 element array for each structure was etched on a glass-epoxy dielectric sheet (normally used for making PCB's) of dimension 300 X 300 X 2mm, using the photo lithography technique. The dielectric sheet was backed by a perfectly conducting layer.

Table 6.1

Aperture	Parameters (mm)
Circular	$a = 4$; $d = 10$.
Annular Ring	$a = 4$; $b = 3$; $d = 10$.
Jerusalem Cross	$a = 19$; $b = 6$; $c = 2$; $d = 10$; $e = 2$.
Double Square Loop	$a = 15$; $d_1 = 13$; $d_2 = 5$; $w_1 = 2$; $w_2 = 1$; $g_1 = 2$; $g_2 = 4$.

The composite structure formed by the perforated conducting screen, absorber and the perfectly conducting backing as shown in Fig 6.2, is termed as Impedance Matched Absorber (IMA)

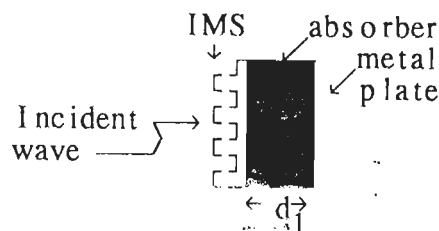


Fig 6.2 Side view of IMA

A quasi mono static free space measurement setup operating in X-Band as shown in Fig 3.4 was employed for the measurement of reflection loss or absorption. The reflectivity of the IMA and that due to a metal plate of the same dimensions as the IMA were measured. The absorption provided by the IMA were then deduced by the two measured values.

The measured absorption for the four IMA's fabricated as well as that due to only the epoxy sheet, that was used in the making of IMA's, are plotted in Fig 6.3.

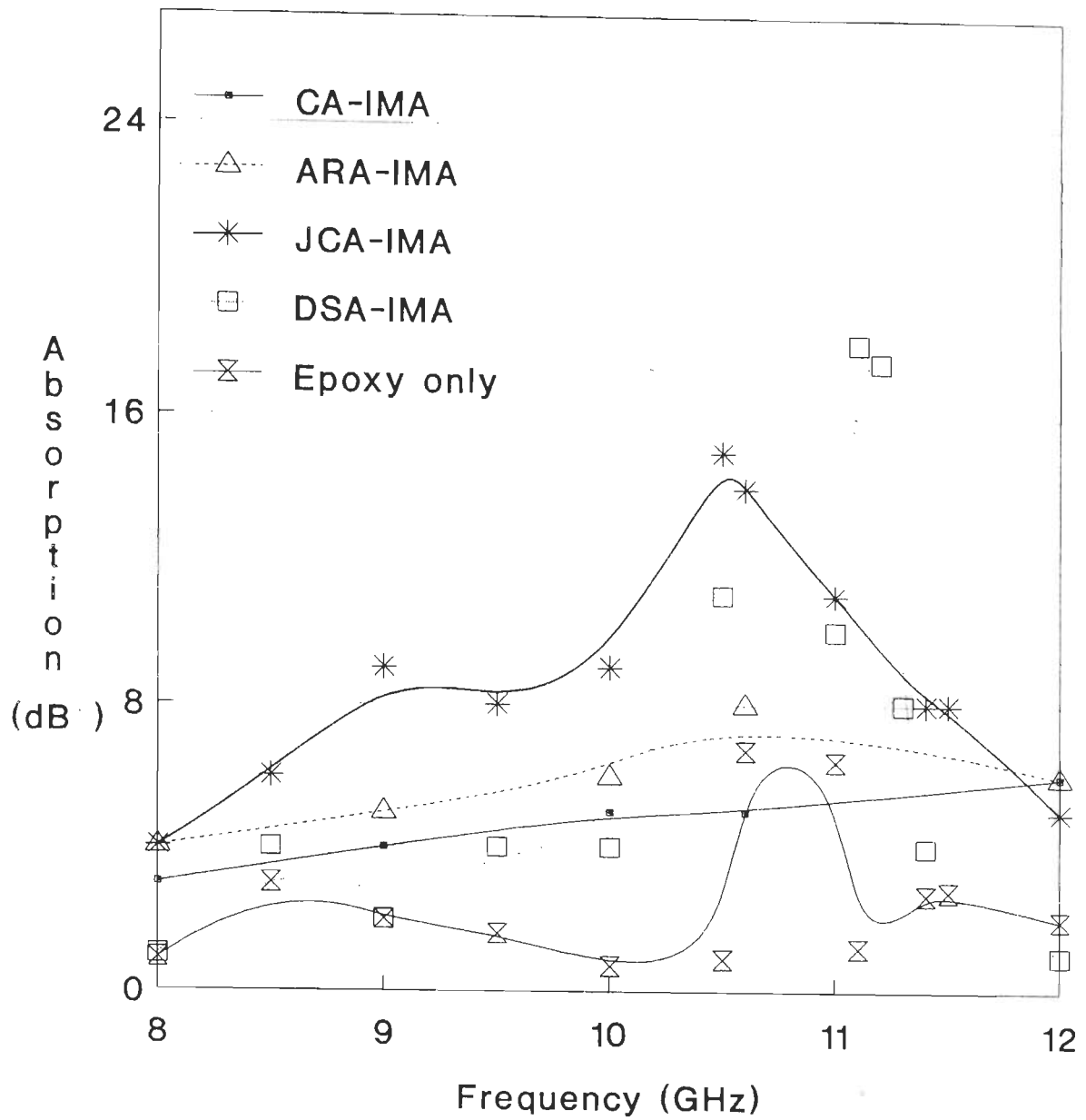


Fig 6.3 Experimentally obtained absorption characteristics for different IMS structures that were considered.

The CA-IMA has provided a minimum 5 dB absorption over a 2.5 GHz bandwidth, while ARA-IMA over a 4 GHz band. But JCA-IMA displays higher and better absorption characteristics than the above two considered. DSA-IMA, though the bandwidth is small when compared with JCA-IMA, displays higher peak absorption. Thus JCA and DSA promise to be good candidate materials for IMS operation.

6.3 THEORY OF IMPEDANCE MATCHED ABSORBER

The overall transmission line equivalent circuit [153] for the IMA construction depicted in Fig 6.2, is shown in Fig 6.4. In which $Z(3)$ is the effective impedance at the absorber-metal plate interface, $Z(2)$ is the effective input impedance at the IMS and absorber interface, while $Z(1)$ is the effective input impedance at the IMS and absorber interface, while $Z(1)$ is the effective input impedance at air - IMS interface. Further Z_1 and Z_2 are the impedance of the IMS and intrinsic impedance of the absorber respectively.

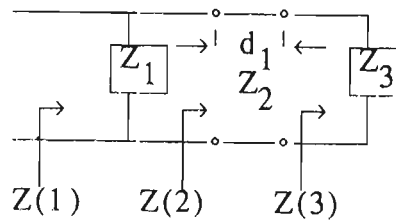


Fig 6.4 Transmission line equivalent

Since the absorber is backed by a metal plate, hence $Z(3)=0$. Thus for normal incidence

$$Z(2) = Z_2 \tanh(jkd_1) \quad 6.1$$

where d_1 is the thickness of the absorber, k is the complex wave number and $Z_2 = \sqrt{\mu/\epsilon}$, where μ and ϵ are the complex permeability and permittivity of the

absorbing media.

Further the absorption can be computed by using Eq. (4.15), where

$$R = \frac{Z(1) - Z_0}{Z(1) + Z_0} \quad 6.2a$$

$$\text{and } Z(1) = \frac{Z(2)Z_1}{Z(2) + Z_1}; \quad 6.2b$$

Z_1 the impedance of the IMS can be determined by using the equivalent circuit model proposed by Langley and Drinkwater and others [110-113].

6.4.0 ANALYSIS OF AN IMA WITH PERIODIC ARRAY OF JERUSALEM CROSS APERTURES AS THE IMS

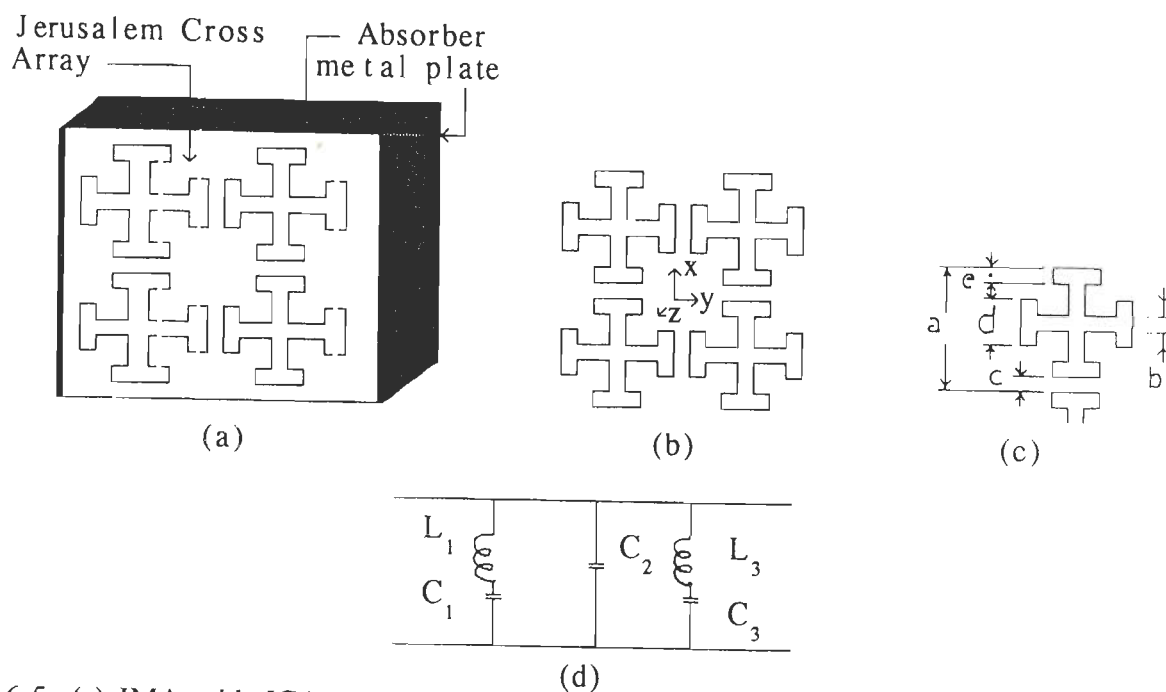


Fig 6.5. (a) IMA with JCA as IMS, (b) An array of Jerusalem Crosses, (c) Unit Cell of the array and (d) Equivalent circuit for the array of Jerusalem Cross.

The construction of the IMA with periodic array of Jerusalem cross apertures as the IMS, is shown in Fig 6.5a. The equivalent circuit model proposed by Langley and Drinkwater [110] has been utilized to arrive at the impedance of the Jerusalem cross array, an IMS.

The unit cell of the jerusalem cross array and its equivalent circuit model [110], are shown in Fig 6.5. The two series LC combinations represent the lower and upper cut off frequencies of the transmission band, while C_2 mainly determines f_T , the peak transmission frequency.

The parameters of the equivalent circuit are computed as follows-

The inductive reactance for the array is given as

$$X_1 = F(a,b,\lambda_L) \quad 6.3$$

where $F(a,b,\lambda)$ is given [113] as

$$F = \frac{a}{\lambda} \left[\ln \left(\text{Cosec} \frac{\pi b}{2a} \right) + G(a,b,\lambda) \right] \quad 6.4a$$

and λ is the free space wavelength.

The correction term $G(a,b,\lambda)$ is defined as

$$G(a,b,\lambda) = \frac{1}{2} \frac{(1-\beta^2) [(1-\beta^4/4)v + 4\beta^2 A_+ A_-]}{(1-\beta^2/4) + \beta^2(1+\beta^2/2 - \beta^4/8)v + 2\beta^6 A_+ A_-} \quad 6.4b$$

where

$$A_{\pm} = \left[1 \pm \frac{2a \sin \theta}{\lambda} - \left(\frac{a \cos \theta}{\lambda} \right)^2 \right]^{-1/2} - 1; \quad 6.4c$$

$$v = A_+ + A_- \quad 6.4d$$

$$\beta = \sin(\pi b/2a) \quad 6.4e$$

and $\theta = 0$ for normal incidence.

The susceptance for the array is given as

$$B_1 = \frac{4d}{a} F(a,c,\lambda_L) + \frac{4(2e+c)}{a} F(a,a-d,\lambda_L) \quad 6.5$$

where c is the gap between the vertical dipoles and $(a-d)$ is the gap between horizontal dipoles.

C_3 is calculated by assuming a upper resonant frequency to be given by $\lambda_H = d/0.49$, then

$$C_3 = 1.0/\sqrt{2\pi L f_H} \quad 6.6a$$

where L is deduced from the end-cap inductance

$$X = (d/p) F(p,e,\lambda_H) \quad 6.6b$$

L_3 is derived from the inductive reactance,

$$X_3 = \frac{1}{2} \left[(d/a)F(a,2e+c,\lambda_H) + F(a/2,b,\lambda_H) \right] \quad 6.7$$

and further C_2 is the sum of two end capacitances C_4 and C_5 , C_4 is given by

$$C_4 = 1.0/\sqrt{2\pi L f_T} \quad 6.8a$$

where L is deduced from the end-cap inductance

$$X = (d/a)F(a,e,\lambda_T) \quad 6.8b$$

and finally C_5 is obtained through the susceptance between the horizontal main arm and the parallel end caps given by $(4d/a)F(a/2,t,\lambda_H)$ where $t = (a-b-c-2h)/2$

Then the impedance of the IMS is given by

$$Z_1 = \frac{jPQ}{\omega(QC_1 + PQC_2 + PC_3)} \quad 6.9$$

where $P = 1 - \omega^2 L_1 C_1$ and $Q = 1 - \omega^2 L_3 C_3$

A computer code was developed to evaluate the impedance of the IMS using Eq.'s (6.3)-(6.9) and the absorption provided by the IMA using Eq's. (6.1)-(6.3). The program listing is given in Appendix 6.1.

The single layer absorber designed and fabricated in chapter III (BBA), has been utilized as the absorber in the analysis of JCA incorporated IMA. For a fixed

periodicity the effect of various parameters of the IMS-array on the operating performance of the IMA [153] are plotted in Fig 6.6a, 6.6b, 6.6c and 6.6d. The corresponding details of the IMS array's are listed in Table 6.2.

It is observed that all the four parameters b, c, d, and e shift the peak absorption frequency, f_p .

In the non resonance region of the absorber, it is significant to note that an increase in strip width 'b' of the JC increases (Fig 6.6a) the absorption.

The element separation parameter 'c', does not alter the absorption pattern (Fig 6.6b) but has the effect of shifting f_p towards the upper side of the frequency spectrum.

Table 6.2

IMS	a	b	c	d	e (mm)
b1	20	0.75	3	10	3
b2	20	1.50	3	10	3
b3	20	2.25	3	10	3
b4	20	3.00	3	10	3
c1	20	3	0.75	10	3
c2	20	3	1.50	10	3
c3	20	3	2.25	10	3
c4	20	3	3.00	10	3
d1	20	3	3	9.9	3
d2	20	3	3	10.0	3
d3	20	3	3	10.1	3
d4	20	3	3	10.2	3
e1	20	3	3	10	0.75
e2	20	3	3	10	1.50
e3	20	3	3	10	2.25
e4	20	3	3	10	3.00

The most significant change in the behavior of the IMA is brought about by the end cap length 'd', and it is seen from the Fig 6.6c, that even a small change in 'd', (0.5% of 'a') will induce significant change in both f_p as well as the

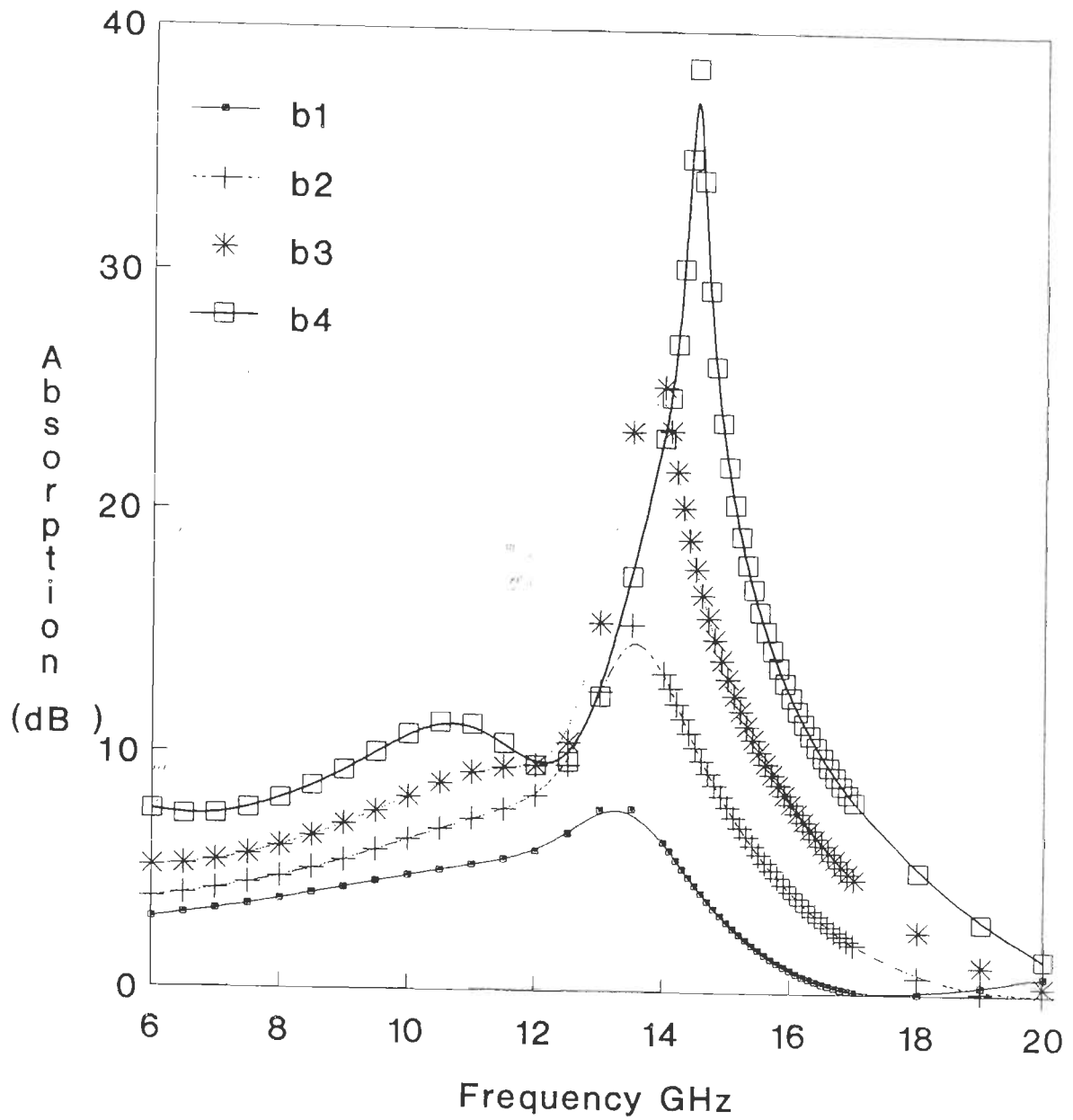


Fig 6.6a Variation of absorption performance of IMA with IMS parameter 'b'. (Details in Table 6.2)

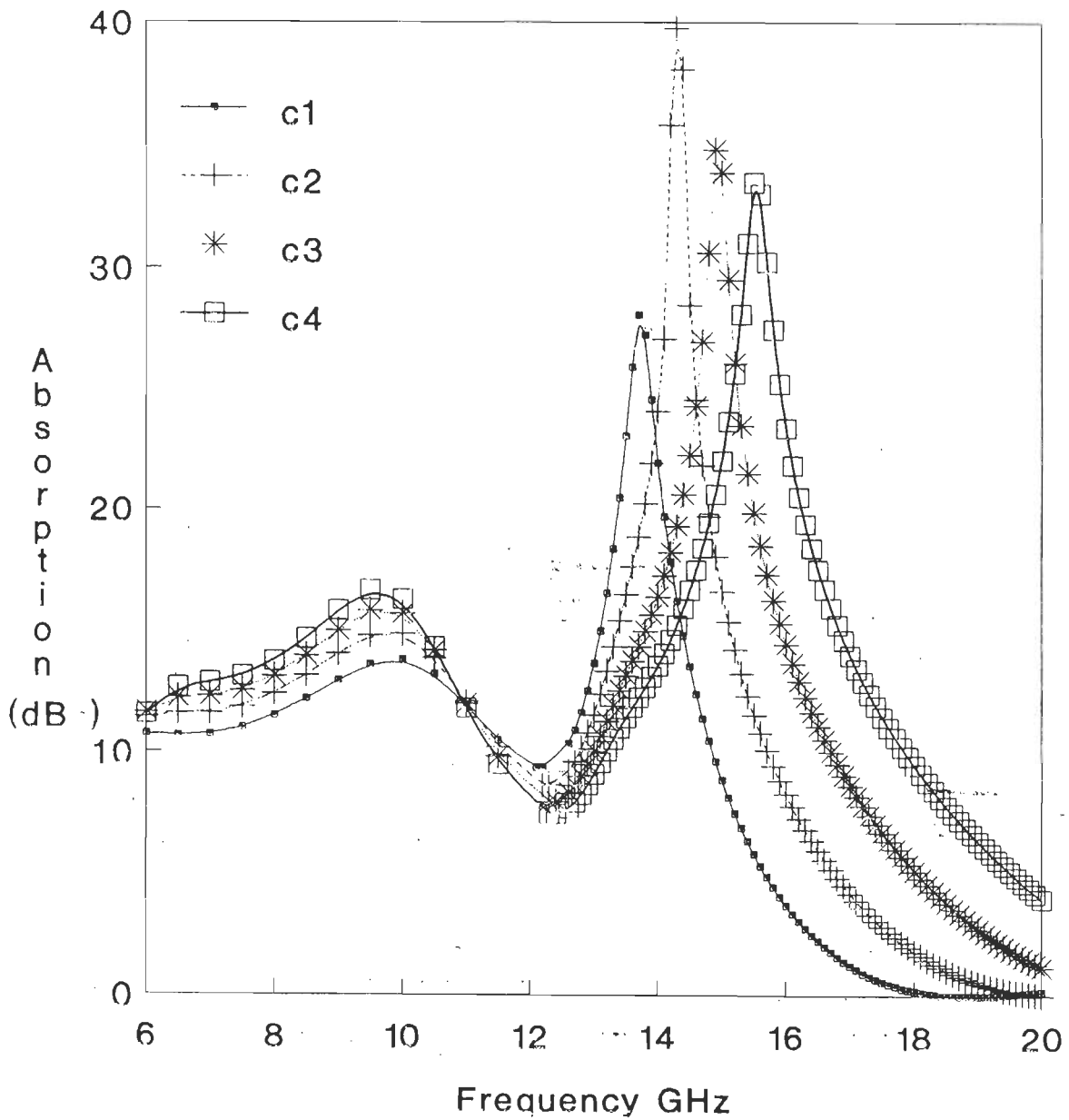


Fig 6.6b Variation of absorption performance of IMA with IMS parameter 'c'. (Details in Table 6.2)

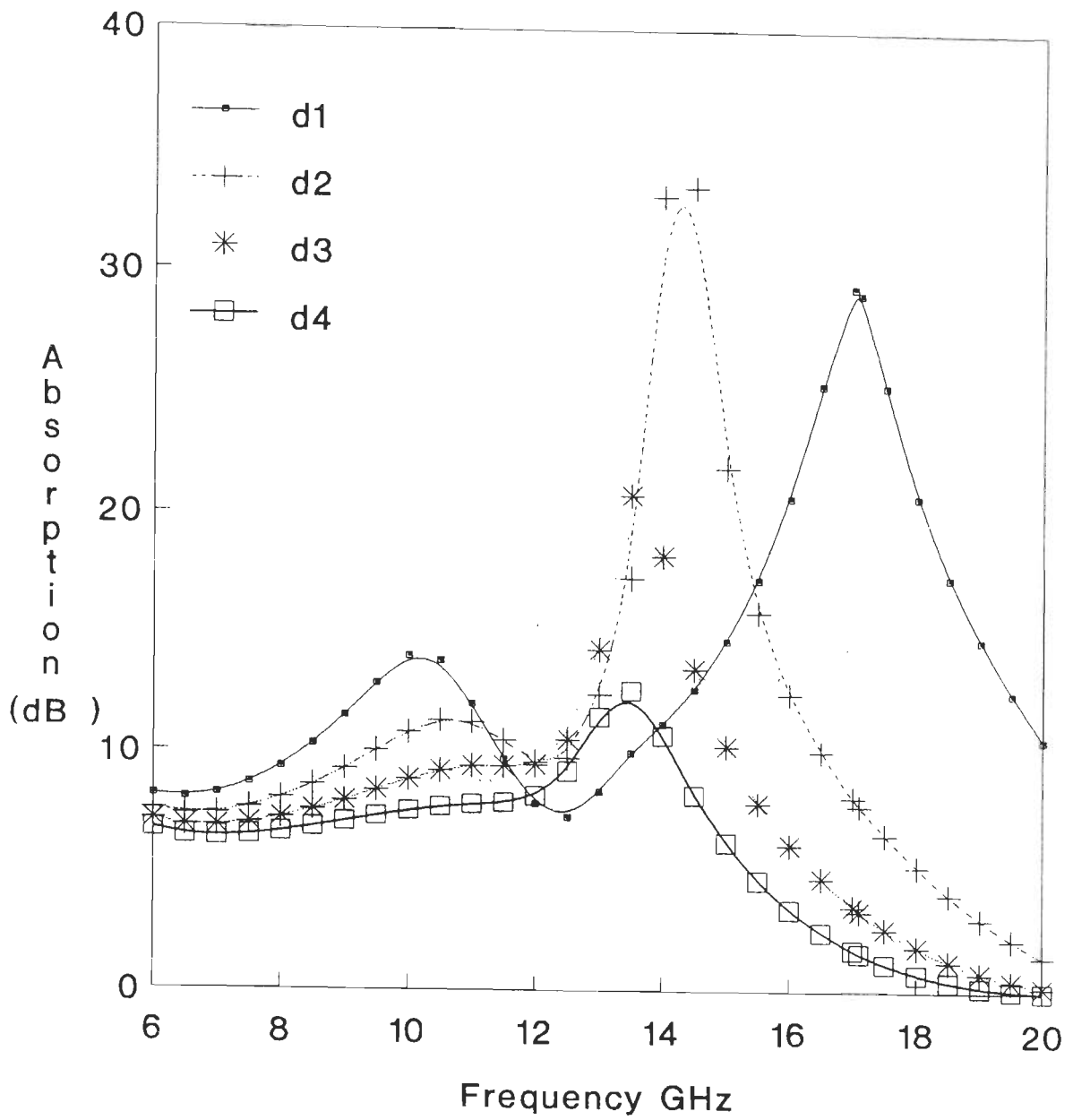


Fig 6.6c Variation of the absorption characteristics of the IMA with IMS parameter 'd'.
(Details in Table 6.2)

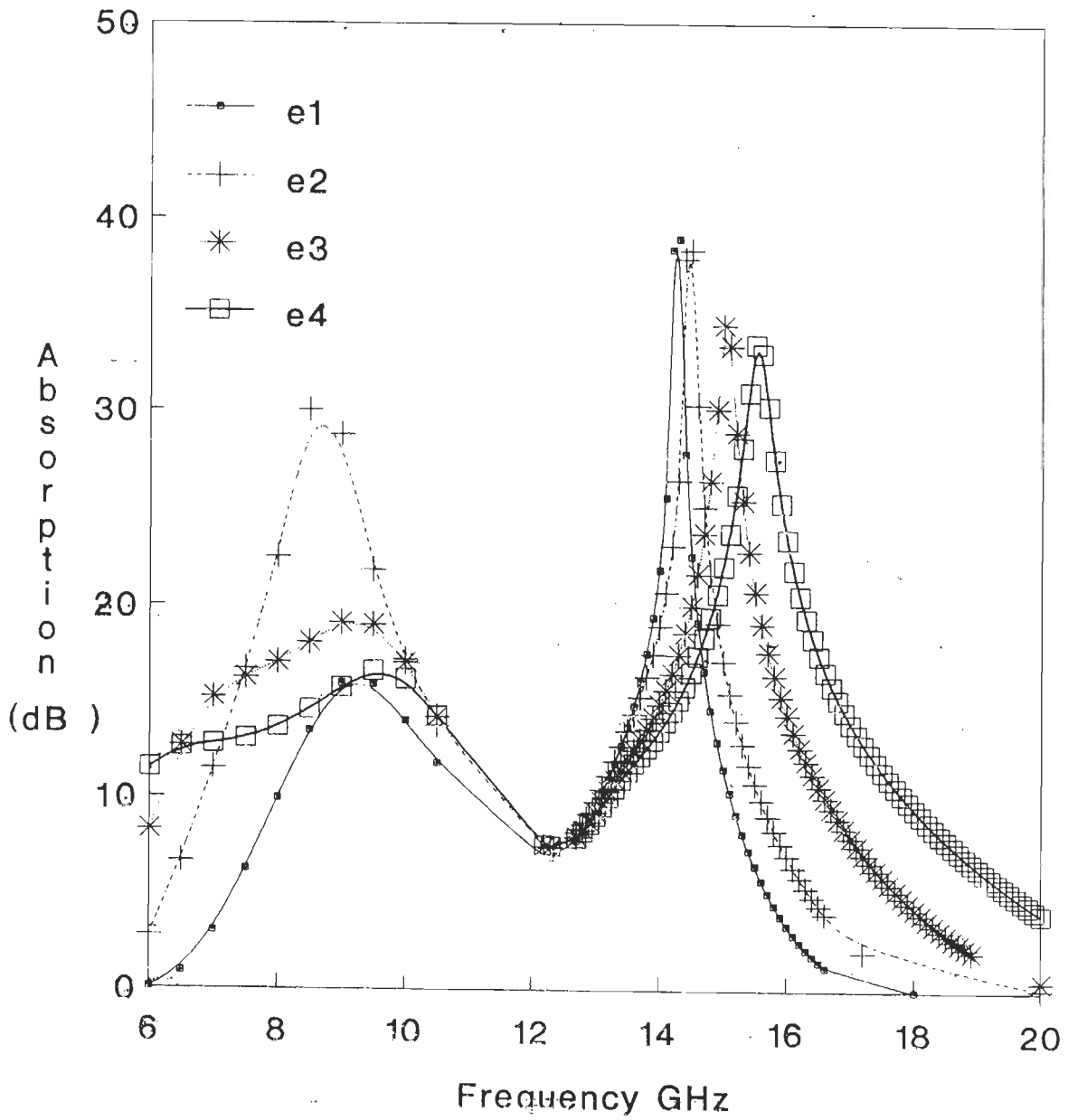


Fig 6.6d Variation of absorption characteristics of the IMA with IMS parameter 'e'.
(Details in Table 6.2)

absorption provided. Further it was observed that absorption decreases with an increase in 'd'.

While the thickness of the end cap 'e' induces significant change (Fig 6.6d) in the operating characteristics, with absorption increasing and then decreasing at the lower end of the band with an increase in the value of 'e'.

It can be observed from the graphs, that an increase in the values of parameter 'b', 'c', and 'e' results in a shift of the peak absorption frequency towards the upper side of the frequency spectrum. While a similar change in parameters 'd' causes f_p to shift towards the lower side of the spectrum.

It should be noted that the effect of IMS parameters 'd' and 'e' are critical not only during the design process, but also during the fabrication. Thus for a given absorber and a particular application, the parameters of the IMS will have to be optimized.

6.4.1 DESIGN EXAMPLES

For a broad band specification of minimum 10dB absorption from 6-18 GHz., and for a narrow band specification of minimum 15dB absorption over a one GHz bandwidth to operate in the Ku-Band, within a thickness constraint of 2mm, BBA was impedance matched using the optimization subroutine. The optimized parameters for the IMS's listed as 'CK' [153] and 'K' [151] in Table 6.3, were selected to meet the desired broad band and narrow band specification respectively. The two IMA's are labelled as CK-IMA and K-IMA.

Table 6.3

JCA	a	b	c	d	e mm
CK	20	4	3	10	4
K	19	6	2	10	2

6.4.2 FABRICATION OF IMS AND IMA :

A 12X12 element array for each of the two designed IMS's were prepared using the photo lithography technique of preparing PCB's on a 100 microns thick copper sheet. The IMS's were then incorporated at the front end of the absorber to form the Impedance Matched Absorber, IMA.

6.4.3 DISCUSSION AND EXPERIMENTAL RESULTS

A free space quasi mono static measurement set up operating in X- or Ku-bands as shown in Fig 3.4 were employed. The reflectivity of the IMA's and the reflectivity of a metal plate of the same dimensions as that of the absorber or IMA were measured. The absorption provided by the IMA is the difference of the two measurements.

The simulated normalized complex wave number for the designed parameters for the absorber, as a function of frequency is shown in Fig 6.7, while the theoretical absorption characteristics of BBA are reproduced in Fig 6.8, along with the experimentally obtained values. The attenuation capabilities of the absorbing media are inferred from the imaginary part of the wave number. It can be noted from Fig 6.7 and 6.8, that though the attenuation constant is reasonably high, the absorption practically provided by the absorber is around 8dB only, in the desired frequency range. This was attributed to poor matching at the air-material

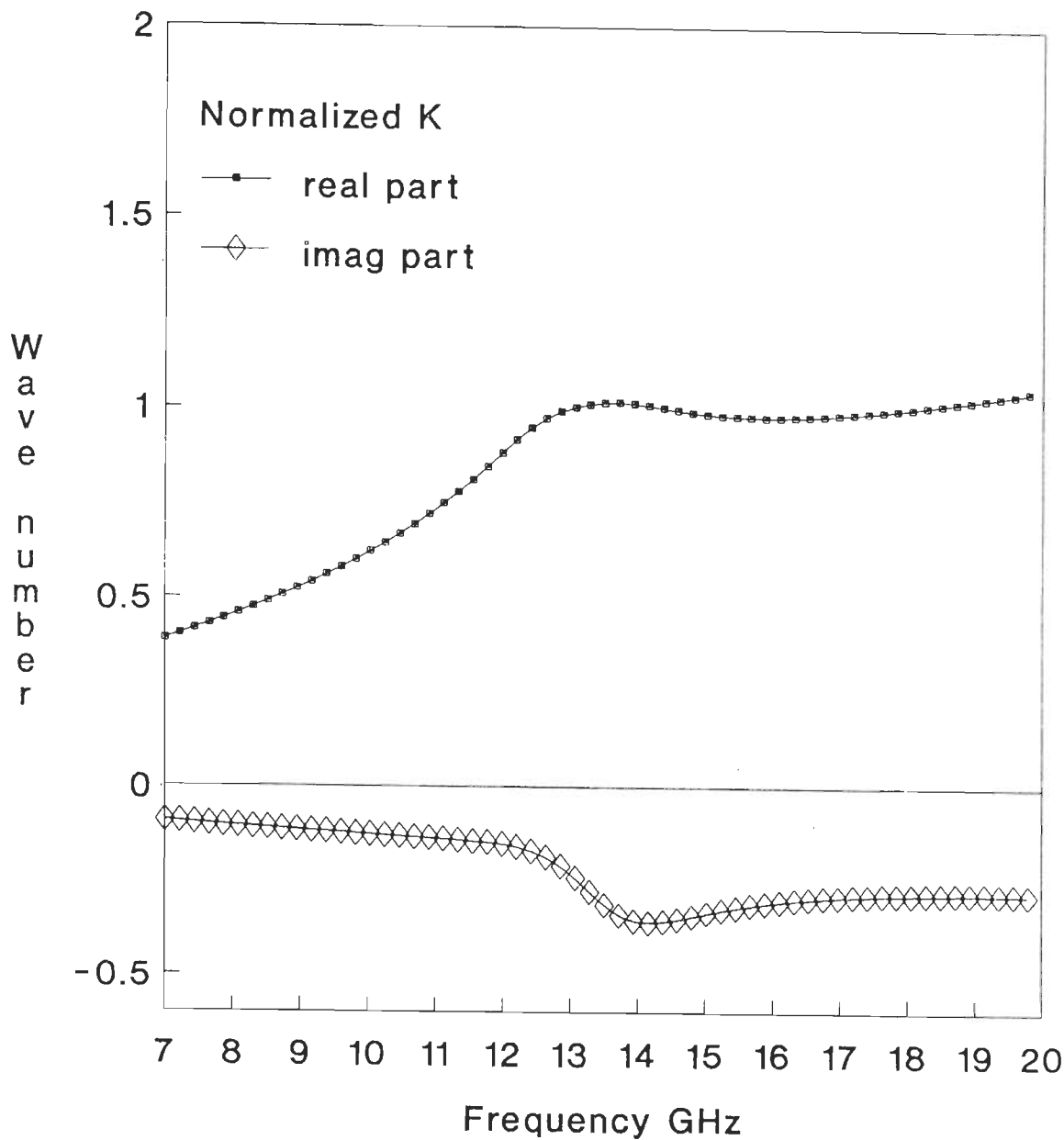


Fig 6.7 Variation of the normalized wave number in the absorber media with frequency.

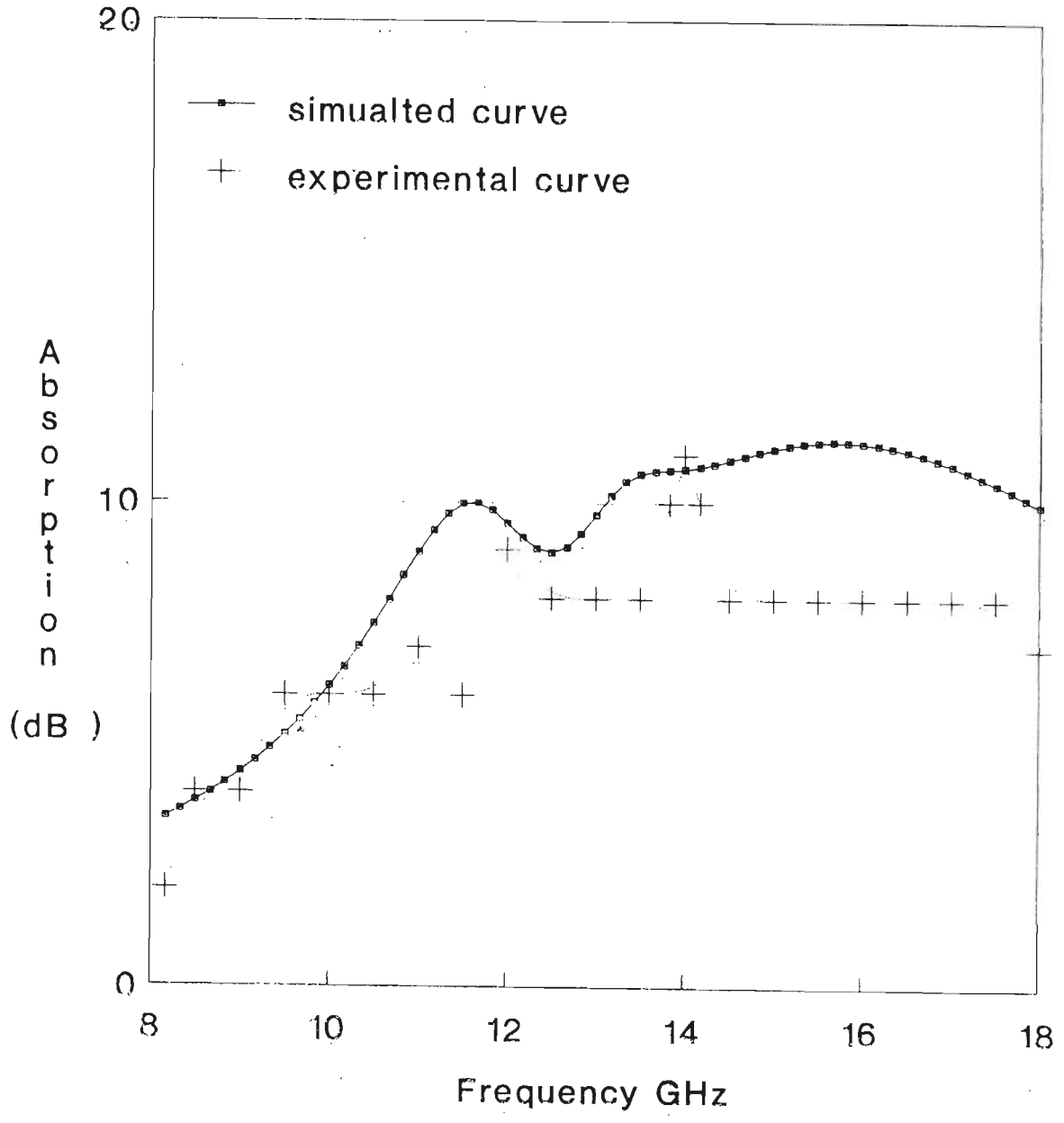


Fig 6.8 Simulated and experimentally determined absorption characteristics for BBA.

interface, which can be readily observed from the impedance of the absorber plotted in Fig 6.9.

The impedance $Z(1)$, for CK-IMA as a function of frequency is plotted in Fig 6.10. The impedance of the CK-IMA, can be observed to match closely with that of free space than, that of the absorber (Fig 6.9), in the frequency band of interest. This can be better appreciated from the simulated absorption characteristics for the CK-IMA, using Eq. (6.1)-(6.9) shown in Fig 6.11. It can also be noted that CK-IMA provides theoretically a minimum 10 dB absorption from 6-18 GHz.

Further from Fig 6.9 and 6.10, it can be observed that the absorber resonates around 12 GHz. due to its thickness effect, while the IMA displays two resonant frequency one around 10.5 GHz and another at 15.5 GHz. These two resonances account for the two peaks observed in the absorption characteristics of the CK-IMA. These two peaks are controlled by the parameters of the IMS, as seen from Fig 6.6, and they can thus, be shifted to any where in the frequency band.

A similar analysis on K-IMA will readily show that K-IMA is matched better with free space for narrow band operation. The simulated absorption characteristics for the K-IMA, using Eq. (6.1)-(6.9) along with that for the absorber are shown in Fig 6.12.

The experimentally determined absorption characteristics for the absorber; and CK-IMA, and K-IMA are plotted in Fig 6.13 and 6.14 respectively. On comparing Fig 6.11 and 6.13, we can see that the experimentally obtained absorption characteristics for CK-IMA follows very closely with the theoretically predicted values. Further from Fig 6.12 and 6.14, the fabricated narrow band, K-IMA has experimentally reproduced the theoretically simulated curve, with a small shift in

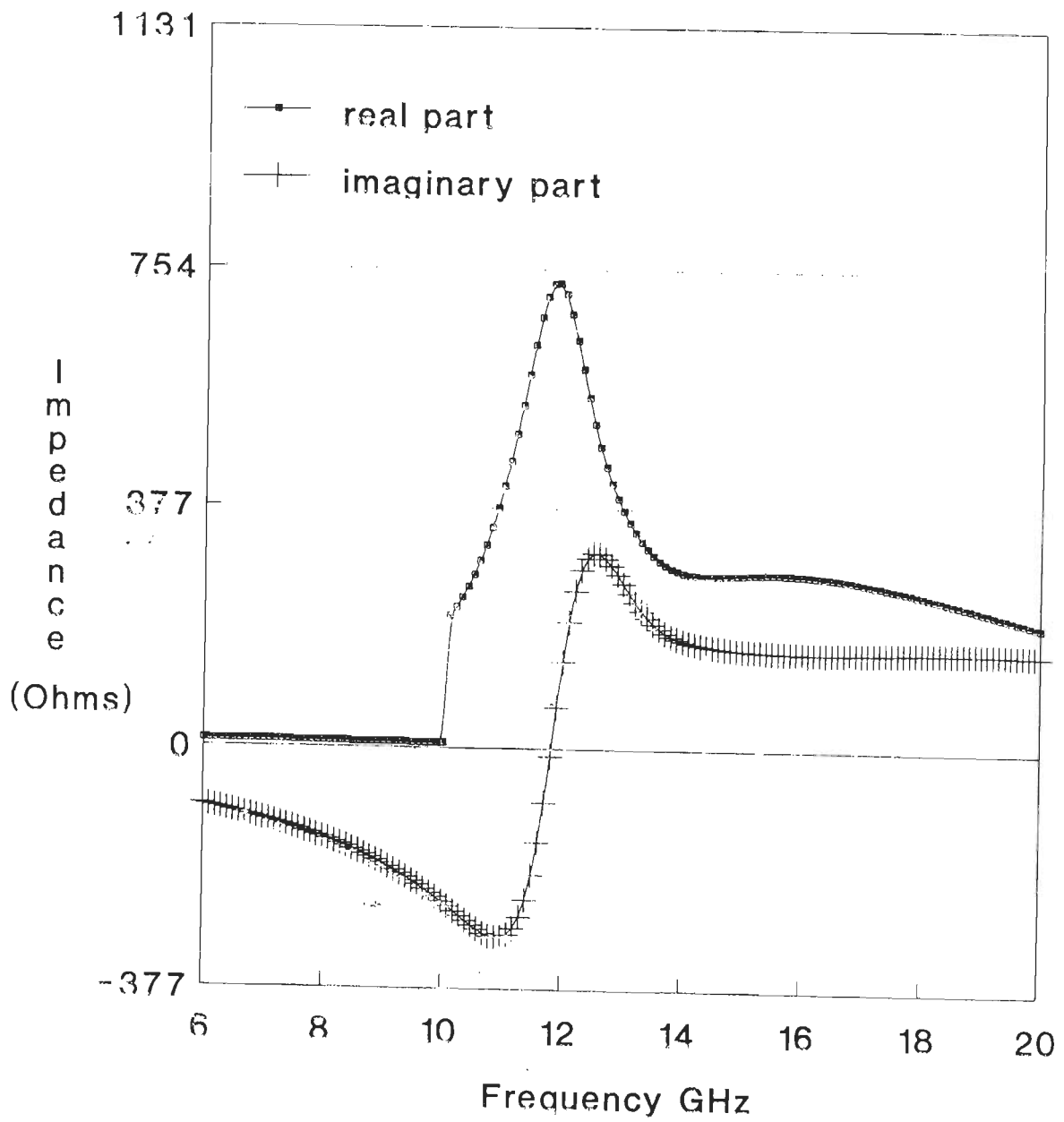


Fig 6.9 Theoretically simulated impedance of BBA.

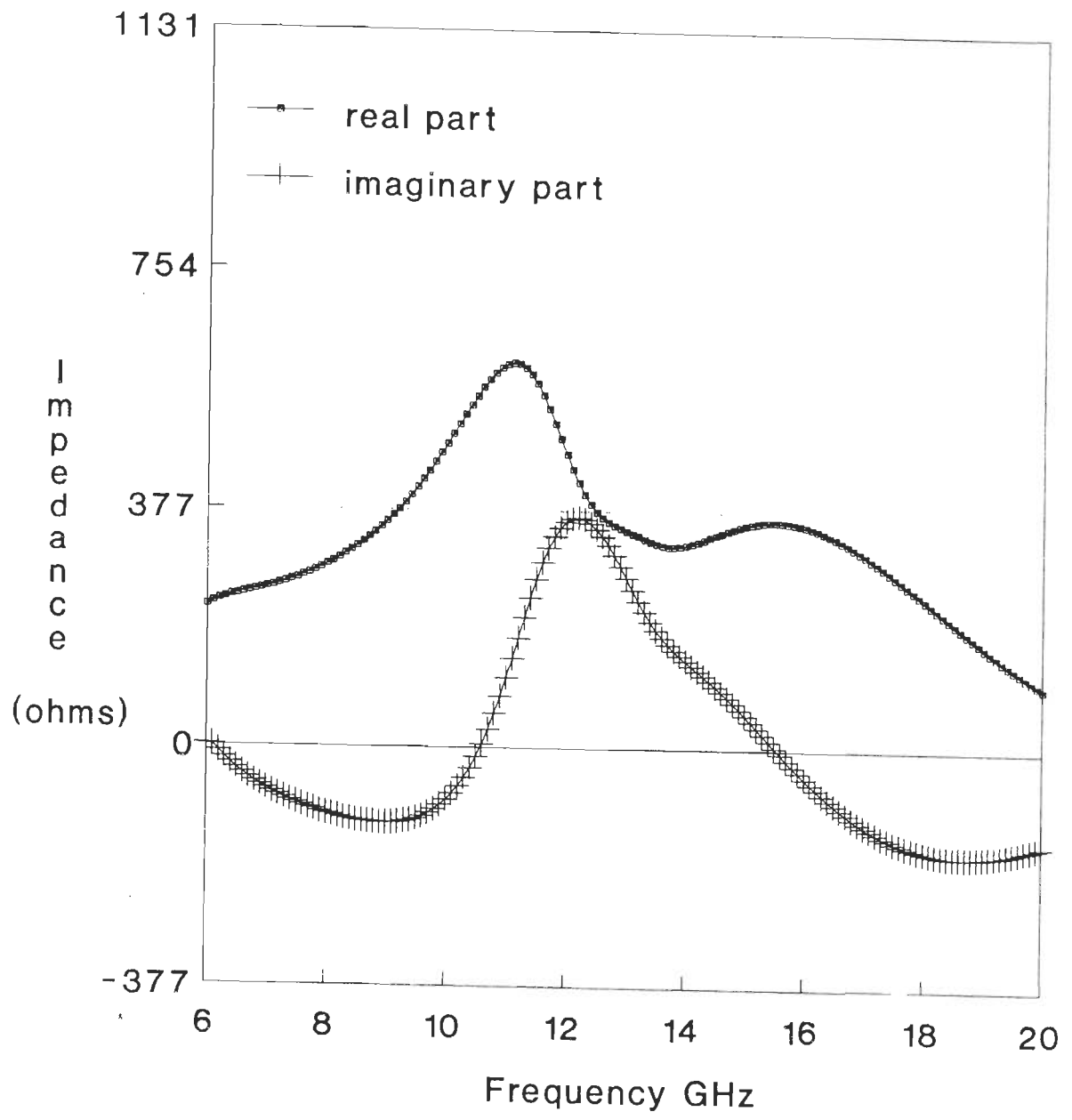


Fig 6.10 Theoretically simulated impedance characteristics for CK-IMA

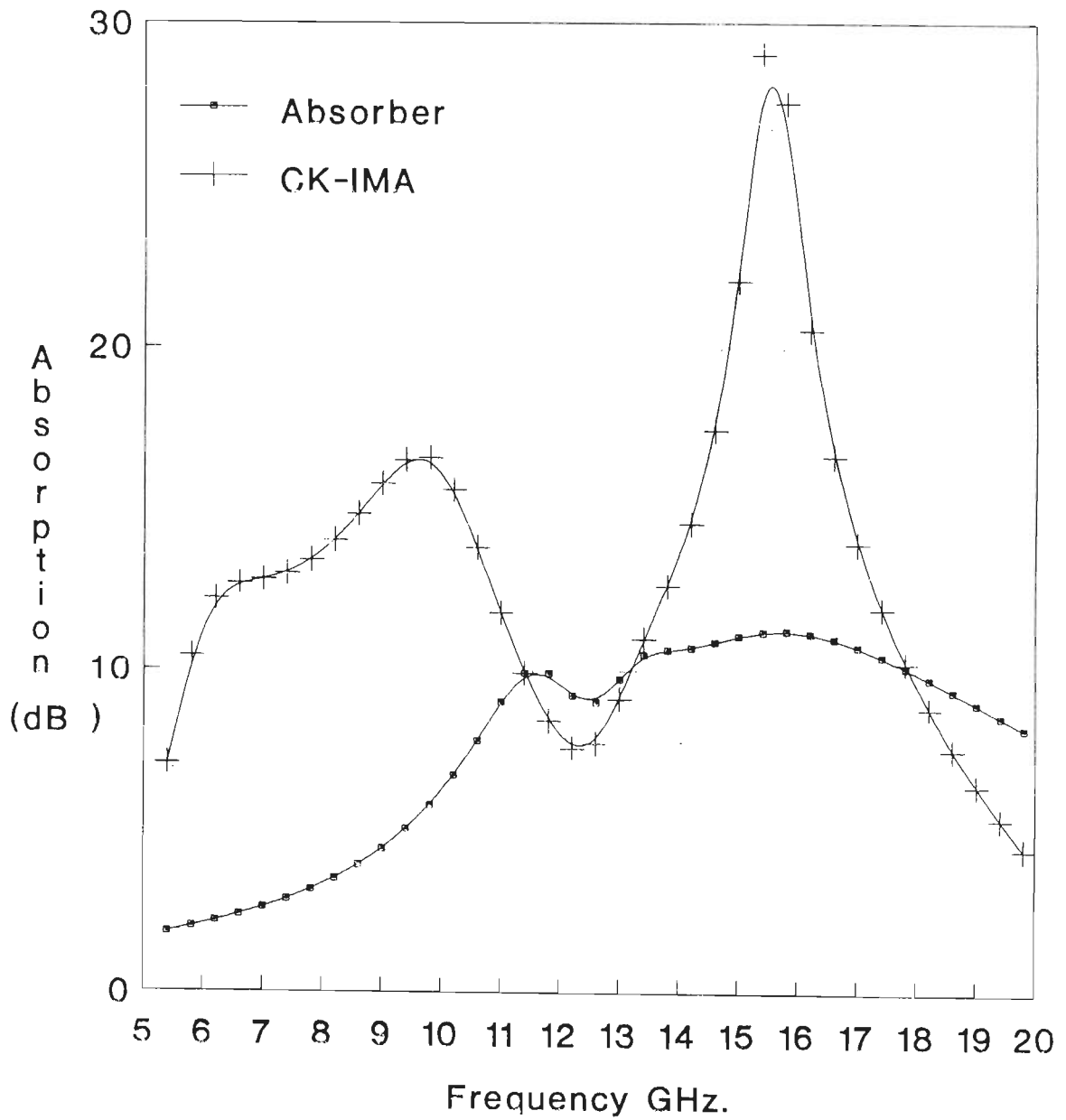


Fig 6.11 Theoretically simulated absorption characteristics for the designed CK-IMA and absorber (BBA).

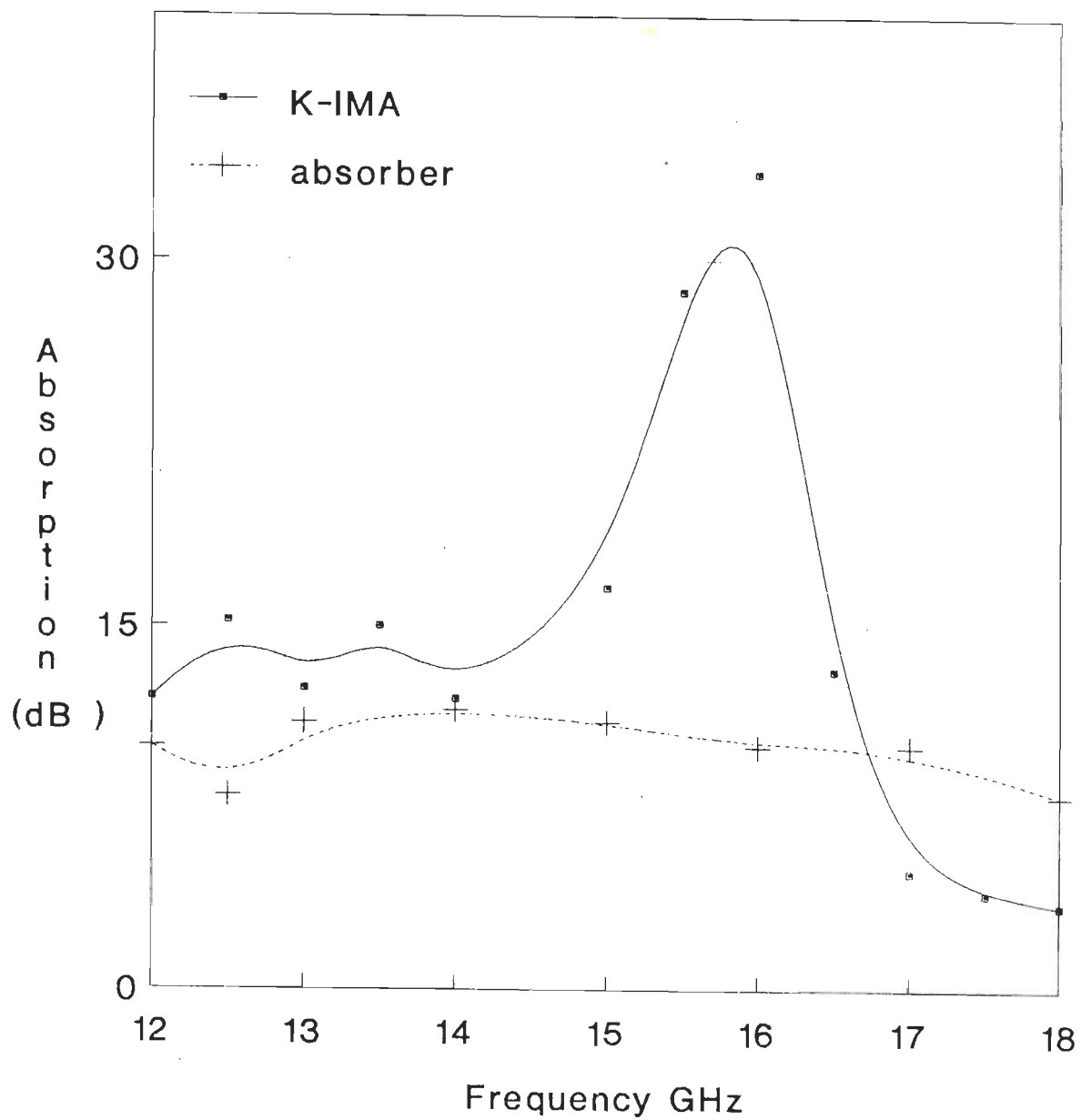


Fig 6.12 Theoretically simulated absorption characteristics for the K-IMA and absorber (BBA).

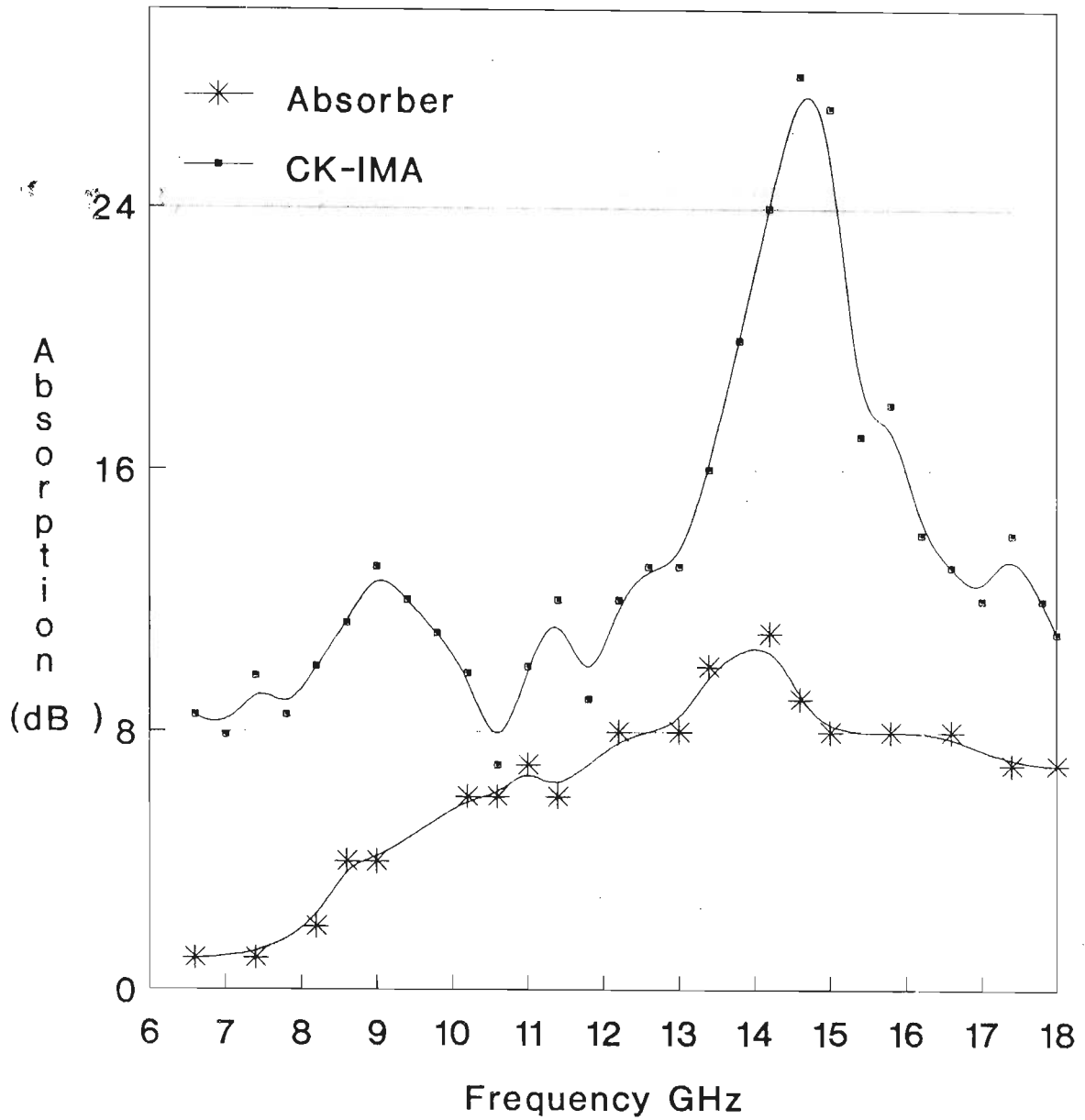


Fig 6.13 Experimentally obtained absorption characteristics for the CK-IMA and absorber (BBA).

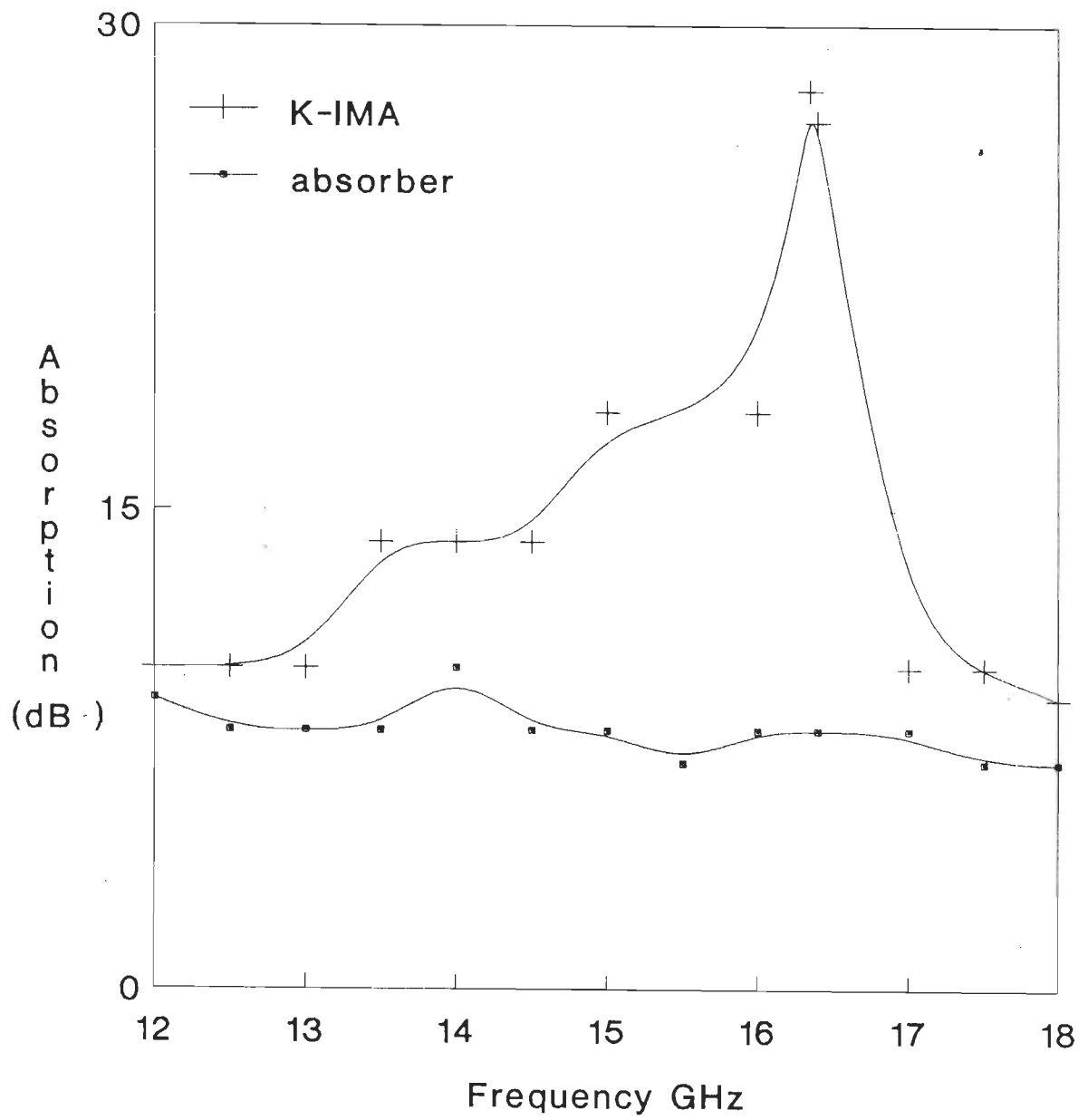


Fig 6.14 Experimentally obtained absorption characteristics for the K-IMA and absorber (BBA).

the peaking frequency.

6.5.0 FREE STANDING PERIODIC ARRAY OF DOUBLE-SQUARE

LOOPS AS AN IMS

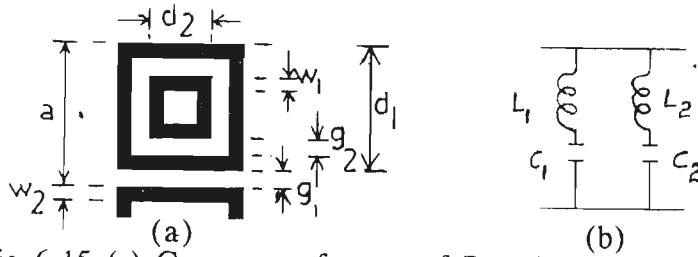


Fig 6.15 (a) Geometry of array of Double Square Loops and (b) its equivalent circuit model.

In the proposed model by [112], as shown in Fig 6.15 the array is represented by two series LC circuits shunted across a transmission line of impedance Z_0 , where Z_0 is the characteristic impedance of free space. The two series LC combinations represent the lower and upper resonant frequencies of the array.

The four circuit elements given in fig. 6.15(b) i.e., L_1 , C_1 , L_2 and C_2 are calculated as follows :

$$L_1 = 2.0 * (L_a || L_b) * \frac{d_1}{p}; \quad 6.10$$

$$\text{where } L_a = F(p, w_1, \lambda) \quad 6.11a$$

$$\text{and } L_b = F(p, w_2, \lambda) \quad 6.11b$$

$$C_1 = 0.75 * C_a * \frac{d_1}{p}; \quad 6.12$$

$$\text{where } C_a = 4f(p, g_1, \lambda) \quad 6.13$$

$$L_2 = L_c * \frac{d_2}{p} \quad 6.14$$

$$\text{where } L_c = F(p, 2w_2, \lambda); \quad 6.15a$$

$$C_2 = (C_a \text{ in series with } C_b) * \frac{d_2}{p}; \quad 6.15b$$

$$\text{and } C_b = 4F(p, g_2, \lambda). \quad 6.15c$$

With the help of above four circuit elements the equivalent circuit for the Double-Square Loop array can be deduced. Thus the impedance of the DSA can be obtained. The procedure for design analysis for a DSA-IMA is exactly similar to the approach described in the previous section with JCA and its equivalent circuit being replaced with DSA and its equivalent circuit.

6.5.1 DESIGN EXAMPLES

Using the technique proposed with a DSA backed by a glass-epoxy sheet of 2mm, as the IMS, Chaitanya et al [152], have modified the single layer absorber designed and fabricated in chapter III, to operate as a broad band IMA. The design details for the array are listed in Table 6.1. The simulated impedance characteristics of the DSA-IMA as a function of frequency is plotted in Fig 6.16. It can be observed from Fig 6.16 that the impedance of DSA-IMA matches closely with that of free space. The theoretically predicted and experimentally determined absorption characteristics for the DSA-IMA of total thickness 3.8mm are plotted in Fig 6.17. It can be noted that the experimental curve follows the theoretically predicted values, and a minimum 8 dB absorption has been achieved over 8 to 18 GHz frequency spectrum.

6.6 CONCLUSION

A simple technique in which an array of Jerusalem cross apertures and a free standing or dielectric backed array of Double Square loops can be used to match a

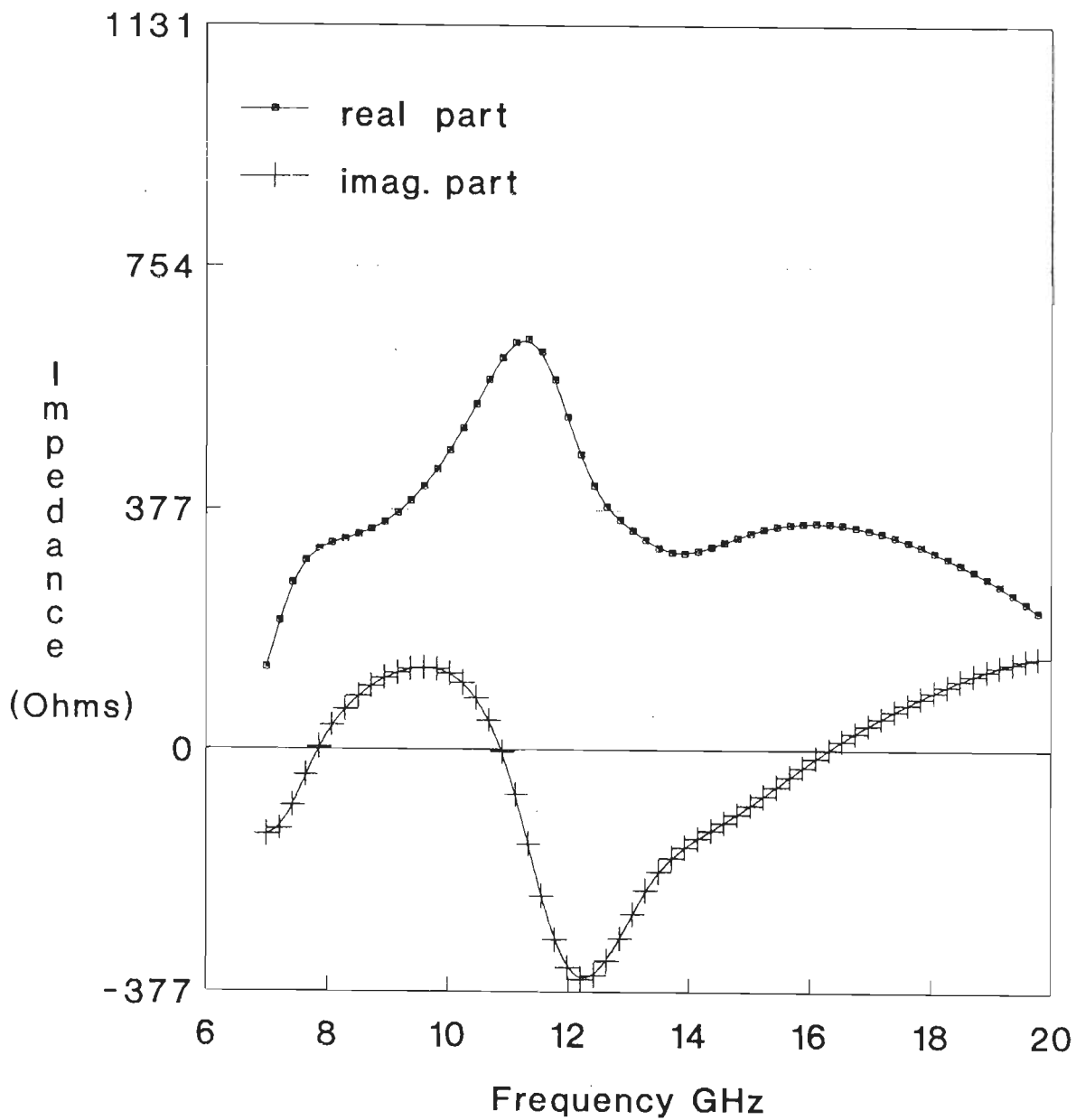


Fig 6.16 Theoretically simulated impedance characteristics for the DSA-IMA

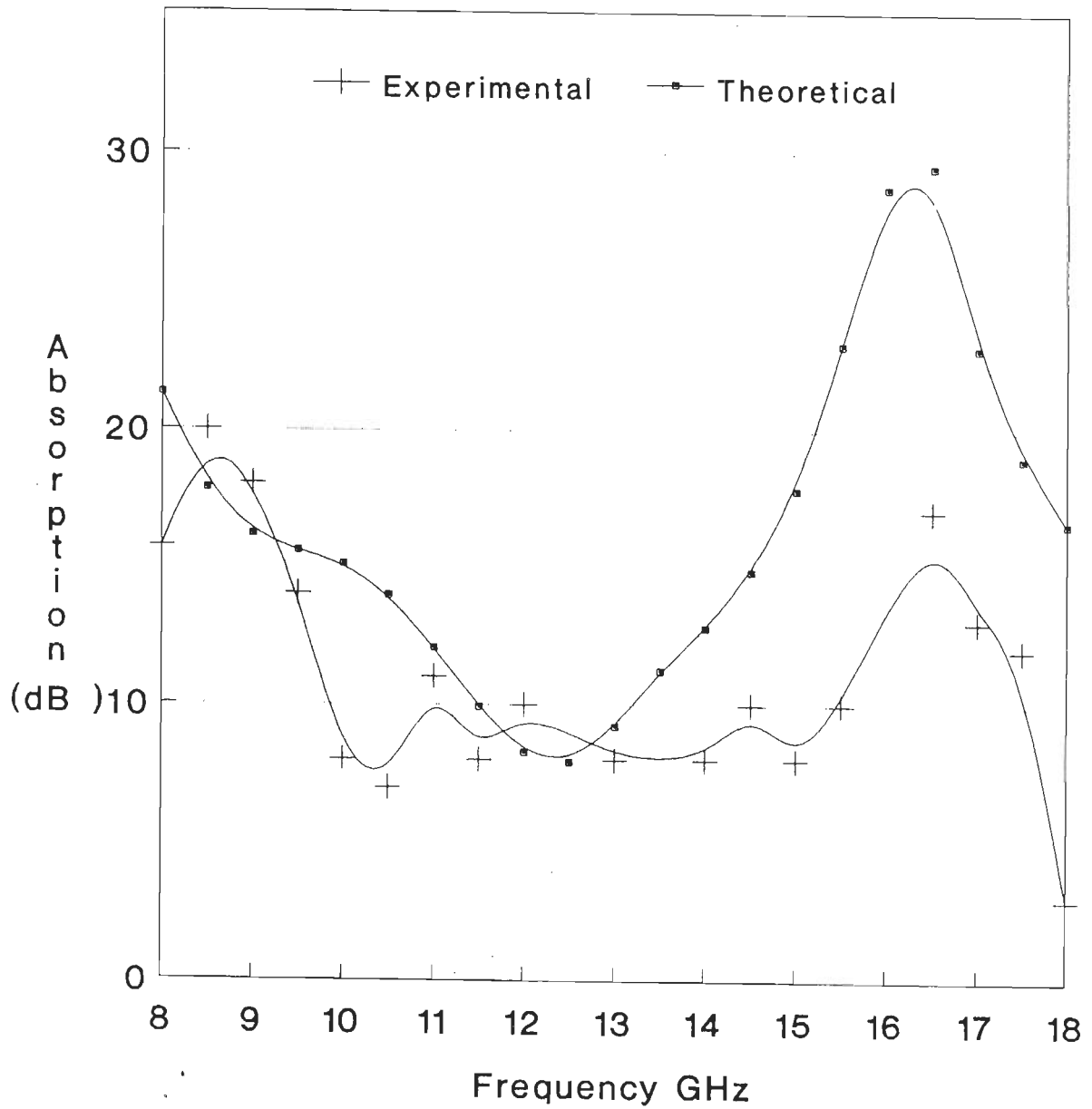


Fig 6.17 Theoretically and experimentally determined absorption characteristics for the DSA-IMA

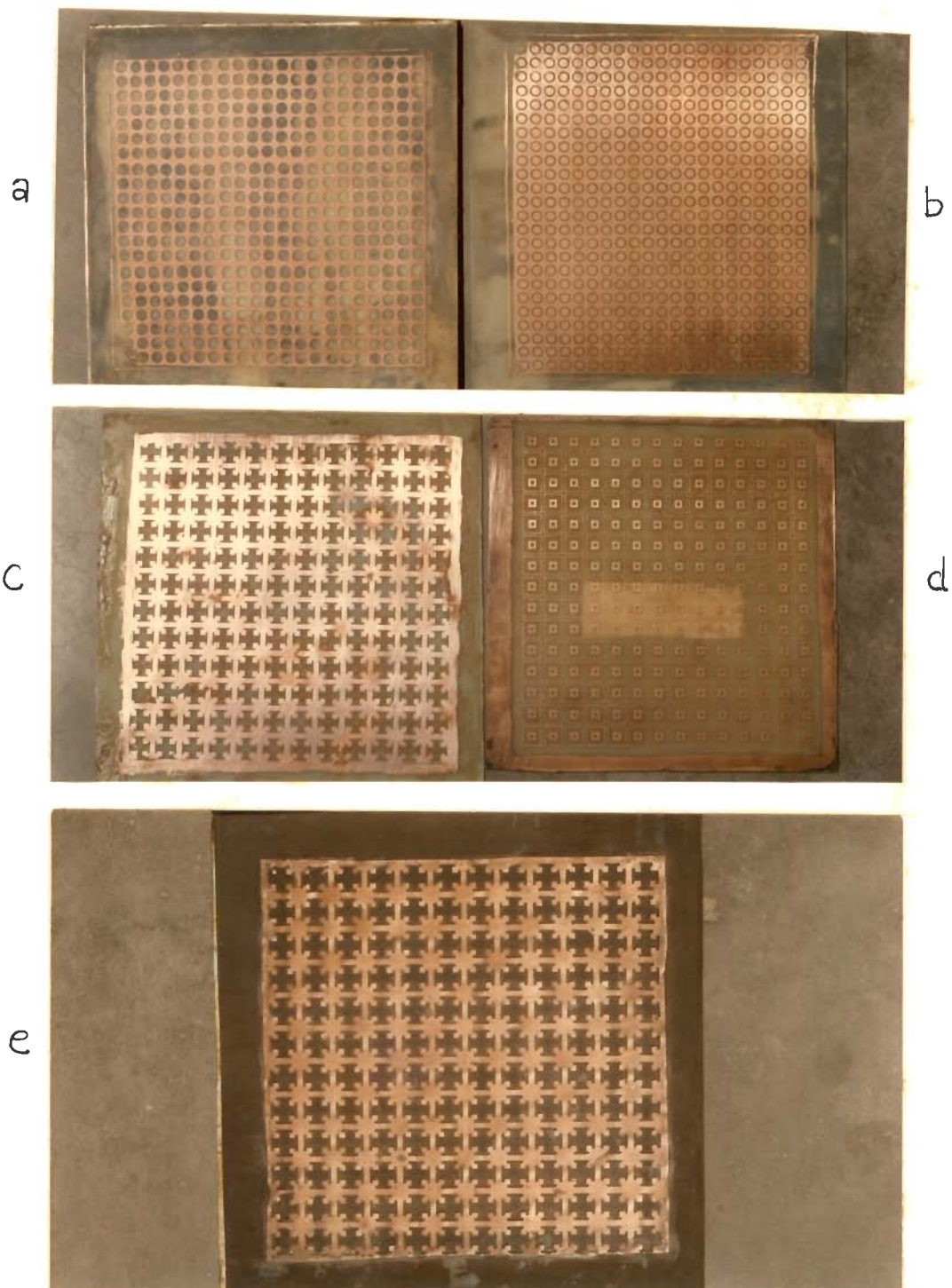
single layer absorber with free space is discussed. Based on the technique discussed a broad band absorber to provide a minimum 10 dB absorption over a frequency range of 6-18 GHz. has been designed and fabricated. Further a narrow band absorber operating in the Ku-Band has also been designed and fabricated. The close agreement shown by the experimental results with the theoretically predicted curves validates the proposed technique for the design. The design of a single layer microwave absorber is also discussed.

The first two photographs attached in the next sheet are showing the fabricated IMA's discussed in section 6.2 and the last one depicts the K-IMA designed and fabricated in section 6.4 (in which the K-IMS is incorporated on the BBA absorber, considered in 3rd chapter).

It is important to note here that Marcuvitz [16], has obtained equation (6.4), with an assumption that periodicity $a \ll \lambda$, in his analysis on strip gratings. However based on our analysis and the practical results obtained for different types of structures, we observe that this assumption on periodicity, is not rigid while considering such an array for IMS application.

Further in the above design and analysis of IMS we have, neglected the effect of thickness 't' of the IMS. It is found [19] that, the thickness of the IMS will have to be accounted in the design as it will influence the peaking frequency, but will have negligible effect on the bandwidth of operation as long as the thickness of IMS, $t \ll d$ is satisfied. Which is confirmed from the experimental results obtained.

A free standing array of Double square array was also fabricated. The experimentally obtained results when this IMS was incorporated at the front end of



Array's of (a) Circular apertures, (b) Annular ring apertures, (c) Jerusalem cross apertures and (d) Double square loops incorporated on a dielectric sheet (e) K-IMS incorporated at the front end of BBA.

a carbon-rubber absorber [154] of thickness 1.8mm, is plotted in Fig 6.18 (The carbon-rubber absorber had equal part by weight of filler and binder). It can be noted that the IMA provides a minimum 10 dB absorption over a 4 GHz bandwidth (10 - 14 GHz). Fig 6.19 shows the experimental observation when the free standing CK-IMS was incorporated at the front end of the carbon-rubber absorber [154]. It can be noted that the performance of the absorber has significantly increased both with respect to the level of absorption provided as well as the bandwidth of operation. Further it provides a minimum 9 dB absorption over a 9 GHz bandwidth. These experimental results confirm the importance of impedance matching in the design of absorbers. Further they also fortify the impedance matching formalism adopted in this chapter.

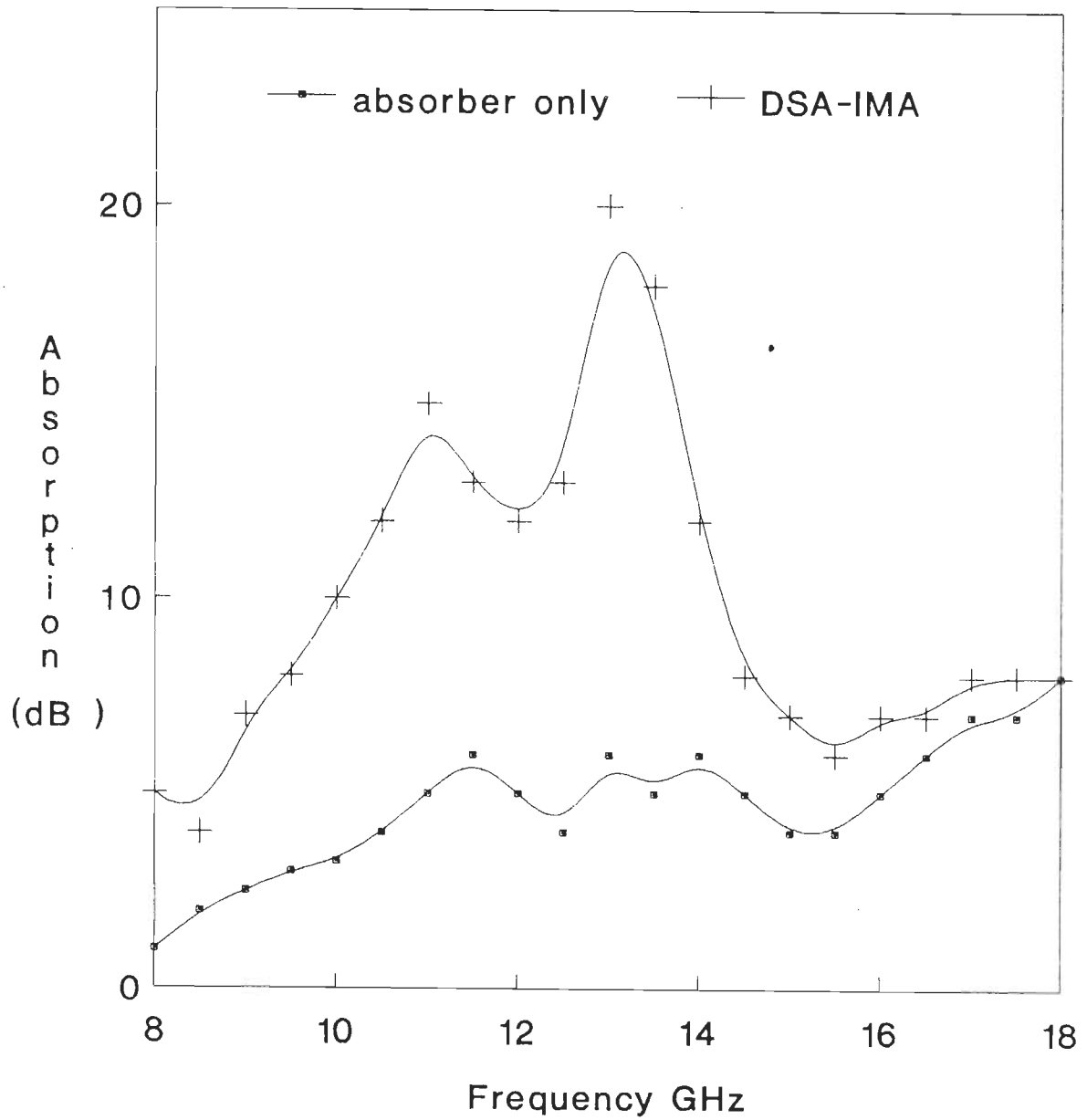


Fig 6.18 Experimentally obtained absorption characteristics for carbon-rubber absorber and DSA-IMA (DSA-IMA : DSA incorporated to Carbon-rubber absorber)

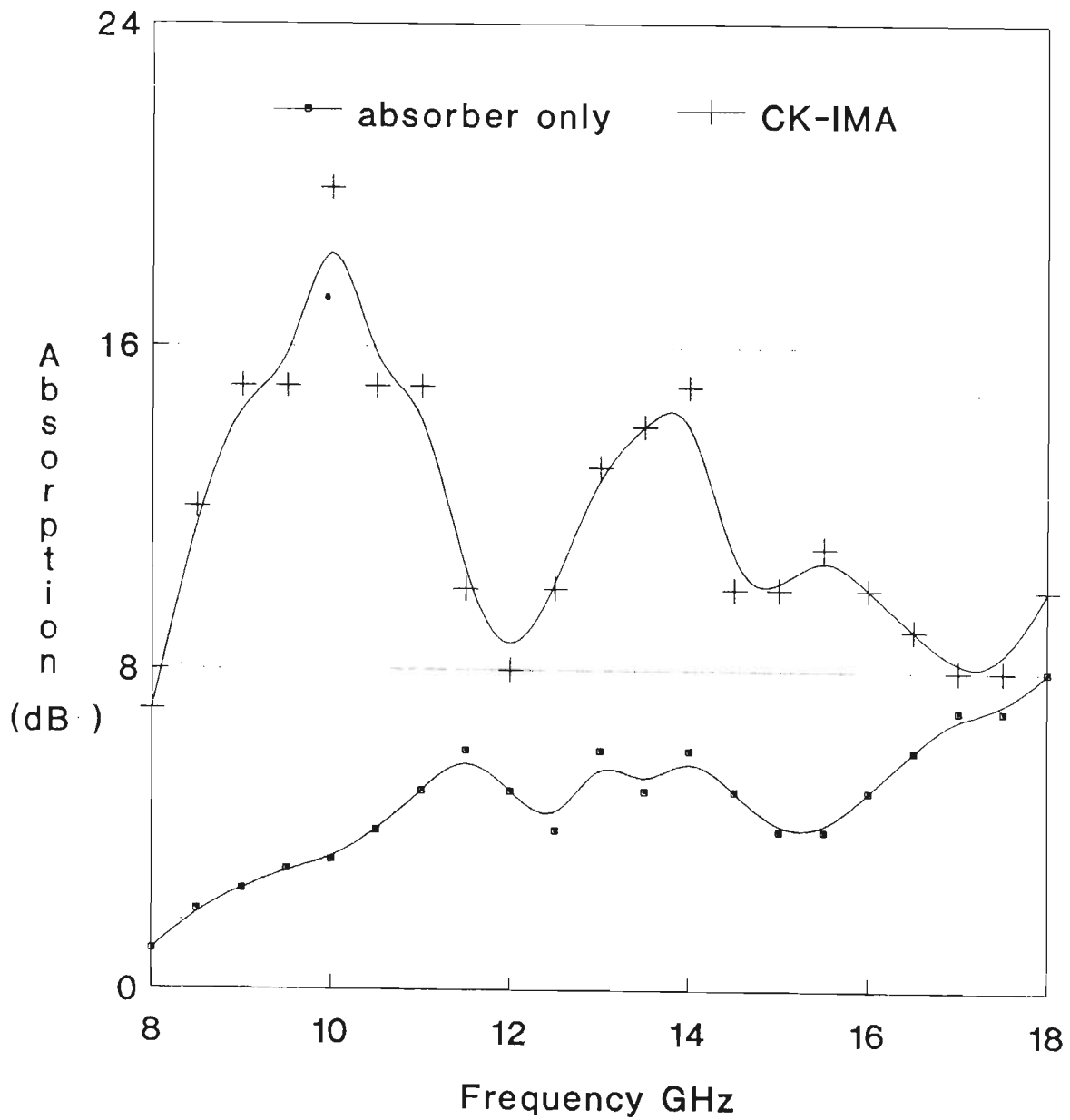


Fig 6.19 Experimentally obtained absorption characteristics for carbon-rubber absorber and CK-IMA
 CK-IMA : CK (IMS) incorporated to Carbon-rubber absorber)

```

C PROGRAM TO COMPUTE THE ELEMENTS OF THE EQUIVALENT
C CIRCUIT FOR THE JERUSALEM CROSS ARRAY
C BASED ON LANGLEY MODEL
C EQ. 6.3 TO 6.8
C MAIN PROGRAM (JCA.FOR)
C P,W,D,G,H,THE,FL ARE a,b,d,c,e, of the JC array,  $\theta$  the incident angle and
C initial value of lower cut of frequency for the array.
C EPR(1) EPI(1),EPR(2),EPI(2) are the real and imaginary parts of permeittivity
C of filler and binder respectively.
C PF(1) AND PF(2) are packinf factor of filler and binder,
C FR(1) the ferromagnetic resonance frequency of Co-BHF and
C DA the thickness of the absorber.
DIMENSION PF(2),FR(10),EPR(2),EPI(2),AJC(4)
OPEN(UNIT=1,FILE='abs.in',STATUS='OLD')
OPEN(UNIT=2,FILE='jca.out',STATUS='NEW')
PIE = 3.1415927
Z0 = 377.
C1 = CMPLX(1.,0.)
U0 = 12.56637E-07
E0 = 8.854E-12
CS = 3.E+11
CSP = 2.*PIE*CS
READ(1,*)P,W,D,G,H,THE,FL
WRITE(2,*)P,W,D,G,H
READ(1,*)EPR(1),EPI(1),EPR(2),EPI(2)
READ(1,*)PF(1),PF(2),FR(1),DA
WRITE(*,*)P,W,D,G,H,THE,FL
ALF = CS/(FL*1.E+9)
THE=(PIE/180.)*THE
WRITE(*,*) THE
C COMPUTING L1
CALL BASFUN(P,W,ALF,THE,X1)
AJC(1) = (X1*Z0*ALF)/CSP
WRITE(*,*)' L1 = ',AJC(1)
WRITE(2,*)' L1 = ',AJC(1)
C COMPUTING C1
CALL BASFUN(P,G,ALF,THE,X1)
BG = 4.*(D/P)*X1/Z0
CG = (BG*ALF)/CSP
PD = P-D
CALL BASFUN(P,PD,ALF,THE,X1)
C BD = 4.*(2.*H+G)*X1/(P*Z0)
BD=(4.*(2.*H+G/P))*X1/377.
CD = BD*ALF/CSP
AJC(2)= CG + CD
WRITE(*,*)' C1 = ',AJC(2)
WRITE(2,*)' C1 = ',AJC(2)
C COMPUTING L3
ALH = D/0.49
HG = 2.*H + G
write(*,*)' computing L3 '
CALL BASFUN(P,HG,ALH,THE,X1)

```

```

AL4 = ((D/P)*X1*ALH)/CSP
write(*,*)al4
PB2 = P/2.
CALL BASFUN(PB2,W,ALH,THE,X1)
AL5 = X1*ALH/CSP
write(*,*)al5
AJC(3) = ((AL4+AL5)/2.)*Z0
WRITE(*,*)' L3 = ',AJC(3)
WRITE(2,*)' L3 = ',AJC(3)
C COMPUTING C3
CALL BASFUN(P,H,ALH,THE,X1)
AL = (D/P)*X1*(ALH/CSP)
AJC(4) = 2./((CSP/ALH)**2 * AL * Z0)
WRITE(*,*)' C3 = ',AJC(4)
WRITE(2,*)' C3 = ',AJC(4)
FREQL = 1./(2.*PIE*SQRT(AJC(1)*AJC(2)))
FREQH = 1./(2.*PIE*SQRT(AJC(3)*AJC(4)))
WRITE(*,*)' FL = ',FREQL
WRITE(2,*)' FH = ',FREQH
WRITE(2,*)' FL = ',FREQL
WRITE(*,*)' FH = ',FREQH
CALL RLOSS(FR,PF,DA,EPR,EPI,AJC)
STOP
END

```

```

SUBROUTINE BASFUN(A1,A2,A3,A4,XZ)
C EQ. 6.4
C A4 = ANGLE OF INCIDENCE
PIE = 3.1415927
BE = PIE * A2/(2.*A1)
PBL=A1/A3
B2 = (PBL*COS(A4))**2
B1 = PBL*2.*SIN(A4)
B = SQRT(1.+B1-B2)
AP = (1./B)-1.
B = SQRT(1.-B1-B2)
AN = (1./B)-1.
B = SIN(BE)
B2 = B*B
B4 = B2*B2
G1 = (1.-B2)**2*((1-B4/4.)*(AP+AN)+4.*B2*AP*AN)
G2 = (1.-B2/4.) + B2*(1.+B2/2.-B4/8.)*(AP+AN)+2.*B2*B4*AP*AN
G = 0.5*G1/G2
XZ = PBL*COS(A4)*(ALOG(1/B)+G)
RETURN
END

```

```

subroutine rloss(fr,pf,al,epr,epi,ajc)
c EQ. 6.1 TO 6.3
c Program to compute the reflection loss
complex ep(10),e,u,q,b,a8,a9,qd,qs,c1,ak,b1,xy,up(10)
dimension af(250),epr(10),epi(10),pf(10)

```

```

open(unit=5,file='abs.out',status='new')
fh = 20.
fl = 7.
dinc = abs(fh-fl)/60.0
pi=3.1415927
u0 = 12.56637E-07
e0 = 8.854E-12
z0 = 377.0
af(0) = fl-dinc
c1=(0.0,1.0)
do 10 i = 1,2
10 ep(i) = cmplx(epr(i),-epi(i))
continue
call eque(ep,pf,xy)
e = xy * e0
d = al/1000.
do 50 k = 1,60
af(k) = af(k-1) + dinc
fl = af(k)
call perm(fl,fr,xy)
up(1) = xy
up(2) = cmplx(1.0,0.0)
call eque(up,pf,xy)
u = xy * u0
ak = 2. * pi * af(k) * 1.e+09 * csqrt(e * u)
a8 =-c1*2.0*ak * d
q = cexp(a8)
qd = 1.0 - q
qs = 1.0 + q
b1 = (qd/qs)*csqrt(u/e)
xy = (b1-z0)/(b1+z0)
r = cabs(xy)
da = -20.0 * alog10(r)
call jci(af(k),a9)
b = (b1*a9)/(b1+a9)
xy = (b-z0)/(b+z0)
r = cabs(xy)
df = -20.0 * alog10(r)
write(5,1)af(k),da,df
write(*,1)af(k),da,df
1 format(3f10.2)
50 continue
stop
end

c subroutine eque to compute the equivalent. e & u
C EQ.3.6C (Lichenaker equivalent e & u formula)
subroutine eque(u1,pf,xa)
complex xa,u1(10)
dimension pf(10)
xa = 0.0
pi = 0.0

```

```

ai = 0.0
tx = 0.0
do 100 i = 1,2
as = cabs(u1(i))
as1 = abs(as)
ai = ai + pf(i) * log(as1)
b1 = aimag(u1(i))
b2 = real(u1(i))
tnd = b1/b2
tx = tx + pf(i) * tnd
pi = pi + pf(i)
100 continue
del = atan(tx)
as = exp(ai)
b2 = as * cos(del)
b1 = as * sin(del)
xa = cmplx(b2,b1)
return
end

```

```

subroutine perm(f1,fsr,us)
c subroutine to compute the permeability
c eq. 3.5a and 3.6b
complex us
us = 0.0
s1 = 1.0
afc = f1 + 1.0
do 525 j1=1,2
afc=afc-1.0
a1 = afc - fsr
a2 = fsr + afc/2.0
a3 = 2.0 * a1/a2
ch = cosh(a3)
a4 = a1*a1
a5 = sqrt(s1 + a4)
xy = 4.0 * ch/a5
if (j1.eq.1) then
ur = xy
else
ui = xy
endif
525 continue
us = cmplx(ur,-ui)
return
end

```

```

SUBROUTINE JCI(F,AJC,Z1)
C CALCULATION OF IMPEDANCE OF FREE STANDING
C JERUSALEM CROSS ARRAY
C EQ. 6.9
REAL L1,C1,L31,C31,F,P,Q,AJC(4)
COMPLEX Z1,J,X,Y

```

```
L1 = AJC(1)
C1 = AJC(2)
L31 = AJC(3)
C31 = AJC(4)
PI=3.1415927
J=(0.,1.)
W=2.*PI*F*1.e+09
P=(1.-(W**2)*L1*C1)
Q=(1.-(W**2)*L31*C31)
X=(J*P*Q)
Y=(W*(C1*Q+C31*P))
Z1=(X/Y)
RETURN
END
```

Typical input file

```
20 4 10 3 4 0 3.98
10 1 5 .2 1 0
.45 .55 12.63 1.8
```

CHAPTER VII

DESIGN ANALYSIS OF A MULTILAYERED ABSORBER

7.1 INTRODUCTION

One of the established approaches to overcome the impedance mismatch at the front end of the absorber, is to utilize a multilayer construction. Where in an impedance grading is created between the free space (high impedance) and the highly lossy layer (low impedance). In this chapter the design and development of an absorber, which is effective to all polarization, over a broad band of frequencies and angle of incidence is discussed. The broad band absorption properties are achieved by using a multilayer construction. The design equations are arrived at and utilized to design and develop an absorber for broad band operation over X-Band and over a $\pm 45^\circ$ angle of incidence.

7.2.0 ANALYSIS OF THE MULTILAYERED ABSORBER

Consider the N layered absorber shown in the Fig 7.1, ϵ_{ri} , μ_{ri} , l_{ri} and K_i are the complex relative permittivity, complex relative permeability, thickness and propagation constant of the i^{th} layer respectively. Let a uniform plane wave travelling in the positive Z direction be incident on the absorber at an angle θ_0 . Then the angle of incidence in the i^{th} layer can be written as

$$k_i \sin(\theta_i) = k_{i-1} \sin(\theta_{i-1}) \quad 7.1$$

The plane formed by the direction of the incident wave and normal to the

surface at the point of incidence is defined as the plane of incidence. The general case, in which the direction of the electric field is arbitrary, can be analyzed into two problems. In one, the field is normal to the plane of incidence and parallel to the boundary surface, while in the other, it lies in the plane of incidence. These two components are called as E_p and E_n respectively.

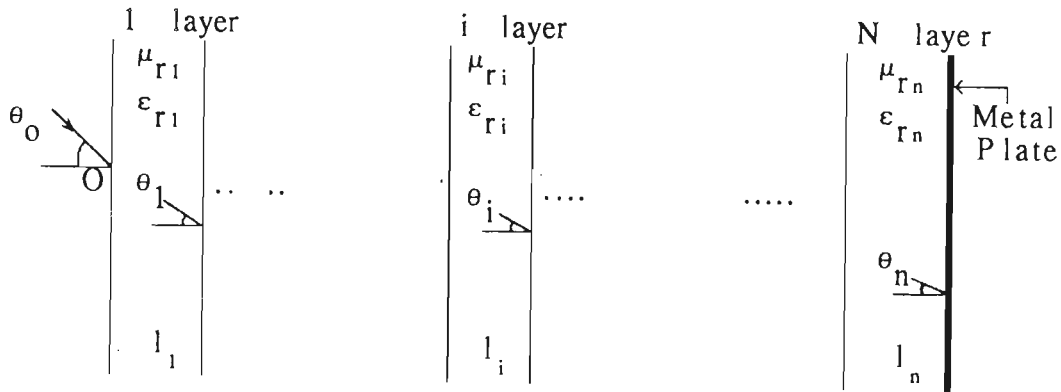


Fig 7.1 Geometry of the Multi-layered absorber

If the interface point 'O' is chosen as the origin of a coordinate system, then the incident field, E_i and reflected field E_r in different layers are given by,

$$E_{ii} = a_i e^{j[\omega t - k_i(x \sin \theta_i + z \cos \theta_i)]} \quad 7.2$$

$$E_{ir} = b_i e^{j[\omega t - k_i(x \sin \theta_i - z \cos \theta_i)]} \quad 7.3$$

where a_i and b_i are the incident and reflected field amplitudes. The time variation $e^{j\omega t}$ is suppressed in the following.

7.2.1 ELECTRIC FIELD PARALLEL TO THE PLANE OF INCIDENCE

The electric and magnetic field vectors E_p and H_n are constant in any X-Y plane. The electric field in different layers can be written as

$$\begin{aligned} E_{po} &= a_{po} \cos \theta_o e^{-jk_o(x \sin \theta_o + z \cos \theta_o)} \\ &+ b_{po} \cos \theta_o e^{-jk_o(x \sin \theta_o - z \cos \theta_o)} \end{aligned} \quad 7.4$$

where $a_{po} = 1$ and b_{po} is the amplitude of the resultant reflected wave from the air-1st layer interface.

$$\begin{aligned} E_{pi} &= a_{pi} \cos \theta_i e^{-jk_i(x \sin \theta_i + z \cos \theta_i)} \\ &+ b_{pi} \cos \theta_i e^{-jk_i(x \sin \theta_i - z \cos \theta_i)} \end{aligned} \quad 7.5$$

where a_{pi} and b_{pi} is the amplitudes of incident and reflected waves respectively in the i^{th} layer.

Using the Maxwell's equations, the corresponding magnetic fields can be obtained as

$$\begin{aligned} H_{pi} &= \frac{K_i}{\omega \mu_i} \left[a_{pi} \cos \theta_i e^{-jk_i(x \sin \theta_i + z \cos \theta_i)} \right. \\ &\quad \left. + b_{pi} \cos \theta_i e^{-jk_i(x \sin \theta_i - z \cos \theta_i)} \right] \end{aligned} \quad 7.6$$

Applying the boundary conditions at successive interfaces between adjacent layers and utilizing the condition that, at the conducting surface $z = L_n$; $E_{pn} = 0$, coefficients a_{pi} 's and b_{pi} 's can be solved [132] as follows

Equating (7.5) to zero at $z=L$, we obtain

$$-b_{pn}/a_{pn} = e^{-j2k_n L_n \cos \theta_n} \quad 7.7$$

$$\text{let } Q_n = -b_{pn}/a_{pn} \quad 7.8$$

At $z = L_{n-1}$, the boundary condition is $E_{pn} = E_{pn-1}$. Hence

$$\begin{aligned} &a_{pn-1} \cos \theta_{n-1} e^{-jk_{n-1}(x \sin \theta_{n-1} + z \cos \theta_{n-1})} \\ &+ b_{pn-1} \cos \theta_{n-1} e^{-jk_{n-1}(x \sin \theta_{n-1} - z \cos \theta_{n-1})} \\ &= a_{pn} \cos \theta_n e^{-jk_n(x \sin \theta_n + z \cos \theta_n)} \\ &+ b_{pn} \cos \theta_n e^{-jk_n(x \sin \theta_n - z \cos \theta_n)} \end{aligned} \quad 7.9$$

Similarly applying the boundary condition on the magnetic field at $z = L_{n-1}$, we obtain

$$\begin{aligned}
 & a_{pn-1} \cos \theta_{n-1} e^{-jk_{n-1}(x \sin \theta_{n-1} + z \cos \theta_{n-1})} \\
 & + b_{pn-1} \cos \theta_{n-1} e^{-jk_{n-1}(x \sin \theta_{n-1} - z \cos \theta_{n-1})} \\
 & = (1/\tau_{pn}) \left(a_{pn} \cos \theta_n e^{-jk_n(x \sin \theta_n + z \cos \theta_n)} \right. \\
 & \quad \left. + b_{pn} \cos \theta_n e^{-jk_n(x \sin \theta_n - z \cos \theta_n)} \right)
 \end{aligned} \tag{7.10}$$

where

$$\tau_{pn} = \sqrt{\frac{\epsilon_{rn} \mu_{rn-1}}{\epsilon_{rn-1} \mu_{rn-1}}} \cdot \frac{\cos \theta_{n-1}}{\cos \theta_n} \tag{7.11}$$

from Eq.s (7.9) and (7.10), we have

$$Q_{n-1} = -b_{n-1}/a_{n-1} = \frac{1 - P_n}{1 + P_n} e^{-j2k_{n-1}L_{n-1}\cos \theta_{n-1}} \tag{7.12}$$

where

$$P_n = \frac{e^{-j2k_n L_{n-1} \cos \theta_{n-1}} - Q_n}{\tau_{pn} \left(e^{-j2k_n L_{n-1} \cos \theta_{n-1}} \right) + Q_n} \tag{7.13}$$

Proceeding in the same manner, at $n-2$ interface or when $z = l_{n-2}$, we obtain

$$Q_{n-2} = -b_{n-2}/a_{n-2} = \frac{1 - P_{n-2}}{1 + P_{n-2}} e^{-j2k_{n-2}L_{n-2}\cos \theta_{n-2}} \tag{7.14}$$

where

$$P_{n-1} = \frac{e^{-j2k_{n-1}L_{n-2}\cos \theta_{n-2}} - Q_{n-1}}{\tau_{pn-1} \left(e^{-j2k_{n-1}L_{n-2}\cos \theta_{n-2}} \right) + Q_{n-1}} \tag{7.15}$$

By successive computation of P_i and Q_{i-1} , it can be shown that, the reflection coefficient at the 1st layer - air interface b_{po} is given by

$$b_{po} = \frac{1 - Q_1 - \tau_{p1}(1+Q_1)}{1 - Q_1 + \tau_{p1}(1+Q_1)} \tag{7.16}$$

7.2.2 ELECTRIC FIELD PERPENDICULAR TO THE PLANE OF INCIDENCE

The electric and magnetic field vectors \mathbf{E}_n and \mathbf{H}_p are constant in any X-Y plane. The electric field in different layers can be written as

$$\begin{aligned} \mathbf{E}_{no} = & a_{no} \cos\theta_o e^{-jk_o(x \sin\theta_o + z \cos\theta_o)} \\ & + b_{no} \cos\theta_o e^{-jk_o(x \sin\theta_o - z \cos\theta_o)} \end{aligned} \quad 7.17$$

where $a_{no} = 1$ and b_{no} is the amplitude of the resultant reflected wave from the air-1st layer interface.

$$\begin{aligned} \mathbf{E}_{ni} = & a_{ni} \cos\theta_i e^{-jk_i(x \sin\theta_i + z \cos\theta_i)} \\ & + b_{ni} \cos\theta_i e^{-jk_i(x \sin\theta_i - z \cos\theta_i)} \end{aligned} \quad 7.18$$

where a_{ni} and b_{ni} are the amplitudes of the incident and reflected wave in the i^{th} layer.

Using the Maxwell's equations, the corresponding magnetic fields can be obtained as

$$\begin{aligned} \mathbf{H}_{ni} = & \frac{K_i}{\omega \mu_i} \left[a_{ni} \cos\theta_i e^{-jk_i(x \sin\theta_i + z \cos\theta_i)} \right. \\ & \left. + b_{ni} \cos\theta_i e^{-jk_i(x \sin\theta_i - z \cos\theta_i)} \right] \end{aligned} \quad 7.19$$

Applying the boundary conditions at successive interfaces between adjacent layers and utilizing the condition that, at the conducting surface $z = L_n$; $\mathbf{E}_n = 0$, coefficients a_{pi} 's and b_{pi} 's can be solved. The reflection coefficient at the 1st layer - air interface b_{no} can be obtained as

$$b_{no} = \frac{1 - Q_1 - \tau_{n1}(1+Q_1)}{1 - Q_1 + \tau_{n1}(1+Q_1)} \quad 7.20$$

where Q_1 is obtained by successive computation of Q 's and P 's as described in the previous section, with τ_{ni} given by

$$\tau_{ni} = \sqrt{\frac{\epsilon_{ri} \mu_{ri-1}}{\epsilon_{ri-1} \mu_{ri}}} \left(\frac{\cos \theta_i}{\cos \theta_{i-1}} \right) \quad 7.21$$

Thus from Eq.'s (7.16) and (7.20), the expression for the reflection coefficient at the air - 1st layer interface can be generalized as

$$b_{xo} = \frac{[1 - Q_1 - \tau_{x1} (1 + Q_1)]}{[1 - Q_1 + \tau_{x1} (1 + Q_1)]} \quad 7.22a$$

where x represents the type of polarization. Q_1 is derived by following the sequence of computing Q_i and P_i , then Q_{i-1} and P_{i-1} and so on, in the descending by using the following equations

$$Q_n = e^{-j2k_n L_n \cos \theta_n} \quad 7.22b$$

$$P_i = \frac{e^{-j2k_i L_{i-1} \cos \theta_{i-1}} - Q_i}{\tau_{pi} [e^{-j2k_i L_{i-1} \cos \theta_{i-1}}] + Q_i} \quad 7.22c$$

$$Q_{i-1} = \frac{1 - P_i}{1 + P_i} e^{-j2k_{i-1} L_{i-1} \cos \theta_{i-1}} \quad 7.22d$$

$$L_i = \sum_{m=1}^i l_m, \quad i = 1, 2, \dots, n \quad 7.22e$$

and τ_{xi} is given by Eq. (7.11) and (7.21) for parallel and perpendicular polarizations respectively. The coefficient b_{xo} is thus a complex function of frequency, individual layer thickness, overall thickness of the absorber, ϵ_i 's and μ_i 's. The voltage reflection coefficient is $\Gamma_x = |b_{xo}|$. The reflection loss or

absorption is then given by

$$A = 20 \log_{10} \Gamma_x \quad 7.23$$

For the case of normal incidence, Eq.'s (7.22) reduces to the form obtained by Amin and James [41] as

$$b_o = \frac{[1 - Q_1 - \tau_1 (1 + Q_1)]}{[1 - Q_1 - \tau_1 (1 + Q_1)]} \quad 7.24a$$

where Q_1 is derived by following the sequence of computing Q_i and P_i , then Q_{i-1} and P_{i-1} and so on, in the descending by using the following equations

$$Q_n = e^{-j2k_n L_n} \quad 7.24b$$

$$P_i = \frac{e^{-j2k_i L_{i-1}} - Q_i}{\tau_{pi} (e^{-j2k_i L_{i-1}}) + Q_i} \quad 7.24c$$

$$Q_{i-1} = \frac{1 - P_i}{1 + P_i} e^{-j2k_{i-1} L_{i-1}} \quad 7.24d$$

$$L_i = \sum_{m=1}^i l_m, \quad i = 1, 2, \dots, n \quad 7.24e$$

$$\text{and } \tau_i = \sqrt{\frac{\epsilon_{ri} \mu_{ri-1}}{\epsilon_{ri-1} \mu_{ri}}} \quad 7.24f$$

7.3 DESIGN AND EXPERIMENTAL RESULTS

Due to the limitation in fabricating a multilayer absorber at our disposal, a single layer absorber as a special case of a multilayer absorber was considered for the validation of the theoretical approach discussed.

The design specification that was set, was a minimum 10 dB absorption over

X-Band at $\pm 45^\circ$ angle of incidence. Further a 3mm limitation on the overall thickness was also set.

Since the absorption required was stringent or had to account for both types of polarization which implies a high loss at normal incidence [124], Iron powder was selected as the lossy material due to its high loss tangents [133] and rubber was used as the binder. The design, using Eq.s (7.22) and (7.23) was made employing the flexible tolerance optimization subroutine [119]. The optimization subroutine was used, because the bandwidth requirement was itself non unique in the sense that beyond a given level, the absorption could fluctuate in an specified manner. The subroutine was run several times with different numerical weights, and the optimized parameters for the single layer microwave absorber sheet were selected, to meet the desired specifications as follows:

Lossy material : Iron powder (average particle size
10 microns);
Binder : Silicone rubber;
L : M : 18:82%; (v/v)
Thickness : 2.3mm.

Commercially available Iron Powder (prepared by electrolysis process was utilized), the average particle was controlled by passing the powder through an appropriate mesh screen in an agitator. Iron powder and rubber were taken in the required ratio and dry mixed in a two roll mill and fabricated into a sheet of 300 X 300 X 2.3mm.

The permittivity and permeability of the fabricated absorber was determined using the method described in section 8.3.12 (next chapter). The experimentally determined permittivity and permeability for the absorber are plotted in Fig 7.2

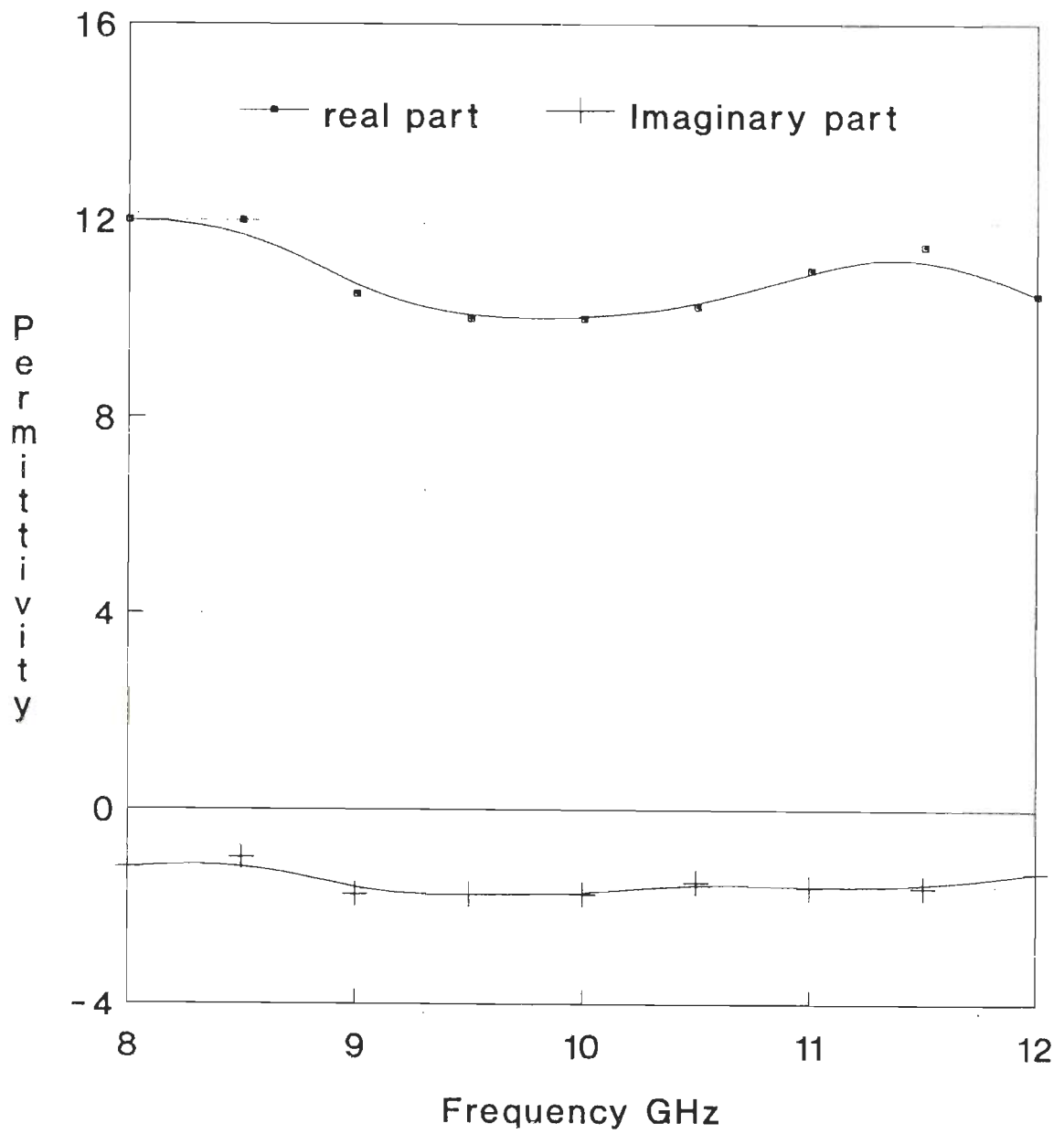


Fig 7.2 Experimentally obtained permittivity characteristics for the designed and fabricated absorber

and 7.3.

The free space measurement set up shown in Fig 3.4, was once again used to measure the absorption provided by the fabricated absorber.

The theoretically predicted absorption and experimentally obtained absorption characteristics for the designed absorber are plotted in Fig 7.4 and 7.5. It can be observed from the figures that the experimentally obtained results are in good agreement with the theoretically predicted values. Experimentally a minimum 10 dB has been achieved at normal incidence as well as $\pm 45^\circ$ angle incidence.

7.4 CONCLUSION

An established approach to overcome the mismatching (at the free space-absorber interface) problem associated with planar absorbers is to construct an impedance taper employing a multilayered structure. This approach has been extended to the case of thin planar absorbers. Generalized design equations have been arrived at, for a plane wave at arbitrary angle of incidence, as a function of number of layers, concentration of the lossy material in each layer, individual layer thickness, and the overall thickness of the absorber.

As a special case of multilayered structure when the number of layers is one, a single layer absorber was designed using the multilayered approach, to operate as a broad band absorber (X-Band) over $\pm 45^\circ$ incidence angle. A limitation on the overall thickness of the absorber of 3mm was also met. Iron powder has been used in the design as the lossy material along with silicone rubber as the binder. The designed and fabricated absorber of 2.3mm thick, displays a practical absorption characteristics which matches very closely with the theoretically predicted curves.

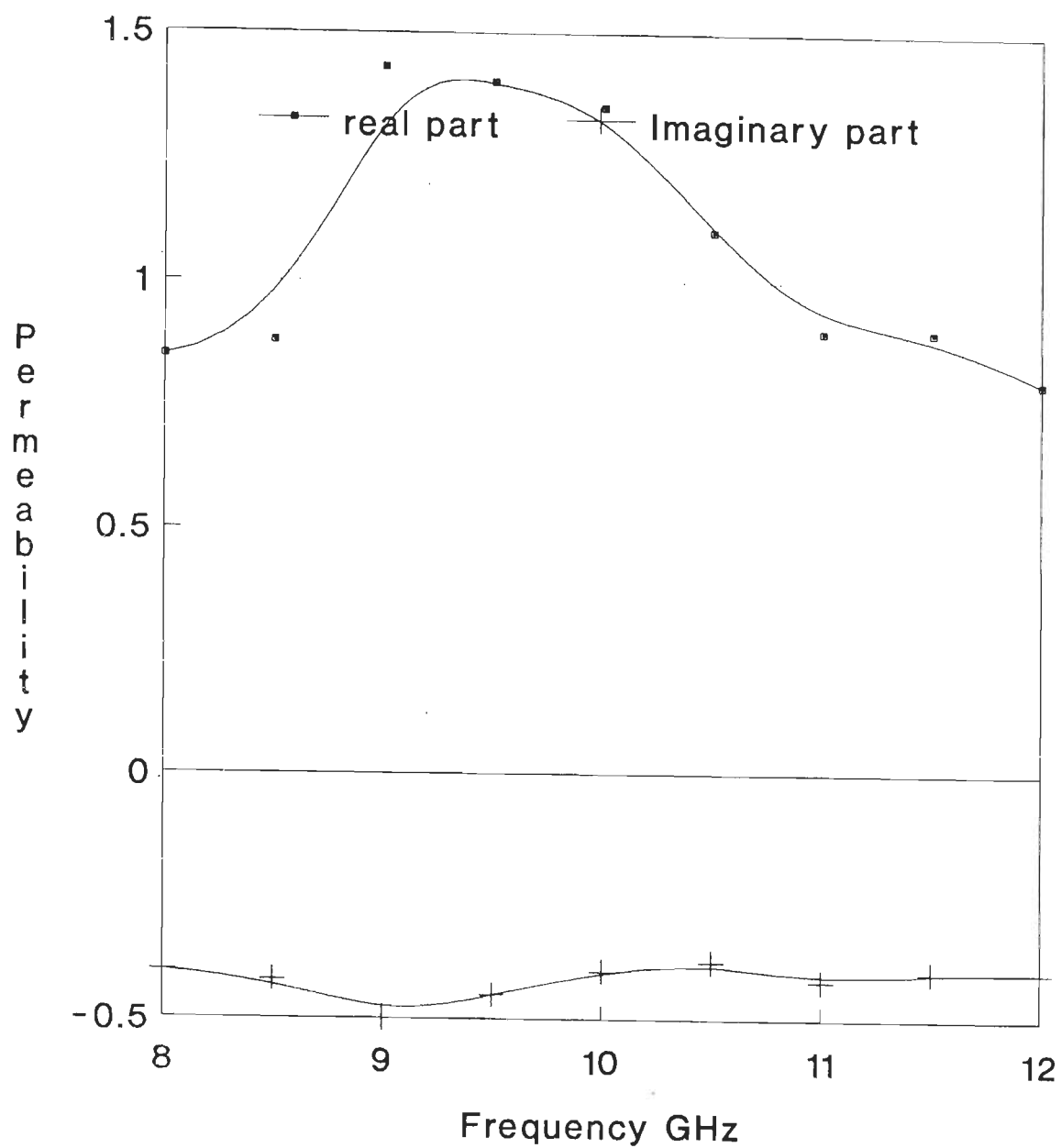


Fig 7.3 Experimentally obtained permeability characteristics for the designed and fabricated absorber

Further from Fig 7.4 and 7.5, it is observed that the absorption characteristics of the absorber is polarization dependent. Since the absorption obtained for perpendicular polarization is more than the corresponding values for parallel polarization. This is due to the following reasons:

The time-averaged power of a beam of electromagnetic wave is equal to the product of P_{av} and A . Where P_{av} is the magnitude of the time averaged Poynting vector and A the cross sectional area of the beam. The ratio of A 's of the reflected to the incident beams is given as $\cos\theta_t/\cos\theta_i$, where subscripts t and i , refer to transmitted and incident beams. Hence, the fraction of the power contained in the transmitted beam is more in perpendicular polarization. Which results in higher absorption. Thus when the absorber is being designed, one needs to satisfy the design specifications only for parallel polarization.

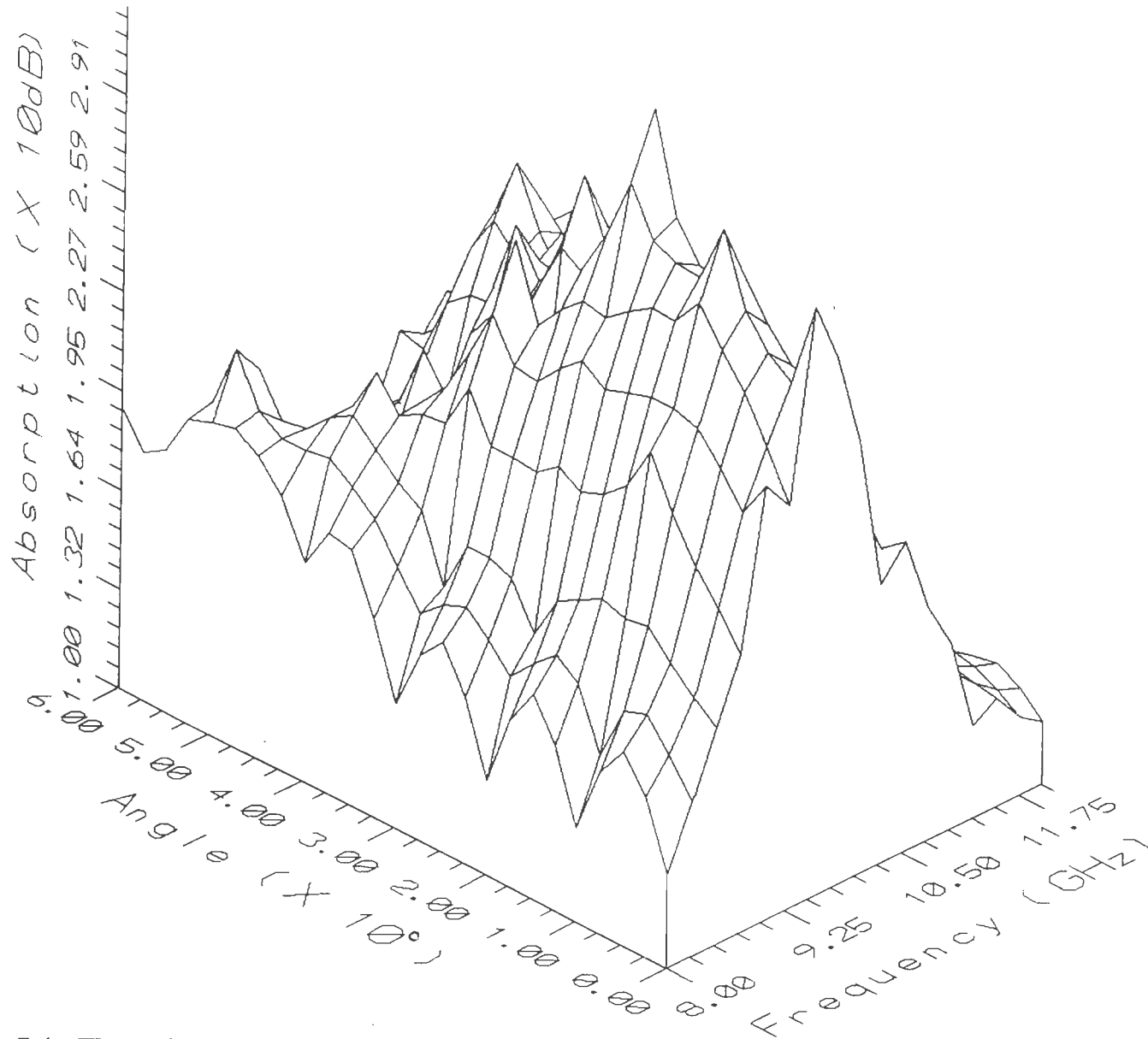


Fig 7.4a Theoretically simulated absorption characteristics for the case of perpendicular polarization.

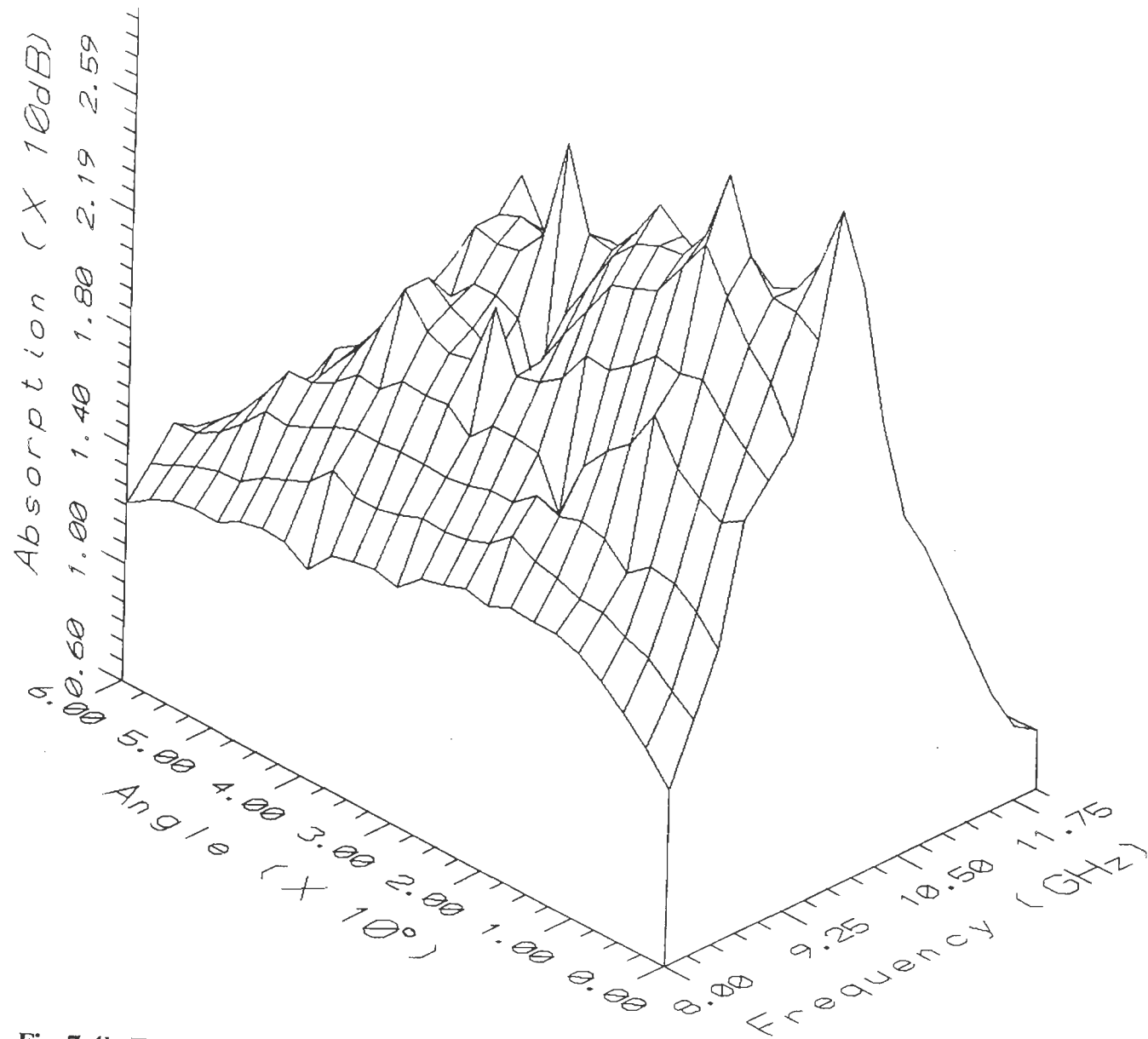


Fig 7.4b Experimentally obtained absorption characteristics for the case of perpendicular polarization.

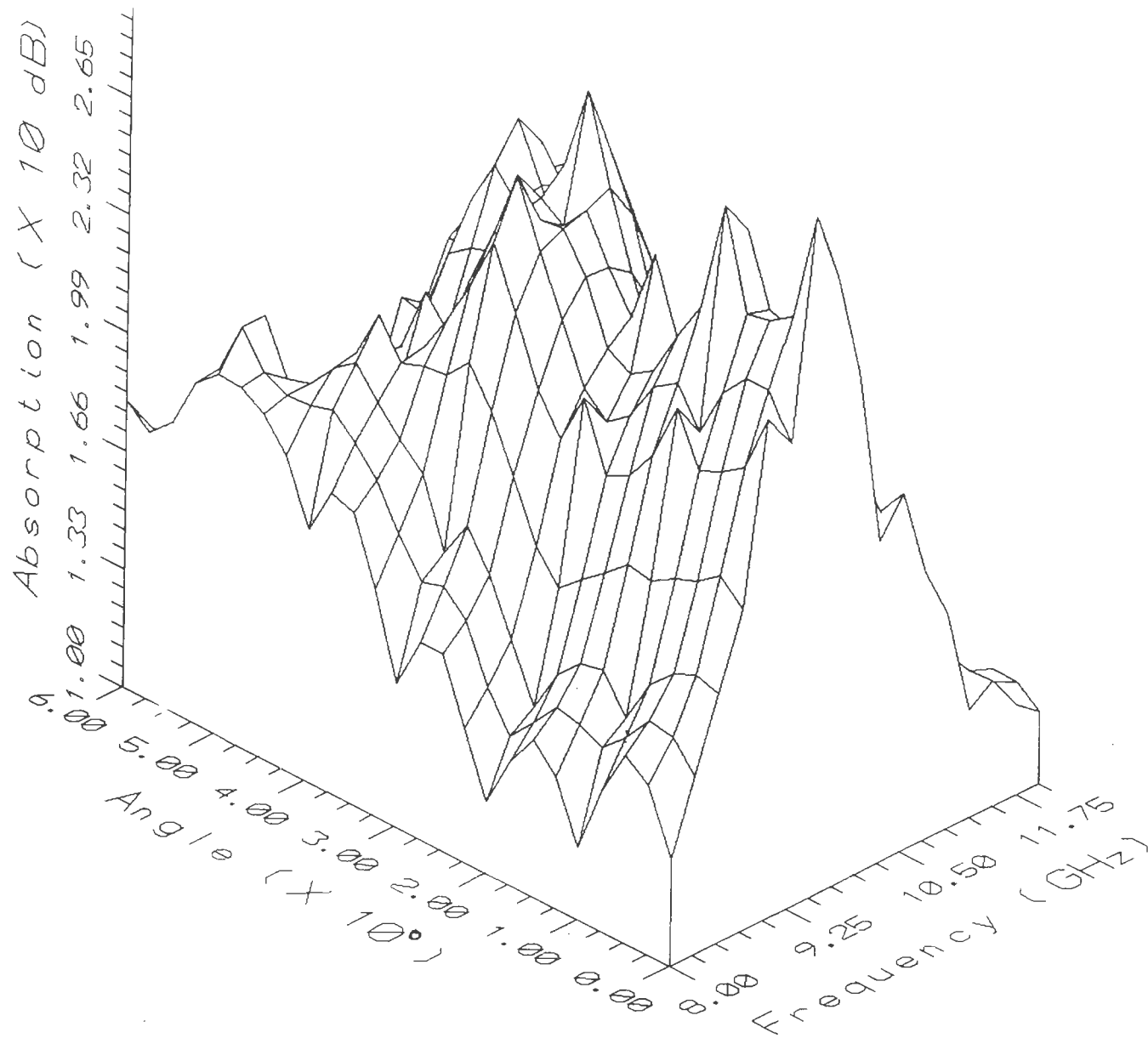


Fig 7.5a Theoretically simulated absorption characteristics for the case of parallel polarization.

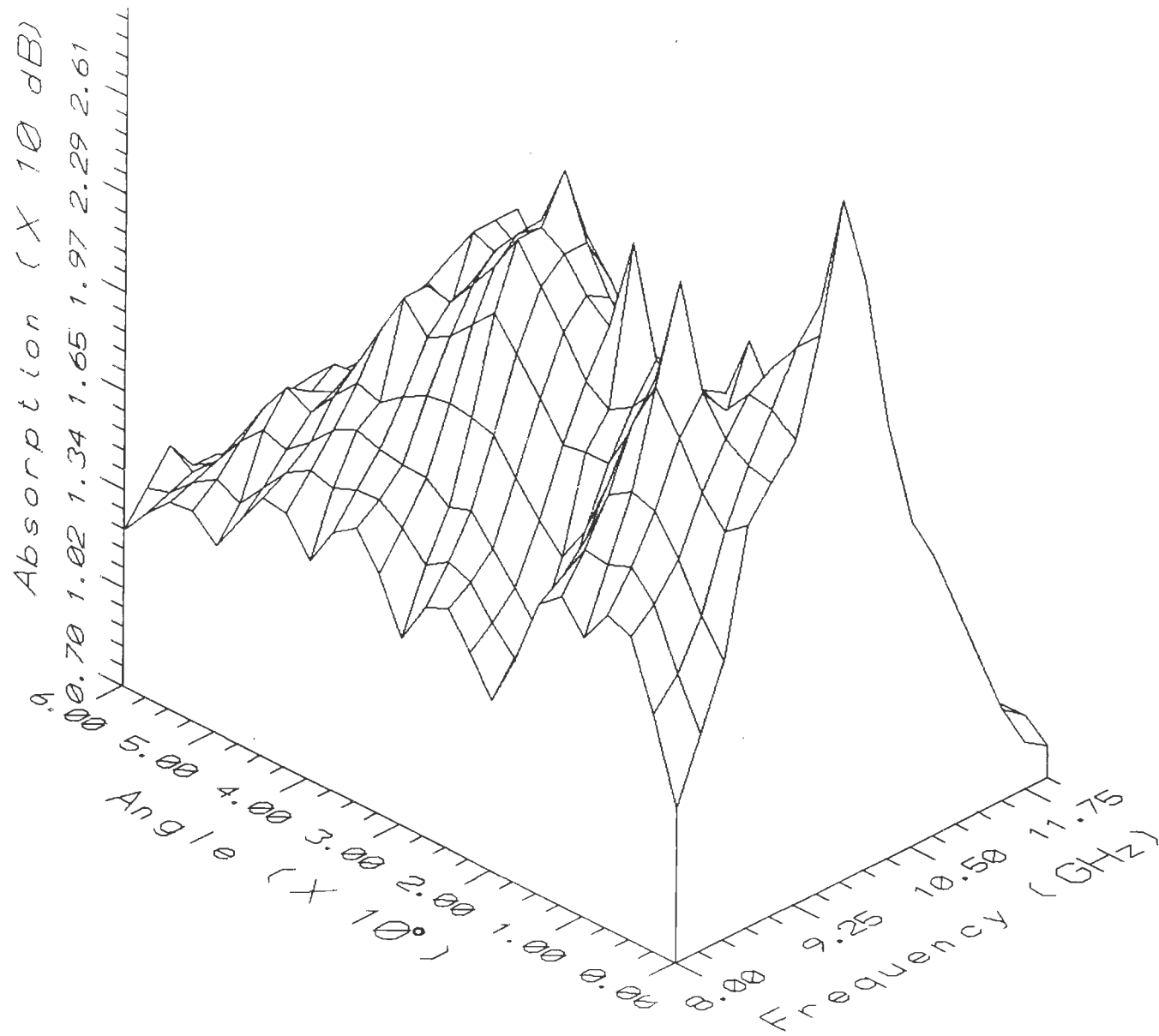


Fig 7.5b Experimentally obtained absorption characteristics for the case of parallel polarization.

CHAPTER VIII

MICROWAVE ABSORBERS : FABRICATIONAL ASPECTS

8.1 INTRODUCTION :

Theoretically designing a microwave absorber for a given specification is just half the way for the complete work. The fabrication process plays an equally important role in the final performance of the absorber. In the theoretical design process, it is assumed that uniform distribution of particles exist in the host media. It becomes imperative to ensure practically uniform distribution of particles. This fact becomes very clear if, we study the results shown in Fig 8.1, for an absorber having iron powder dispersed in rubber matrix (designed in the previous chapter). Curve 'b' is obtained when the sheet was fabricated without considering the dispersion aspects. While curve 'c' is obtained when the sheet was fabricated, using a dispersion aid along with the dispersion technique arrived in the next section. The difference in absorption characteristics is significant highlighting the importance of the dispersion technique.

8.2 AN EXPERIMENTAL INVESTIGATION : ANALYSIS OF PARTICULATE DISPERSION IN RUBBER

To experimentally analyze the dispersion of particulate matter in the binder matrix, an high power optical microscope and Scanning Electron Microscope (SEM), were utilized. The analysis was done on iron powder-rubber samples prepared using different dispersing aids. Commercially available dispersion aids V216 and DMPS

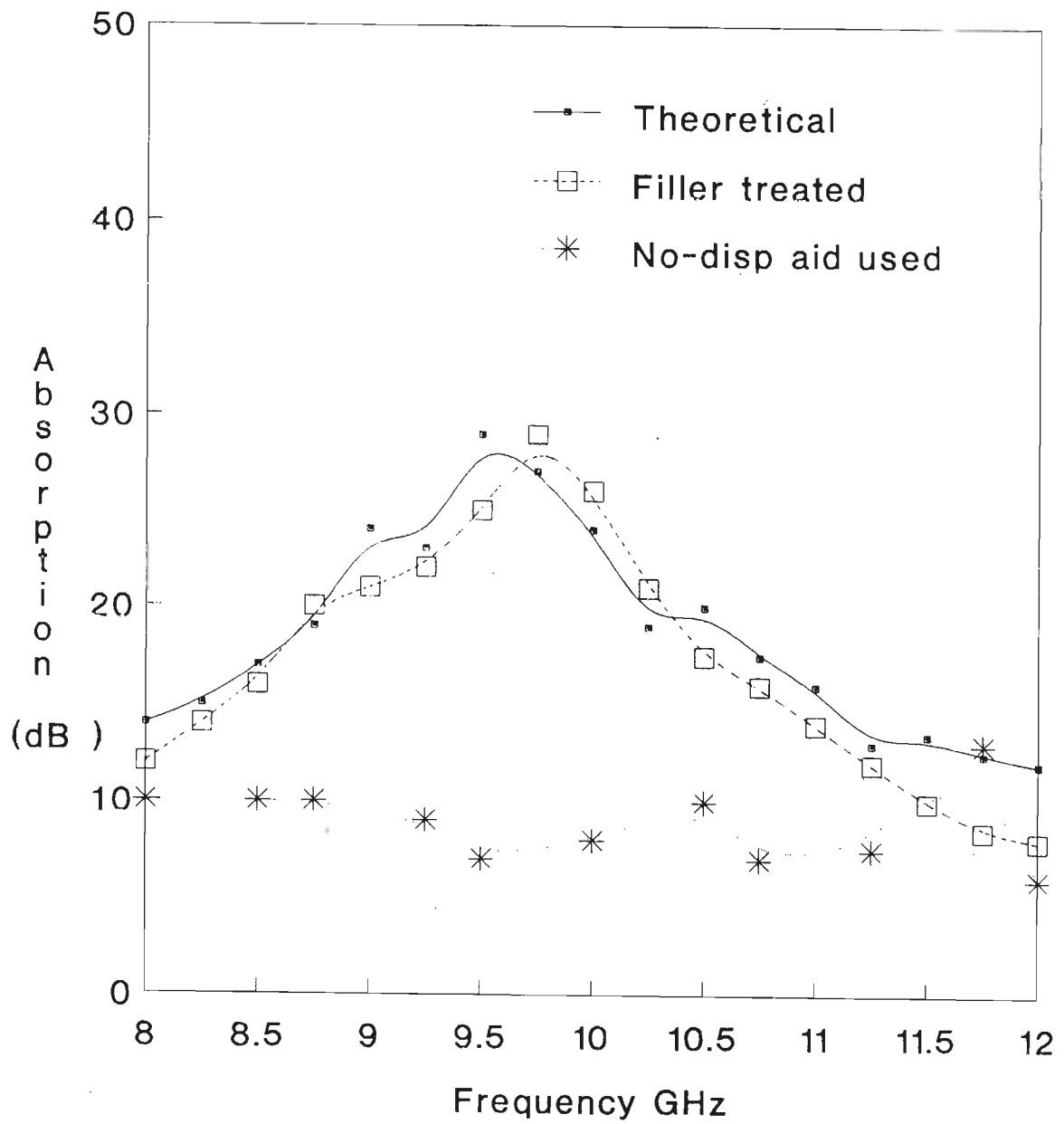


Fig 8.1 Absorption characteristics for iron powder rubber absorber, with and without dispersing aid.

(commercial names of organic emulsions), were employed.

With different concentrations of the two dispersion aids, four samples were fabricated using the method described in section 8.4, named V216-0.5%, V216-1%, DMPS-0.5% and DMPS-1%, corresponding to weight percentage of aid used in rubber. The weight percentage of aid in rubber is indicated in the sample name itself. A sample without any aid (No-aid) was also fabricated. All the samples had equal amount of filler with average particle size of 20 microns, dispersed in an identical binder. The samples were fabricated into 150mm diameter sheets in a specially custom built mould set, employing an identical fabrication procedure.

There may be better dispersing aids available, but only those commercially and locally available were employed.

A large a number of micrographs were obtained from different locations of a sheet, using the high power optical microscope and the SEM. For each composition a minimum of two sheets were considered. Only a few representative micrographs are shown in Fig 8.2, although a number of micrographs were taken. It can be observed from the various micrographs, that DMPS-1% (Fig 8.2f) promises to be the best dispersion aid and concentration among the different combinations that were tried. To improve the dispersion further, a novel idea was tried out. The filler was pretreated with the dispersing aid and then added, instead of dispersing aid and filler being added in sequence during the fabrication process. This resulted in vast improvement in dispersion as observed from Fig 8.2f and 8.2g. Thus, from the experimental investigation described above, it was concluded that DMPS-1%, promises to be the best dispersing aid, coupled with pretreating of the filler. A uniform distribution can be easily obtained practically as can be seen from Fig 8.2g.

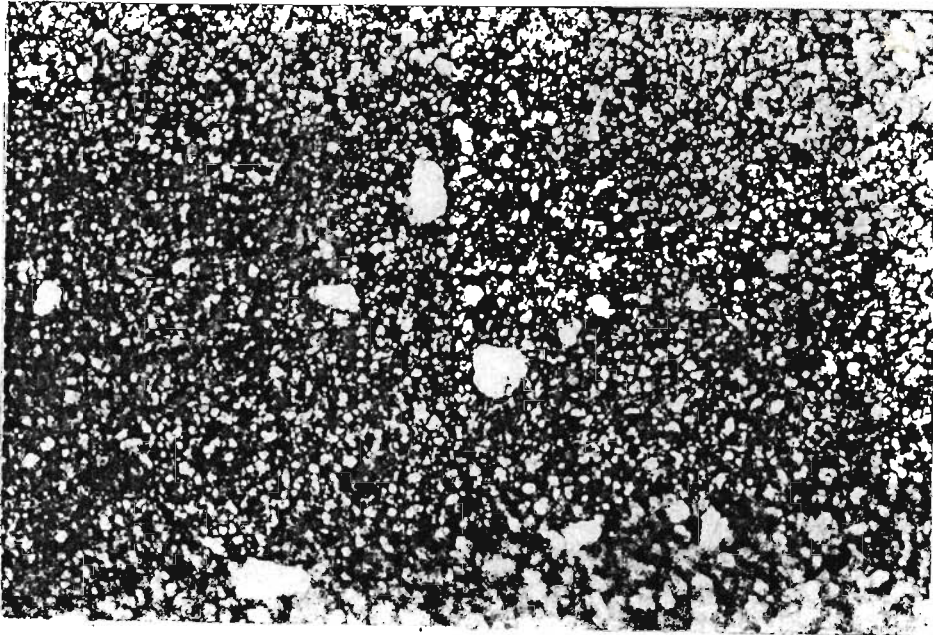


Fig 8.2a Micrograph showing the dispersion obtained when No-dispersion aid was used. The Large are also seen. The distribution is non uniform.

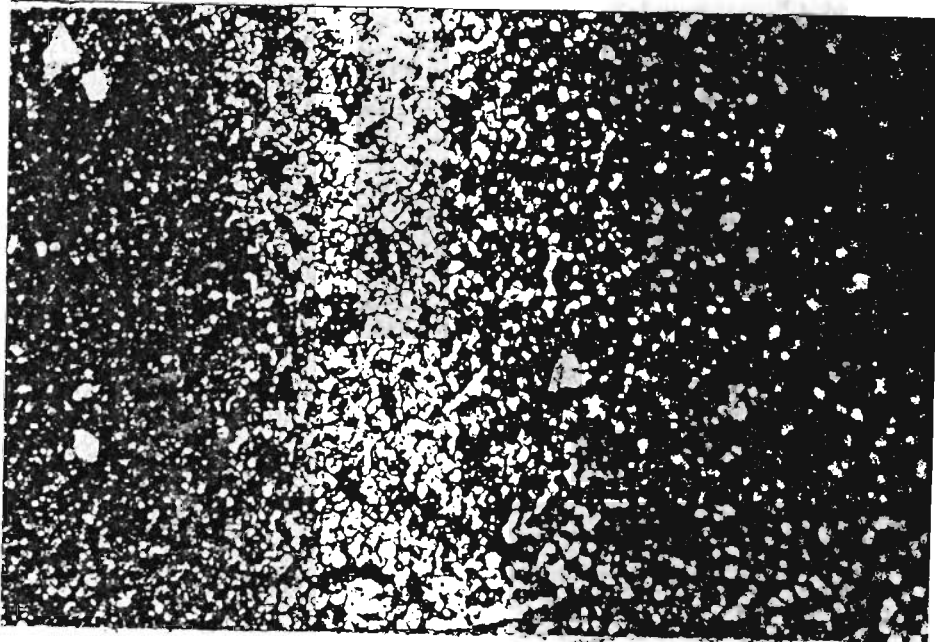


Fig 8.2b Micrograph showing the dispersion obtained when No-dispersion aid was used. The alignment of particles can be seen. The distribution is non uniform.

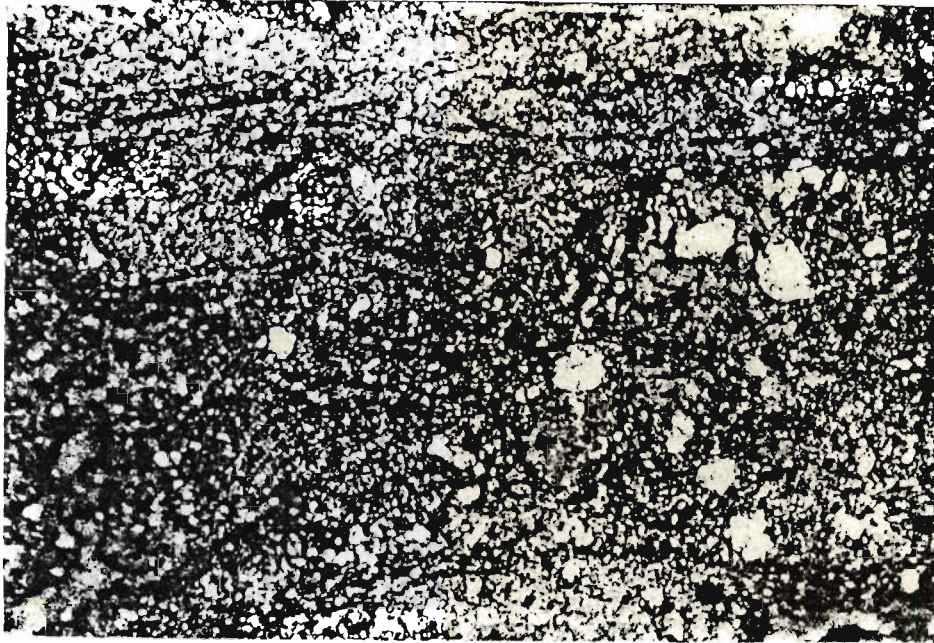


Fig 8.2c Micrograph showing the dispersion obtained when V216-0.5% dispersing aid was used. The Large are also seen in plenty. Alignment of Particles is strong. The distribution is non uniform.

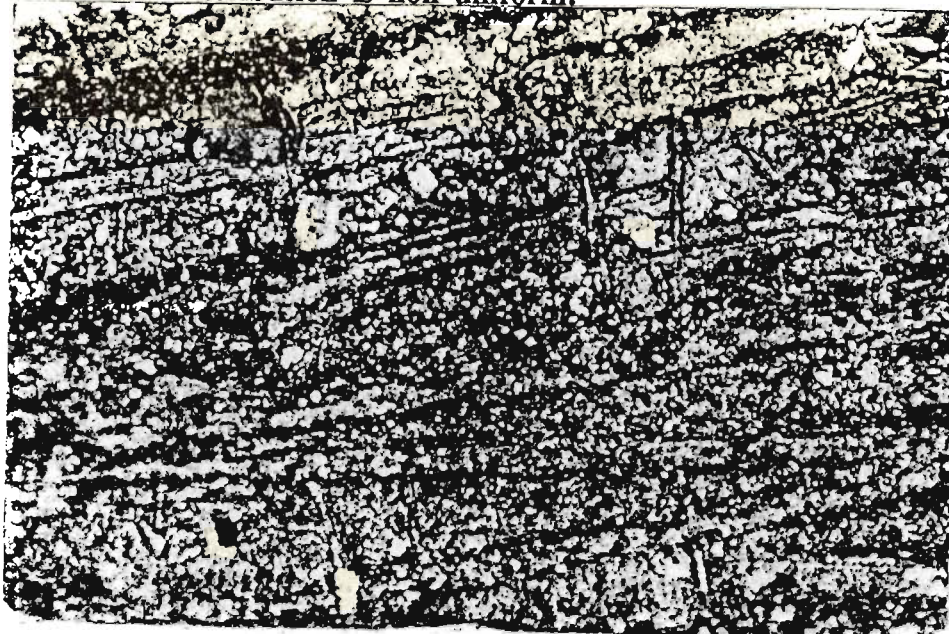


Fig 8.2d Micrograph showing the dispersion obtained when V216-1.0% dispersing aid was used. The Large are also seen in plenty. Alignment of Particles is strong. The distribution is non uniform.



Fig 8.2e Micrograph showing the dispersion obtained when DMPS-0.5% dispersing aid was used. Alignment of Particles as well as few large particles are visible in some regions. The distribution is non uniform.

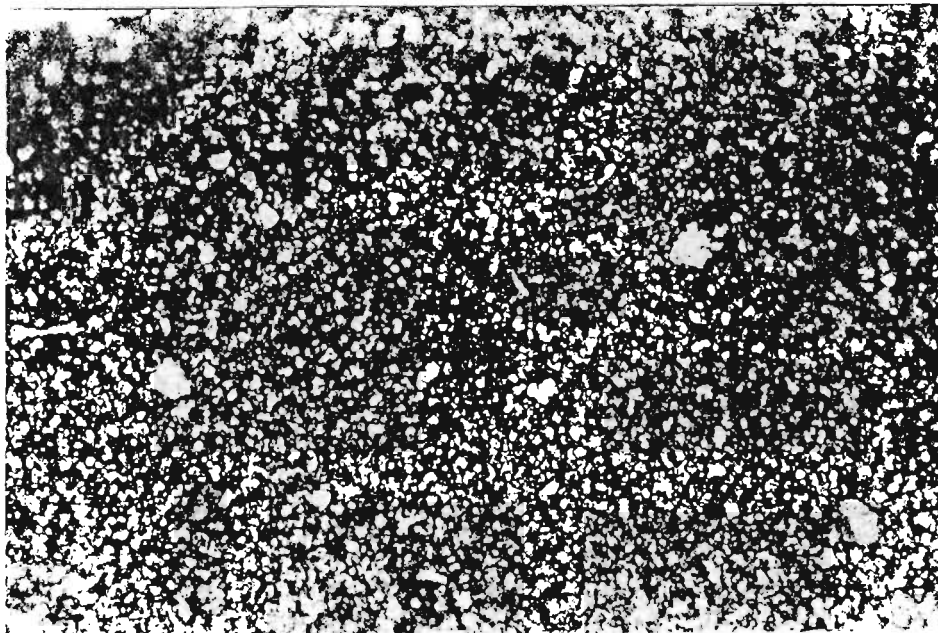


Fig 8.2f Micrograph showing the dispersion obtained when DMPS-1.0% dispersing aid was used. Near uniform distribution. Few large particles are visible in some regions.

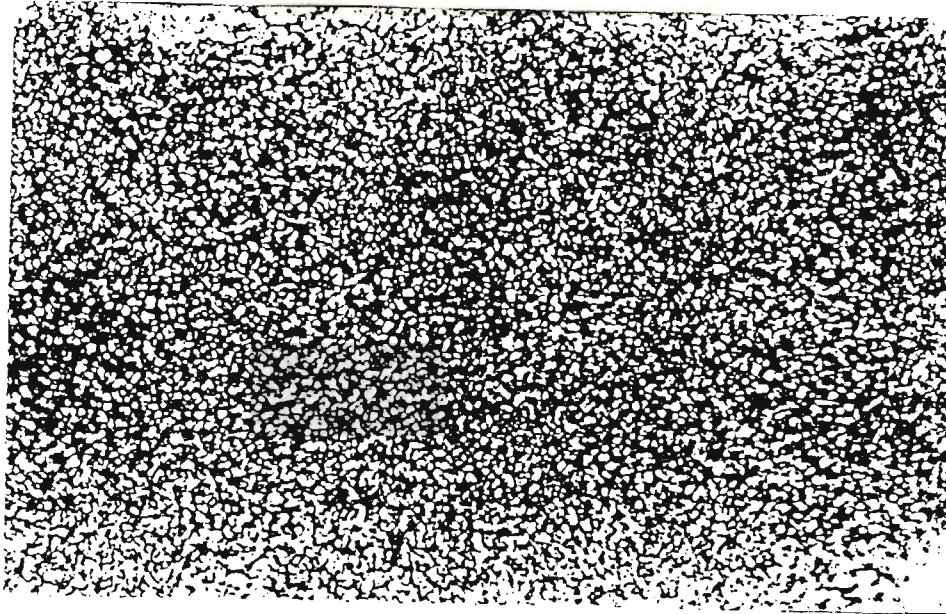


Fig 8.2g Distribution obtained when the filler was pretreated. Large particles are absent. Uniform distribution is obtained through out the sample.

8.3.0 FABRICATION OF THE RUBBER-ABSORBER SHEET

The fabrication process for an absorber sheet is largely dictated by the type of binder selected. Since it was required to design and develop flexible type absorber, so that they may be used to cover existing structures, rubber was selected as the binder. In the following section, a general method of fabricating a rubber sheet with particular application of realizing the properties of a microwave absorber is described.

The fabrication of the rubber-absorber sheet involves the following steps.

- (i) Preparation of the lossy material in powder form;
- (ii) Estimation of the properties of the lossy material; and
- (iii) Fabrication of the sheet.

8.3.1 PREPARATION OF THE LOSSY MATERIAL

The lossy materials that were prepared and used in the design analysis of absorbers are pure ferrite and Cobalt-Substituted Barium Hexagonal Ferrite (Co-BHF). Carbon and Iron powder wherever used, were procured indigenously.

The non availability of highly pure ferrites (Fe_3O_4) and Cobalt Substituted Barium Hexagonal Ferrite (Co-BHF), made it necessary to go in for the preparation of these ferrites. The Co-BHF was prepared using the conventional powder ceramic procedure, while a chemical or wet method was employed to obtain the ferrite.

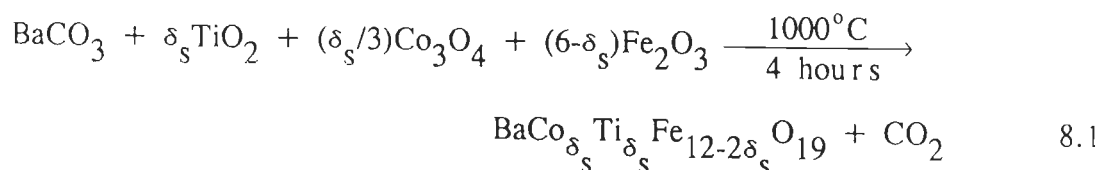
The particle size of the powder was controlled to within the desired value by a repeated process of prolonged grinding in a ball mill and then sieving out the

desired size particles. The particles were ball milled for a minimum period of 48 hours before sieving was employed, to fractionate desired size ranges. The shape of the particles were monitored by observing through a high power optical microscope.

The powders were prepared in the Metal forming and Heat treatment Laboratory, at the Metallurgical department, at the University of Roorkee.

8.3.2 PREPARATION OF Co-BHF

The basic chemical reaction involved in the preparation of Co-BHF is [41]



One part by molecular weight of barium Carbonate, δ_s parts by molecular weight of Titanium dioxide, $\delta_s/3$ parts by molecular weight of Cobaltic oxide, and $(6-\delta_s)$ parts by molecular weight of ferric oxide, were mixed and fired for four hours at 1000°C . This would yield one molecular weight of Co-BHF and δ_s , the amount of Cobalt being doped as per Eq. (4.26) for a required ferromagnetic resonance in the Co-BHF. Table 8.1 gives the amount of the four chemicals required as δ_s varies from 0.75 to 0.99, to make up of 1 Kilogram of the finished product.

During firing Fe^{+++} or trivalent Iron atoms are replaced by Cobalt atoms. Titanium impurity is added for electrical neutrality.

Table 8.1

δ_s	BaCO ₃ grms	Co ₃ O ₄ grms	TiO ₂ grms	Fe ₂ O ₄ grms
0.75	190.1199	57.9917	75.9716	718.3287
0.76	190.5616	58.9015	77.1505	716.7962
0.77	191.0057	59.8156	77.3303	715.2585
0.78	191.4516	60.7339	77.5108	713.7136
0.79	191.8997	61.6565	77.6922	712.1616
0.80	192.3499	62.5834	77.8745	710.6022
0.81	192.8022	63.5147	78.0576	709.0355
0.82	193.2566	64.4504	78.2416	707.4614
0.83	193.7132	65.3905	78.4264	705.8799
0.84	194.1719	66.3350	78.6121	704.2910
0.85	194.6328	67.2841	78.7987	702.6943
0.86	195.0959	68.2376	78.9862	701.0903
0.87	195.5612	69.1957	79.1746	699.4785
0.88	196.0288	70.1584	79.3639	697.8589
0.89	196.4986	71.1257	79.5541	696.2316
0.90	196.9706	72.0976	79.7452	694.5966
0.91	197.4449	73.0743	79.9372	692.9536
0.92	197.9215	74.0556	80.1302	691.3027
0.93	198.4004	75.0417	80.3241	689.6438
0.94	198.8816	76.0326	80.5189	687.9769
0.95	199.3652	77.0283	80.7147	686.3018
0.96	199.8511	78.0288	80.9114	684.6186
0.97	200.3394	79.0342	81.1091	682.9272
0.98	200.8301	80.0446	81.3078	681.2275
0.99	201.3232	81.0599	81.5074	679.5195

8.3.3 PREPARATION PROCEDURE

All the chemicals that were used were of Analytical Reagent grade (98-99% pure). Commercially available Co₃CO₄ was decarbonized at 700°C for 4 hours to obtain Co₃O₄.

The four basic raw chemicals, BaCO₃, Co₃CO₄, TiO₂ and Fe₂O₃ were subjected to wet milling in a ball mill individually for about 72 hours. This was felt necessary, to ensure that all the starting chemicals were of the same relative sizes. The particle size of these were controlled to within 10 microns.

The ground raw chemicals were oven dried at 110°C for 2 hours. They were weighed as per the proportion required, to make up 1½ Kg's of the finished product. The raw materials were now ball milled together for 72 hours, this was felt necessary to ensure a uniform, homogeneous and intimate mixing of the different ingredients. The mixture was then oven dried. The mixture was pressed into three cylindrical cakes under 1 ton per sq.inch pressure. The cakes were then sintered at 1000°C for 4 hours in a furnace. The sintered cakes were allowed to cool, and then crushed to particulate form. The powder thus prepared was then milled to the required average particle size.

A number of Co-BHF samples for different ferromagnetic resonance frequency f_r , were prepared by the ceramic powder preparation technique described above.

It now remains to verify the ferromagnetic resonance frequency of the Co-BHF, so prepared. To this end, the Cobalt content in the Co-BHF was estimated as described in the next section, and then f_r computed using Eq. (4.26).

8.3.4 ESTIMATION OF COBALT CONTENT IN THE BARIUM FERRITE

The cobalt content in any compound can be estimated using the **Spectrospan IV**, which is a computerized plasma emission spectro-photometer. The absorbance of the unknown Cobalt compound solution is measured. The cobalt content is then read off from a predetermined graph of absorbance v/s concentration, of a standard solution. The steps involved in this method are

- (i) Preparation of the standard solution;
- (ii) Determination of the 'concentration curve';
- (iii) Preparation of the solution of the unknown Cobalt compound; and

(iv) Estimation of the Cobalt content in the unknown Cobalt compound.

8.3.5 PREPARATION OF THE STANDARD SOLUTION

One mg Cobalt equivalent of Cobalt nitrate was dissolved in 10% hydrochloric acid, to form a solution of one ppm concentration. This solution is then dissolved in double distilled water to make up 5%, 10%, 15%.....,100% concentrated standard solutions.

8.3.6 DETERMINATION OF THE CONCENTRATION CURVE

The absorbance of the different concentrated standard solution was obtained from the spectrosan. the graph of variation in absorbance with concentration is then plotted to scale, as shown in Fig 8.3.

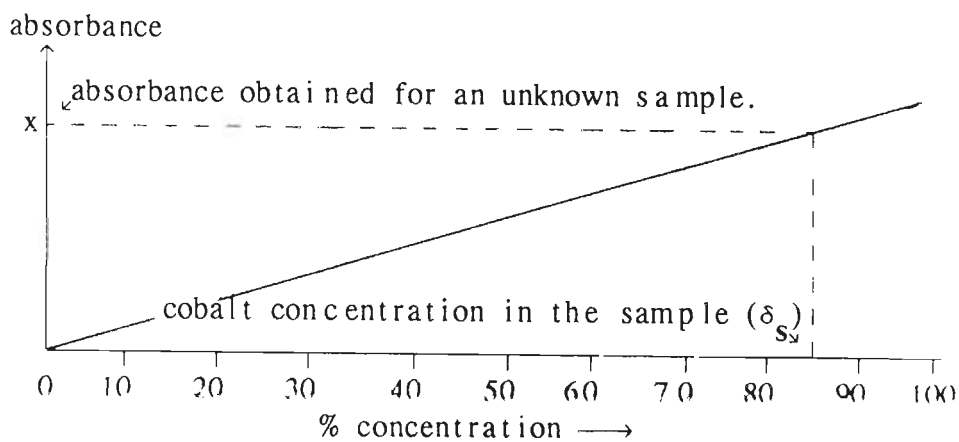


Fig 8.3 Composition curve, showing results obtained for a unknown sample.

8.3.7 PREPARATION OF SOLUTION OF THE UNKNOWN COBALT COMPOUND

A known quantity of the Co-BHF (approximately 20mg, for each sample was taken)

is accurately weighed. It is then digested in 100cc of 10% hydrochloric acid, by continuous heat treatment. The white precipitate that was formed was further digested by adding weak nitric acid along the digestion process. The solution so obtained was a clear solution without any precipitates, as is recommended in the Spectrospan manual.

8.3.8 ESTIMATION OF COBALT CONTENT IN THE SAMPLE

The absorbance of the solution of the unknown cobalt solutions were determined using the Spectrospan. The cobalt content is then estimated from the concentration curve obtained in the previous section, as described in Fig 8.3. The procedure was repeated with all the Co-BHF samples prepared. The practically estimated δ_p and f_{rp} and δ_t , which was computed for a required f_r (f_{rt}) are listed in Table 8.2 for the Co-BHF samples that were prepared.

Table 8.2

Sl No	sample	δ_t	δ_p	Ferromagnetic Resonance frequency in GHz.	
				f_{rt}	f_{rt}
1	a	0.79	0.815	14	12.63
2	b	0.829	0.650	12	20.01
3	c	0.873	0.575	10	23.35
4	d	0.829	0.792	12	13.65
5	e	0.862	0.657	10.5	19.66
6	f	0.885	0.741	9.5	15.90
7	g	0.855	0.909	9.5	8.4
8	h	0.79	0.698	14.0	17.85

8.3.9 ESTIMATION OF COMPLEX PERMEABILITY OF CO-BHF : DETERMINATION OF THE F_r FOR CO-BHF

The non availability of a Vector Network Analyzer (VNA) at this stage of the work, left the author with no other alternative but, to use the time tested but time consuming 'Open Circuit-Short Circuit' (OC-SC) test [157], to determine μ_r of Co-BHF.

8.3.10 EXPERIMENTATION

The experimental procedure to estimate the complex relative permeability involves three steps, first the wave guide sample is prepared, and second, experimentation is carried out to generate a set of data and finally the data is analyzed to obtain μ_r .

8.3.11 PREPARATION OF WAVEGUIDE SAMPLES

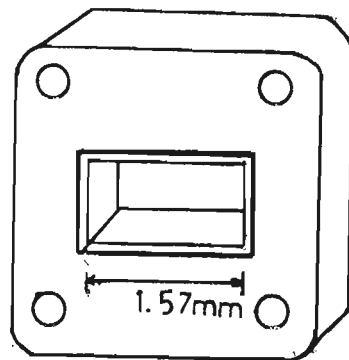


Fig 8.4 Constructional details of the sample holder.

Two wave guide (Ku-Band) sample holders of 3.8 mm and 4.3 mm thick, were fabricated using brass, as described in Fig 8.4 in the departmental workshop. Co-

BHF and Paraffin wax in equal volume proportions, were thoroughly mixed in a power mixer to obtain a homogeneous mixture. A computed quantity of the mix was then, compressed under small pressure in a specially made die-punch set, into samples of dimensions equal to inner dimensions of the Ku-Band wave guide. In order to avoid any mismatch between the sample holders and the ferrite samples, a provision was made in the die-punch set to attach the sample holder at its lower end. So that the sample slowly ejected under pressure from the die, would exactly fit into the waveguide of the sample holders. In this way it was ensured that there was no air gaps between the sample end surfaces and the wave guide walls. The two faces were grinded with suitable emery paper to obtain a smooth planer surfaces.

8.3.12 EXPERIMENTAL PROCEDURE [157]

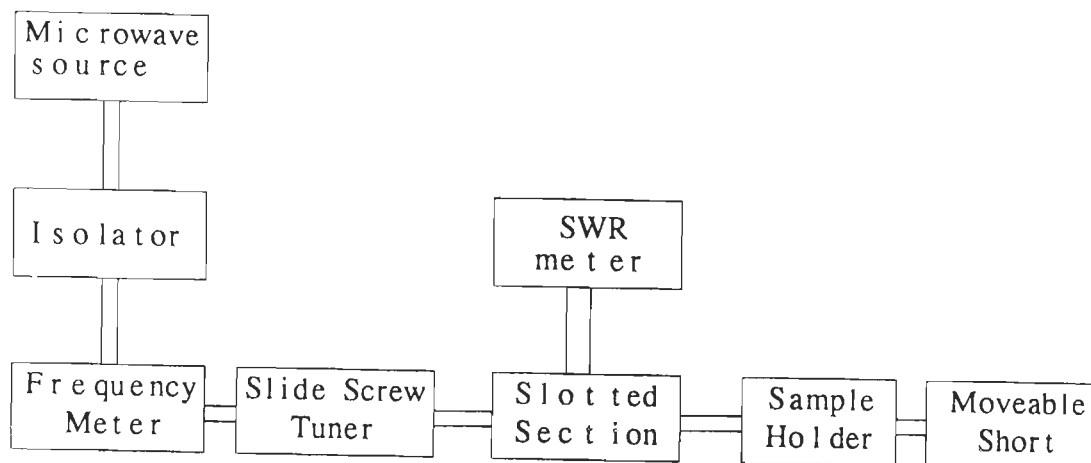


Fig 8.5 Experimental setup for 'Open-circuit and Short-circuit' test.

- Step 1 :** Connect the equipment as shown in Fig 8.5, do not insert the sample at this time. Tune the system for the required frequency.
- Step 2 :** Determine the guide wavelength λ_g , which is twice measured distance between alternate minima in the slotted line.
- Step 3 :** Place the sample in the sample holder and obtain d_{sc} , the position of the

first minima in the wave guide, by measuring the shift in the minima, with the short circuit in perfect contact with the sample. Measure r_{sc} , the standing wave ratio.

Step 4 : Place the short at a $\lambda_g/4$ distance from the sample surface, and obtain d_{oc} and r_{oc} , under open circuit condition.

Step 5 : Repeat steps 1 to 4 above over the entire frequency band at suitable frequency intervals.

Step 6 : Accurately measure the thickness of the sample l_1 and tabulate the results.

Step 7 : Repeat steps 1 to 6 above for a second sample of different thickness l_2 .

8.3.13 ANALYSIS OF THE DATA

1. Compute $K = 2\pi/\lambda_g$ 8.2

2. For each pair of values for d and r , find Y_{sc} and Y_{oc} form

$$Y = \frac{1 + |\Gamma_{in}| e^{j2Kd}}{1 - |\Gamma_{in}| e^{j2Kd}}; \quad 8.3$$

where $|\Gamma_{in}| = (r-1)/(r+1)$.

3. Compute $k_r + jk_i = \pm\sqrt{-Y_{sc}/Y_{oc}}$ 8.4

choose that sign (\pm) of the square root, so that k_i is positive real.

4. Determine two variable, a and b as

$$a = (1/2) \tan[2k_r/x] \quad 8.5$$

$$b = (-1/4) \ln[(4k_r^2 + x)/y] \quad 8.6$$

where $x = k_r^2 + k_i^2 - 1$; and $y = \sqrt{(1 - k_i)^2 + k_r^2}$

5. Repeat steps 1 to 4 above for the data collected for the second sample.

It is clear from the above set of equations that the value of 'b' is

uniquely obtained, while that of 'a' within an additive integral multiple of $\pi/2$. Hence to resolve this ambiguity, measurements are made for two samples of different thickness l_1 and l_2 , the values of 'a's are resolved by satisfying the relation [157] given below

$$(a_1/l_1) = (a_2/l_2) \quad 8.7$$

6. For each pair of 'a's and 'b's selected, compute

$$k_2/K = (a + jb)/Kl \quad 8.8$$

7. Find

$$\mu_r = \pm (k_2/K)/\sqrt{Y_{sc} Y_{oc}} \quad 8.9$$

Choose that sign (\pm) which makes real part positive.

A computer program was developed in FORTRAN to compute μ_r using Eq.'s (8.2) to (8.9) from the measured data.

The permeability of the Co-BHF prepared and indicated as sample 'a' in Table 8.1, was determined as follows :

1. Two samples of 3.8mm and 4.3mm were prepared.
2. The 'OC-SC' test was conducted and the data for the two samples tabulated.
3. The values of μ_r for the Co-BHF was deduced from the measured data, using the program listed in Appendix 8.1 The permeability as a function of frequency is plotted in Fig 8.6.

It can be observed that μ_r' peaks around 12.75 GHz. which is very near to 12.63 GHz., obtained by Cobalt analysis discussed in the previous section. Hence the f_r of the prepared Co-BHF was decided to be 12.63 GHz.

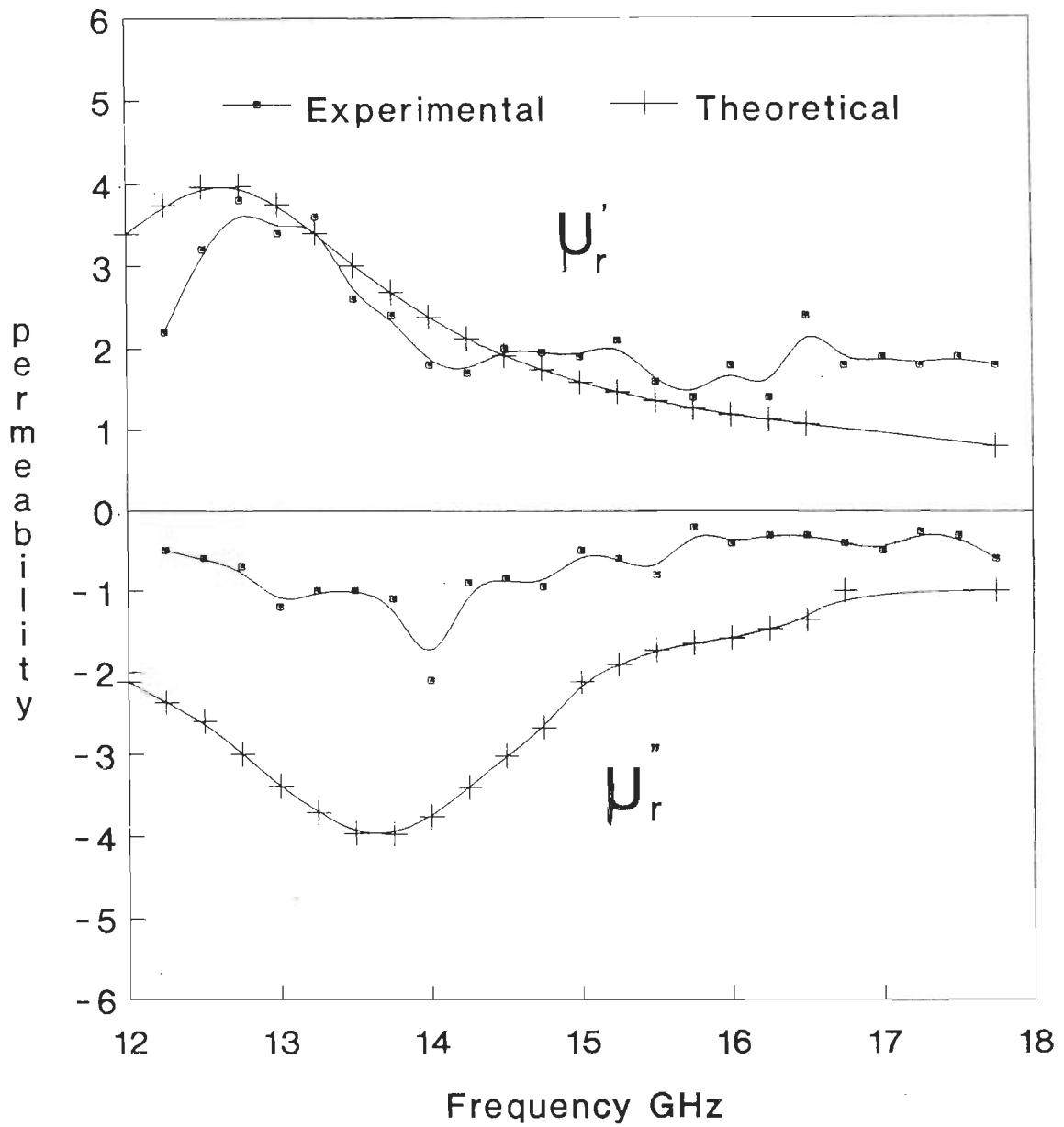


Fig 8.6 Permeability characteristics for the Co-BHF sample listed as 'a' in Table 8.2

8.3.14 PREPARATION OF FERRITE

In this section a procedure for the preparation of pure ferrite (Fe_3O_4) in the laboratory is described briefly.

A known quantity of analytical grade Iron powder was digested in weak hydrochloric acid, with continuous heat treatment. The precipitate that was formed during the digestion process, was further digested by adding small quantities of weak nitric acid. To, the clear but saturated solution, Oxalic acid crystals were added in abundant quantity, with constant stirring. The precipitate of iron oxalate thus formed was distilled out of the solution, dried and then fired at 600°C for 2 hours. Thus pure ferrite was prepared. The ferrite particles were then milled to the required average particle size.

In the manner described above 1.5 Kilograms of finished product, ferrite powder of required average particle size 20 microns was obtained.

8.4 FABRICATION OF THE SHEET

The fabrication of the absorber-sheet involves two steps; mixing of the various fillers into the rubber, and hot curing the green sheet.

A two roll mill was used to dry mix the filler and rubber. A calculated amount of rubber was first thoroughly pulverized in the roll mill, computed quantity of the pretreated filler was then added in very small quantities, with continuous mixing till all the filler was added. The mill was then run for another 10-15 minutes to ensure uniform mixing. The direction of the roll of the mill and the direction of the feed was repeatedly changed to avoid any alignment of the

particles along the direction of rolling [7].

The powder mix so prepared was passed through a calendar machine to size it to the required thickness. The green sheets so obtained were hot pressed in a hydraulic press with a ram of 300mm diameter. Initially the mould set had a provision to fabricate 1.8mm thick sheets only. However this was later on extended to higher thickness by incorporating additional spacers. The custom built mould had a thickness tolerances of $\pm 1.5\%$ at 1.8mm. The curing temperature of the mould was maintained through out the mould surface by having heater elements at every 50mm, and was held constant by a thermostat arrangement. The temperature and pressure that needs to be used during hot curing of the green sheets is largely dictated by the type of binder used. However, the pressure and temperature normally employed during the fabrication of absorber sheets are

Temperature : 130-160°C; and

Pressure : 1.0-1.25 Tons per square inch.

8.5.0 FABRICATION OF IMPEDANCE MATCHING SURFACES

The Impedance Matching Surfaces (IMS); conducting screens perforated with an array of apertures or its complimentary screen, a free standing array of structures were fabricated by using the conventional photo-lithography technique of preparing printed circuit boards. The fabrication process involves the following steps :

1. Preparation of the art work for the designed array dimensions;
2. Preparation of the negatives;
3. Preparation of a mask on the copper sheet (conductive sheet); and
4. Preparation of the IMS in its final form.

8.5.1 PREPARATION OF THE ART WORK

The first step towards fabricating the IMS, was to prepare the art work of the required design. For the designed dimensions of the array and element of the array, the art work was prepared manually for Jerusalem cross aperture. While for the remaining structures like, Circular aperture, annular ring aperture, single square loop and double square loop, the art work was prepared using a Autocad software on a PC-386 and plotted using a plotter. All the art work were drawn to 2:1 scale, and covered an area of 600 X 600 mm.

8.5.2 PREPARATION OF THE NEGATIVES

The art work of the designed IMS, prepared in the previous section were photographically reduced to the required size of 300 X 300mm. The negatives were prepared in the departmental PCB laboratory.

8.5.3 PREPARATION OF A MASK ON THE COPPER SHEET

Since in our design analysis, we have assumed the conducting screen to be of zero thickness, the thinnest copper sheet of thickness 50 microns, that was available commercially was used to fabricate the IMS.

The copper sheet was affixed onto a fibre glass base frame specially made for the purpose, and then the surface of the sheet was thoroughly polished. A film of Photo resist was given to the polished surface. The mask of the required design was then prepared photographically using the negative prepared in the previous section. The copper sheet was then removed from the base frame and a very thin protective film of paint was spray painted on the back surface of the masked copper sheet.

This was necessary, since the mask was obtained on only one face of the copper sheet and the other face was naked and would be etched away, when the copper sheet was passed through the final stage of etching. The sheet was then affixed onto a transparency sheet of 50 microns thick for easy handling, as well as to retain the relative positions of the elements in the array.

8.5.4 PREPARATION OF THE IMS IN ITS FINAL FORM

The final step in the fabrication of the IMS, was to etch out the unwanted conductive portions in the sheet. This was done using a weak ferric chloride solution. It is important to note here, one needs to be very careful during this process because the thickness of the copper sheet and the protective film at the back is very small. Further the dimensions of array are also critically small. Hence if etching is carried on, without monitoring, it is the experience of the author, that the whole sheet would be etched out!

The etched copper sheet was thoroughly washed and cleaned, thus the IMS was fabricated.

8.6.0 MATERIALS USED TO ABSORB ELECTROMAGNETIC ENERGY AT MICROWAVE FREQUENCIES

Since it is not the purpose of this work to tackle the microwave loss or absorption by a lossy material, from a physicist point of view and our work is application oriented, only a brief mention is made here to the general types and properties of lossy materials that are utilized to design and develop thin sheet microwave absorbers.

As discussed in the introduction chapter, materials which have an imaginary component to their refractive index can be employed to absorb electromagnetic energy. However the most extensively used materials for microwave absorption are Carbon in various forms, Iron powder and Ferrites. These are employed individually as well as in combination to obtain the necessary microwave absorption. In addition loss aiding structures like dipoles, brass and aluminum fibers or small cylinders, chiral molecules, in the form of conducting helix are also added.

8.6.1 Carbon :

Due to its high permittivity in the microwave spectrum and low density, carbon in various forms is widely used in resonant absorbers at microwave frequencies.

8.6.2 Iron powder :

Due to its high permeability in the microwave spectrum iron powder is an excellent material for microwave absorption, but due its high density, absorbers made using iron powder are very heavy which is a great disadvantage.

8.6.3 Ferrites :

During the past three to four decades, ferrites have become firmly established as an important class of magnetic materials, finding use in a wide range of linear, digital, and microwave applications. However the use of ferrites as a Radar Absorbing Material is relatively recent. A ferrite may be described as a magnetizable insulator. More specifically, it is a metal oxide which contains

magnetic ions arranged in a manner which produces spontaneous magnetization, while maintaining good dielectric properties. The spontaneous magnetization of these materials arises from a peculiar alignment of the magnetic dipoles of trivalent iron ions (Fe^{3+}) which form opposing sub lattices. Since one sub lattices is stronger than the other, a net magnetization results and the material behaves very much like metallic iron or nickel, but with lower magnetization. Since the material is an oxide, ideally there are no conduction electrons and the material is an insulator. To appreciate the value of ferrites in microwave applications, it is important to understand the basic physical phenomena that are involved in successful device operation. In general the microwave device depends on the interaction between the magnetic vector of the incident wave and the magnetization of the ferrite for its operation.

Magnetism of materials has its origin in the magnetic moments of orbiting electrons-usually separable into orbital and spin contributions. For spontaneous magnetism (magnetism which does not depend on the presence of an external field) to exist in a material, some of its atomic or ionic constituents must be individually magnetic. Ferromagnetism arises from the alignment of individual atomic magnetic moments caused by magnetic exchange forces.

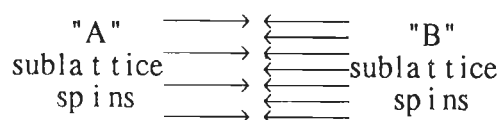


Fig 8.7

To produce the ferrimagnetic combination of parallel and anti parallel spin arrangements shown in the Fig 8.7, the material must possess two types of crystallographic sites occupied by Fe^{3+} ions. For each type of site, a separate

ferromagnetic sublattice exists within the overall crystal lattice and the two sublattices are interwoven in such a manner that an individual ionic moment couples parallel to its neighbor of its own sublattice while coupling anti parallel to a neighbor in the opposite sublattice.

8.6.4 LOSS MECHANISM IN FERRITES (MAGNETIC LOSSES)

When an electromagnetic field is incident on the ferrite the total magnetic field undergoes a change and is given by

$$H = H_i + h e^{j\omega t}$$

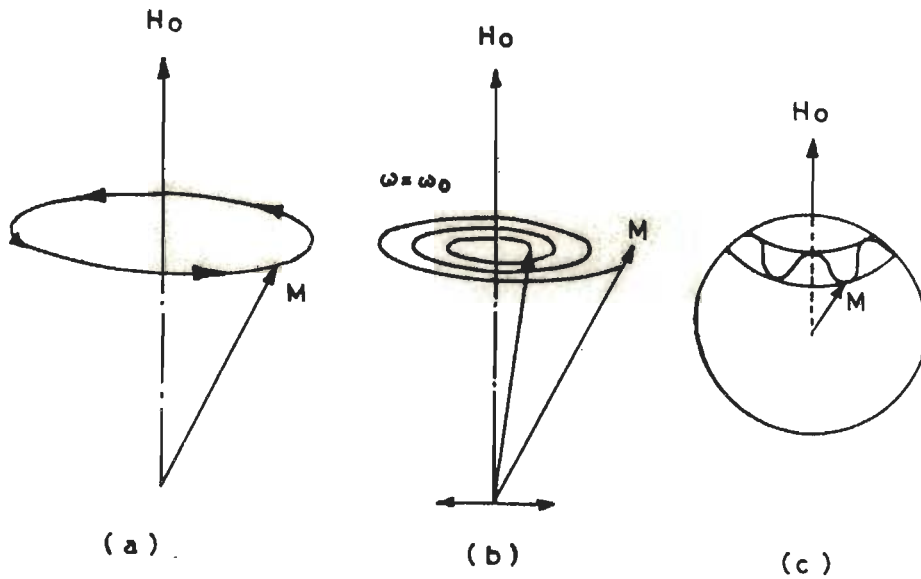


Fig 8.8

where H_i is the vector sum of d.c. fields within the material including that due to the externally applied d.c. field H_0 ; and any time independent internal field. The applied term contains the amplitude h and the microwave frequency ω . It is possible to transfer energy from the microwave field to the system if the driving frequency equals the natural precession frequency ω_0 . Consider the Fig 8.8a, the

effect of adding an alternating component at ω_0 along the y-axis to a large constant field directed along the z-axis, is to cause the oscillating component of the torque M , to be in phase with the precessional motion of the magnetic dipole under the influence of the constant magnetic field in the steady state condition. Thus the amplitude of the precession will grow as shown in Fig. 8.8b and energy will be transferred from the microwave field. At any other frequency, the situation is complicated but it is sufficient to mention that the oscillating component of the torque is no longer in phase with the precessional motion of the magnetic dipole, giving rise to both in and out of phase components between the two resulting in less transfer of microwave energy to the system. Thus closer the applied microwave frequency to the natural precession frequency greater the absorption.

8.7 CONCLUSION

The fabrication procedure that was employed in fabricating the absorber-rubber sheets and Impedance Matching Surfaces have been described briefly.

A dispersion analysis was made to ascertain the type of dispersing aid and the method that has to be adopted during mixing to obtain a uniform distribution of particles in the host matrix. Based on the analysis, pretreating the filler particles with dispersing aid DMPS, 1% w/w of rubber would give near uniform dispersion with very few accumulated large particles in the media.

The results of dispersion analysis done on the No-aid sample, reflects the findings of Nishikata and Shimizu [7]. The alignment of particles in the direction of rolling can be very clearly seen in the micro graph for various samples shown in Fig 8.2. This anisotropy can be regularized, estimated and utilized in the design

analysis of absorbers as described in [7], or can be avoided as described in previous section.

Co-BHF's in fine powder form have been prepared to suit the demands of the theoretical design. Conventional ceramic powder preparation method has been utilized for the preparation of Co-BHF. Their ferromagnetic resonance frequency has been determined through a chemical method. The chemical method to determine ferromagnetic resonance frequency has been verified by measuring the complex relative permeability for one Co-BHF sample. The ferro-magnetic resonance frequency obtained compares well with the chemically determined values.

A small but, sufficient quantity of ferrite was also prepared using the wet method. A brief description of various lossy materials used in the design and development of microwave absorbers are also given.

```

c calculation of complex permittivity and
c permeability by "oc" & "sc" test on the sample
complex c,a1,a2,y(5),bk,ake,u(2),e(2)
dimension d(2),s(2),r(2),el(2),a(50),ur(2)
dimension b(2),rl(50),gl(2),af(100)
character *7 name
write(*,*) ' Give the output file name '
read(*,11)name
open(unit=5,file=name,status='new')
write(*,*) ' Give the input file 1 name '
read(*,11)name
open(unit=6,file=name,status='old')
write(*,*) ' Give the input file 2 name '
read(*,11)name
11 format(a7)
open(unit=7,file=name,status='old')
write(*,*) ' enter the No. of computations '
read(*,*)n1
write(*,*) ' enter el1 & el2 in cm '
read(*,*)(el(i),i=1,2)
write(*,*) ' f : ', u : ', e : '
write(5,*) ' f : ', u : ', e : '
c = cmplx(0.0,1.0)
pie = 3.1415927
pie2 = pie*2.0
hpie = pie/2.0
do 60 k = 1,n1
do 30 j = 1,2
c i=1--sc * i=2--oc
if(j.eq.1) then
read(6,*)af(k),(d(i),s(i),i=1,2)
else
read(7,*)af(k),(d(i),s(i),i=1,2)
endif
al = 30.0/af(k)
alsq = ((al)/(2.0*2.286))**2
alg = al/sqrt(1.0-alsq)
ak = pie2/alg
do 10 i = 1,2
r(i) = (s(i)-1.)/(s(i)+1)
r1 = abs(r(i))
a5 = c*2.0*ak*d(i)
a1 = cexp(a2)*r1
y(i) = (1.0+a1)/(1.0-a1)
10 continue
y(j+2) = csqrt(y(1)*y(2))
bk = c*csqrt(y(1)/y(2))
b1 = aimag(bk)
if(b1.lt.0.0)then
bk = -bk

```

```

else
endif
x = real(bk)
p = aimag(bk)
xsq = x*x
xysq = xsq+p*p-1.0
a(j) = 0.5*atan(2.0*x/xysq)
if(a(j).lt.0.0) then
a(j) = a(j) + hpie
else
go to 29
endif
29 b1 = 4.0*xsq+xysq*xysq
b3 = xsq+(1.0-p)*(1.0-p)
b2 = b3*b3
b(j) = -(alog(b1/b2))/4.0
30 continue
a(0) = a(1) - hpie
a(11) = a(2) - hpie
do 40 j = 1,10
a(j) = a(j-1) + hpie
a(10+j) = a(10+(j-1)) + hpie
rl(j) = a(j)/el(1)
rl(10+j) = a(10+j)/el(2)
40 continue
alow = 1.0
do 45 il = 1,10
do 45 jl = 11,20
diff = abs(r(il)-r(jl))
if(diff.lt.alow) then
alow = diff
il = il
jl = jl
else
go to 45
endif
45 continue
r1 = 0.5 * (r(il)+r(jl))
a(1) = r1 * el(1)
a(2) = r1 * el(2)
do 50 j = 1,2
ake = cmplx(a(j),b(j))
ake = ake/(ak*el(j))
u(j) = ake/y(j+2)
b1 = aimag(u(j))
if(b1.gt.0.0) then
b1 = -b1
else
go to 48
endif
48 b2 = real(u(j))
if(b2.lt.0.0) then

```

```

b2 = -b2
else
go to 49
endif
u(j) = cmplx(b2,b1)
49 a1 = (ake*ake*(1-alsq))+alsq
e(j) = a1/u(j)
bk = csqrt(e(j)*u(j))
b1 = real(bk) * 4.0
gl(j) = a1/b1
50 continue
ur1 = real(u(1))
ur2 = real(u(2))
er2 = real(e(2))
er1 = real(e(1))
ui1 = aimag(u(1))
ui2 = aimag(u(2))
ei1 = aimag(e(1))
ei2 = aimag(u(2))
write(*,5)af(k),ur1,ui1,er1,ei1,ur2,ui2,er2,ei2
write(5,5)af(k),ur1,ui1,er1,ei1,ur2,ui2,er2,ei2
5 format(1x,3f7.2,2x,2f7.2,5x,2f7.2,2x,2f7.2)
60 continue
stop
end

```



DISCUSSIONS AND CONCLUSIONS

9.1 DISCUSSIONS AND CONCLUSIONS

A generalized design approach is formulated in the 3rd chapter with Cobalt-substituted Barium Hexa Ferrite (Co-BHF) as the lossy material for the design of broad band absorbers [Chaitanya et al, 121]. Broad banding is achieved by combining the material and thickness absorption effects in the absorber. The theoretical analysis has been done to estimate the absorption of a single layer absorber in section 3.2. The design formulation has been practically verified by fabricating of an absorber for broad band operation over Ku-band, with a constraint of 2mm on the thickness of the absorber [Chaitanya et al, 120, 155]. Experimental details to measure the absorption provided by the absorber are given in section 3.4. The experimentally obtained absorption characteristics follows very closely the theoretically predicted curve (Fig 3.5). The experimental values of absorption are less than theoretical values by 2-3 dB, these could be due to the limitation of the fabrication process. A minimum of 8 dB has been achieved practically through out the 12 - 18 GHz (6 GHz. bandwidth) frequency band, which is 2 dB less than the desired value.

The range of frequencies in which this technique can be adopted is limited by the lossy material used. In the present case this technique is limited to within 2-46 GHz, through which the ferromagnetic resonance frequency of the Co-BHF can be varied. The maximum absorption as well as the maximum bandwidth that can be achieved are limited by the practical limitation on the volume of filler that can be loaded in a given binder.

A mathematical model for the theoretical analysis and design of microwave absorbers has been formulated in the 4th chapter, based on the evaluation of the overall reflection coefficient of the absorber. The design criteria for two types namely, matched and resonant absorbers are established [Chaitanya et al, 123]. The design criteria for the matched absorber (Eq. 4.24 and 4.19) indicates that it is best suited for broad band operation and a predominantly magnetic type of material will have to be employed to realize matched absorber in practice. The design criteria for the resonant absorber (Eq. 4.24 and 4.25) implies that, resonant absorbers are narrow band absorbers.

Absorbers one each for matched (broad band operation over Ku-Band) and resonant (narrow band operation in X-Band) criteria with an added constraint on thickness of 2mm were designed and fabricated. Co-BHF and carbon have been used as the lossy materials along with silicone/neoprene rubber as the binder in the design [Chaitanya et al, 130, 131]. The experimentally obtained absorption characteristics for both types follow very closely the theoretically predicted curves (Fig 4.2 and 4.3). The experimental absorption values for the matched absorber are less than theoretical values by 3-4 dB, these could be due to the limitation of the fabrication process. A minimum of 10 dB has been achieved practically over 13 - 18 GHz frequency region. Further for the resonant absorber, the experimentally obtained resonant frequency has shifted by 0.5 GHz, from its theoretical value of 9 GHz. This could be due to the fact that the theoretically computed thickness was 1.76 mm, while the fabricated thickness was 1.8 mm. Further the resonant absorber has provided a minimum 15 dB absorption over a 7.75 - 9 GHz, band thus full filling the specification for narrow band absorber. The technique can be applied to develop absorbers in any desired frequency range.

Waterman's T-matrix approach has been utilized in a multiple scattering formulation in the 5th chapter, to determine the bulk or effective propagation constant for the composite absorbing medium, as a function of particle (scatterer) size and shape, volume concentration of the lossy material, orientation and position of the scatterer in the binder or host matrix. In the multiple scattering model, T-matrix is used to represent the effect of size and shape of individual lossy particles and the random nature of orientation of the particles in the host matrix. An average over all possible position is performed using the two-point joint probability function, which in turn is defined by the radial distribution function obtained under the self consistent approximation. A closed form solution of the dispersion equation for a ferrite polymer composite is obtained under the long wavelength approximation (Eq. 5.30).

The designed and fabricated matched absorber performance was verified using this approach. This model describes more closely the practical behavior of the absorbers (BBA and MBA, which were considered in 3rd and 4th chapter respectively) than the earlier methods (Fig 5.7 and 5.8), thus proving that bulk properties have to be considered, when high loss materials are employed in the design. For the BBA this model predicts the small resonance that was observed in the experimentally determined (Fig 5.8) absorption characteristics. This method predicts very clearly the flatter absorption characteristics displayed experimentally by the MBA (Fig 5.8).

Employing the proposed model, the optimum configuration for a ferrite-rubber composite, such as size of the spherical particles (scatterer), volume concentration of the ferrite and thickness of the absorber were determined for broad band operation over X-Band within 3mm thickness limitation. The

experimentally determined absorption characteristics for the designed and fabricated absorber of thickness 2.3mm, (Fig 5.11) displays good agreement with the theoretically predicted curve as a broad band absorber, except for the shift in the absorption peak. Experimentally the fabricated absorber has provided a minimum 10 dB absorption over 8 - 12 GHz (X-Band) frequency range. In addition a number of absorbers have been analyzed and designed [154], in different frequency ranges and the experimental results fortify, the multiple scattering formulation adopted, to describe the bulk or effective properties of the absorbing media.

An impedance matching technique is formulated in the 6th chapter, to overcome the mismatching (at the free space-absorber interface) problem associated with thin planar absorbers. A thin conducting screen perforated with an array of structures has been employed as the Impedance Matching Screen (IMS). Jerusalem cross and double square loop array structures were found (Fig 6.3) to be promising candidates for IMS application from a number of structures that were experimentally examined [Chaitanya et al, 156].

A simple equivalent circuit approach is formulated for the design analysis of the composite structure formed by incorporating the IMS at the front end of the absorber in section 6.3. Equivalent circuit models available in literature, to analyze the array of Jerusalem cross and double square loops have been utilized in the design of the IMS's. The effect of the various parameters of the array on the overall performance of the absorber have been analyzed and critical parameters identified in section 6.4 [Chaitanya et al, 153].

Using the proposed equivalent circuit model, with Jerusalem cross as the IMS structure, the Co-BHF rubber absorber designed in chapter III, which practically

provides around 8db absorption over 12-18 GHz., was impedance matched into (i) operating as a narrow band absorber (Fig 6.11) with a peak absorption of over 30dB; and (ii) operating as broad band absorber with bandwidth over 8 to 18 GHz (Fig 6.12), with a marked increase in the level of absorption through out the band. The close agreement between the theoretically predicted absorption characteristics and the experimentally determined values for both the cases (Fig 6.11 - 6.14) consolidates the proposed impedance technique.

The CK-IMA designed as a broad band absorber, has practically provided 8 dB absorption over 8-18 GHz. (10 GHz bandwidth) frequency range. The experimentally determined characteristics follow the theoretical predicted curve. Further it is to be noted that the general decrease of 2-3 dB absorption over the frequency band by the BBA has also been reflected in the response of the CK-IMA.

The K-IMA designed as a narrow band absorber, has practically provided a minimum 15 dB absorption over 15 - 17 GHz. (2 GHz) frequency range. The experimentally determined characteristics follow the theoretical predicted curve. The shift in the resonant frequency observed experimentally is due to the fact that the IMS, had to be attached on to the surface of the absorber by means of a glue and the thickness of the IMS has been assumed to zero in our theoretical analysis. It is the experience [154] of the author that the thickness of the glue used to attach the IMS onto the absorber shifts the resonant frequency. Thicker the glue larger will be the shift in the resonant frequency towards the lower side of the frequency spectrum. To overcome this problem it was suggested that the IMS could be incorporated onto the absorber during the fabrication process of the absorber itself, and this method was subsequently followed in the fabrication of a number of IMA's in [154], with satisfactory results.

The author wishes to put on record the fact that, it was possible to fabricate the IMS's only after a number of unsuccessful attempts. The disability of etching a free standing copper sheet of less than 50 microns thick to within 0.05mm track tolerance, within the available facilities was a major handicap.

An established approach to overcome the mismatching (at the free space-absorber interface) problem associated with planar absorbers is to construct an impedance taper employing a multi layered structure. This approach has been extended to the case of thin planar absorbers in the 7th chapter. Generalized design equations have been arrived at, for a plane wave at arbitrary angle of incidence, as a function of number of layers, concentration of the lossy material in each layer, individual layer thickness, and the overall thickness of the absorber in section 7.2.1 and 7.2.2.

As a special case of multi layered structure when the number of layers is one, a single layer absorber was designed using the multi layered approach, to operate as a broad band absorber (X-Band) over $\pm 60^\circ$ incidence angle. A limitation on the overall thickness of the absorber of 3mm was also met. Iron powder has been used in the design as the lossy material along with silicone rubber as the binder. The designed and fabricated absorber of 2.3mm thick, displays a practical absorption characteristics which matches very closely with the theoretically predicted curves. Theoretically the absorber provides a minimum 10dB absorption over X-Band, at $\pm 45^\circ$ incidence (Fig 7.4 and 7.5), while the experimentally obtained absorption characteristics provides a minimum 10 dB absorption over X-Band. The peak absorption experimentally determined is 4 dB less than the theoretically predicted value.

One of the major problems faced in translating the theoretical design into practical absorbers is dispersing the lossy particles uniformly in the host medium. In this context in 8th chapter, Secondary Electron and Optical Microscopic Analysis were done on samples fabricated with different dispersing aids (section 8.2). The type and critical concentration of the dispersing aid, and the method for dispersion, to obtain a uniform dispersion of particles in the binder matrix have been identified. A representative micro graph of the type of dispersion obtained is shown in Fig 8.2f. Wherein Iron powder particles are dispersed in Silicone rubber.

Due to the non availability of Co-BHF and ferrite to the required specification, the above two types of raw materials were prepared in the laboratory and their parameters have been determined.

The design of all the absorbers have been done with the aid of an existing optimization subroutine. The mathematical optimization technique was utilized due to the non uniqueness of the specifications (section 2.5) of the absorbers. The specifications were set as per the requirement of [Project Report on Development of Thin Radar Absorber, DRDO, Ministry of Defence, Govt. of India, India., 154]. The flexible tolerance optimization technique was found suitable due to two reasons: i) optimization does not involve differentiation of the objective function; and ii) the objective function and the constraints are incorporated into the optimization routine separately via the PROBLEM(INQ) subroutine.

Summarizing, we note that the analysis done on the development and characterization of microwave absorbers, indicate that in the design and fabrication of thin planar absorbers, the absorbing media has to be represented by its bulk characteristics.

The design criteria for thin planar absorbers have been arrived at for both broad band as well as narrow band operation. The criteria indicates that to achieve broad band operation predominantly magnetic type of fillers will have to be employed.

A technique has been formulated to achieve broad band operation with single layer absorbers, by combining material and resonant absorption properties of the absorber.

The impedance matching technique is a very powerful tool to improve, modify the absorber performance or for the design of composite absorbers. In addition for a given absorption-bandwidth specification the impedance matching technique provides a solution to reduce the overall thickness and weight of the absorber.

Translating the design into practical absorbers demands special fabrication procedures depending on the type of absorber.

Although a large number of absorbers with various design specification, have been designed and fabricated in [154]. Using the various design and analysis approaches formulated in this work and the repeatability of the results obtained, only a few and representative results have been included in this dissertation. Since to discuss all the results would only serve to increase the volume of this presentation.

9.2 SCOPE OF FUTURE WORK

The design and analysis done on absorbers in this work can be extended to the case of structurally strong microwave absorbing materials.

Different types of high loss materials (other than Co-BHF) or a combination of them, can be utilized in the generalized design approach to realize higher absorption and wider bandwidths.

The T-matrix analysis done to realize the effective properties of the absorbing media can be extended to the case of arbitrary shaped particles.

The Impedance Matching technique developed can be extended to the case of arbitrary angle of incidence and polarization. Other types of Structures can also be tried in the design for IMS. The conducting screen IMS's can be replaced by lossy screens IMS's to achieve better results. A multilayered construction can be formulated and designed interleaving IMS and absorbers to achieve better absorber performance.

References

- [1] Skolnik, M.J., 'Introduction to Radar Systems', McGraw Hill Co., 1962.
- [2] Knott, E.F., Shaeffer, J.F. and Tuley, M. T., 'Radar Cross Section, Its Prediction and Reduction', Artech House Inc., North Bergen., New Jersey, 1985.
- [3] Dax, P.R., 'ECM Verses ECCM In Search Radar', Space/Aeronautics, Vol. 33, p34, April 1960.
- [4] Salisbury, W.W., 'Absorbent Bodies For Electromagnetic Waves', U.S. Patent 2 599 944, June 10, 1952.
- [5] Knott, E.F., 'Thickness Criterion For A Single Layer Radar Absorbent', IEEE Trans. Antennas and Propagation, Vol. AP-27., No.5, pp 698-701, 1979.
- [6] Nishikata, A. and Shimizu, Y., 'Analysis Of Lamda/4 Type Wave Absorber By Resistive Cloth', Electronics and Communication in Japan, Part 1, Vol. 73, No. 4, pp 66-75, 1990.
- [7] Nishikata, A. and Shimizu, Y., 'Absorbing Rubber Sheet Mixed With Carbon For X-Band Marine Radar Frequencies', Electronics and Communication in Japan, Part 1, Vol. 69, No. 12, pp 65-71, 1986.
- [8] Mirtaheri, S.A., Mizumota, T. and Natio, Y., 'The Electromagnetic And Dispersion Characteristics Of Materials Composed Of Rubber, Carbon And Ferrite', Trans. of Institute of Electronics, Information and communication Engg., Part E, Vol. E-73, No.12, pp1746- 52, 1990.
- [9] Mirtaheri, S.A., Yin, J., Mizumota, T. and Natio, Y., 'The Characteristics Of Electromagnetic Wave Absorber Composed Of Rubber, Carbon, And Ferrite', Trans. of Institute of Electronics, Information and communication Engg., Part E, Vol. E-72, No.12, 1447- 52, 1989.

- [10] Natio, Y., Yin, J. and Mizumoto, T., 'Electromagnetic Wave Absorbing Properties Of Carbon-Rubber Doped With Ferrite', Electronics and Commun. in Japan, Part 2, Vol. 71, No.7, pp77-83, 1988.
- [11] Dong II Kim, Chung, S.M., Park, Y.W. and Natio, Y., 'Characteristics Of Carbon-Ferrite Microwave Absorber', J.of Korean Institute of Telematics and Electronics, Vol. 26, pp67-71, 1989.
- [12] Natio, Y, Mizumota, T., 'Effect of Doping Carbon In An Electromagnetic Wave absorber', Electronics and Commun. in Japan, Part 2, Vol. 70, No.2, pp12-17, 1987.
- [13] Natio, Y., 'Thickness Of Ferrite Absorbing Wall', Electronics and Communication in Japan, Vol. 52-B, No.1, pp71-75, 1969.
- [14] Natio, Y. and Suetaka, K., 'Characteristics Of The Ferrite Absorbing Wall', Electronics and Commun. in Japan, Vol. 52-B, No.1, pp76-80, 1969.
- [15] Chino, M., Yamamota, T. and Oshimoto, A., 'Microwave Absorbers Using Ferroelectric/Rubber Composite Structure And Their Evaluation', Ferroelectrics, Vol. 93, pp67-71, 1989.
- [16] Fernandez, A. and Valenzuela, A., 'General Solution For Single Layer Electromagnetic Wave Absorber', Electronics Letters, Vol. 21, No.1, pp20-21, 1985.
- [17] Ahmad, A.H. and Abdul Dada, J.W., 'Reduction Of Radar Cross Section Using Absorption Technique', IE(I) Journal-ET., Vol. 71., pp 29-32, May 1990
- [18] Plas, G.V.D., Barel, A. and Schweicher, E., 'A Spectral Iteration Technique For Analyzing Scattering From Circuit Analog Absorbers', IEEE Trans. on Antennas and Propagation, Vol. 37, No. 10, pp1327-32, 1989.

- [19] Tsao, C.H. and Mittra, R., 'A Spectral-Iteration Approach For Analyzing Scattering From Frequency selective Surfaces', IEEE Trans. on Antennas and Propagation, Vol. 30, pp303-308, 1982.
- [20] Varadan, V.K., Varadan, V.V., Ma, Y. and Hall, W.F., 'Design Of Ferrite-Impregnated Plastics (PVC) As Microwave Absorbers', IEEE Trans. On Microwave Theory and Techniques, Vol. 34, No.2, pp251-258, 1986.
- [21] Ueno, R. and Ogasawara, N., 'Ferrites- or Iron oxides-Impregnated Plastics Serving As Radio Wave Scattering Suppressors', Proc. of the International Conference on Ferrites-3, Japan, pp890-93, Oct., 1980.
- [22] Kakimi, Y., Yoshida, N. and Fukai, I., 'Analysis Of Absorbing Characteristics Of Thin-type Absorber For Generalized Condition Of Incident Wave', IEEE Trans. on Electromagnetic compactibility, Vol. 31, No.3, pp323-28, 1989.
- [23] Aoto, T., Yoshida, N. and Fukai, I., 'Transient Analysis Of Electromagnetic Field For Resonance-Type Absorber In Three Dimensional Space', Trans of IECE, Japan, Vol. J70B, No.1, pp148-158, 1987.
- [24] Aoto, T., Yoshida, N. and Fukai, I., 'Transient Analysis Of The Electromagnetic Field For A Wave Absorber In Three Dimensional Space', IEEE Trans. on Electromagnetic compactibility, Vol. 29, No.1, pp18-23, 1987.
- [25] Jaggard, D.L. and Engheta, N., 'ChirosorbTM As An Invisible Medium', Electronics Letters, Vol. 25, No.3, pp173-74, 1989.
- [26] Jaggard, D.L., Engheta, N. and Liu, J.C., 'Chiroshield, A Salisbury/Dallenbach Shield Alternative', Electronics Letters, Vol. 26, No.17, pp1332-34, 1990.
- [27] Jaggard, D.L., Liu, J.C. and Sun, X., 'Spherical Chiroshield', Electronics Letters, Vol. 27, No.1, pp77-79, 1991.

- [28] Bassiri, S., Papas, C.H. and Engheta, N., 'Electromagnetic Wave Propagation Through A Dielectric-Chiral Interface and Through a Chiral Slab', *J.Opt.Soc.Am.A*, 5, pp1450-59, 1988.
- [29] Gurie, T., Varadan, V.V. and Varadan, V.K., 'Influence Of Chirality On The Reflection Of EM Waves By Planar Dielectric Slabs', *IEEE Trans. on Electromagnetic Compactibility*, Vol. 32, No.4, pp300-303, 1990.
- [30] Lakhtakia, A., Varadan, V.V. and Varadan, V.K., 'A Parametric Study Of Microwave Reflection Characteristics Of A Planar Achiral-Chiral Interface', *IEEE Trans. on Electromagnetic Compactibility*, Vol. 28, No.2, pp90-95, 1986.
- [31] Varadan, V.K., Varadan, V.V., Ma, Y. and Lakhtakia, A., 'Ferrite and Chiral Polymer Composites : Electromagnetic Applications', *SPIE Vol.927, Wave Propagation and scattering in varied media*, pp213-219, 1988.
- [32] Pitman, K.C., Lindely, M.W., Simkin, D. and Cooper, J.F., 'Radar Absorbers: Better By Design', *Proc. of IEE, Part F*, Vol. 138, No.3, pp223-28, 1991.
- [33] Fante, R.L. and Michael, T.M., 'Reflection Properties Of The Salisbury Screen', *IEEE Trans. on Antennas and Propagation*, Vol. 36, No.10, pp1443-54, 1988.
- [34] Morris, S.B., 'Optimization Of Thin Planar Absorbers And The Effect On Bandwidth', *IEE Colloquium digest No.125*, p3/1-6, 1992.
- [35] Perni, J. and Cohen, L.S., 'Design Of Radar Absorbing Material (RAMs) For Wide Range Of Angles Of Incidence', *Proc. Of IEEE-S, International Symposium On Electromagnetic compactibility*, pp418-24, 1991.
- [36] Natio, Y. and Suetake, K., 'Construction Of Multi-Layer Absorbing Wall For Microwaves', *Electronics and Communication in Japan*, Vol. 48, pp112-121, 1965.

- [37] Ono, M. and Suzuki, M., 'An Improved Synthesis Of The Multi Layer Absorber', Electronics and Communication in Japan, Vol.54B, No.4, pp64-69, 1971.
- [38] Ono, M. and Suzuki, M., 'A Design Method For Multilayer Microwave Absorber Of Wideband Type', Electronics and Communication in Japan, Vol. 53B, No.11, pp81-89, 1970.
- [39] Ono, M. and Suzuki, M., 'Reflection And Attenuation Characteristics Of Multilayered Absorber At Oblique Incidence', Electronics and Communication in Japan, pp 84-92, 1967.
- [40] Ono, M. and Ikuta, A., 'Synthesis Of An EMW Absorber With Good Reflection Characteristics At Both Normal And Oblique Incidence', Electronics and Communication in Japan, Vol. 62B, No.10, pp 54-62, 1979.
- [41] Amin, M.B. and James, J.R., 'Techniques For The Utilization Of Hexagonal Ferrites In Radar Absorbers. Part 1.' The Radio and Electronics Engineers., Vol. 51, pp 209 - 218, 1981
- [42] Kyung, Y.K., Wang, S.K. and Jong, K.L., 'Behaviour Of Laminates Of Ferrites On Electromagnetic Wave Absorber', IEEE Trans. On Magnetics, Vol. 29, No.4, pp2134-38, 1993.
- [43] Miyazaki, Y. and Tanoue, K., 'Electromagnetic Absorption And Shield Properties Of Lossy Composite Multilayers', Proc. of IEEE-S, International Symposium On Electromagnetic Compactibility, pp370-74, 1990.
- [44] Ruck, G.T., Barriek, D.E., Straut, W.D. and Krichbaum, C.K., 'Radar Cross Section Hand Book, Vol.-II', Plenum press, New York, 1970
- [45] Hatakeyama, K. and Inui, T., 'Electromagnetic Wave Absorber Using Ferrite Absorbing Material Dispersed With Short Metallic Fibres', IEEE Trans. on Magnetics, Vol. 20, NO.5, pp1261-63, 1984.

- [46] Varaprasad, A.M. and Parameswaran, S., '123 Oxide In Double Layer Microwave Absorber', *Ferroelectrics Letters Section*, Vol. 9, No.5, pp123-30, 1988.
- [47] Svirgelj, J., Michielssen, E. and Mittra, R., 'Absorption Characteristics Of Periodic Arrangement Of Infinite Helices', *IEEE Microwave And Guided Wave Letters*, Vol. 2, No.12, pp 495-96, 1992.
- [48] Jha, V. and Banthia, A.K., 'Composites Based On Waste-ferrites As Microwave Absorber', *Indian J. Phys.* 63(A), (5), pp514-524, 1989.
- [49] Kumar, A., 'Acctylene Black: A Single Layer Microwave Absorber', *Electronics Letters*, Vol. 23, No.5, pp184-85, 1987.
- [50] Kumar, A., 'Complex Permittivity Of Rubber-Carbon Mixtures', *IEEE Trans. on Electrical Insulation*, Vol. 14, pp175-78, 1979.
- [51] Hashimoto, O. and Shimizu, Y., 'Reflecting Characteristics Of Anisotropic Rubber Sheets And Measurement Of Complex Permittivity Tensor', *IEEE Trans. on Microwave Theory and Techniques*, Vol. 34, No.11, pp1202-07, 1986.
- [52] Veinger, A.I., Zabrodskii, A.G., Krasikov, L.A. and Khorosheva, N.E., 'Anamolous Microwave Absorption In Magnetically Filled Low-molecular Weight Rubbers', *Soviet technical physical letters*, Vol. 15, No.21-22, pp59-61, 1989.
- [53] Ishimaru, A., 'Wave Propagation And Scattering In Random Media', Vol. 2, Academic press, New York, 1978.
- [54] Holt, A.R., 'The Fredholm Integral Equation Method And Comparison With The T-matrix Approach', in *Acoustic, electromagnetic and elastic wave scattering: Focus on the T-matrix approach*. Varadan, V.V. and Varadan V.K. Eds., U.K., Pergamon press, p255-68, 1980.

- [55] Antar, Y.M., Kishk, A.A., Shafai, L. and Allan, L.E., 'Radar Backscattering From Partially Coated Targets With Axial Symmetry', IEEE Trans. on Antennas and Propagation, Vol. 37, No.5, pp564-75, 1989.
- [56] Umashankar, K., Taflove, A. and Rao, S.M., 'Electromagnetic Scattering By Arbitrary Shaped Three-dimensional Homogeneous Lossy Dielectric Objects', IEEE Trans. on Antennas and Propagation, Vol. 34, pp758-66, 1986.
- [57] Schaubert, D.H., Wilton, D.R. and Glisson, A.W., 'A Tetrahedral Modelling Method For Electromagnetic Scattering By Arbitrarily Shaped Inhomogeneous Dielectric Bodies', IEEE Trans. on Antennas and Propagation, Vol. 32, pp77-85, 1984.
- [58] Tsai, C.T., Massoudi, H., Durney, C.H. and Iskander, M.F., 'A Procedure For Calculating Fields Inside Arbitrarily Shaped Inhomogeneous Dielectric Bodies Using Linear Basis Function With The Moment Method', IEEE Trans. on Microwave Theory and Techniques, Vol. 34, No.11, pp1131-38, 1986.
- [59] Taflove, A. and Umashankar, K., 'Radar Cross Section Of General Three Dimensional Scatterers', IEEE Trans. on Electromagnetic Compactibility, Vol. 25, pp433-40, 1983.
- [60] Zienkiewicz, O.C. and Cheung, Y.K, 'Finite Elements In The Solution Of Field Problems', The Engineer, pp507-10, 1965.
- [61] Morgan, M.A., 'Finite Element Computation Of Scattering By Inhomogenous Penetrable Bodies Of Revolution', IEEE Trans. on Antennas and Propagation, Vol. 27, No.2, pp202-14, 1979.
- [62] D'Angelo, J. and Mayergoyz, I., 'Finite Element Method for The Solution Of RF Radiation And Scattering Problems', Electromagn., Vol. 10, pp177-99, 1990.

- [63] Barber, P., Yeh, C., 'Scattering Of Electromagnetic Waves By Arbitrary Shaped Dielectric Bodies', *Applied Optics*, Vol. 14, No.12, pp2684, 1975.
- [64] Brangi, V.N. and Seliga, T.A., 'Scattering From Axisymmetric Dielectrics or Perfect Conductors Imbeded In An Axisymmetric Dielectrics', *IEEE Trans. on Antennas and Propagation*, Vol. 25, pp575-80, July 1977.
- [65] Tsang, L. and Kong, J.A., 'Effective Propagation Constants For Coherent Electromagntic Wave Propagation In Media Embedded With Dielectric Scatters', *J.Appl.Phys.*, Vol. 53, No.11, pp7162-73, 1982.
- [66] Holt, A.R., 'The Scattering Of Electromagnetic Waves By Single Hydrometers', *Radio Sci.*, Vol. 17, pp929-45, 1982.
- [67] Wills, T.M. and Weil,H., 'Disk Scattering and Absorption By An Improved Computational Method', *Appl.Opt.*, Vol. 26, No.18, pp3987-95, 1987.
- [68] Wilton, D.R., 'Review Of Current Status And Trends In The Use Of Integral Equations In Computational Electromagnetics', *Electromagnetics*, Vol. 12, pp287-341, 1992.
- [69] Bates, R.H.T., 'General Introduction To The Extended Boundary Condition', in *Acoustic, electromagnetic and elastic wave scattering: Focus on the T-matrix approach*. Varadan, V.V. and Varadan V.K. Eds., U.K., Pergamon press, p21-31, 1980.
- [70] Waterman, P.C., 'Matrix Formulation Of Electromagnetic scattering', *Proc. of IEE*, Vol. 53, pp805-12, 1965.
- [71] Waterman, P.C., 'Symmetry, Unitary And Geometry In Electromagentic Scattering', *Phys.Rev.D.*, Vol. 3, No.4, pp825-39, 1971.
- [72] Foldy, L.L., 'The Multiple Scattering Of waves', *Phys.Rev.*, Vol. 67, 107-19, 1945.

- [73] Lax, M., 'Multiple Scattering Of Waves', *Rev.Mod.Phys.*, Vol. 23, pp289-310, 1951.
- [74] Lax, M., 'The Effective Field In Dense System', *Phys.Rev.*, Vol. 88, pp621-29, 1952.
- [75] Twersky, V., 'On Scattering Of Waves By Random Distribution, I, Free Space Scatterer Formalism', *J.Math.Phys.*, Vol. 3, 700-15, 1962.
- [76] Twersky, V., 'On Scattering Of Waves By Random Distribution, II, Two-Space Scatterer Formalism', *J.Math.Phys.*, Vol. 3, 724-34, 1962.
- [77] Twersky, V., 'Multiple scattering Of Waves And Optical Phenomena', *J.Opt.Soc.Am.*, Vol. 52, pp145-171, 1962.
- [78] Twersky, V., 'Coherent Scalar Field In Pair-correlated Random Distributions Of Aligned Scatterers', *J.Math.Phys.*, Vol. 18, pp2468-86, 1977.
- [79] Twersky, V., 'Coherent Electromagnetic Waves In Pair-correlated Random Distributions Of Aligned Scatterers', *J.Math.Phys.*, Vol. 19, pp215-30, 1978.
- [80] Twersky, V., 'Acoustic Bulk Parameters In Distributions Of Pair-correlated Scatterers', *J.Opt.Soc.Am.*, Vol. 64, pp1710-19, 1978.
- [81] Tsang, L. and Kong, J.A., 'Multiple Scattering Of Electro-magnetic Waves By Random Distribution Of Discrete Scatterers With Coherent Potential and Quantum Mechanical Formulism', *J.Appl.Phys.*, Vol. 51, pp3465-85, 1980.
- [82] Varadan, V.K., Bringi, V.N. and Varadan V.V., 'Coherent Electromagnetic Wave Propagation Through Randomly Distributed Dielectric Scatterers', *Phys.Rev.D.*, Vol. 19, No. 8, pp2480-89, 1979.
- [83] Varadan, V.V. and Varadan V.K., 'Multiple Scattering Of Electromagnetic Waves By Randomly Distributed And Oriented Dielectric Scatterers', *Phys.Rev.D.*, Vol. 21, No. 2, pp388, 1980.

- [84] Varadan, V.K., 'Multiple Scattering Of Acoustic, Electromagnetic And Elastic Waves', in Acoustic, electromagnetic and elastic wave scattering: Focus on the T-matrix approach. Varadan, V.V. and Varadan V.K. Eds., U.K., Pergamon press, pp103-34, 1980.
- [85] Bringi, V.N., Varadan, V.K. and Varadan V.V., 'Average Dielectric Properties Of Discrete Random Media Using Multiple Scattering Theory', IEEE Trans. on Antennas and Propagation, Vol. 31, No.2, pp371-75, 1983.
- [86] Varadan, V.K., Bringi, V.N., Varadan V.V. and Ishimaru, A., 'Multiple Scattering Theory For Waves In Discrete Random Media And Comparison With Experiments', Radio Sci., Vol. 18, pp321-327, 1983.
- [87] Varadan, V.K., Ma, Y, Varadan V.V., 'Coherent Electromagnetic Wave Propagation Through Randomly Distributed and Oriented Pair-Correlated Dielectric Scatterers', Radio Sci., Vol. 19, No. 6, pp1445-49, 1984.
- [88] Ma, Y., Varadan, V.V. and Varadan, V.K., 'Wave Propagation In inhomogeneous Media Containing Randomly Oriented Nonspherical Scatterers', proc. of SPIE, Vol. 927, Wave Propagation and Scattering in Varied Media, pp17-24, 1988.
- [89] Cohn, S.B., 'Dielectric Properties Of A Lattice Of Anisotropic Particles', J.Appl.Phys., Vol. 27, pp1106-07, 1956.
- [90] Pelton, E.L. and Munk, B.A., 'A Streamlined Metallic Radome', IEEE Trans. on Antennas and Propagation, pp799-803, 1974.
- [91] Chen, C.C., 'Transmission Through A Conducting Screen Perforated Periodically With Apertures', IEEE Trans. on Microwave Theory and Techniques, Vol. 18, No. 2, pp627-32, 1970.
- [92] Lee, S.W., 'Scattering By Dielectric-loaded Screen', IEEE Trans. on Antennas and Propagation, Vol. 19, pp656-665, 1971.

- [93] Chen, C.C., 'Transmission Of Microwave Through Perforated Flat Plates Of Finite Thickness', IEEE Trans. on Microwave Theory and Techniques, Vol. 21, No. 1, pp1-6, 1973.
- [94] Anderson, I., 'On The Theory Of Self-Resonant Grids', Bell Syst. Tech.Journal, Vol. 54, pp1725-31, 1975.
- [95] Agrawal, V.D. and Imbriale, W.A., 'Design Of Dichroic Cassegrain Subreflector', IEEE Trans. on Antennas and Propagation, Vol. 27, pp466-73, 1979.
- [96] Schennum, G.H., 'Frequency Selective Surfaces For Multiple Frequency Antennas', Microwave J., Vol. 16, pp55-57, 1973.
- [97] Durschlag, M.S. and DeTemple, T.A., 'Far-IR Optical Properties Of Free Standing And Dielectric Backed Metal Meshes', Appl.Opt., Vol. 20, No.7, pp1245-53, 1981.
- [98] McPhedran, R.C. and Maystre, D., 'On The Theory And Solar Application Of Inductive grids', Appl.Phys. Vol. 14, pp1-20, 1977.
- [99] Montgomery, J.P., 'Scattering By An Infinite Periodic Array Of Thin Conductors On A Dielectric Sheet', IEEE Trans. on Antennas and Propagation, Vol. 23, No.1, pp70-75, 1975.
- [100] Montgomery, J.P., 'Scattering By An Infinite Periodic Array Of Microstrip Elements', IEEE Trans. on Antennas and Propagation, Vol. 26, No.6, pp850-53, 1978.
- [101] Pelton, E.L. and Munk, B.A., 'Scattering From Periodic Arrays Of Crossed Dipoles', IEEE Trans. on Antennas and Propagation, Vol. 27, No.3, pp323-30, 1979.

- [102] Tsao, C.H. and Mittra, R., 'Spectral-Domain Analysis Of Frequency Selective Surfaces Comprised Of Periodic Arrays Of Cross Dipoles And Jerusalem Crosses', IEEE Trans. on Antennas and Propagation, Vol. 32, No.5, pp478-86, 1984.
- [103] Mittra, R., Chan, C.H. and Cwik, T., 'Techniques For Analyzing Frequency Selective Surfaces- A Review', Proc. of IEEE, Vol. 76, No. 2, pp1593-1615, 1988.
- [104] DeLyser, R.R. and Kuester, E.F., 'Homogenization Analysis Of Electromagnetic Strip Gratings', Journal of Electromagnetic Waves and Applications, Vol. 5, No.11, pp1217-36, 1991.
- [105] Carbonini, L., 'The Natural Current Expansion Approach To The Numerical Analysis Of Finite Arrays', Electromagnetics, Vol. 12, pp273-83, 1992.
- [106] Compton, R.C. and Rutledge, D.B., 'Approximation Techniques For Planar Periodic Structures', IEEE Trans. on Microwave Theory and Techniques, Vol. 33, No.10, pp1083-88, 1985.
- [107] Lee, S.W., Zarrillo, G. and Law, C.L., 'Simple Formulas For Transmission Through Periodic Metal Grids Or Plates', IEEE Trans. on Antenna and Propagation, Vol. 30, No.5, pp904-09, 1982.
- [108] Chen, C.C., 'Differation of Electromagnetic Waves By A Conducting Screen Perforated Periodically With Circular Holes', IEEE Trans. on Microwave Theory and Techniques, Vol. 19, No.5, pp475-81. 1971.
- [109] Roberts, A. and McPhedran, R.C., 'Bandpass Grids With Annular Apertures', IEEE Trans. on Antennas and Propagation, Vol. 36, No.5, pp607-11, 1988.
- [110] Langley, R.J. and Drinkwater, A.J., 'Improved Empirical Model For The Jerusalem Cross', IEE proc., Vol.129, Pt.H, No.1, pp1-6, 1982.

- [111] Langley, R.J. and Parker, E.A., 'Equivalent Circuit Model For Arrays Of Square Loops', *Electronics Letters*, Vol. 18, No.7, pp294-96, 1982.
- [112] Langley, R.J. and Parker, E.A., 'Double Square Frequency Selective Surfaces And Their Equivalent Circuit', *Electronics Letters*, Vol. 19, No.17, pp675-76, 1983.
- [113] Marcuvitz, N., 'Waveguide Handbook', McGraw-Hill Co., 1951.
- [114] Cwik, T. and Mittra, R., 'The Effects Of The Truncation And Curvature Of Periodic Surfaces: A Strip Grating', *IEEE Trans. On Antennas and Propagation*, Vol. 36, No.5, pp612-22, 1988.
- [115] Severin, H. and Stoll, P.J., 'Permeabilitat einiger Ferrite mit magnetischen Verlusten im Bereich der Zentimeter- und Millimeterwellen', *Z. Angew Physik.*, Bd. 23, No.3, pp 209-212, 1967
- [116] Nedkov, I., Petkov, A. and Karpov, V., 'Microwave Absorption in Sc- And Co-substituted Ba Hexa Ferrite Powders', *IEEE Trans. on Magnetics*, Vol.26, No.5, pp 1483-84, 1990.
- [117] Crispin, J.W. and Siegel., 'Methods of Radar Cross Section Analysis', Academic Press, New York, 1968.
- [118] Lichtenecker K. and Rother K., 'Die Herleitung der Logarithmischen Mischungsgesetzes. als allgemeinen Prinzipien der Stationasen Strömung', *Physik.Zeitscher*, 32, pp.225-260., 1931
- [119] David, H., 'Applied NonLinear Programming', McGraw Hill Book Co.
- [120] Gupta, S.C., Agrawal, N.K. and Chaitanya Kumar, M.V., 'Design Of A Single Layer Broad Band Microwave Absorber Using Cobalt Substituted Barium Hexagonal Ferrite', *Proc. of the IEEE-S, International Symposium on MTT*, New Mexico, USA, pp 317-320, June 1992.

- [121] Gupta, S.C., Agrawal, N.K. and Chaitanya Kumar, M.V., 'Broad Band Absorbers For S-, C-, X- and KU-bands', Journal of IETE, Vol. 39, No.3, pp 197-200, 1993.
- [122] Wickersham, A.F., 'Microwave And Fiber Optics Communication', Prentice-Hall Inc., N.J., 1988.
- [123] Chaitanya Kumar, M.V., Agrawal, N.K. and Gupta, S.C., 'An Approach For The Design Analysis Of Add-On Types Of Electromagnetic Wave Absorbers', Accepted for publication in the Journal of IE(ET), India., 1994.
- [124] Straton, J.A., 'Electromagnetic Theory', New York, McGraw Hill Co., 1941.
- [125] Inui, T. and Ogasawara, N., 'Grain Size Effects On Microwave Ferrite Magnetic Properties', IEEE Transaction on Magnetics, Vol. MAG.13, No.6, pp.1729-34., Nov. 1977.
- [126] Neelakantaswamy, P.S., Chowdari B.V.R. and Rajaratnam A., 'Estimation Of Permittivity Of A Compact Crystal by Dielectric Measurement On Its Powders: A Stochastic Model For The Powder Dielectric', Journal Physics. D: Applied Physics, Vol. 16, pp1785-1799, 1983.
- [127] Lal, K. and Prasad, R., 'Permittivity of Conductor-Dielectric Hetrogenous Mixtures', J.Phys D., pp 2098-2110., 1973.
- [128] Dionne, G.F., 'A Review of Ferrite for Microwave Application', Proc. IEEE, Vol.63, No.5, pp 777-788. 1975.
- [129] Von Aulock, W.H., 'Handbook of Microwave Ferrite Materials.', Academic Press, New York.
- [130] Chaitanya Kumar, M.V., Agrawal, N.K. and Gupta, S.C., 'Microwave Interference Suppression Through Absorption', Accepted at IEEE-S, International symposium on Euro-Electromagnetics and Environment, France, May-June 1994.

- [131] Chaitanya Kumar, M.V., Agrawal, N.K. and Gupta, S.C., 'Design Analysis Of Add-On Type Of Microwave Absorber', Proc. of the IX National Convention of Institutions of Engineers (ET), University of Roorkee, Roorkee, India., pp 347-350, March 1994.
- [132] Chaitanya Kumar, M.V., 'Development Of A Broad band Single Layer microwave Absorber', M.E. Dissertation report., Electronics and Computer Engineering Department., University of Roorkee., Roorkee., India., 1991.
- [133] Von Hippal, A.R., 'Dielectric Materials And Applications.' The Technology Press of MIT and John Wiley & Sons., New York, 1954.
- [134] Oguchi, T., 'Scattering From Hydrometers: A Survey', Radio Sci., Vol. 16, pp 691-729, 1981.
- [135] Olsen, R.I., 'A Review Of Theories Of Coherent Radio Wave Propagation Through Precipitation Media Of Randomly Oriented Scatterers, And The Role Of Multiple Scattering', Radio Sci., Vol. 17, pp 913-928, 1982.
- [136] Bringi, V.N., Varadan, V.K. and Varadan V.V., 'Coherent Wave Attenuation By A Random Distribution Of Particles', Radio Sci., Vol. 18, pp 946-952, 1982.
- [137] Mathur, N.C. and Yeh, K.C., 'Multiple Scattering Of Electromagnetic Waves By Random Scatterers Of Finite Size', J. Math. Phys., Vol. 5, pp 1619-1628, 1964.
- [138] Varadan, V.V., Varadan V.K., Ma. Y. and Steele, W.A., 'Effects Of NonSpherical Statistics On EM Wave Propagation In Discrete Random Media', Radio Sci., Vol. 22, No. 4, pp 491 -498, 1987.
- [139] Cruzan, O.R., 'Translational Addition Theorem For Spherical Vector Wave Equations', Q.App.Maths, Vol. 20, pp30-39, 1962.

- [140] Varadan, V.V. and Varadan V.K. Eds., Acoustic, electromagnetic and elastic wave scattering: Focus on the T-matrix approach. Pergamon press, U.K., 1980.
- [140a] Barber, P., 'Scattering And Absorption By Homogeneous and Layered Dielectrics', in Acoustic, electromagnetic and elastic wave scattering: Focus on the T-matrix approach. Varadan, V.V. and Varadan V.K. Eds., Pergamon press, U.K., pp191-209, 1980.
- [140b] Srinivasan, A., 'Propagational Characteristics Of Centimeter And Millimeter Waves By Numerical And Experimental Techniques', Ph.D. thesis, University Of Roorkee, India, 1984.
- [141] Edmonds, A.R., 'Angular Momentum In Quantum Mechancis', Princeton university press, Princeton, New Jersey , 1957.
- [142] Papolius, A., 'Probability, Random, Variables and Stochastic Processes', McGraw Hill Co., 1965.
- [143] Atkinson, K.E., 'An Introduction To Numerical Analysis', John Wiley & Sons, New York, pp 73-77, 1989.
- [144] Twersky, V., 'Reflection And Scattering Of Sound By Correlated Rough Surfaces', J.Acoust. Soc. Am., Vol. 73, pp 86-94, 1983.
- [145] Percus, J.K. and Yewick, G.J., 'Analysis Of Classical Statistics Mechanics By Means Of Collective Coordinates', Phys. Rev., Vol. 110, pp 1-3, 1958.
- [146] Fisher, I.Z., 'Statistical Theory Of Liquids', Univerity of Chicago press, Chicago, 1965.
- [147] McQuarrie, D.A., 'Statistical Mechanics', Harper and Row, New York, 1976.
- [148] Rowlinson, J.S., 'Self-consitent Approximation For Molecular Distribution Function', Mol. Phys., Vol. 9, pp 217-217, 1965.
- [149] Watts, R.O. and Henderson, D., 'Pair Distribution Function For Fluid Hard Spheres', Mol. Phys., Vol. 16, pp 217-233, 1969.

- [150] Ott, R.H., R.G.Kaouyoumjain and L.Peter's Jr., 'Scattering By A Two Dimensional Periodic Array Of Narrow Plates'., Radio Sci., Vol. 2., PP 1347-49, Nov 1967.
- [151] Chaitanya Kumar M.V., Kak, V., Gupta, S.C. and Agrawal, N.K., 'An Improved Radar Absorber using Frequency Selective surface', Proceedings of The Discussion Meeting On NTAD, IISc, Bangalore, India, pp28-31, Dec. 1992.
- [152] Chaitanya Kumar M.V., Moolri, M., Gupta, S.C. and Agrawal, N.K., 'A Technique To Improve The Performance Of resonant Absorbers', Accepted at International Conference on Radar, Paris, France., May, 1994.
- [153] Chaitanya Kumar M.V., Gupta, S.C. and Agrawal, N.K., 'An Array Of Jerusalem Crosses As An Impedance Matching Surface', Submitted to Defense Science Journal, India.
- [154] Gupta, S.C. and Agrawal, N.K., 'Project Report On Development Of Thin Radar Absorbers', Submitted to DRDO, Ministry of Defence, Govt. of India., 1994.
- [155] Chaitanya Kumar M.V., Gupta, S.C. and Agrawal, N.K., 'Measurement Technique For Thin Sheet Microwave Absorbers', Proc. of the 3rd International Symposium On Recent Advances In Microwave Technology, Nevada, USA, pp 145-148, 1991.
- [156] Chaitanya Kumar M.V., Gupta, S.C. and Agrawal, N.K., 'Conducting Screens Perforated With Apertures As An Impedance Matching Layer'. Proc. of the IX National Convention of Institution of Engineers (ET), University of Roorkee, Roorkee, India., pp 412-415, March 1994.
- [157] Max Sucher and Jerome Fox, 'Handbook of Microwave Measurement., Vol. II.', John Wiley & Sons., New York, pp.536, 1963.

APPENDIX I

```

DIMENSION X(50),X1(50,50),X2(50,50),R(100),SUM(50),
1 F(50),SR(50),ROLD(100),H(50),af(250),pf(10)
DIMENSION COF(25),COEFN(25),COEFD(25),TDI(50),RRP(20),
1 RQ(20),RIP(10),RIQ(10),CRR(25),RR(25),RI(25)
COMMON/A/ NX,NC,NIC,STEP,ALFA,BETA,GAMA,IN,INF,FDIFER,
1 SEQL,K1,K2,K3,K4,K5,K6,K7,K8,K9,X,X1,X2,R,SUM, F,SR,
1 ROLD,SCALE,FOLD
COMMON /C/ WI,WIN,W0,W1,W2,NN,COEFN,COEFD,NN1,NN2
COMMON /B/ LFEAS,L5,L6,L7,L8,L9,R1A,R2A,R3A,TOL
OPEN(UNIT=1,FILE='FL',STATUS='OLD')
OPEN(UNIT=6,FILE='FLOUT',STATUS='NEW')
READ (1,*) NX,NC,NIC,SIZE,CONVER,TOL,NCON,NNC
WRITE(*,*) NX,NC,NIC,SIZE,CONVER,TOL,NCON,NNC
ALFA = 1.
BETA = 0.5
GAMA = 2.
STEP=SIZE
C SECOND(TIME)
10 CONTINUE
NNC=NNC+1
C TEMPORARY DATA FOR THE PROBLEM, SUCH AS VARIABLE
COEFFICIENTS OR
C NEW PARAMETERS SHOULD BE READ IN AFTER THIS CARD
C THE ASSUMED INTIAL VECTOR IS READ IN AFTER THIS CARD
IF(NNC.GT.2) GO TO 9999
READ (1,*,END=11) (X(I), I = 1, NX)
11 WRITE(6, 106)
WRITE(6, 759)
WRITE(6, 756) NX,NC,NIC,SIZE,CONVER,TIME
C TYPE *, 'STEP1'
K1 = NX + 1
K2 = NX + 2
K3 = NX + 3
K4 = NX + 4
K5 = NX + 5
K6 = NC + NIC
K7 = NC + 1
K8 = NC + NIC
K9 = K8 + 1
N = NX - NC
N1 = N + 1
IF(N1.GE.3) GO TO 50
N1 = 3
N=2
50 N2 = N + 2
N3 = N + 3
N4 = N + 4
N5 = N + 5
N6 = N + 6
N7 = N + 7
N8 = N + 8

```



```

XN = N
XNX = NX
XN1 = N1
R1A = 0.5*(SQRT(5.)-1.)
R2A = R1A * R1A
R3A = R2A * R1A
L5 = NX + 5
L6 = NX + 6
L7 = NX + 7
L8 = NX + 8
L9 = NX + 9
ICONT = 1
NCONT = 1
WRITE(6, 115)
WRITE(6,116) (X(J), J = 1,NX)
FDIFER = 2.*(NC + 1)*STEP
FOLD = FDIFER
IN = N1
CALL SUMR
SR(N1) = SQRT(SEQL)
WRITE(6, 763) FDIFER,SR(N1)
IF(SR(N1).LT.FDIFER) GO TO 341
CALL WRITEX
WRITE(6, 757)
INF = N1
STEP = 0.05*FDIFER
CALL FEASBL
WRITE(6, 764)
WRITE(6,116) (X2(INF,J),J = 1, NX)
WRITE(6,765) SR(INF)
IF(FOLD.LT.TOL) GO TO 80
341 WRITE(6, 35)
WRITE(6,758) ICONT, FDIFER
CALL WRITEX
FTER = R(K9)
C COMPUTE CENTROID OF ALL VERTICES OF INITIAL POLYHEDRON
237 STEP1 = STEP*(SQRT(XNX + 1.) + XNX-1.)/(XNX*SQRT(2.))
STEP2 = STEP*(SQRT(XNX+1.) - 1.)/(XNX*SQRT(2.))
ETA = (STEP1 + (XNX - 1.)*STEP2)/(XNX + 1.)
DO 4 J = 1, NX
X(J) = X(J) - ETA
4 CONTINUE
CALL START
DO 9 I = 1, N1
DO 9 J = 1, NX
X2(I,J) = X1(I,J)
9 CONTINUE
DO 5 I = 1, N1
IN = I
DO 6 J = 1, NX
6 X(J) = X2(I,J)
CALL SUMR
SR(I) = SQRT(SEQL)

```

```

IF(SR(I).LT.FDIFER) GO TO 8
CALL FEASBL
IF(FOLD.LT.TOL) GO TO 80
C IF(FOLD.LT.1.0E-09) GO TO 80
8 CALL PROBLEM(3)
F(I) = R(K9)
5 CONTINUE
1000 STEP = 0.05 * FDIFER
ICONT = ICONT + 1
C SELECT LARGEST VALUE OF OBJECTIVE FUNCTION FROM
POLYHEDRON VERTICES
FH = F(1)
LHIGH = 1
DO 16 I = 2, N1
IF(F(I).LT.FH) GO TO 16
FH = F(I)
LHIGH = I
16 CONTINUE
C SELECT MINIMUM VALUE OF OBJECTIVE FUNCTION FROM
POLYHEDRON VERTICES
41 FL = F(1)
LOW = 1
DO 17 I = 2, N1
IF(FL.LT.F(I)) GO TO 17
FL = F(I)
LOW = I
17 CONTINUE
DO 86 J = 1, NX
86 X(J) = X2 (LOW, J)
IN = LOW
CALL SUMR
SR(LOW) = SQRT(SEQL)
IF(SR(LOW).LT.FDIFER) GO TO 87
INF = LOW
CALL FEASBL
IF(FOLD.LT.TOL) GO TO 80
C IF(FOLD.LT.1.0E-09) GO TO 80
CALL PROBLEM(3)
F(LOW) = R(K9)
GO TO 41
87 CONTINUE
C FIND CENTROID OF POINTS WITH I DIFFERENT THAN LHIGH
DO 19 J = 1, NX
SUM2 = 0.
DO 20 I = 1, N1
20 SUM2 = SUM2 + X2(I,J)
19 X2(N2,J) = 1./XN*(SUM2-X2(LHIGH,J))
SUM2 = 0.
DO 36 I = 1, N1
DO 36 J = 1, NX
SUM2 = SUM2 + (X2(I,J) - X2(N2,J)) **2
36 CONTINUE
FDIFER = (NC+1)/XNI*SQRT(SUM2)

```

```

IF(FDIFER.LT.FOLD) GO TO 98
FDIFER = FOLD
GO TO 198
98  FOLD = FDIFER
198 CONTINUE
    FTER = F(LOW)
137 NCONT = NCONT + 1
    IF(NCONT.LT.4*N1) GO TO 37
    IF(ICONT.LT.NCON) GO TO 337
    FOLD = 0.5*FOLD
337 NCONT = 0
    WRITE(6,35)
    WRITE(6,758) ICONT, FDIFER
    CALL WRITEX
37  IF(FDIFER.LT.CONVER) GO TO 81
C   SELECT SECOND LARGEST VALUE OF OBJECTIVE FUNCTION
    IF(LHIGH.EQ.1) GO TO 43
    FS = F(1)
    LSEC = 1
    GO TO 44
43  FS = F(2)
    LSEC = 2
44  DO 18 I = 1, N1
    IF(LHIGH.EQ.I) GO TO 18
    IF(F(I).LT.FS) GO TO 18
    FS = F(I)
    LSEC = I
18  CONTINUE
C   REFLECT HIGH POINT THROUGH CENTROID
    DO 61 J = 1, NX
    X2(N3,J) = X2(N2,J) + ALFA*(X2(N2,J) - X2(LHIGH,J))
61  X(J) = X2(N3,J)
    IN = N3
    CALL SUMR
    SR(N3) = SQRT(SEQL)
89  IF(SR(N3).LT.FDIFER) GO TO 82
    INF = N3
    CALL FEASBL
    IF(FOLD.LT.TOL) GO TO 80
C   IF(FOLD.LT.1.0E-09) GO TO 80
8   CALL PROBLEM(3)
    F(N3) = R(K9)
    IF(F(N3).LT.F(LOW)) GO TO 84
    IF(F(N3).LT.F(LSEC)) GO TO 92
    GO TO 60
92  DO 93 J = 1, NX
93  X2(LHIGH,J) = X2(N3,J)
    SR(LHIGH) = SR(N3)
    F(LHIGH) = F(N3)
    GO TO 1000
84  DO 23 J = 1, NX
    X2(N4,J) = X2(N3,J) + GAMA*(X2(N3,J) - X2(N2,J))
23  X(J) = X2(N4,J)

```

```

IN = N4
CALL SUMR
SR(N4) = SQRT(SEQL)
IF(SR(N4).LT.FDIFER) GO TO 25
INF = N4
CALL FEASBL
IF(FOLD.LT.TOL) GO TO 80
C   IF(FOLD.LT.1.0E-09) GO TO 80
25  CALL PROBLEM(3)
    F(N4) = R(K9)
    IF(F(Low).LT.F(N4)) GO TO 92
    DO 26 J = 1, NX
26  X2(LHIGH,J) = X2(N4,J)
    F(LHIGH) = F(N4)
    SR(LHIGH) = SR(N4)
    GO TO 1000
60  IF(F(N3).GT.F(LHIGH)) GO TO 64
    DO 65 J = 1, NX
65  X2(LHIGH,J) = X2(N3,J)
64  DO 66 J = 1, NX
    X2(N4,J) = BETA*X2(LHIGH,J) + (1. - BETA) * X2(N2,J)
66  X(J) = X2(N4,J)
    IN = N4
    CALL SUMR
    SR(N4) = SQRT(SEQL)
    IF(SR(N4).LT.FDIFER) GO TO 67
    INF = N4
    CALL FEASBL
    IF(FOLD.LT.TOL) GO TO 80
C   IF(FOLD.LT.1.0E-09) GO TO 80
67  CALL PROBLEM(3)
    F(N4) = R(K9)
    IF(F(LHIGH).GT.F(N4)) GO TO 68
    DO 69 J = 1, NX
    DO 69 I = 1, N1
69  X2(I,J) = 0.5*(X2(I,J) + X2(Low,J))
    DO 70 I = 1, N1
    DO 71 J = 1, NX
71  X(J) = X2(I,J)
    IN = I
    CALL SUMR
    SR(I) = SQRT(SEQL)
    IF(SR(I).LT.FDIFER) GO TO 72
    INF = I
    CALL FEASBL
    IF(FOLD.LT.TOL) GO TO 80
C   IF(FOLD.LT.1.0E-09) GO TO 80
72  CALL PROBLEM(3)
70  F(I) = R(K9)
    GO TO 1000
68  DO 73 J = 1, NX
73  X2(LHIGH,J) = X2(N4,J)
    SR(LHIGH) = SR(N4)

```

```

      F(LHIGH) = F(N4)
      GO TO 1000
81  WRITE(6,760) ICONT, FDIFER
      CALL WRITEX
C   CALL SECOND(TIME
      TIME=1.0
      WRITE(6,755) TIME
      WRITE(6,761)
      WRITE(6,'(1X,80(''**'))')
      GO TO 10
80  WRITE(6,760) ICONT, FDIFER
      CALL WRITEX
      WRITE(6,762)
      GO TO 10
1   FORMAT(3I5,F10.5,E10.3)
2   FORMAT(8F10.5)
35  FORMAT(/,80('**'))
106 FORMAT(1H1,/)
115 FORMAT(/,10X, ' THE STARTING VECTOR SELECTED BY USER
1 IS ')
116 FORMAT(10X,8E16.6)
755 FORMAT(/, 10X,35H THE COMPUTATION TIME IN SECONDS =
1 E12.5)
756 FORMAT(/,10X,'NUMBER OF INDEPENDENT
1 VARIABLES=',I5,/,10X,' NUMBER OF EQUALITY
1 CONSTRAINTS=',I5,/,10X,'NUMBER OF INEQUALITY
1 CONSTRAINTS=',I5,/,10X,'SIZE OF INITIAL POLY
1 3HEDRON=',E12.5,/,10X,'THE DESIRED CONVERGENCE
1 IS=',E12.5,
4/,10X,'THE COMPUTATION TIME IN SECONDS=',E12.5)
757 FORMAT(/,10X,'THE INITIAL X VECTOR DOES NOT SATISFY
1 THE INITIAL TO LERANCE CRITERION')
758 FORMAT(/,10X,'STAGE CALCULATION NUMBER =',I5,/,
1 20X,'THE TOLE2RANCE CRITERION =', E14.6)
759 FORMAT(/)
760 FORMAT(/,10X,'TOTAL NUMBER OF STAGES CALCULATIONS
1 =',I5,/, 10X,'THE CONVERGENCE LIMIT =',E14.6)
761 FORMAT(/,30X,'THESE ARE THE FINAL ANSWERS')
762 FORMAT(/,30X,'THESE ARE NOT THE FINAL ANSWERS')
763 FORMAT(/,10X,40H THE INITIAL TOLERANCE CRITERION IS
1 E12.5,/, 10X,40H THE SUM OF VIOLATED CONSTRAINTS IS',
1 E12.5)
764 FORMAT(/,70H THE VECTOR FOUND BY PROGRAM WHICH
1 SATISFIES THE INITIAL TOLERANCE IS )
765 FORMAT(/,10X,31H SUM OF VIOLATED CONSTRAINTS = E17.7)
9999 STOP
      END
      SUBROUTINE FEASBL
      DIMENSION X(50),X1(50,50),X2(50,50),R(100),SUM(50),
1 F(50),SR(50),ROLD(100),H(50),af(250),pf(10)
      DIMENSION COF(25),COEFN(25),COEFD(25),TDI(50),RRP(20),
1 RQ(20),RIP(10),RIQ(10),CRR(25),RR(25),RI(25)
      COMMON/A/ NX,NC,NIC,STEP,ALFA,BETA,GAMA,IN,INF,FDIFER,

```

```

1  SEQL,K1,K2,K3,K4,K5,K6,K7,K8,K9,X,X1,X2,R,SUM, F,SR,
1  ROLD,SCALE,FOLD
COMMON /C/ WI,WIN,W0,W1,W2,NN,COEFN,COEFD,NN1,NN2
COMMON /B/ LFEAS,L5,L6,L7,L8,L9,R1A,R2A,R3A,TOL
ALFA = 1.
BETA = 0.5
GAMA = 2.
XNX = NX
ICONT = 0
LCHEK = 0
ICHEK = 0
25  CALL START
DO 3 I = 1, K1
DO 4 J = 1, NX
4   X(J) = X1(I,J)
IN = I
CALL SUMR
3   CONTINUE
C   SELECT LARGEST VALUE OF SUM(I) IN SIMPLEX
28  SUMH = SUM(1)
INDEX = 1
DO 7 I = 2, K1
IF(SUM(I).LE.SUMH) GO TO 7
SUMH = SUM(I)
INDEX = I
7   CONTINUE
C   SELECT MINIMUM VALUE OF SUM(I) IN SIMPLEX
SUML = SUM(1)
KOUNT = 1
DO 8 I = 2, K1
IF(SUML.LE.SUM(I)) GO TO 8
SUML = SUM(I)
KOUNT = I
8   CONTINUE
C   FIND CENTROID OF POINTS WITH I DIFFERENT THAN INDEX
DO 9 J = 1, NX
SUM2 = 0.
DO 10 I = 1, K1
10  SUM2 = SUM2 + X1(I,J)
X1(K2,J) = 1./XNX*(SUM2 - X1(INDEX,J))
C   FIND REFLECTION OF HIGH POINT THROUGH CENTROID
X1(K3,J) = 2.*X1(K2,J) - X1(INDEX,J)
9   X(J) = X1(K3,J)
IN = K3
CALL SUMR
IF(SUM(K3).LT.SUML) GO TO 11
C   SELECT SECOND LARGEST VALUE IN SIMPLEX
IF(INDEX.EQ.1) GO TO 38
SUMS = SUM(1)
GO TO 39
38  SUMS = SUM(2)
39  DO 12 I = 1, K1
IF((INDEX - 1).EQ.0) GO TO 12

```

```

        IF(SUM(I).LE.SUMS) GO TO 12
        SUMS = SUM(I)
12     CONTINUE
        IF(SUM(K3).GT.SUMS) GO TO 13
        GO TO 14
C     FORM EXPANSION OF NEW MINIMUM IF REFLECTION HAS
PRODUCED ONE MINIMUM
11     DO 15 J = 1, NX
        X1(K4,J) = X1(K2,J) + 2.*(X1(K3,J) - X1(K2,J))
15     X(J) = X1(K4,J)
        IN = K4
        CALL SUMR
        IF(SUM(K4).LT.SUML) GO TO 16
        GO TO 14
13     IF(SUM(K3).GT.SUMH) GO TO 17
        DO 18 J = 1, NX
18     X1(INDEX,J) = X1(K3,J)
17     DO 19 J = 1, NX
        X1(K4,J) = 0.5*X1(INDEX,J) + 0.5*X1(K2,J)
19     X(J) = X1(K4,J)
        IN = K4
        CALL SUMR
        IF(SUMH.GT.SUM(K4)) GO TO 6
C     REDUCE SIMPLEX BY HALF IF REFLECTION HAPPENS TO PRODUCE
A LARGER VALUE
C     THAN THE MAXIMUM
        DO 20 J = 1, NX
        DO 20 I = 1, K1
20     X1(I,J) = 0.5*(X1(I,J) + X1(KOUNT,J))
        DO 29 I = 1, K1
        DO 30 J = 1, NX
30     X(J) = X1(I,J)
        IN = I
        CALL SUMR
29     CONTINUE
5     SUML = SUM(1)
        KOUNT = 1
        DO 23 I = 2, K1
        IF(SUML.LT.SUM(I)) GO TO 23
        SUML = SUM(I)
        KOUNT = I
23     CONTINUE
        SR(INF) = SQRT(SUM(KOUNT))
        DO 27 J = 1, NX
27     X(J) = X1(KOUNT,J)
        GO TO 26
6     DO 31 J = 1, NX
31     X1(INDEX,J) = X1(K4,J)
        SUM(INDEX) = SUM(K4)
        GO TO 5
16     DO 21 J = 1, NX
        X1(INDEX,J) = X1(K4,J)
21     X(J) = X1(INDEX,J)

```

```

SUM(INDEX) = SUM(K4)
SR(INF) = SQRT(SUM(K4))
GO TO 26
14 DO 22 J = 1, NX
X1(INDEX,J) = X1(K3,J)
22 X(J) = X1(INDEX,J)
SUM(INDEX) = SUM(K3)
SR(INF) = SQRT(SUM(K3))
26 ICONT = ICONT + 1
DO 36 J = 1, NX
36 X2(INF,J) = X(J)
IF(ICONT.LT.2*K1) GO TO 50
ICONT = 0
DO 24 J = 1, NX
24 X(J) = X1(K2,J)
IN = K2
CALL SUMR
DIFER = 0.
DO 57 I = 1, K1
57 DIFER = DIFER + (SUM(I) - SUM(K2)) **2
DIFER = 1./(K7*XNX)*SQRT(DIFER)
IF(DIFER.GT.TOL) GO TO 50
C IF(DIFER.GT.1.0E-14) GO TO 50
51 IN = K1
STEP = 20.*FDIFER
CALL SUMR
SR(INF) = SQRT(SEQL)
DO 52 J = 1, NX
52 X1(K1,J) = X(J)
DO 53 J = 1, NX
FACTOR = 1.
X(J) = X1(K1,J) + FACTOR*STEP
X1(L9,J) = X(J)
IN = L9
CALL SUMR
X(J) = X1(K1,J) - FACTOR*STEP
X1(L5,J) = X(J)
IN = L5
CALL SUMR
56 IF(SUM(L9).LT.SUM(K1)) GO TO 54
IF(SUM(L5).LT.SUM(K1)) GO TO 55
GO TO 97
54 X1(L5,J) = X1(K1,J)
SUM(L5) = SUM(K1)
X1(K1,J) = X1(L9,J)
SUM(K1) = SUM(L9)
FACTOR = FACTOR + 1.
X(J) = X1(K1,J) + FACTOR * STEP
IN = L9
CALL SUMR
GO TO 56
55 X1(L9,J) = X1(K1,J)
SUM(L9) = SUM(K1)

```



```

X1(K1,J) = X1(L5,J)
SUM(K1) = SUM(L5)
FACTOR = FACTOR + 1.
X(J) = X1(K1,J) - FACTOR * STEP
IN = L5
CALL SUMR
GO TO 56
97  H(J) = X1(L9,J) - X1(L5,J)
    X1(L6,J) = X1(L5,J) + H(J)*R1A
    X(J) = X1(L6,J)
    IN = L6
    CALL SUMR
    X1(L7,J) = X1(L5,J) + H(J) * R2A
    X(J) = X1(L7,J)
    IN = L7
    CALL SUMR
    IF(SUM(L6).GT.SUM(L7)) GO TO 68
    X1(L8,J) = X1(L5,J) + (1. - R3A) * H(J)
    X1(L5,J) = X1(L7,J)
    X(J) = X1(L8,J)
C   X(J) = X1(L8,J)
    IN = L8
    CALL SUMR
    IF(SUM(L8).GT.SUM(L6)) GO TO 76
    X1(L5,J) = X1(L6,J)
    SUM(L5) = SUM(L6)
    GO TO 75
76  X1(L9,J) = X1(L8,J)
    SUM(L9) = SUM(L8)
    GO TO 75
68  X1(L9,J) = X1(L6,J)
    X1(L8,J) = X1(L5,J) + R3A*H(J)
    X(J) = X1(L8,J)
    IN = L8
    CALL SUMR
    STEP = SIZE
    SUM(L9) = SUM(L6)
    IF(SUM(L7).GT.SUM(L8)) GO TO 71
    X1(L5,J) = X1(L8,J)
    SUM(L5) = SUM(L8)
    GO TO 75
71  X1(L9,J) = X1(L7,J)
    SUM(L9) = SUM(L7)
75  IF(ABS(X1(L9,J) - X1(L5,J)).GT.0.01*FDIFER)
    GO TO 97
    X1(K1,J) = X1(L7,J)
    X(J) = X1(L7,J)
    SUM(K1) = SUM(L5)
    SR(INF) = SQRT(SUM(K1))
    IF(SR(INF).LT.FDIFER) GO TO 760
53  CONTINUE
    ICHEK = ICHEK + 1
    STEP = FDIFER

```

```

IF(ICHEK.LE.2) GO TO 25
FOLD=TOL
C FOLD = 1.0E-12
WRITE(6,853)
WRITE(6,850)
WRITE(6,851) (X(J), J = 1, NX)
WRITE(6,852) FDIFER, SR(INF)
GO TO 46
760 DO 761 J = 1, NX
X2(INF,J) = X1(K1,J)
761 X(J) = X1(K1,J)
50 IF(SR(INF).GT.FDIFER) GO TO 28
IF(SR(INF).GT.0.) GO TO 35
CALL PROBLEM(3)
FINT = R(K9)
DO 139 J = 1, NX
139 X(J) = X2(INF,J)
CALL PROBLEM(2)
DO 40 J = K7,K8
40 R1(J) = R(J)
DO 41 J = 1, NX
41 X(J) = X1(KOUNT,J)
CALL PROBLEM(2)
DO 42 J = K7, K8
42 R3(J) = R(J)
DO 43 J = 1, NX
H(J) = X1(KOUNT,J) - X2(INF,J)
43 X(J) = X2(INF,J) + 0.5*H(J)
CALL PROBLEM(2)
FLG(1) = 0.
FLG(2) = 0.
FLG(3) = 0.
C WRITE(6,*) (R(III),III=1,10)
C WRITE(6,*) (X(III),III=1,10)
C WRITE(6,*) K7,K8
DO 44 J = K7,K8
IF(R3(J).GE.0.) GO TO 44
FLG(1) = FLG(1) + R1(J)*R1(J)
FLG(2) = FLG(2) + R(J)*R(J)
FLG(3) = FLG(3)+ R3(J)*R3(J)
44 CONTINUE
SR(INF) = SQRT(FLG(1))
IF(SR(INF).LT.FDIFER) GO TO 35
ALFA1 = FLG(1) - 2.*FLG(2) + FLG(3)
BETA1 = 3.*FLG(1) - 4.*FLG(2) + FLG(3)
C IF(R3(J).GE.0.0) RATIO=1.0
RATIO = BETA1/(4.*ALFA1)
DO 45 J = 1, NX
45 X(J) = X2(INF,J) + H(J) *RATIO
IN = INF
CALL SUMR
SR(INF) = SQRT(SEQL)
IF(SR(INF).LT.FDIFER) GO TO 465

```

```

DO 49 I = 1, 20
DO 48 J = 1, NX
48 X(J) = X(J) - 0.05*H(J)
CALL SUMR
SR(INF) = SQRT(SEQL)
IF(SR(INF).LT.FDIFER) GO TO 465
49 CONTINUE
465 CALL PROBLEM(3)
IF(FINT.GT.R(K9)) GO TO 46
SR(INF) = 0.
GO TO 35
46 DO 47 J = 1, NX
47 X2(INF,J) = X(J)
35 CONTINUE
DO 335 J = 1, NX
335 X(J) = X2(INF,J)
850 FORMAT(/108H IT IS NOT POSSIBLE TO SATISFY THE
1 VIOLATED CONSTRAINT SET FROM THIS VECTOR. THE SEARCH
1 WILL BE TERMINATED. /68H PLEASE CHOOSE A NEW STARTING
1 VECTOR AND REPEAT SOLUTION AGAIN )
851 FORMAT(/,63H THE VECTOR FOR WHICH THE CONSTRAINTS
1 COULD NOT BE SATISFIED IS /,(8E16.6))
852 FORMAT(/,27H THE TOLERANCE CRITERION = E14.6,20X, 49H
1 THE SQUARE ROOT OF THE CONSTRAINTS SQUARED IS = E16.6)
853 FORMAT(/,81H * * * * * SUBROUTINE FEASBL FAILS TO
1 FIND A FEASIBLE POINT * * * * * )
RETURN
END
SUBROUTINE START
DIMENSION A(50,50)
DIMENSION X(50),X1(50,50),X2(50,50),R(100),SUM(50),
1 F(50),SR(50),ROLD(100),H(50),af(250),pf(10)
DIMENSION COF(25),COEFN(25),COEFD(25),TDI(50),RRP(20),
1 RQ(20),RIP(10),RIQ(10),CRR(25),RR(25),RI(25)
COMMON/A/ NX,NC,NIC,STEP,ALFA,BETA,GAMA,IN,INF,FDIFER.
1 SEQL,K1,K2,K3,K4,K5,K6,K7,K8,K9,X,X1,X2,R,SUM, F,SR.
1 ROLD,SCALE,FOLD
COMMON /C/ WI,WIN,W0,W1,W2,NN,COEFN,COEFD,NN1,NN2
COMMON /B/ LFEAS,L5,L6,L7,L8,L9,R1A,R2A,R3A,TOL
VN = NX
STEP1 = STEP/(VN*SQRT(2.))*(SQRT(VN + 1.) + VN - 1.)
STEP2 = STEP/(VN*SQRT(2.))*(SQRT(VN + 1.) - 1.)
DO 1 J = 1, NX
1 A(1,J) = 0.
DO 2 I = 2, K1
DO 4 J = 1, NX
4 A(I,J) = STEP2
L = I - 1
A(I,L) = STEP1
2 CONTINUE
DO 3 I = 1, K1
DO 3 J = 1, NX
3 X1(I,J) = X(J) + A(I,J)

```

```

RETURN
END
SUBROUTINE WRITEX
DIMENSION X(50),X1(50,50),X2(50,50),R(100),SUM(50),
1 F(50),SR(50),ROLD(100),H(50),af(250),pf(10)
DIMENSION COF(25),COEFN(25),COEFD(25),TDI(50),RRP(20),
1 RQ(20),RIP(10),RIQ(10),CRR(25),RR(25),RI(25)
COMMON/A/ NX,NC,NIC,STEP,ALFA,BETA,GAMA,IN,INF,FDIFER,
1 SEQL,K1,K2,K3,K4,K5,K6,K7,K8,K9,X,X1,X2,R,SUM, F,SR,
1 ROLD,SCALE,FOLD
COMMON /C/ WI,WIN,W0,W1,W2,NN,COEFN,COEFD,NN1,NN2
COMMON /B/ LFEAS,L5,L6,L7,L8,L9,R1A,R2A,R3A,TOL
CALL PROBLEM(3)
WRITE(6,1) R(K9)
1 FORMAT(/, ' OBJECTIVE FUNCTION VALUE = 'E17.7)
WRITE(6,2) (X(J), J = 1, NX)
2 FORMAT(/, ' THE INDEPENDENT VECTORS ARE' /,6E17.7)
IF(NC.EQ.0) GO TO 6
CALL PROBLEM(1)
WRITE(6,3) (R(J), J = 1, NC)
3 FORMAT(/, ' THE EQUALITY CONSTRAINT VALUES ARE
/,6E17.7)
6 IF(NIC.EQ.0) GO TO 5
CALL PROBLEM(2)
WRITE(6,4) (R(J), J = K7, K6)
4 FORMAT(/, ' THE INEQUALITY CONSTRAINT VALUES' /,6E17.7)
5 RETURN
END
SUBROUTINE SUMR
DIMENSION X(50),X1(50,50),X2(50,50),R(100),SUM(50),
1 F(50),SR(50),ROLD(100),H(50),af(250),pf(10)
DIMENSION COF(25),COEFN(25),COEFD(25),TDI(50),RRP(20),
1 RQ(20),RIP(10),RIQ(10),CRR(25),RR(25),RI(25)
COMMON/A/ NX,NC,NIC,STEP,ALFA,BETA,GAMA,IN,INF,FDIFER,
1 SEQL,K1,K2,K3,K4,K5,K6,K7,K8,K9,X,X1,X2,R,SUM, F,SR,
1 ROLD,SCALE,FOLD
COMMON /C/ WI,WIN,W0,W1,W2,NN,COEFN,COEFD,NN1,NN2
COMMON /B/ LFEAS,L5,L6,L7,L8,L9,R1A,R2A,R3A,TOL
SUM(IN) = 0.
CALL PROBLEM(2)
SEQL = 0.
IF(NIC.EQ.0) GO TO 4
DO 1 J = K7, K8
IF(R(J).GE.0.) GO TO 1
SEQL = SEQL + R(J) * R(J)
1 CONTINUE
4 IF(NC.EQ.0) GO TO 3
CALL PROBLEM(1)
DO 2 J = 1, NC
2 SEQL = SEQL + R(J) * R(J)
3 SUM(IN) = SEQL
5 RETURN
END

```

```

SUBROUTINE PROBLEM(INQ)
DIMENSION X(50),X1(50,50),X2(50,50),R(100),SUM(50),
1 F(50),SR(50),ROLD(100),af(250),pf(10)
COMMON/A/ NX,NC,NIC,STEP,ALFA,BETA,GAMA,IN,INF,FDIFER,
1 SEQL,K1,K2,K3,K4,K5,K6,K7,K8,K9,X,X1,X2,R,SUM,F,SR,
1 ROLD,SCALE,FOLD
COMMON /C/ WI,WIN,W0,W1,W2,NN,COEFN,COEFD,NN1,NN2
COMMON /B/ LFEAS,L5,L6,L7,L8,L9,R1A,R2A,R3A
C EQUALITY CONSTRAINTS
IF(INQ.EQ.1) GO TO 1
IF(INQ.EQ.2) GO TO 2
IF(INQ.EQ.3) GO TO 3
1 CONTINUE
C EQUALITY CONSTRAINTS ARE TO BE ENTERED HERE

GO TO 5
2 CONTINUE
C INEQUALITY CONSTRAINTS ARE TO BE ENTERED HERE

GO TO 5
3 CONTINUE
C OBJECTIVE FUNCTIN
C PROGRAM'S LISTED IN APPENDIX 3.1/APPENDIX 5.3/
C APPENDIX 6.1 IS TO BE INCLUDED HERE.

RETRURN
END

```